DEVELOPING GENETIC THERAPIES FOR POLYGLUTAMINE DISORDERS

Melvin Evers

DEVELOPING GENETIC THERAPIES FOR POLYGLUTAMINE DISORDERS

MELVIN EVERS

Cover design: M.J.J. Langewouters || Fruto internet, concepts & design
Layout: M.M. Evers
Printed by: Proefschriftmaken.nl || Uitgeverij BOXPress
Published by: Uitgeverij BOXPress, 's-Hertogenbosch

ISBN: 978-90-8891-992-3

Printing of this thesis was financially supported by: Vereniging van Huntington
Prosensa Therapeutics B.V.

DEVELOPING GENETIC THERAPIES FOR POLYGLUTAMINE DISORDERS

Proefschrift

ter verkrijging van
de graad van Doctor aan de Universiteit Leiden,
op gezag van Rector Magnificus prof.mr. C.J.J.M. Stolker,
volgens besluit van het College voor Promoties
te verdedigen op woensdag 7 januari 2015
klokke 16.15 uur

door

Melvin Maurice Evers

geboren te Rhenen
in 1982

Promotiecommissie

Promotor:
Prof. dr. G.J.B. van Ommen

Co-promotor:
Dr. W.M.C. van Roon-Mom

Overige leden:
Prof. dr. R.A.C. Roos
Prof. dr. Y. Temel (Maastricht UMC+)
Dr. J.C. Dorsman (VU Medisch Centrum, Amsterdam)

Promovendi hebben lange en zware dagen omdat er meer mis dan goed gaat in het onderzoek,
maar aan het einde van de dag gaan ze naar huis om andere dingen te doen.
Patiënten met polyglutamine aandoeningen kunnen nooit een pauze nemen.

Table of Contents

Melvin M. Evers [1]
Ioannis Zalachoras [2]
Lodewijk J.A. Toonen [1]
Rinkse Vlamings [3,4]
Annemieke Aartsma-Rus [1]
Onno C. Meijer [2]
Yasin Temel [3,4]
Willeke M.C. van Roon-Mom [1]

[1] Department of Human Genetics, Leiden University Medical Center
[2] Department of Endocrinology, Leiden University Medical Center
[3] Departments of Neuroscience and Neurosurgery, Maastricht University Medical Center
[4] European Graduate School of Neuroscience (EURON)

1

General introduction: Genetic therapies for polyglutamine disorders

Frontiers in Molecular Neuroscience 2011, 4:10
Huntington's Disease - Core Concepts and Current Advances 2012, InTech
Molecular Neurobiology 2014, 49(3):1513-1531

1.1. Introduction

More than two decades ago for the first time an expansion of a repeated microsatellite sequence was discovered to be the cause of a disease. A CGG triplet repeat expansion in the gene responsible for fragile X syndrome was found (Verkerk *et al.*, 1991). In the same year the mutation in fragile X syndrome was identified, a CAG trinucleotide repeat expansion in the *AR* gene was found to be the cause of a X-linked progressive neurodegenerative disorder called spinal and bulbar muscular atrophy (SBMA), or Kennedy disease (La Spada *et al.*, 1991). The CAG trinucleotide repeat expansion in the *AR* gene results in a mutant androgen receptor (AR) with an expanded polyglutamine (polyQ) tract (La Spada *et al.*, 1991). Next to SBMA, eight other neurodegenerative disorders have since been identified resulting from an expanded polyQ protein (**Table 1**). These disorders are Huntington disease (HD), the spinocerebellar ataxias (SCAs) 1, 2, 3, 6, 7, and 17), and dentatorubro-pallidoluysian atrophy (DRPLA) (**Table 1**).

This chapter will first introduce a group of inherited disorders caused by a triplet repeat expansion and provide a short overview of the main characteristics of polyQ disorders (**paragraph 1.2**). The underlying clinical and molecular genetics of the most prevalent and best studied polyQ disorders, HD and SCA3, will be extensively reviewed in **paragraph 1.3 and 1.4**. While I will provide a short overview of the disease-causing polyQ proteins and the role of known disease mechanisms of the other polyQ disorders; DRPLA, SBMA, and SCAs 1, 2, 6, 7 and 17, in **paragraph 1.5**. Next, opportunities for protein lowering approaches of polyQ disorders will be discussed (**paragraph 1.6**). What can we learn from other neurodegenerative disorders where genetic therapies are in development or already used as therapy (**paragraph 1.7**). The challenges in delivery and cellular uptake of genetic therapies for neurodegenerative disorders to the brain and specifically neurons will be discussed in **paragraph 1.8.** Finally, the scope and outline of this thesis "developing genetic therapies for polyglutamine disorders" will be defined.

1.2. Triplet repeat expansion disorders

Since the early nineties, 14 inherited triplet repeat expansion disorders have been identified. Over the years other repeat expansions, such as tetra, penta and dodecanucleotide repeats, have also been linked to human diseases (Mirkin, 2007). In this thesis I will only focus on neurological and neuromuscular disorders caused by triplet repeat expansions. These triplet repeat disorders are categorised according to their disease mechanism, being (1) functional cellular impairment due to loss of function of the gene containing the repeat, (2) cellular impairment due to production of RNA containing an expanded CUG tract, or (3) functional cellular impairment due to production of a protein containing an expanded polyQ. Here, I will provide a short overview of all three categories and successively I will focus on polyQ disorders.

Loss of protein function

As described previously, in 1991 the Human Genome Project led to the discovery of the gene responsible for fragile X syndrome (Verkerk *et al.*, 1991). Fragile X syndrome is characterized by mental retardation, macroorchidism, and distinct facial features (Jacquemont *et al.*, 2007). The CGG repeat is located in the 5′ untranslated region (UTR) of the *FMR1* gene (Kremer *et al.*, 1991; Verkerk *et al.*, 1991). A trinucleotide repeat expansion of over 200 CGGs results in decreased FMR1 expression due to hypermethylation at the promoter, decreased fragile X mental retardation protein (FMRP) levels and loss of function (Pieretti *et al.*, 1991; Meijer *et al.*, 1994). The CGG repeat in fragile X syndrome is considered to be highly unstable once it exceeds a certain threshold length (Richards and Sutherland, 1992). This phenomenon where the triplet repeat size increases upon the next generation, causing symptoms at an earlier age, is called anticipation. The full mutation alleles are derived from meiotically unstable maternal premutation alleles, with 55 to 200 CGG repeats (Fu *et al.*, 1991). Patients with 45 to 54 repeats do not transmit directly to the full mutation, even though these intermediate alleles are slightly unstable, particularly when maternally transmitted (Zhong *et al.*, 1996).

Gain of RNA toxicity

A decade after the discovery of the CGG triplet repeat expansion responsible for fragile X syndrome, it was found that carriers with premutation alleles developed a late age of onset neurodegenerative disorder called fragile X-associated tremor/ataxia syndrome (FXTAS) (Hagerman *et al.*, 2001; Jacquemont *et al.*, 2003). Although not fully penetrant, especially males with premutation alleles containing of more than 70 CGG repeats develop FXTAS with intention tremor and cerebellar ataxia (Jacquemont *et al.*, 2006). Remarkably, FXTAS patients had close to normal FMRP protein levels, ruling out the loss of protein function as shown in fragile X syndrome (Kenneson *et al.*, 2001). Peripheral blood leucocytes derived from FXTAS patients did show elevated FMRP mRNA levels in (Kenneson *et al.*, 2001). Likewise, *post-mortem* brain tissue showed intranuclear mRNA inclusions (RNA foci) containing the expanded CGG-repeat (Tassone *et al.*, 2004), suggesting RNA-mediated neurodegeneration.

Originally, the idea for gain of toxic function at RNA level came from myotonic dystrophy type 1 (DM1) (Davis *et al.*, 1997). DM1 is a member of CTG expansion disorders that derive from triplet repeat expansions located in non-coding regions of the corresponding genes. Other CTG repeat expansion disorders are HD-like 2 (HDL2), SCA8 and SCA12. DM1 is caused by a CTG expansion in the 3' UTR of the *dystrophia myotonica-protein kinase* (*DMPK*) gene (Brook *et al.*, 1992; Fu *et al.*, 1992; Mahadevan *et al.*, 1992). This unstable CTG triplet repeat expansion results in the most common form of adult muscular atrophy. Like other triplet repeat expansions, DM1 shows genetic anticipation with an earlier onset and more severe phenotype after transmission from one generation to the next (Howeler *et al.*, 1989). Patients with DM1 were shown to have RNA foci with sequestration of the muscleblind-like 1 (MBNL1) splicing factor in muscle nuclei (Miller *et al.*, 2000; Fardaei *et al.*, 2001). The CUG repeat mRNA can form stable hairpin structures which can sequester RNA binding proteins, such as MBNL1. This binding of MBNL1 to double stranded CUG RNA is believed to result in depleted MBNL1 function and consequently misregulation of alternative splicing, resulting in cellular toxicity (Wheeler and Thornton, 2007).

Gain of toxic polyQ protein function

Since the discovery that an expanded CAG repeat in the *AR* gene and subsequent translation of a mutant polyQ-repeat containing androgen receptor result in SBMA, eight other neurodegenerative polyQ disorders have been identified (**Table 1**). All polyQ disorders are caused by a CAG triplet repeat expansion in exons of different genes and are the result of a gain of toxic polyQ protein function. These disorders are HD, SCAs 1, 2, 3, 6, 7, and 17, and DRPLA (**Table 1**). PolyQ disorders can be subdivided based on their main clinical feature: SBMA is mainly characterized by motor weaknesses, HD by chorea and the other 7 polyQ disorders by ataxia.

It is known that the prevalence of each polyQ disorder significantly varies per country and ethnicity. The prevalence of the polyQ SCAs was estimated to be about 3 per 100,000 individuals in the Netherlands (van de Warrenburg *et al.*, 2005) and for DRPLA 0.1 per 100,000 individuals in Japan (Hirayama *et al.*, 1994). Worldwide HD (3-5 per 100,000), SBMA (1-2 per 100,000), and SCA3 (0.5-1 per 100,000) are the most prevalent polyQ disorders (Schols *et al.*, 2004; Banno *et al.*, 2012; Pringsheim *et al.*, 2012).

Although the mutations occur in very different genes, polyQ disorders have a lot in common (Fischbeck, 2001). They all result in progressive neurodegeneration with psychiatric, cognitive and motor symptoms. Except for SBMA, they are all autosomal dominant and disease onset is around midlife. For all disorders the CAG repeat length correlates with the age of onset, which means that the longer the CAG repeat, the earlier the disease manifestation (Doyu *et al.*, 1992; Ikeuchi *et al.*, 1995; Lund *et al.*, 2001; van de Warrenburg *et al.*, 2005; Roos, 2010). All polyQ disorders have a CAG repeat threshold, meaning that carriers with a CAG repeat above this threshold will certainly develop the disorder (**Table 1**). PolyQ diseases also have genetic anticipation, mainly upon paternal transmission, which means that the next generation will likely inherit a longer CAG repeat, resulting in a more severe disease with an earlier age of

Table 1: Overview of polyQ disorders and CAG repeat location and number of causative genes.

disease		gene		CAG repeat	repeat number	
symbol	full name	symbol	full name	location	wt	mut
HD	Huntington disease	*HTT*	huntingtin	exon 1	< 29	≥ 40
SCA3/ MJD	spinocerebellar ataxia type 3/ Machado-Joseph disease	*ATXN3*	ataxin 3	exon 10	< 40	≥ 52
SBMA	spinal and bulbar muscular atrophy/ Kennedy disease	*AR*	androgen receptor	exon 1	< 31	≥ 40
SCA1	spinal and bulbar muscular atrophy/	*ATXN1*	ataxin 1	exon 8	< 36	≥ 39
SCA2	Kennedy disease	*ATXN2*	ataxin 2	exon 1	< 31	≥ 32
SCA6	spinocerebellar ataxia type 6	*CACNA1A*	calcium channel, voltage-dependent, P/Q type, alpha 1A subunit	exon 47	< 18	≥ 19
SCA7	spinocerebellar ataxia type 7	*ATXN7*	ataxin 7	exon 3	< 35	≥ 38
SCA17	spinocerebellar ataxia type 17	*TBP*	TATA box-binding protein	exon 3	< 42	≥ 50
DRPLA	dentatorubral-pallidoluysian atrophy	*ATN1*	atrophin 1	exon 5	< 35	≥ 49

Abbreviations: wt: normal repeat size, mut: full penetrant repeat size

onset (Rub *et al.*, 2013).

As described above, the polymorphic polyQ tract consists of CAG repeats. However, polyQ is also encoded by CAA codons and usually a combination of both CAG and CAA triplets encodes the polyQ tract. In polyQ disease-causing proteins the polyQ tracts are commonly composed of long uninterrupted CAG triplets. The polyQ tracts encoded by mixtures of CAG and CAA codons seems to be less prone to expansion and more stable upon transmission to the next generation (Frontali *et al.*, 1999). In accordance, interruption of the CAG repeat by CAA (silent) or CAT (missense) mutations results is altered aggregation properties and delay the onset age (Menon *et al.*, 2013).

Except for SCA6, polyQ disease-causing proteins are ubiquitously expressed throughout the body. Apart from the expanded polyQ repeat, mutant polyQ proteins have no homologous sequences or functional domains, assuming that the expanded polyQ repeat is causative for the observed pathogenesis (Zoghbi and Orr, 2000). It has been suggested that in polyQ disorders increasing oxidative stress and inability to protect against free radicals with age could lead to mitochondrial dysfunction and cell damage (Kim *et al.*, 2003; Goswami *et al.*, 2006; Miyata *et al.*, 2008; Ajayi *et al.*, 2012).

A prominent pathological hallmark of these diseases is the accumulation of aggregated polyQ proteins in the brain (Davies *et al.*, 1997). However, the exact role of protein aggregation in disease pathogenesis is controversial and whether the aggregates are neurotoxic or neuroprotective is still under debate (Klement *et al.*, 1998; Saudou *et al.*, 1998; Yamada *et al.*, 2006). Probably the smaller soluble polyQ species generated by proteolytic cleavage during the aggregation process are the toxic entities and the large SDS-insoluble aggregates may likely be less harmful end products of the upstream toxic event (Shao and Diamond, 2007). Misfolding of the expanded polyQ proteins probably results in proteolytic cleavage and altered interactions, resulting in neurodegeneration and neuronal loss (Shao and Diamond, 2007).

1.3. Huntington disease

HD is an autosomal, dominantly inherited neurodegenerative disorder. HD is rare, but more common in Western countries. The prevalence of HD in America is approximately 5 in 100,000 (Shoulson and Young, 2011) and in Europe, the prevalence of HD may be even higher with estimates in England and Wales as high as 12 in 100,000 individuals (Rawlins, 2010).

Post-mortem studies show that there is a 10-20 percent weight reduction in HD brains (Vonsattel *et al.*, 1985). Neurodegeneration occurs throughout the forebrain and specifically affects GABAergic medium spiny neurons of the striatum (Levesque *et al.*, 2003). Severe cell loss in the striatal complex, the caudate nucleus and putamen, results in striatal atrophy (Halliday *et al.*, 1998). This causes an enlargement of the lateral ventricles. The medium spiny projection neurons, containing enkephalin, are more susceptible to degeneration than substance P containing projection neurons while interneurons seem to be spared (Walker, 2007). With disease progression, degeneration expands throughout the brain and other structures become affected (Tabrizi *et al.*, 2009). Cortical atrophy is characterized by thinning of the cerebral cortex and the underlying white matter. Neuronal loss is abundant in cortical layers III, V and VI (Rosas *et al.*, 2008) but is also prominent in the *Cornu Ammonis* (CA1) region of the hippocampus, with a reduction of about 9 percent (Rosas *et al.*, 2003).

Disease onset usually occurs around midlife and is clinically characterized by a combination of symptoms: cognitive impairments, movement abnormalities, and emotional disturbances (Roos, 2010). Motor symptoms of HD include chorea and occasionally bradykinesia and dystonia (Tabrizi *et al.*, 2009). Choreic movements, recognized as involuntary and unwanted movements, start in the distal extremities. During the course of HD these movements become more profound and eventually all muscles of the body are affected. These symptoms can initially appear as lack of concentration or nervousness and unsteady gait (Kremer *et al.*, 1992). Psychiatric symptoms often precede the onset of motor symptoms. Irritability is commonly one of the first signs and occurs throughout the course of the disease. Other psychiatric symptoms involve anxiety, obsessive and compulsive behaviour while apathy and psychosis can appear in advanced stages. However, the most frequent psychiatric symptom is depression (Reedeker *et al.*, 2012). Like psychiatric symptoms, cognitive symptoms can be present prior to the onset of the motor symptoms. The cognitive symptoms comprise mainly of impairment in executive functions, including abstract thinking, problem solving, and attention (Paulsen and Long, 2014). Furthermore, the ability to learn new skills is affected (Paulsen *et al.*, 2001). Altogether these symptoms dramatically impede social and professional functioning. Eventually patients are incapable to adequately perform daily activities finally leading to progressive disability, requiring full-time care, followed by death (Simpson, 2007). Death generally occurs 15 to 20 years post diagnosis due to complications such as pneumonia, falls, dysphagia, heart disease or suicide (Roos *et al.*, 1993).

The disease is caused by a CAG trinucleotide repeat expansion in the first exon of the *HTT* gene. The *HTT* gene was the first autosomal disease locus to be mapped by genetic linkage

analysis in 1983 (Gusella *et al.*, 1983) on the short arm of chromosome 4 (4p16.3). The huntingtin protein (htt) was found to be ubiquitously expressed throughout the body, with highest expression in testis and brain (Strong *et al.*, 1993), however, cells in the brain are specifically vulnerable to the toxic function of mutant htt. The CAG repeat expansion in the *HTT* gene results in an expanded polyQ repeat in the htt protein (The Huntington's Disease Collaborative Research Group, 1993). When the number of CAG repeats exceeds 39, the gene encodes a mutated form of the htt protein that is prone to aggregation. Alleles ranging from 36 to 39 repeats, lead to reduced penetrance of the disease or to a very late onset (Kremer *et al.*, 1992; McNeil *et al.*, 1997; Losekoot *et al.*, 2013) and both sexes are affected with the same frequency (Walker, 2007). Repeat numbers exceeding 55-60 result in clinical manifestation of the disease before the age of 20, known as juvenile HD (Andresen *et al.*, 2007). Intergenerational CAG repeat changes are extremely rare on normal chromosomes but on expanded chromosomes changes in CAG repeat size take place in approximately 70 percent of meioses and expansion is more likely via the paternal line (Kremer *et al.*, 1995).

There is a strong inverse correlation between repeat numbers and the age of onset of the disease. The repeat length accounts for approximately 70 percent of the variance in age of onset (Roos, 2010). The relationship between repeat size is and rate of progression and duration of the disease is still under debate (Rosenblatt *et al.*, 2012). Neuropathological changes, such as atrophy and the number of aggregates found in the brain are clearly correlated with the CAG repeat number.

For patients, only symptomatic treatment is available and a treatment to slow down the progression or delay the onset of the disease remains elusive.

Huntingtin protein

When the *HTT* gene was discovered in 1993, the htt protein had an unknown function. Since then, enormous research efforts have revealed many functions of the wild-type protein (discussed in the present paragraph) and many toxic gain of functions of the mutant protein (discussed in the next paragraph) (**Figure 1**).

Wild-type htt is mainly localized in the cytoplasm, although a small proportion is present in the nucleus (Hoogeveen *et al.*, 1993; de Rooij *et al.*, 1996; Kegel *et al.*, 2002). The protein is known to be associated with microtubules, the plasma membrane, Golgi complex, the endoplasmic reticulum (ER), and mitochondria. Furthermore htt is associated with vesicular structures, such as clathrin-coated and non-coated vesicles, autophagic vesicles, endosomal compartments or caveolae (Kegel *et al.*, 2005; Atwal *et al.*, 2007; Rockabrand *et al.*, 2007; Strehlow *et al.*, 2007; Caviston *et al.*, 2011).

Three of the first 17 amino acids at the amino terminus of htt are lysines, which are targets for post translational modifications that regulate htt half-life and are proposed to be involved in targeting htt to various intracellular membrane-associated organelles (Kalchman *et al.*, 1996; Steffan *et al.*, 2004; Kegel *et al.*, 2005; Atwal *et al.*, 2007; Rockabrand *et al.*, 2007). The polyQ repeat starts at the 18th amino acid and is thought to form a polar zipper structure, important for the interaction between different polyQ-containing transcription factors (Perutz *et al.*, 1994; Harjes

and Wanker, 2003). The polyQ stretch is followed by a polymorphic polyproline repeat, which is thought to be involved in keeping the protein soluble (Steffan *et al.*, 2004). Additionally, three main HEAT (htt, elongation factor 3, protein phosphatase 2A, and the yeast PI3-kinase TOR1) repeat motifs are present which are known to form superhelical structures and are involved in protein-protein interactions (Takano and Gusella, 2002; Li *et al.*, 2006). Htt is palmitoylated at the cysteine residue 214 by htt interacting protein (Hip) 14, which is thought to be involved in htt trafficking (Huang *et al.*, 2004). Htt has various proteolytic cleavage motifs, with a hotspot between amino acid 500 and 600 that are recognized by various proteases, such as caspases 1, 3, 6, 7 and 8 and calpain (Gafni and Ellerby, 2002; Wellington *et al.*, 2002; Kim *et al.*, 2006). The significance of wild-type htt cleavage is not completely clear, but the N-terminal proteolytic cleavage products tend to be trafficked across the nuclear membrane (Warby *et al.*, 2008). In the case of mutant htt, the accumulation of N-terminal proteolytic cleavage products in the nucleus has major impact on the pathogenesis (see below).

Mutant huntingtin: gain of toxic function

Although countless toxic gain of functions of the mutant htt have been proposed in the last two decades, the exact order of pathogenic events in HD, as well as interactions between mutant htt and other cellular proteins, are still poorly understood. Mutant htt is known to undergo conformational changes and interferes with various cellular processes, such as cellular trafficking, inhibition of chaperones, proteasomes, and autophagy, causing accumulation of htt and other abnormally folded proteins (**Figure 1**).

The characteristic protein aggregates are located throughout the brain and can already be found before the onset of the first symptoms (Weiss *et al.*, 2008). The rate of aggregate formation is correlated to the length of the polyQ repeat (Legleiter *et al.*, 2010), although there is growing evidence suggesting that these aggregates are not good indicators for disease onset and progression (Wanker, 2000; van Roon-Mom *et al.*, 2006). Whether accumulation of these aggregates is neurotoxic or neuroprotective is still under debate but increasing evidence suggests that soluble shorter mutant htt, and fragments thereof, are the main toxic components (Davies *et al.*, 1997; Saudou *et al.*, 1998; Arrasate *et al.*, 2004; Sathasivam *et al.*, 2013). Mutant htt is more subject to increased caspase activity and proteolytic cleavage of mutant htt results in the formation of small toxic N-terminal mutant htt fragments (**Figure 1**) (Cooper *et al.*, 1998). In HD brains, more htt protein fragments are found within the striatum compared to control brains, as well as upregulation of caspases, suggesting that cleavage may be disease specific (Mende-Mueller *et al.*, 2001; Graham *et al.*, 2010). Furthermore, strong evidence was presented for an important role of htt protein fragments in the pathogenesis of HD, as a HD mouse model containing capase-6-resistant expanded htt did not show neuronal dysfunction in contrast to the same mouse with caspase-6-sensitve expanded htt (Graham *et al.*, 2006). The only difference between these mice was the presence or absence of a 586 amino acid caspase-6 cleaved htt fragment containing the expanded polyQ repeat.

Although many genes and proteins have been identified to be involved in the HD pathogenesis, there is not one main cellular process affected in HD. Below I will review the

best studied cellular processes known to be involved in HD pathology.

Transcriptional deregulation

Like other polyQ disorders, altered gene expression is a prominent molecular hallmark of HD. As described above, mutant htt is proteolytically cleaved and N-terminal fragments are abundant in the nucleus, where they form aggregates (Cooper *et al.*, 1998). Various transcription factors have been found to co-localize with htt aggregates, such as TATA box-binding protein (TBP), cAMP response element-binding protein binding protein (CBP) and p53 (Steffan *et al.*, 2000; van Roon-Mom *et al.*, 2002). These co-aggregated proteins can no longer assert their normal function and could thereby contribute to transcriptional deregulation (Nucifora, Jr. *et al.*, 2001). A large set of genes involved in cellular processes affected have been found to be differentially expressed in various cellular and animal models of HD (Cha, 2007) and HD patient-derived *post-mortem* brain (Hodges *et al.*, 2006). In HD, mutant htt binds less efficient to the RE1 silencing transcription factor (REST), causing transcriptional repression of various genes, including the brain-derived neurotrophic factor (BDNF) (Zuccato *et al.*, 2001; Zuccato *et al.*, 2007). BDNF is vital for neuronal survival and is involved in synaptic plasticity processes (Huang and Reichardt, 2001). Next to reduced gene transcription, mutant htt also disrupts vesicular transport and release of BDNF, possibly leading to excitotoxicity (Gauthier *et al.*, 2004).

Impaired protein degradation

Protein aggregates in HD patient-derived brain material shows a clear co-localization of htt and ubiquitin (Difiglia *et al.*, 1997), suggesting an involvement of the ubiquitin-proteasomal protein degradation in the disease. Mutant htt is misfolded, resulting in an aggregation-prone conformation (Rousseau *et al.*, 2009). Misfolded, aggregation-prone proteins are generally cleared either by the ubiquitin-proteasome system (UPS) (short-lived proteins) or through the autophagy-lysosome pathway (long-lived cytoplasmic proteins and protein complexes) (Rubinsztein, 2006). Aggregated htt protein and long stretches of Qs are known to impair the UPS *in vitro* and in *post-mortem* brain tissue (Bence *et al.*, 2001; Venkatraman *et al.*, 2004; Diaz-Hernandez *et al.*, 2006; Raspe *et al.*, 2009; Park *et al.*, 2013b), resulting in an inefficient degradation of mutant htt. The UPS is also involved in ER-associated protein degradation (ERAD). In an overexpressing cell system mutant htt was found to sequester various ERAD proteins, thereby inhibiting their function (Duennwald and Lindquist, 2008), which can result in ER stress-induced autophagy. To note, the involvement of the UPS in processing of expanded polyQ repeats has been the subject of controversy. Overexpressed N-terminal polyQ fragments were found to be entirely degraded by cellular proteasomes (Juenemann *et al.*, 2013). Also the entrapment of components of the UPS in aggregates could not be validated in HD mouse models (Bett *et al.*, 2009; Maynard *et al.*, 2009). Still, UPS activity is known to decrease with age and this reduced UPS activity is associated with increasing N-terminal expanded polyQ fragments aggregates in an HD knock-in mouse model (Zhou *et al.*, 2003), suggesting an involvement of UPS impairment in the HD pathogenesis.

In HD, two types of autophagy are affected, being macroautophagy and chaperone-mediated

autophagy (Cortes and La Spada, 2014). By macroautophagy cytosolic materials are sequestered in double membrane vesicles called autophagosomes. Although in HD cells autophagosomes are formed correctly and fused with lysosomes, its cargo recognition is disrupted by mutant htt, leading to empty autophagosomes (Martinez-Vicente *et al.*, 2010). Thus, it seems that the in HD reduced macroautophagy is not caused by comprised autophagosomes formation, but due to impaired toxic substrate removal. Blockage of macroautophagy results in upregulation of chaperone-mediated autophagy (Kaushik *et al.*, 2008). Chaperones usually assist target substrates, including phosphorylated (mutant) htt, directly to the lysosome (Thompson *et al.*, 2009; Qi *et al.*, 2012). In HD, this chaperone-mediated autophagy is impaired, probably by reduced phosphorylation of mutant htt (Thompson *et al.*, 2009), or by binding of mutant htt to chaperone proteins (Qi *et al.*, 2012), resulting in a reduced clearance of mutant htt. The reduced macroautophagy seen in HD is perhaps initially compensated by chaperone-mediated autophagy, but this overcompensation decreases with age, resulting in impaired clearance of toxic entities, increased oxidative damage and eventually neuronal cell death (Cortes and La Spada, 2014).

Mitochondrial dysfunction

N-terminal mutant htt fragments were found to be associated with the surface of mitochondria in transgenic and knock-in HD mice (Panov *et al.*, 2002; Orr *et al.*, 2008). The accumulation of mutant htt on mitochondria increases with age and correlates with disease progression. Soluble mutant htt impairs microtubule-based transport of proteins that are involved in the transport of mitochondria, which could lead to decreased ATP supply in nerve terminals (Orr *et al.*, 2008). Mutant htt is also suggested to be involved in mitochondrial energy metabolism defects. Metabolic energy defects could be the result of mutant htt's capability to induce mitochondrial permeability transition pore opening (Choo *et al.*, 2004). This leads to low mitochondrial membrane potential and high glutamate transmission, resulting in overactive glutamate receptors (excitotoxicity) (Choo *et al.*, 2004). Abnormal mitochondrial respiratory chain function seen in HD leads to reduced ATP levels and subsequent partially depolarized membrane (Milakovic and Johnson, 2005). This voltage change leads to chronic calcium influx and activation of proteases, causing more reactive oxygen species production and eventually oxidative stress. Nevertheless, this respiratory chain impairment is probably not caused by mutant htt directly but as late secondary event of autophagy pathway impairment and transcriptional deregulation (Oliveira, 2010).

Impaired axonal transport

In HD, axonal transport of mitochondria is impaired (Chang *et al.*, 2006). Next to transport of mitochondria, also transport of other organelles, such as BDNF-containing organelles and vesicles that store neurotransmitters and other peptides, exists in synapses (Gauthier *et al.*, 2004; Li *et al.*, 2009). In *C. elegans* and *D. melanogaster* HD models, mutant htt overexpression resulted in axonal aggregate formation and subsequently impaired axonal trafficking of synaptic vesicles and mitochondria (Parker *et al.*, 2001; Gunawardena *et al.*, 2003; Sinadinos *et al.*,

2009). This impaired transport of vesicles is confirmed by the finding that in early stage HD patients synaptic vesicle proteins show an altered subcellular location (Modregger *et al.*, 2002). Finally, various proteins involved in exocytosis are known to have decreased expression levels in HD patients. Proteins involved in docking and fusion of vesicles show reduced transcript expression, suggesting a defect in the neurotransmitter release machinery in HD patients (Smith *et al.*, 2007).

To conclude, many cellular processes have been identified that are impaired in HD, making it difficult to pinpoint offhand which processes are crucial for the disease pathology. Nevertheless, the toxic N-terminal polyQ protein fragments are thought to be crucial in the pathogenesis of HD. Why certain neuronal populations are more vulnerable to polyQ-containing peptides than others, remains elusive.

Loss of wild-type htt function

As described above, the main cause of HD is a gain of toxic mutant htt function. Mutant htt can bind and sequester wild-type htt into aggregates, potentially causing loss of wild-type htt function (Kazantsev *et al.*, 1999; Busch *et al.*, 2003). Since wild-type htt has anti-apoptotic properties and is important for cell survival in adult brain, loss of wild-type htt function could also be involved. Knock-out of the homologous *htt* mouse gene was found to be early embryonic lethal (Duyao *et al.*, 1995; Nasir *et al.*, 1995; Zeitlin *et al.*, 1995) and htt inactivation in the forebrain and testis of adult mice was shown to result in progressive neurodegeneration, sterility and reduced lifespan (Dragatsis *et al.*, 2000). Removal of endogenous htt in a *D. melanogaster* HD model was found to exacerbate the neurodegenerative phenotype (Zhang *et al.*, 2009). Htt is reported to be involved in BDNF-mediated neurotrophic support (Zuccato *et al.*, 2001) and act as protector of brain cells from apoptotic stimuli (Rigamonti *et al.*, 2000). These neuronal survival pathways are compromised due to mutant htt, once more supporting the view that loss of wild-type htt function is also involved in the disease pathogenesis.

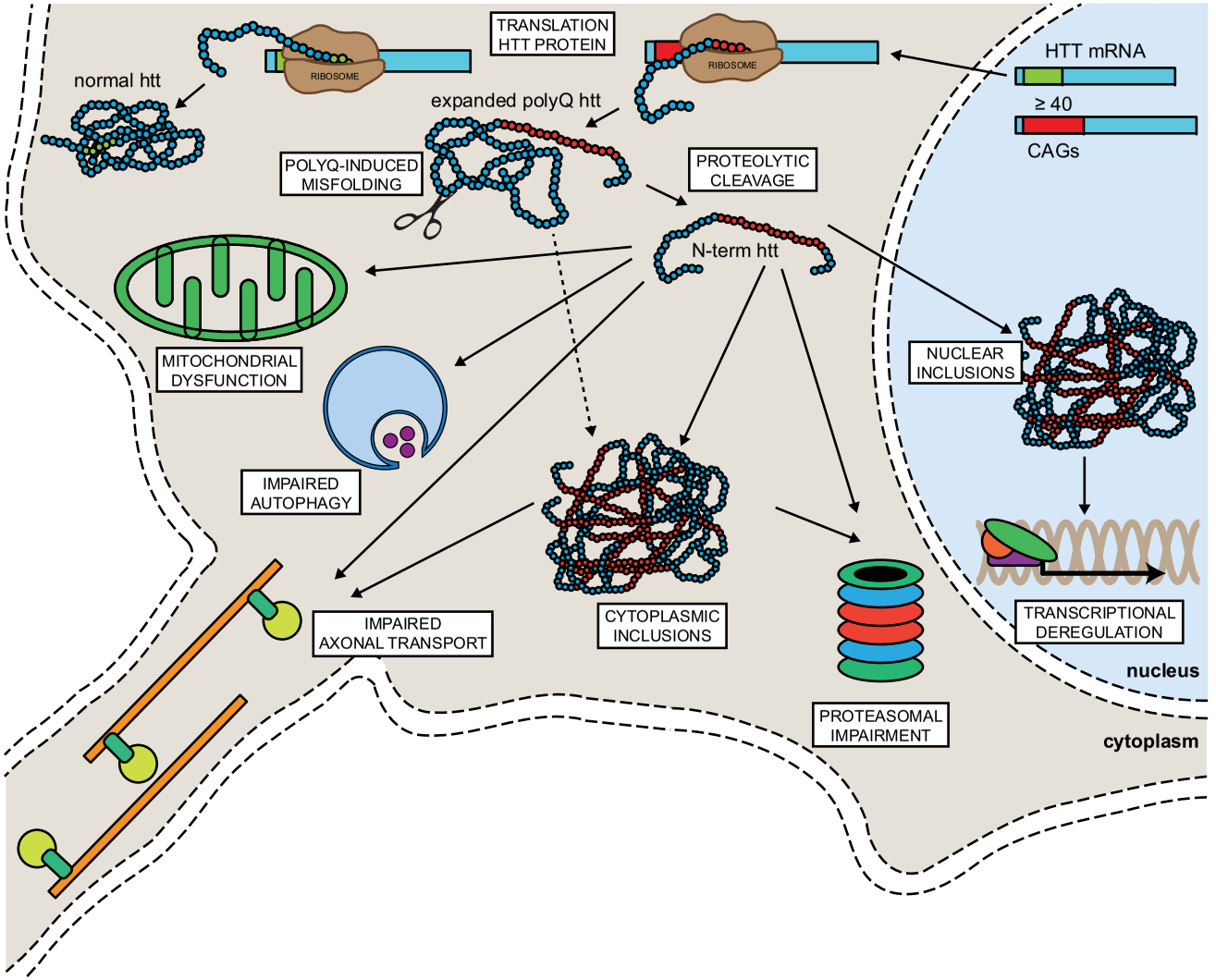

Figure 1. Schematic representation of cellular pathogenesis in Huntington disease (HD). The *HTT* gene is transcribed into pre-mRNA containing 67 exons which is spliced into mature mRNA. The expanded CAG repeat is located in the first exon and the transcript is translated into a mutant polyglutamine (polyQ) repeat-containing huntingtin (htt) protein. This polyQ repeat triggers conformational changes, resulting in abnormally folded mutant htt. Mutant htt is proteolytically cleaved, giving rise to N-terminal fragments that are aggregation-prone. Full-length and cleaved forms of htt form soluble monomers, oligomers or large insoluble aggregates, both in the nucleus and in the cytoplasm that cause toxicity. Other cellular disturbances resulting from mutant htt presence involved in HD pathogenesis include: transcriptional deregulation, impaired autophagy, mitochondrial dysfunction, proteasomal impairment, and compromised axonal transport.

1.4. Spinocerebellar ataxia type 3

SCA3, or Machado-Joseph disease (MJD) (Haberhausen *et al.*, 1995), is the most common spinocerebellar ataxia (Ranum *et al.*, 1995; Silveira *et al.*, 1996) and the second most common polyQ disease after HD (Pringsheim *et al.*, 2012). Similar to the other polyQ disorders is SCA3 inherited in an autosomal dominant fashion (Coutinho and Andrade, 1978), neurodegeneration is progressive and is ultimately fatal. Current therapeutic strategies are only able to provide symptomatic relief (Bauer and Nukina, 2009). SCA3 is clinically heterogeneous, but the main feature is progressive ataxia, affecting balance, gait and speech. Other frequently described symptoms include pyramidal signs, progressive external ophthalmoplegia, dysarthria, dysphagia, rigidity, distal muscle atrophies and double vision (Coutinho and Andrade, 1978; Rosenberg, 1992; Soong *et al.*, 1997; Teive *et al.*, 2012). Neuropathological studies have detected widespread neuronal loss in the cerebellum, thalamus, midbrain, pons, medulla oblongata and spinal cord of SCA3 patients, as reviewed by Riess *et al.*, (Riess *et al.*, 2008).

SCA3 is caused by an expanded stretch of CAG triplets in the penultimate exon of the *ATXN3* gene on chromosome 14q32.1, encoding the ataxin-3 protein (Kawaguchi *et al.*, 1994). Healthy individuals have up to 44 CAG repeats, whilst affected individuals have between 52 and 86 glutamine repeats. A repeat range from 45 to 51 is associated with incomplete penetrance of the disease (Kawaguchi *et al.*, 1994; Durr *et al.*, 1996; Padiath *et al.*, 2005). SCA3 patients with two mutant alleles show a more severe disease phenotype than those with a single mutant allele (Carvalho *et al.*, 2008). Also, there is a clear correlation between CAG repeat size and age of onset, though CAG repeat length only accounts for approximately 50% of the total variability in age of onset (Maciel *et al.*, 1995). The expanded CAG repeat leads to formation of an expanded polyQ tract in the C-terminal region of the ataxin-3 protein, leading to a toxic gain of function of the protein and formation of characteristic neuronal aggregates (Paulson *et al.*, 1997b). As is the case in HD, the neurotoxic properties of these aggregates are still under debate since the number of aggregates does not mirror the level of neurodegeneration or *ATXN3* CAG repeat length (Rub *et al.*, 2006).

Extensive studies in cell and animal models over the last decade have led to the identification of several cellular processes potentially involved in SCA3 pathology. Nonetheless, much remains to be elucidated regarding the toxicity resulting from mutant ataxin-3 RNA and protein, and a more comprehensive understanding of the many cellular processes involved would be of great benefit for the development of therapeutic strategies.

Ataxin-3 protein

The ataxin-3 protein has a molecular weight of approximately 42 kDa, depending on the isoform and size of the polyQ repeat. The CAG repeat, located in the penultimate exon, is translated into a polyQ repeat located at the C-terminus of the protein. In blood, 56 splice variants of ATXN3 have been identified, of which 20 could potentially be translated into a functional ataxin-3 protein (Bettencourt *et al.*, 2010). Of these 20 isoforms, only two isoforms, which differ in their C-terminal tail, have been studied extensively thus far. The isoform of ATXN3 most commonly expressed in brain consists of 11 exons, and is translated into an ataxin-3 protein consisting of 361 amino acids (Schmidt *et al.*, 1998; Trottier *et al.*, 1998; Harris *et al.*, 2010), based on a polyQ repeat length of 13 [Ensembl transcript ID ENST00000393287] (**Figure 2**).

Ataxin-3 is found throughout the cell and is able to translocate from the cytoplasm to the nucleus and back (Paulson *et al.*, 1997a; Schmidt *et al.*, 1998; Tait *et al.*, 1998; Trottier *et al.*, 1998; Pozzi *et al.*, 2008). Different regions of the ataxin-3 protein influence its subcellular localisation. It is not yet known if ataxin-3 plays a more important role in the nucleus or the cytoplasm, but enzymatically active ataxin-3 has been shown to localise to the nucleus more frequently compared to its inactive form (Todi *et al.*, 2007). In silico analysis predicted a nuclear localisation signal (NLS) in the proximity of the polyQ repeat at amino acid 273 to 286 (**Figure 2**) (Tait *et al.*, 1998; Albrecht *et al.*, 2004; Antony *et al.*, 2009; Macedo-Ribeiro *et al.*, 2009). This NLS showed a weak nuclear import activity *in vitro* (Antony *et al.*, 2009). However, mutating or deleting the proposed core NLS sequence from amino acid 282 to 285 had no effect on subcellular distribution, thus questioning the importance of the ataxin-3 NLS in its cellular localisation (Mueller *et al.*, 2009; Breuer *et al.*, 2010).

Another region that has been implicated in regulating ataxin-3 cellular localisation lies in the first 27 amino acids. Ataxin-3 lacking these first 27 amino acids could not be found in the nucleus, though the responsible mechanism involved is still unknown (Pozzi *et al.*, 2008). Furthermore, ataxin-3 contains six potential nuclear export signals (NES) (Albrecht *et al.*, 2004; Antony *et al.*, 2009; Macedo-Ribeiro *et al.*, 2009), of which two (amino acid 77 to 99 and 141 to 158) (**Figure 2**), showed significant nuclear export activity (Antony *et al.*, 2009; Macedo-Ribeiro *et al.*, 2009).

The N-terminus of ataxin-3 contains a large Josephin domain (**Figure 2**) that is known to have a low isopeptidase activity (Winborn *et al.*, 2008), implicating a role for ataxin-3 in the UPS pathway (Burnett *et al.*, 2003). The Josephin domain, together with the ubiquitin interacting motifs (UIM), can either rescue proteins from degradation or stimulate breakdown, by the removal of inhibitory poly-ubiquitin chains and by the regeneration of free and reusable ubiquitin(Burnett *et al.*, 2003; Winborn *et al.*, 2008; do Carmo *et al.*, 2010). The UPS pathway is involved in various cellular processes, such as protein degradation, endocytosis, transcriptional regulation and antigen presentation. Ubiquitination is a cascade of processes involving activating enzyme E1, transfer to ubiquitin conjugating enzymes E2 and association with ubiquitin ligases E3, resulting in addition of ubiquitins via isopeptide linkages to lysines

in the targeted protein (Fang and Weissman, 2004). Ubiquitins can bind individually, or as a poly-ubiquitin chain. Polyubiquitin chains linked through lysines 6, 11, 27, 29, 33, and 48 target proteins for proteasomal degradation. In contrast, lysine 63 or linear polyubiquitin chains have non-proteolytic functions such as activation of kinases and autophagy, where it is proposed to be involved in the biogenesis of protein inclusions (Lim and Lim, 2011). Amino acid cysteine 14, histidine 119, and asparagine 134 of the Josephin domain (**Figure 2**) of ataxin-3 are essential for its isopeptidase function and are highly conserved between Josephin and other ubiquitin C-terminal hydrolases and ubiquitin-specific proteases (Mao *et al.*, 2005; Nicastro *et al.*, 2005). The UIMs mediate selective binding to ubiquitin chains and restrict the types of chains that can be cleaved by the Josephin domain. Ataxin-3 is known to recognise poly-ubiquitin chains of four or more ubiquitins (Burnett *et al.*, 2003; Berke *et al.*, 2005) and binds the poly-ubiquitin linkages at lysine 48, lysine 63 and mixed linkage ubiquitin chains, with preference for lysine 63-tagged ubiquitins (Fang and Weissman, 2004; Winborn *et al.*, 2008). Especially the first and second UIMs are very important for binding of poly-ubiquitin chains, since mutations of leucine 229 and 249 resulted in almost abolished binding to ubiquitins (Burnett *et al.*, 2003).

Ataxin-3 has been found to bind the valosin-containing protein (VCP/p97) (**Figure 2**) (Wang *et al.*, 2000; Zhong and Pittman, 2006). VCP/p97 has numerous functions, of which one is the regulation of ERAD (Zhong and Pittman, 2006; Liu and Ye, 2012). A potential VCP/p97 binding domain has been mapped to an arginine/lysine-rich motif just prior to the polyQ repeat (Boeddrich *et al.*, 2006). The ataxin-3-VCP/p97 complex is involved in assisting targeted proteins to the proteasome (Wang *et al.*, 2006). Ataxin-3 is also known to interact with the human homologues of yeast protein RAD23, hHR23A and hHR23B (**Figure 2**) (Wang *et al.*, 2000). hHR23A and hHR23B are involved in DNA repair pathways as well as the delivery of ubiquitinated substrates to the proteasome for degradation (Wang *et al.*, 2000). The binding site of hHR23B to ataxin-3 is located in the second ubiquitin binding site of the Josephin domain, and in concordance, hHR23B was shown to compete with ubiquitin binding (Nicastro *et al.*, 2005). Cell stress resulted in altered interactions with both VCP/p97 and HR23B, which were found mainly in the cytoplasm, although no effect on protein degradation was reported (Laco *et al.*, 2012a).

Besides the clear role of ataxin-3 in protein degradation, ataxin-3 has been shown to be capable of regulating the transcriptional process. Ataxin-3 is, for instance, able to repress matrix metalloproteinase-2 (MMP-2) transcription, and improved nuclear localisation of ataxin-3 through phosphorylation enhances this transcriptional repression (Mueller *et al.*, 2009). Transcriptional regulation by ataxin-3 might arise through different mechanisms, since ataxin-3 is known to interact with numerous transcriptional regulators such as TBP-associated factor 4 (TAF4) (Shimohata *et al.*, 2000), CBP (McCampbell *et al.*, 2000; Chai *et al.*, 2002; Li *et al.*, 2002), p300 (Li *et al.*, 2002), p300/CBP-associated factor (PCAF) (Li *et al.*, 2002), nuclear receptor co-repressor (NCoR1), histone deacetylase (HDAC) 3 and 6 (Burnett, 2005; Evert *et al.*, 2006), forkhead box O (FOXO) transcription factor FOXO4 (Araujo *et al.*, 2011), and RAD23 (Wang *et al.*, 2000). Also, direct binding of ataxin-3 to DNA can likely take place through a leucine zipper motif located at amino acid 223 to 270 (**Figure 2**) (Evert *et al.*, 2006). This basic leucine zipper

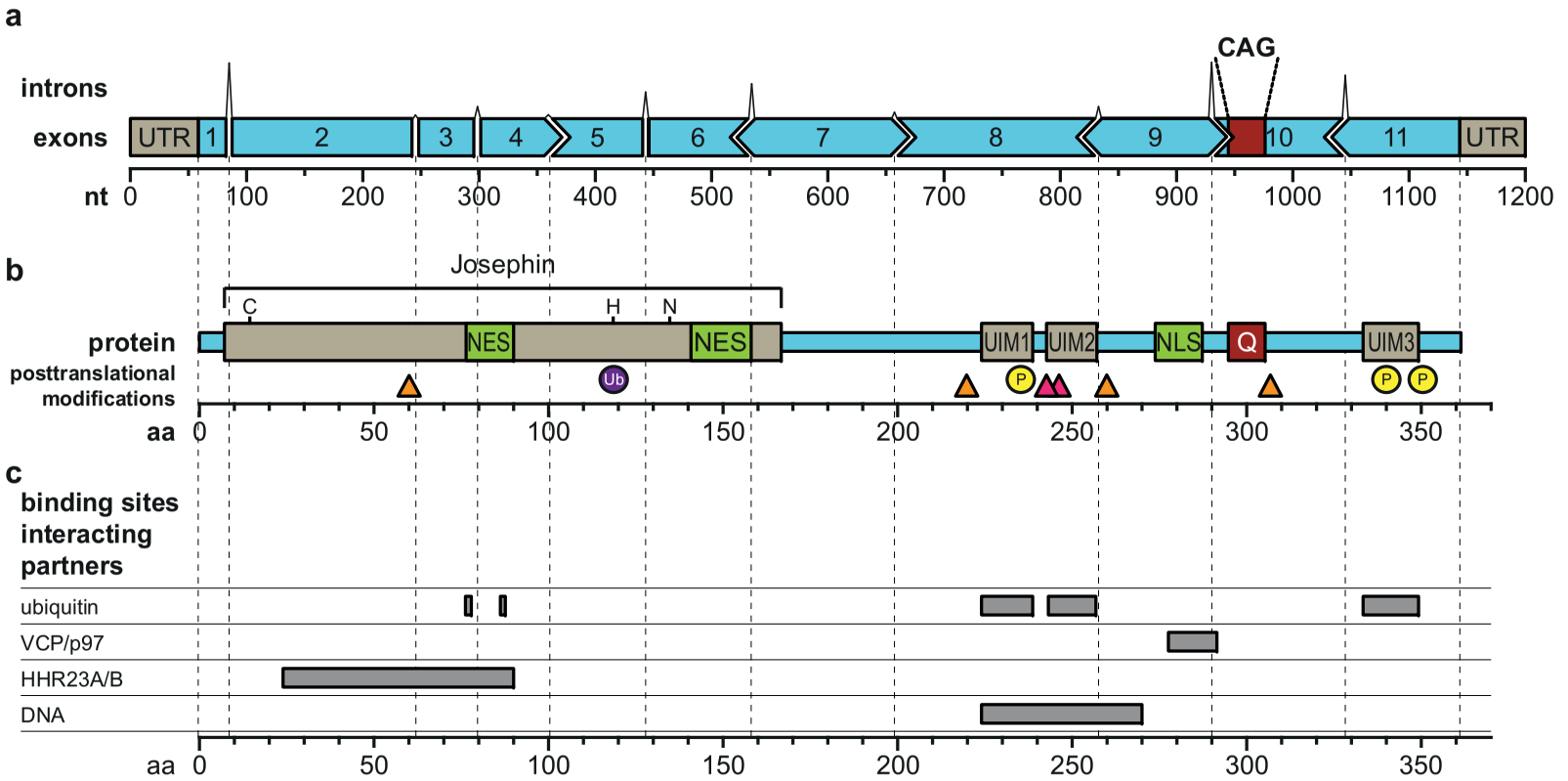

Figure 2. Schematic representation of the *ATXN3* gene, exon-intron structure and protein product showing protein functional domains, posttranslational modifications and binding domains of the main interacting partners. (a) The *ATXN3* gene (Ensembl ENST00000393287 transcript ID) consists of 11 exons with the start codon in exon 1 and the CAG repeat in exon 10. The shape of the boxes depict the reading frame, nt = nucleotides. The height of the introns are relative to their size. **(b)** The ataxin-3 protein consists of 361 amino acids (aa) with a Josephin domain in the N-terminal part that contains crucial amino acids for its isopeptidase activity (cysteine 14 **(C)**, histidine 119 **(H)**, and asparagine 134 **(N)**) and two nuclear export signals (NES). The C-terminal part contains three ubiquitin interacting motifs (UIM 1 to 3), a nuclear localisation signal (NLS) and the polyQ repeat. Specific amino acids known to undergo posttranslational modifications are indicated as follows: Yellow circles, phosphorylation **(P)**; purple eclipse, ubiquitination (Ub); orange triangle, calpain cleavage site; pink triangle, caspase cleavage motif. **(c)** Binding domains of the main interacting partners: ubiquitin; VCP/p97, valosin-containing protein; hHR23A and hHR23B, human homologs of yeast protein RAD23; and DNA.

motif was previously shown to bind to the GAGGAA consensus sequence in DNA (Landschulz *et al.*, 1988).

In summary, ataxin-3 is a well-established deubiquitinating enzyme, directly regulating the UPS machinery. Next to the proteasomal degradation, ataxin-3 is also implicated to be involved in regulation of misfolded ER protein degradation and might also directly interact with important transcriptional regulators and components of the DNA repair pathway.

Mutant ataxin-3 gain of toxic function

In SCA3, the expanded polyQ stretch in the C-terminus of ataxin-3 most likely leads to conformational changes of the protein, in turn resulting in altered binding properties, loss of protein function, altered subcellular localisation, aggregation, and perhaps altered proteolytic cleavage (Jana and Nukina, 2004). Although in the past decade there has been extensive research into the SCA3 disease mechanisms, it is still not well understood how the ataxin-3 polyQ expansion results in the observed pathology. In brain, the *ATXN3* gene expression levels were not found to be higher in the predominantly affected brain regions, suggesting that ATXN3 gene expression levels do not directly correlate with the selective neurodegeneration seen in SCA3 patients (Schmitt *et al.*, 1997). Therefore, other alterations induced by the mutant ataxin-3 protein are most likely important in SCA3 pathogenesis as well.

One of the first observations made in SCA3 patient derived brain material were the intracellular aggregates in neurons of the ventral pons and less frequently in the substantia nigra, globus pallidus, dorsal medulla, and dentate nucleus (Paulson *et al.*, 1997b), a feature that was reproduced in cell and animal models overexpressing mutant ataxin-3 (Ikeda *et al.*, 1996; Evert *et al.*, 1999; Schmidt *et al.*, 2002). Mutant ataxin-3 is known to accumulate in the cell nucleus, a property that is required for *in vivo* toxicity (Paulson *et al.*, 1997b; Schmidt *et al.*, 1998; Bichelmeier *et al.*, 2007). In line with this, transgenic SCA3 mice show a decrease of soluble mutant ataxin-3 protein in the cerebellum during disease progression, whilst aggregate formation increases and the disease phenotype progresses (Nguyen *et al.*, 2013). The nuclear environment has been suggested to promote the formation of nuclear aggregates, and additional proteins, such as TBP and CBP, were found to be recruited to the aggregates in human brain (van Roon-Mom *et al.*, 2005) and SCA3 animal models (Perez *et al.*, 1998). Indeed, reducing nuclear localisation of mutant ataxin-3 led to a reduction in nuclear inclusions (Fei *et al.*, 2007; Mueller *et al.*, 2009). The intranuclear aggregates only arise when ataxin-3 contains the expanded polyQ tract (Paulson *et al.*, 1997b).

In SCA3, proteolytic cleavage of mutant ataxin-3 is thought to lead to generation of cytotoxic and aggregation prone shorter soluble fragments containing the expanded polyQ toxic entity (Berke *et al.*, 2004; Haacke *et al.*, 2006; Takahashi *et al.*, 2008; Koch *et al.*, 2011). In a mouse model, ataxin-3 derived cleavage fragments were shown to contain expanded polyQ-containing protein fragments C-terminal of amino acid 221 (Goti *et al.*, 2004). Interestingly, in the two SCA3 brains tested, the ataxin-3 C-terminal fragments were enriched in disease-relevant brain structures, such as the cerebellum and substantia nigra, compared to an unaffected brain region or control brain material (Goti *et al.*, 2004). In subsequent studies, several caspase and

calpain proteolytic enzymes were identified that could be responsible for the generation of the potentially toxic ataxin-3 fragments. These mutant ataxin-3 fragments are highly susceptible to aggregation (Hubener *et al.*, 2012), and capable of inducing both aggregation and toxicity to a larger extent than full length mutant ataxin-3 (Ikeda *et al.*, 1996; Teixeira-Castro *et al.*, 2011).

In the past decade there has been extensive research into the SCA3 disease mechanisms, and various cellular processes, which I will review below, were found to be altered in SCA3.

Impaired protein degradation

Though ubiquitin chain proteolytic activity does not appear to vary between wild-type and mutant ataxin-3 (Winborn *et al.*, 2008), a widespread reduction of protein deubiquitination was reported in a mutant ataxin-3 cell model (Winborn *et al.*, 2008). This potential loss of deubiquitination function in SCA3 might in part be explained by trapping of ataxin-3 and various other components of the proteasomal machinery in the large ubiquitin-rich aggregates (Paulson *et al.*, 1997b; Chai *et al.*, 1999). Mutant ataxin-3 binds the ERAD-mediated protein degradation component VCP/p97 more efficiently than wild-type ataxin-3, possibly because of conformational changes (Hirabayashi *et al.*, 2001; Zhong and Pittman, 2006; Laco *et al.*, 2012a). In spite of this more efficient binding, mutant ataxin-3 seems to interfere with the degradation of target substrates (Doss-Pepe *et al.*, 2003; Laco *et al.*, 2012a). Additionally, N-terminal ataxin-3 fragments of 259 amino acids lacking the VCP/p97 binding domain were found to result in ER stress and impaired ER mediated unfolded protein response when expressed in a mouse model, though ERAD component levels appeared unchanged (Hubener *et al.*, 2011).

Not only ER degradation is altered in SCA3 but also autophagy, in which the degradation of cellular components through the lysosomal machinery, is impaired (**Figure 3**). Aggregates of mutant ataxin-3 were found to contain molecular components involved in autophagy. For instance, beclin-1, a protein crucial in the autophagy pathway was found to be trapped in protein aggregates in SCA3 brains (Nascimento-Ferreira *et al.*, 2011). In a rat model overexpressing mutant ataxin-3, increased beclin-1 expression resulted in clearance of the mutant protein (Nascimento-Ferreira *et al.*, 2011). This observation is in accordance with impairments in autophagy seen in other neurodegenerative disorders (Wong and Cuervo, 2010), and the fact that stimulation of autophagy was found to alleviate symptoms *in vivo* (Ravikumar *et al.*, 2004).

These observations suggest that the SCA3 pathology may partly be the result of loss of function of ERAD machinery as well as compromised autophagy, together resulting in impaired protein degradation, accumulation of ubiquitinated proteins, and cellular stress.

Mitochondrial dysfunction

A cell model overexpressing mutant ataxin-3 with 78 CAGs showed reduced antioxidant enzyme levels, increased mitochondrial DNA damage, and reduced energy supply, which indicates impaired mitochondrial function (Yu *et al.*, 2009). Recently, mitochondrial DNA damage was also seen in SCA3 transgenic mice expressing full length ataxin-3 with 98 to 104 glutamines (Kazachkova *et al.*, 2013). In the disease affected pontine nuclei of these transgenic SCA3 mice less mitochondrial DNA copies were seen, as compared to the unaffected

hippocampus (Kazachkova *et al.*, 2013). Additionally, less mitochondrial DNA copy numbers were observed in the mutant cells and SCA3 patient samples, implying mitochondrial DNA damage due to oxidative stress (Yu *et al.*, 2009). In line with this, the antioxidant enzyme superoxide dismutase was found downregulated in pontine brain tissue of SCA3 patients (Araujo *et al.*, 2011), suggesting diminished antioxidant enzyme function.

Additionally, mitochondrial dysfunction was verified by the finding that the mitochondrial respiratory chain complex II activity was somewhat compromised in SCA3 (Laco *et al.*, 2012b). As damaged mitochondria will not be able to scavenge free radicals and prevent cell energy impairment as effectively, this process may therefore further increase oxidative stress in the cell. Oxidative stress is then able to interfere with vital cellular functions, potentially resulting in activation of apoptosis or excitotoxicity, two of the main causes of neuronal death (Emerit *et al.*, 2004).

Above described findings indicate that, like other polyQ disorders, defects in the cellular defence mechanism against oxidative stress could play a role in the pathogenesis of SCA3.

Transcriptional deregulation

Since ataxin-3 has DNA-binding properties and interacts with transcriptional regulators, transcriptional deregulation has been suggested to play a central role in the SCA3 pathogenesis (Riley and Orr, 2006). In SCA3 and other polyQ disorders, transcription factors, together with polyQ proteins, are sequestered into nuclear aggregates, resulting in deregulation of their function as transcriptional co-repressor or activator (Perez *et al.*, 1998; van Roon-Mom *et al.*, 2005). Transcription of genes involved in inflammatory processes, cell signalling, and cell surface-associated proteins were found to be altered in SCA3 cell and mouse models, suggesting transcriptional deregulation in SCA3 (Evert *et al.*, 2001; Evert *et al.*, 2003; Chou *et al.*, 2008). Likewise, some corresponding proteins like MMP-2, amyloid-β precursor protein (APP) and interleukins were found to be significantly increased in SCA3 patient brain material (Evert *et al.*, 2001). However, thus far no gene expression studies have been performed on SCA3 patient material to replicate above described findings.

Ataxin-3 was shown to inhibit histone acetylase activity. When mutated, this inhibition of histone acetylase is impaired, and increased acetylation of total histone H3 was indeed observed in mutant ataxin-3 overexpressing cells and human SCA3 brain material, resulting in an increase of transcription in SCA3 cells (Evert *et al.*, 2006). This transcriptional upregulation was supported by the discovery that in cells overexpressing mutant ataxin-3, MMP-2 was found upregulated (Evert *et al.*, 2003).

Although in SCA3 changes in gene expression have not been as extensively studied as the impaired protein degradation, the discovery of altered transcription of many genes suggests a role of transcriptional deregulation in SCA3 pathogenesis.

Loss of wild-type ataxin-3 function

Although the ataxin-3 protein has been well studied, it is still uncertain to what extent ataxin-3 is an essential protein for normal cellular functioning. In support of an essential role for ataxin-3, depletion of ataxin-3 using small-interference RNA (siRNA) in cultured non-neuronal human and mouse cells resulted in accumulation of ubiquitinated material in the cytoplasm, cytoskeletal disorganisation, loss of cell adhesion and increased cell death (Rodrigues *et al.*, 2010). Likewise, knock-out of ataxin-3 was found to result in lower levels of stress-induced chaperone proteins in mouse brain, proposing an significant role for ataxin-3 in cellular homeostasis (Reina *et al.*, 2012). Other evidence however suggests that ataxin-3 is not necessary for normal cellular functioning. First, ataxin-3 knock-out in *C. elegans* did not alter the lifespan (Rodrigues *et al.*, 2007), and remarkably resulted in resistance to stress (Rodrigues *et al.*, 2011). In mice, local knock-down of endogenous ataxin-3 in the striatum for 2 months did not show any toxicity (Alves *et al.*, 2010). Likewise, ataxin-3 knock-out mice, loss of ataxin-3 did not affect viability or fertility (Schmitt *et al.*, 2007; Boy *et al.*, 2009; Switonski *et al.*, 2011). However, these mice did show a mild behavioural phenotype with increased anxiety, as well as increased levels of ubiquitinated proteins, particularly in cells that are known to express high levels of ataxin-3 in wild-type mice (Schmitt *et al.*, 2007). Furthermore, ataxin-3 has also been proposed to serve as a neuroprotectant, since in flies expressing mutant polyQ proteins overexpression of ataxin-3 was found to alleviate neurodegeneration (Warrick *et al.*, 2005). In contrast, double transgenic mice, co-expressing mutant and wild-type ataxin-3, did not show any phenotypic improvement as compared to single transgenic SCA3 mice, suggesting that ataxin-3 may not act as neuroprotectant (Hubener and Riess, 2010)

Whilst absence of ataxin-3 thus does not appear to be directly detrimental to cellular vitality in most studies, the subtle phenotypes observed in rodent ataxin-3 knock-out models and the fact that ataxin-3 contains several well conserved regions amongst different species (Albrecht *et al.*, 2003) indicate that the protein may not be completely dispensable.

1.5. Clinical and molecular genetics of other polyQ disorders

Spinal and bulbar muscular atrophy

SBMA is X-linked and females typically exhibit a reduced pathology (Banno *et al.*, 2012). Next to lower motor weakness, males affected by SBMA suffer from muscle cramps, gynecomastia with abdominal obesity, and progressive loss of libido (Katsuno *et al.*, 2012). There is marked degeneration of anterior horn cells, bulbar neurons, and dorsal root ganglion cells (Orr and Zoghbi, 2007). Patients with 40 or more CAGs in the first exon of the *AR* gene will develop SBMA (La Spada *et al.*, 1991).

The AR protein is a well characterized nuclear hormone with the polyQ repeat located in its N-terminal transactivation domain. Next to this transactivation domain, the AR contains a DNA binding domain and an androgen binding domain. Binding of android to the AR in the cytoplasm results in translocation into the nucleus, where it dimerizes and subsequently stimulates transcription of androgen responsive genes. AR is essential for male foetus development, male sexual characteristics and spermatogenesis maintenance (Brinkmann, 2011). The main pathological mechanisms leading to SBMA are altered protein-protein interactions and transcriptional deregulation. Intranuclear aggregates have been found to sequester AR binding partners (Beitel *et al.*, 2013). Other known polyQ gain of function mechanisms like mitochondrial deregulation, autophagy, and impaired transport were also suggested to be involved in SBMA (Beitel *et al.*, 2013).

Spinocerebellar ataxia type 1

SCA1 is clinically characterized by dysphagia, oculomotor disturbance, pyramidal and extrapyramidal disease signs, sensory deficits as well as mild cognitive decline (Sasaki *et al.*, 1996). SCA1 is caused by a repeat expansion of 39 or more CAGs in the first coding exon (exon 8) of the *ATNX1* gene, resulting in severe cerebellar and brain stem atrophy (Orr *et al.*, 1993). In healthy individuals, when the repeat is longer than 21 CAGs, it is interrupted by one to three histidine-encoding CAT triplets. Loss of one of these CAT codons results in an uninterrupted CAG repeat which is instable upon transmission (Menon *et al.*, 2013). There is a clear inverse correlation between the pure CAG repeat number and the age of onset (Menon *et al.*, 2013). Patients with 70 or more CAG repeats will develop a juvenile form of SCA1 (Donato *et al.*, 2012).

The function of the ataxin-1 protein is largely unknown, although various domains and phosphorylation sites have been identified that are involved in protein-protein interactions, cellular localisation and stability (Chen *et al.*, 2003; La Spada and Taylor, 2010). Ataxin-1 is able to translocate from the cytoplasm to the nucleus where it can interact with various transcription factors (Orr, 2012). Mutant ataxin-1 can still translocate to the nucleus, but transport back to the cytoplasm is impaired (Irwin *et al.*, 2005).

Spinocerebellar ataxia type 2

Compared to SCA1, patients with SCA2 show slower eye movements and more pronounced hyporeflexia and tremor (Giunti *et al.*, 1998). SCA2 is characterized by olivopontocerebellar, spinal and cortical atrophy (Geschwind *et al.*, 1997a). SCA2 is caused by a CAG repeat expansion in the first exon of the *ATXN2* gene which is translated into an expanded polyQ containing ataxin-2 protein (Imbert *et al.*, 1996). The CAG repeat is interrupted by one or two CAA triplets and loss of one of the CAA triplets makes the repeat very unstable upon transmission to the next generation. SCA2 is an unique polyQ disorder as it does not show reduced penetrance. Patients with 32 or more CAGs will develop SCA2, whereas individuals with 31 do not (Magana *et al.*, 2013).

Though no reduced penetrance has been reported for SCA2, an expansion between 27 to 33 CAGs in ATXN2 has been associated with sporadic and familial amyotrophic lateral sclerosis (ALS). In these cases, an altered interaction between ataxin-2 and the ALS related TAR DNA-binding protein (TARDBP) is thought to result in cytoplasmic aggregations in neurons derived from ALS patients (Elden *et al.*, 2010). The ataxin-2 protein is thought to be involved in transcriptional regulation via its interaction with mRNA metabolism complexes (Orr, 2012).

Spinocerebellar ataxia type 6

SCA6 is a slow progressing pure cerebellar ataxia with mainly cerebellar atrophy mild peripheral neuropathy (Schols *et al.*, 1998). Patients show pronounced oculomotor disturbance and problems with the vestibulo-ocular reflex (Yabe *et al.*, 2003). SCA6 is the only non-fatal polyQ disease, probably because the brain stem is not affected (Zhuchenko *et al.*, 1997; Geschwind *et al.*, 1997b). The CAG repeat located in the 3'UTR of the *CACNA1A* gene on chromosome 19p13 was found when mapping the gene responsible for familial hemiplegic migraine (FHM) and episodic ataxia type-2 (EA-2) (Ophoff *et al.*, 1996). SCA6 is the result of an expansion of 20 till 33 CAG repeats, usually located in the 3'UTR of the *CACNA1A* gene (Riess *et al.*, 1997). However, in SCA6 alternative splicing leads to an alpha 1A subunit of the voltage-dependent P/Q type calcium channel ($Ca_v2.1$) isoform containing the toxic polyQ repeat at its C-terminus. This alternative splicing disrupts the reading frame at the 3' end of the CACNA1A transcript due to a GGCAG pentamer read-through at the intron 46 and exon 47 boundary (Tsunemi *et al.*, 2008).

The pathogenic polyQ expansion in the encoded C-terminus of $Ca_v2.1$ is by far the smallest of all polyQ disorders and within the range of normal repeats in other polyQ disease-causing proteins. $Ca_v2.1$ is highly expressed in the cerebellar cortex and is expressed in only a few neuronal specific cell types. The pathology of SCA6 is thought to be a straightforward channelopathy, although SCA6 knock-in mice, which displayed aggregation of mutant $Ca_v2.1$, did not show an electrophysiological phenotype, suggesting that the polyQ repeat itself does not affect the intrinsic electrophysiological properties of the channels (Watase *et al.*, 2008). Proteolytic processing is implicated in disease pathogenesis, because C-terminal fragments and cytoplasmic protein aggregates have been reported in SCA6 *post-mortem* brain tissue (Ishikawa *et al.*, 1999; Kubodera *et al.*, 2003).

Spinocerebellar ataxia type 7

Next to ataxia and dysarthria, the clinical presentation of SCA7 consists of oculomotor disturbance, pyramidal disease signs, and visual loss due to pigmentary retinopathy (Enevoldson *et al.*, 1994). This clinical presentation resulting from the olivopontocerebellar atrophy is highly variable and depends on the length of the CAG repeat in exon 3 of the *ATXN7* gene (David *et al.*, 1997). Individuals with 36 or more CAG repeats will certainly develop the disease around midlife and in the case of more than 100 repeats the disease manifests itself in infancy or early childhood (van de Warrenburg *et al.*, 2001). Intermediate alleles of 28 to 35 CAG repeats are meiotically unstable and were shown to result in pathological repeat lengths after paternal transmission (Stevanin *et al.*, 1998).

The ataxin-7 protein is part of various transcription regulating complexes, where it functions as transcriptional repressor via histone acetylation (Strom *et al.*, 2005). The pathogenic role of expanded ataxin-7 is still not exactly known and expanded ataxin-7 overexpression systems showed conflicting results on its histone acetylation activation (Martin, 2012). Although its gain of function mechanism is thus far unidentified, proteolytic cleavage and entrapment of truncated and full-length ataxin-7 in nuclear aggregates are part of the disease process (Holmberg *et al.*, 1998; Garden *et al.*, 2002).

Spinocerebellar ataxia type 17

SCA17 was the last identified polyQ disorder. In SCA17 patients the repeat size correlates with clinical characteristics; patients with 43 to 50 repeats display a reduced penetrance and show an HD-like phenotype (Rolfs *et al.*, 2003), patients with 50 to 60 Qs show intellectual disability, dystonia and pyramidal signs, whereas patients with over 60 Qs have early childhood onset with rapid progression (Cloud and Wilmot, 2012). The expanded CAG repeat, interspersed by CAAs, is located in exon 3 of the *TBP* gene (Nakamura *et al.*, 2001). Because the CAG repeat is interrupted by CAA codons, the expanded repeat is quite stable upon inheritance, and anticipation is rare in SCA17.

The expanded mixed repeat encodes a polyQ expansion in the transcription initiation factor TBP. TBP has the longest pure glutamine stretch in the healthy human proteome and can contain up to 42 Qs. An homozygous expanded polyQ repeat in TBP does not impair normal function during development, ruling out loss of function in SCA17 (Zuhlke *et al.*, 2003; Toyoshima *et al.*, 2004). Although transcriptional deregulation has been suggested, the exact mechanism by which expanded TBP cause neurotoxicity is not yet known (Friedman *et al.*, 2008).

Dentatorubro-pallidoluysian atrophy

DRPLA is characterized by progressive ataxia, dementia, choreoathetosis, myoclonus, and epilepsy (Naito and Oyanagi, 1982). It is caused by an expanded CAG repeat in exon 5 of the *atrophin-1* (*ATN1*) gene, resulting in degeneration of the dentatorubral and pallidoluysian systems of the central nervous system (CNS) (Naito and Oyanagi, 1982). Patients with a repeat of 49 or more will develop symptoms (Nagafuchi *et al.*, 1994). Patients with a repeat number of 65

or more will develop myoclonic epilepsy during childhood, whilst infantile onset with severe atrophy was reported in patients with more than 90 CAGs (Shimojo *et al.*, 2001).

Although the exact function of atrophin-1 is still unknown, it was suggested to act as transcriptional co-repressor (Zhang *et al.*, 2002). Mutant atrophin-1 is prone to proteolytic cleavage and N-terminal fragments accumulate in nuclei of neurons (Nucifora, Jr. *et al.*, 2001). This transcriptional deregulation is thus far the only pathogenic mechanism proposed to contribute to the neurodegeneration in DRPLA.

1.6. Protein lowering approaches for polyQ disorders

Most therapeutic strategies for polyQ diseases under investigation are targeting one of the many altered cellular processes caused by toxic mutant polyQ protein. To date, several clinical trials with small patient numbers have been carried out for polyQ disorders as symptomatic treatment to reduce depression, chorea, parkinsonian phenotype, restless leg syndrome, and sleepiness (Ogawa, 2004; Bettencourt and Lima, 2011; Scott, 2011). Clearly, there is demand for polyQ disorder therapies directed at preventing or slowing the progression of neurodegeneration. Targeting a single cellular process might be inadequate to be clinically beneficial. A more effective approach would be to reduce the expression of the mutant gene and thereby inhibiting all downstream toxic effects. Since polyQ disorders are monogenic and are the result of a gain of toxic polyQ protein, reducing the expression of the CAG repeat expansion containing gene should ideally halt the disease progression. However, for most of the polyQ disorders, the exact function and importance of the polyQ-containing protein is not fully understood, and therefore specific lowering of the mutant polyQ protein levels, leaving wild-type levels unchanged, would be favoured over a generic downregulation (Miller *et al.*, 2003; Rodriguez-Lebron and Paulson, 2006). For instance, TBP haploinsufficiency was already shown to cause cognitive deficits in mice, indicating that complete knockdown of TBP cannot be used as potential therapy for SCA17 (Rooms *et al.*, 2006).

For SCA2 and SCA17, no reports are available that use oligonucleotide-mediated modulating therapeutics as potential treatment, although if there would be therapies existing for these disorders, rodent models that nicely mimic phenotypic characteristics, are available to test these protein lowering strategies (Kelp *et al.*, 2013; Magana *et al.*, 2013). For the remaining polyQ disorders, there have been reports on protein lowering strategies, which will be shortly outlined below. I will first in short describe the basic principles of oligonucleotide-mediated therapies. Next I will focus on studies showing non-allele-specific lowering of total polyQ protein levels (**Figure 3a and b**), followed by different approaches for allele-specific lowering of mutant polyQ proteins (**Figure 3c**), than oligonucleotide-mediated modulating therapeutics targeting the common denominator of polyQ disorders, being the expanded CAG repeat (**Figure 3d**), and finally I will discuss lowering polyQ protein levels by targeting its binding partner.

Basic principles of antisense oligonucleotide-mediated therapies

Oligonucleotide-mediated therapies are widely used to manipulate the expression of specific disease-causing genes, as well as modulating splicing to rescue protein expression. Nowadays, there are many types of nucleic acid molecules that can interfere at the RNA level, such as double stranded RNAs (siRNAs, short hairpin RNAs (shRNA), and microRNAs (miRNA or miR)) (Maxwell, 2009) or single stranded RNAs (single-stranded silencing RNA (ss-siRNA)) (Yu *et al.*, 2012), that promote selective degradation of homologous cellular mRNAs through the RNA-induced silencing complex. In this thesis I will mainly focus on antisense oligonucleotides (AON), which are small pieces of modified RNA or DNA that can hybridize to RNA. They can

generate different effects depending on the AON chemistry and target site (**Figure 3 and 4**).

Initially, AONs were used to induce gene knockdown (Dias and Stein 2002). This can be achieved through RNase H, a ubiquitous enzyme that cleaves RNA:RNA or RNA:DNA hybrids. The AONs used for this application are generally modified with a phosphorothioate (PS) backbone, which increases AON stability and enhances uptake of the AON across cell membranes. AONs modified further containing DNA molecules with 2'sugar moieties at the wings (DNA gapmers) will, upon binding to target mRNA, recruit RNase H to this RNA:DNA heteroduplex, resulting in cleavage and degradation of the target by nucleases (Wu *et al.*, 2004) (**Figure 3a**).

Suppressing RNA translation into protein is also achieved by AONs targeting the translation start site by sterically blocking the binding of RNA binding protein complexes, such as ribosomal subunits (Kole *et al.*, 2012) (**Figure 3b**). Here, AONs can be modified further to render them RNase H resistant by addition of a methyl (Me) or methoxyethyl (MOE) group to the 2'O sugar ribose, which is the target cleavage site of the RNase H enzyme. The 2' sugar PS AONs targeted at pre-mRNA splicing elements can also block the access of proteins involved in the splicing machinery, causing exon skipping or inclusion (**Figure 4**).

Alternatively, nucleotides have been modified even further, e.g. using phosphorodiamidate morpholino oligomers (PMO), peptide nucleic acids (PNA) or locked nucleic acids (LNA). PMOs have been widely used for developmental studies in zebrafish embryos (Nasevicius and Ekker 2000; Nasevicius *et al.*, 2000). Multiple RNase H-dependent AONs are in clinical trials including one against high-grade glioma in phase IIb (trabedersen (Bogdahn *et al.*, 2011), and one has even been registered as a drug for cytomegalovirus induced retinitis (vitravene) (Marwick 1998).

Lowering total polyQ protein levels

For HD, various synthetic oligonucleotides with different modifications and backbones have been used in rodents to lower htt expression (Sah and Aronin, 2011). A partial reduction of 25 to 35% of both normal and mutant htt by using shRNAs was well-tolerated in wild-type rats up to 9 months without signs of toxicity or striatal degeneration (Drouet *et al.*, 2009). Non-allele-specific reduction of htt transcripts up to 75% by using shRNAs (McBride *et al.*, 2008; Boudreau *et al.*, 2009; Grondin *et al.*, 2012) and chimeric MOE PS AONs (**Figure 3b**) (Kordasiewicz *et al.*, 2012) was found to be well tolerated in HD rodents and non-human primates. Intracerebroventricular (ICV) infusion of MOE PS AONs in transgenic HD mice for two weeks targeting both the human HTT transgene and endogenous murine htt resulted in reduced toxicity, extended survival, and improved motor performance up to 3 months post treatment (Kordasiewicz *et al.*, 2012). Interestingly, the observed phenotypic improvement was comparable to the mice who were treated with exclusively the human HTT-specific AON, suggesting that the therapeutic reversal is caused by total lowering of htt protein levels (Kordasiewicz *et al.*, 2012). Since htt lowering strategies will be most beneficial for patients when administered over many years, the long-term safety needs to be assessed.

Reducing AR protein expression using siRNAs was shown to reduce truncated mutant AR-induced toxicity in mutant AR overexpressing *D. melanogaster* and human cell models of SBMA (Caplen *et al.*, 2002). However, no follow-up studies have been published since showing

an *in vivo* effect of reduced AR protein expression levels.

In a transgenic mouse model of SCA1, it also has been shown that ataxin-1 is an essential protein for cellular functioning (Burright *et al.*, 1995). Depletion of endogenous ataxin-1 resulted in learning deficits and decreased hippocampal paired-pulse facilitation. This suggests that complete knockdown of ataxin-1 is not favourable (Matilla *et al.*, 1998). The first attempt to use oligonucleotides as treatment for SCA1 was performed in a SCA1 transgenic mouse model, where injection of lentiviral shRNAs into the cerebral ventricles resulted in reduced mutant ataxin-1 protein expression, causing improved neuropathology and motor coordination (Xia *et al.*, 2004). Silencing of mutant ataxin-1 *in vivo* was also achieved with miRNAs (Keiser *et al.*, 2013). However, these shRNAs or miRNAs are uniquely attacking the transgenic human 82 CAGs-containing *ATXN1* gene, whereas the endogenous ataxin-1 is left untouched, limiting its value as a model for the human intervention where all the ataxin-1 protein will probably be affected.

As potential gene silencing treatment for SCA3, non-allele-specific downregulation of all ataxin-3 transcripts has been tested in both wild-type and SCA3 rats (Alves *et al.*, 2010). Striatal knock-down of endogenous ataxin-3 by injection of lentiviruses encoding shRNAs into the brain of wild-type rats did not show any toxicity (Alves *et al.*, 2010). Interestingly, in SCA3 rats, this non-allele-specific silencing of ataxin-3 in the striatum for a 2 month period resulted in locally reduced neuropathology (Alves *et al.*, 2010).

Lowering specifically mutant polyQ protein

Suppression of human mutant htt by 50% to 80%, for 4 months in transgenic rodent models of HD (expressing one human mutant htt and two wild-type murine htt transcripts) was found to improve motor and neuropathology abnormalities and prolonged longevity in HD mice (Harper *et al.*, 2005; Wang *et al.*, 2005). These studies showed that allele-specific lowering mutant htt without reducing wild-type htt levels, result in an improved pathology. Various studies have shown that a pronounced decrease of mutant htt levels with only minor reduction in wild-type htt is feasible using allele-specific oligonucleotides (Krol *et al.*, 2007; van Bilsen *et al.*, 2008; Hu *et al.*, 2009b; Lombardi *et al.*, 2009; Pfister *et al.*, 2009; Carroll *et al.*, 2011). One way to design a molecule that can distinguish between the wild-type and polyQ disease-causing allele is to target a single nucleotide polymorphism (SNP) that is unique to the mutant transcript (Miller *et al.*, 2003). SNPs are DNA sequences in which a single nucleotide is different between the two alleles of a gene. The first study showing allele-specific silencing in HD using SNP-specific siRNAs was obtained in human cells overexpressing an additional copy of HTT containing the targeted SNP (Schwarz *et al.*, 2006). The first proof of principle of endogenous mutant htt silencing using this approach was shown in fibroblasts derived from HD patients (van Bilsen *et al.*, 2008). Next to siRNAs, SNP-targeting RNase H-dependent AONs (**Figure 3c**) were shown to allele-specifically reduce mutant htt expression in patient-derived cells and a humanized HD mouse model (Carroll *et al.*, 2011; Ostergaard *et al.*, 2013). Subsequent genotyping revealed a group of 22 SNPs that are highly associated with mutant htt alleles in a European HD cohort (Warby *et al.*, 2009). Since then, various groups have shown that the vast majority of the HD

patient population could be treated in this way using 5 (75% of HD patients) or 7 (85% of the HD patients) different siRNAs (Lombardi *et al.*, 2009; Pfister *et al.*, 2009). The most promising SNP is located in exon 67 of the *HTT* gene. This SNP is strongly associated with the mutant allele while 48% of the total Western HD population was heterozygous at this site (Pfister *et al.*, 2009). Although the allele specificity obtained from above described SNP targeting siRNAs are very promising, there are some limitations. The diversity of SNPs within patient populations would make it necessary to develop multiple oligonucleotides. Furthermore, for HD patients that do not exhibit heterozygosity at any of the most frequent SNPs this approach is not applicable.

A cre-recombinase conditional knock-out SCA1 mouse model proved that removal of mutant ataxin-1 at an early stage of the disease results in clearance of nuclear inclusions and reversal of disease symptoms (Zu *et al.*, 2004). To date, there is only one report on allele-specific silencing of mutant ataxin-1 by targeting a heterozygous SNP. Using SNP-specific siRNAs in SCA1 patient-derived fibroblasts, only a moderate reduction of the mutant ataxin-1 transcript was achieved, whereas the normal ataxin-1 allele was also somewhat reduced (Fiszer *et al.*, 2012).

Whilst absence of ataxin-3 does not appear to be directly detrimental to cellular vitality in most studies, subtle phenotypes were observed in rodent ataxin-3 knock-out models (Schmitt *et al.*, 2007; Boy *et al.*, 2009; Switonski *et al.*, 2011). The fact that ataxin-3 contains several well conserved regions amongst different species (Albrecht *et al.*, 2003), together with its important function in protein degradation, transcription and possibly DNA repair, suggests that a strategy which reduces mutant ataxin-3 protein toxicity, whilst maintaining wild-type ataxin-3 protein levels, would be a preferable approach for therapeutic application in SCA3. Allele-specific silencing was achieved using shRNAs directed against a SNP unique to the mutant ataxin-3 transcript (Alves *et al.*, 2008). This targeted SNP at the 3' end of the *ATXN3* gene was found to be present in over 70% of SCA3 patients (Gaspar *et al.*, 2001). The SNP-specific shRNA was able to specifically silence mutant ataxin-3 and was found to be neuroprotective in SCA3 mouse and rat models (Alves *et al.*, 2008; Nobrega *et al.*, 2013), thus showing good promise of allele-specific reduction for clinical implementation in SCA3 patients.

In the case of SCA6, complete removal of the $Ca_v2.1$ protein would probably result in cerebellar dysfunction due to Purkinje cell loss (Saito *et al.*, 2009). However, mice with one functional *CACNA1A* allele are phenotypically normal (Fletcher *et al.*, 2001). Therefore, an allele-specific, or even better, a specific reduction of the $Ca_v2.1$ isoform containing the toxic polyQ repeat at its C-terminus would be preferred. This splice isoform-specific knockdown of polyQ-containing $Ca_v2.1$ was performed *in vitro* in transiently transfected human cells using siRNAs, as well as in human neuronal cells using miRNAs targeting a specific sequence encoding the polyQ-containing C-terminus of $Ca_v2.1$ (Tsou *et al.*, 2011).

Recently, conditional knockdown of mutant ataxin-7, one month after onset of motor symptoms, resulted in reversal of aggregation and alleviated some behavioural deficits in a tamoxifen-inducible SCA7 transgenic mouse model (Furrer *et al.*, 2013). They concluded that a 50% downregulation of the mutant ataxin-7 protein expression already would show

major impact on the SCA7 phenotype. On the other hand, complete removal of the ataxin-7 homolog in *D. melanogaster* was shown to be lethal at the larval stage (Mohan *et al.*, 2014). Furthermore, knockdown of ataxin-7 in *D. melanogaster* resulted in reduced deubiquitinase activity, pronounced neurodegeneration, reduced locomotion, and decreased life span (Mohan *et al.*, 2014), suggesting that complete removal of ataxin-7 is not a proper strategy for SCA7. Thus far only one potential treatment for SCA7 showed to some extent an allele-specific reduction of mutant ataxin-7. Using shRNAs, a reduction of mutant ataxin-7 was achieved by targeting an expanded CAG repeat-linked SNP located in the last coding exon of ATXN7 (Scholefield *et al.*, 2009; Scholefield *et al.*, 2014). In a heterozygous wild-type and mutant ataxin-7 overexpressing cell model it was found that using this SNP-specific shRNA a 97% and 26% reduction of respectively mutant and wild-type ataxin-7 was achieved, which ameliorated the SCA7 phenotype (Scholefield *et al.*, 2009). However, in patient-derived fibroblasts this allele-specific reduction of mutant ataxin-7 transcript levels was less pronounced and was only found at very low doses of SNP-specific shRNAs (Scholefield *et al.*, 2014), questioning the allele-specificity of this particular small RNA, especially at higher dosage or of more realistic (less favourable) agent : target ratios.

PolyQ expansion-specific protein lowering

Another approach to achieve allele-specific silencing targets the common denominator of all polyQ disorders; their expanded CAG repeat (**Figure 3d**). Here selective silencing is either based on the hypothesis that there are structural differences between wild-type and mutant HTT mRNA, or based on the larger number of CAGs in the expanded repeat and subsequent more binding possibilities of CAG-targeting oligonucleotides. The first proof for allele discrimination by targeting the CAG repeat was achieved in HD human fibroblasts using an siRNA with 7 consecutive CUG nucleotides (Krol *et al.*, 2007). Further studies with CAG repeat targeting siRNAs showed a low selectivity for the mutant allele, making siRNAs unsuitable for CAG repeat-directed allele-specific silencing (Hu *et al.*, 2009b). Other chemical modifications and oligomers show much higher specificity for expanded CAG repeat transcripts. Single stranded PNAs, LNAs and 2OMePS AONs targeting CAG repeats (**Figure 3d**) have been used to specifically reduce expanded HTT transcripts *in vitro* in patient-derived fibroblasts (Hu *et al.*, 2009b; chapter 3). Other endogenous CAG repeat containing transcripts with important cellular functions were unaffected by the tested CUG oligonucleotides (Hu *et al.*, 2009b; chapter 3). To note, PNA selectivity was less pronounced in CAG repeat lengths (40 to 45 CAGs) that occur most frequently in the HD patient population. The allele-specific reduction with 2OMePS AONs and LNAs with 7-mer CUG repeats was more pronounced in the average HD CAG repeat length, making these 2OMePS AONs and LNAs more suitable for polyQ expansion-specific protein lowering.

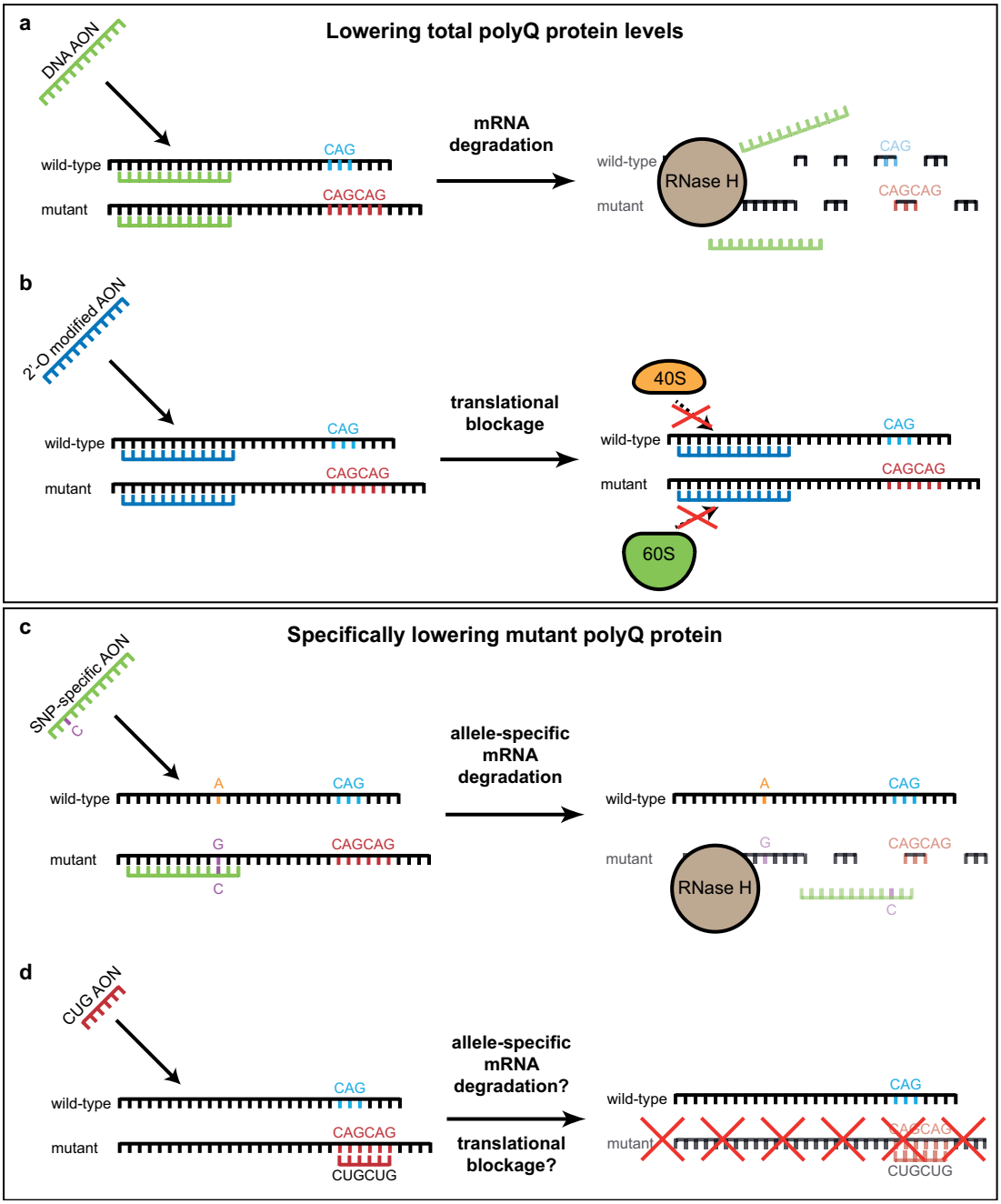

Figure 3. AON-mediated therapeutic approaches for lowering polyQ protein levels. Two different polyQ protein lowering strategies used for polyQ disorders are: 1) Lowering total polyQ protein levels by **(a)** using 2'-O-modified-phosphorothioate (PS) AONs blocking translation from both transcripts or **(b)** using (chimeric 2'-O-modified-PS) DNA AONs resulting in a RNA:DNA hybrid, which activates RNase H. RNase H will cleave the mRNA and prevents the translation into a protein. 2) Specifically lowering mutant polyQ protein by **(c)** targeting a unique heterozygous SNP linked to the mutant transcript and subsequently RNase H-induced cleavage of the mutant mRNA or **(d)** targeting the expanded CAG repeat by using CUG triplet AONs complementary to the CAG repeat, resulting in polyQ expansion-specific protein lowering.

Lowering polyQ protein levels by targeting its modulating partner

Next to targeting the (mutant) transcript directly, targeting binding partners to lower polyQ protein levels have been recently proposed as potential therapeutic intervention for various polyQ disorders. For SBMA, a possible approach to lower AR protein levels that does not directly target the AR, but targets a binding partner of AR, acts through miRNAs. Exploration of miRNA expression differences in the spinal cords of mice expressing full length wild-type AR and mutant AR resulted in the identification of upregulated miR-196a (Miyazaki *et al.*, 2012). This miR-196a regulated CUGBP Elav-like family member 2 (CELF2). CELF2 recognizes the AR exon 1-internal CUGCUGCUG sequence and by binding increases AR mRNA stability (Miyazaki *et al.*, 2012). Lentiviral miR-196a injection in the hind limb skeletal muscle of SBMA mice resulted in reduced levels of the polyQ-specific antibody 1C2-positive aggregate formation in the spinal cord and improved motor symptoms (Miyazaki *et al.*, 2012).

For SCA1, it was recently found that multiple components of the cell-signalling RAS–MAPK–MSK1 pathway influence ataxin-1 protein expression levels (Park *et al.*, 2013a). Pharmacological inhibition of this pathway was found to decrease ataxin-1 protein levels and knockout of MSK1 rescued both behavioural and pathological phenotypes in SCA1 mice (Park *et al.*, 2013a). These results suggest that components of this pathway are potential target for oligonucleotide-mediated lowering of mutant ataxin-1 protein levels.

In summary, most research has been performed on protein lowering treatments for HD and SCA1 and SCA3. Concerning the rarer polyQ disorders, less is known about the importance of the wild-type functions of polyQ proteins and the gain of toxic pathological mechanisms of the expanded polyQ proteins. For none of the polyQ disorders, much data is available elucidating the levels of mutant and wild-type transcript and protein present in the brain. Knowledge of wild-type and mutant polyQ protein levels are required to allow researchers to better assess the impact of non-allele-specific reduction of wild-type htt protein. Knowledge on these basal levels, together with better understanding of the significance of the polyQ protein for normal cellular functioning, will eventually define which protein lowering strategy to follow; an allele-specific or general reduction.

1.7. Antisense oligonucleotides in therapy for other neurodegenerative diseases

Like polyQ disorders, many other neurodegenerative diseases originate from a mutation in a single gene, resulting in a loss- or gain of one or more toxic functions, eventually initiating disease onset. There are several neurodegenerative disorders where the use of AONs is a promising therapeutic strategy. I will show some examples where AON treatment resulted in therapeutic benefit in animal models and/or clinical trials. In neurodegenerative diseases such as polyQ disorders, multiple sclerosis (MS), ALS and Alzheimer disease (AD), the aim of AON treatment can be to reduce transcript levels of disease-causing proteins. Alternatively, the deleterious allele can be reduced or knocked-out using allele-specific approaches or the mutated element can be eliminated by modulating pre-mRNA splicing events. The latter approaches are being followed for HD (chapter 4), SCA3 (chapter 5), and spinal muscular atrophy (SMA). In SMA, altering splicing can also be used to restore the expression of a gene or increase expression of a particular isoform.

Prevent translation of mutant protein in neurodegenerative diseases

ALS is a progressive neurodegenerative disorder caused by degeneration of motor neurons in the brain and spinal cord. This eventually leads to muscle weakening, twitching, and an inability to move the arms, legs, and body (Al-Chalabi and Leigh, 2000). Only 5% of ALS cases are familial and about 20% of all familial cases result from a specific genetic defect that leads to mutation of the enzyme known as superoxide dismutase 1 (SOD1) rendering the protein toxic and prone to aggregation (Bossy-Wetzel *et al.*, 2004). The AONs that have been used in ALS were designed to lower mRNA levels of the SOD1 transcripts and were PS modified chimeric nucleotides with five MOE modifications on both the 5′ and 3′ ends and 10 deoxynucleotides in the center to support RNase H activity. Continuous ventricular infusion reduced levels of mutant SOD1 in a rodent model of ALS and significantly slowed disease progression (Smith *et al.*, 2006). A phase I study to test the safety of this AON in subjects with familial ALS with a SOD1 mutation showed no serious adverse side effects after intrathecal injection into the CSF (Miller *et al.*, 2013).

MS is an autoimmune disease of the CNS where multifocal infiltration of autoreactive T lymphocytes across the blood brain barrier (BBB) takes place. Lymphocytes in MS patients display high levels of α-4 integrin on their surface (Cannella and Raine, 1995) and this plays an important role in lymphocyte migration to sites of inflammation (Rose *et al.*, 2007). Decreasing leukocyte trafficking into various organs has been successful using monoclonal antibodies against α-4 integrin (Lobb and Hemler, 1994). In a commonly used mouse model of MS, the experimental autoimmune encephalomyelitis model, AON-induced blocking of α-4 integrin expression reduced the incidence and severity of paralytic symptoms (Myers *et al.*, 2005). The 20-mer AONs with MOE modifications and a PS backbone were designed to target a sequence just 3′ of the translation start site of the murine α-4 integrin mRNA to block its translation.

Subcutaneous daily injections reduced α-4 integrin surface expression. Although the site of actions of this particular AON is unknown, it is thought that α-4 integrin levels are reduced in peripheral lymphoid tissue and this prevents trafficking of activated mononuclear cells into brain and spinal cord (Myers *et al.*, 2005).

AD is the most common form of dementia, in which AONs are considered in yet another mode. Cleavage of amyloid β precursor protein (APP) at the β-secretase and γ-secretase site causes elevated levels of β-amyloid peptide (Aβ). This is considered a key event in the pathogenesis of AD (Van Broeck *et al.*, 2007). Point mutations near the β-secretase site in the human gene for APP lead to a dominantly inherited form of AD (Selkoe and Kopan 2003). In a transgenic mouse model of AD containing this mutated β-secretase site, translation of the APP-mRNA was blocked by AONs that bind specifically to the mutated β-secretase site. The AONs used in this study had a MOE group and capped at 5'- and 3'-ends with a PS backbone. Repeated injections into the third ventricle (once a week for 4 weeks) reduced the levels of toxic Aβ and increased the levels of soluble α-cleaved APP indicating that this could be a possible strategy to treat familial AD (Chauhan and Siegel, 2007).

Modulating pre-mRNA splicing neuromuscular diseases

Other AON applications that do not induce the lowering of transcript levels are gaining more interest. The best-known application is the manipulation of splicing. Using AONs that target splice sites or exonic/intronic inclusion signals, exons can be hidden from the splicing machinery, resulting in skipping of the target exon (**Figure 4**). This can have multiple applications, e.g. switching from one isoform to another, skipping an aberrantly introduced exon to restore the normal transcript, removing disease-causing mutations from genes, or introducing an out-of-frame deletion that results in knock down expression of a gene. The latter approach is an alternative approach to AON-induced knockout through RNAse H-dependent cleavage of RNA:DNA hybrids (Aartsma-Rus *et al.*, 2009).

The most advanced clinical application of exon skipping is the exclusion of an exon allowing the production of an internally deleted, partially functional protein. This has been extensively studied as a therapeutic approach for Duchenne muscular dystrophy (DMD). Protein restoration has been shown in patient-derived cell cultures and in animal models this led to a rescued phenotype (Aartsma-Rus *et al.*, 2006; Heemskerk *et al.*, 2009; Heemskerk *et al.*, 2010). The results in phase I and I/II clinical trials were very encouraging (Lu *et al.*, 2003; Alter *et al.*, 2006; van Deutekom *et al.*, 2007; Kinali *et al.*, 2009; Goemans *et al.*, 2011). Although the primary endpoint in a recently conducted phase III clinical trial was not reached (Flanigan *et al.*, 2014), a very clear phenotypical improvement in young children was seen (press release January 16th 2014, Prosensa Holding N.V.), indicating that exon skipping is successful in DMD patients.

Intron splicing silencers can also be targeted resulting in exon inclusion. This can be used to restore expression of a gene or inducing expression of a particular isoform. Here, the most prominent application is rescue of SMA by AON mediated stimulation of the expression of a functional homologue. SMA is an autosomal recessive neuromuscular disorder caused by dysfunction and loss of motor neurons in the anterior horn of the spinal cord and lower brain

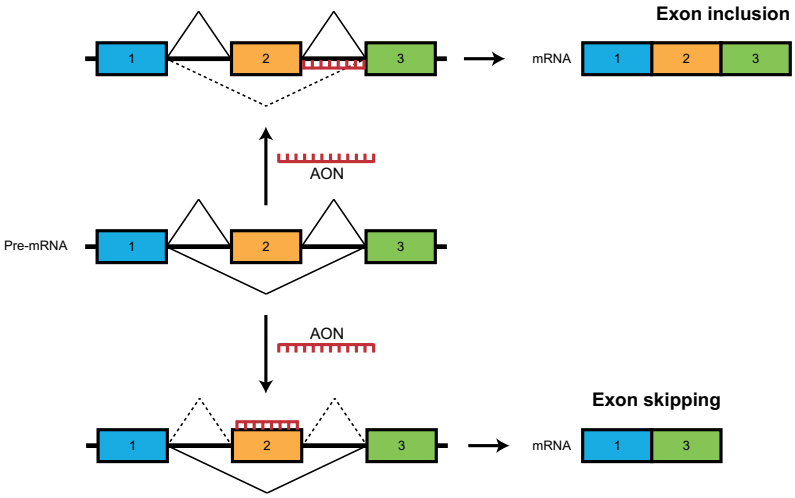

Figure 4. Schematic representation of anti-sense oligonucleotide-mediated modulation of pre-mRNA splicing. 2'OH modified RNase H-resistant or alternatively modified AONs complementary to the target pre-mRNA can result in: 1) inclusion of an exon by binding to the exonic splicing silencers (ESSs) or intronic splicing silencers (ISSs). 2) exclusion of an exon by binding to the 3' or 5' splice sites or exon-internal sequences, resulting in an in-frame transcript and translation of a shorter partly functional protein. Full lines indicate possible splicing events while dashed lines indicate non-possible events.

stem. The underlying cause of SMA is a homozygous deletion of survival motor neuron 1 (SMN1). SMN1 depletion is viable because of the presence of the almost identical *SMN2* gene. However, the majority of SMN2 mRNA transcripts lack exon 7, due to a silent mutation within this exon. This reduces the inclusion of exon 7 which results in a truncated protein and reduced expression of functional SMN protein (Lorson *et al.*, 2010). Current therapeutic strategies are aimed at modulation the splicing of SMN2 by blocking exonic splicing silencers (ESE) or intronic splicing silencers (ISS), thereby increasing exon 7 inclusion. Transfecting fibroblasts with an AON (termed ISS-N1) blocking an ISS in intron 7 of SMN2 was found to result in inclusion of SMN2 exon 7 (Singh *et al.*, 2006). Improved efficacy of the AON was achieved by incorporation of a uniform MOE chemistry and a single injection of this AONs into the cerebral ventricles in a severe mouse model of SMA showed increased exon 7 inclusion and SMN protein levels in the spinal cord resulting in increased muscle size and strength (Passini *et al.*, 2011). An increased exon 7 inclusion could also be achieved by targeting the 3' splice site region of exon 8 with 2OMe and PS backbone modified AONs (Lim and Hertel, 2001). These 2OMePS AONs were found to result in exon 7 inclusion and elevated SMN protein expression levels *in vivo* (Williams *et al.*, 2009; Hua *et al.*, 2010).

Recently, a phase I clinical trial has been completed evaluating the safety of a MOE-modified AON which aims at exon 7 inclusion and increased SMN protein levels (ClinicalTrials.gov, 2011). The so called ISIS-SMNRx was intrathecally injected in 4 increasing doses in children with SMA. In this open label safety tolerability dose-escalating study, the MOE-modified AON was well tolerated with no significant safety or tolerability findings after a single dose up to 9 mg. The intrathecal injection procedure was well tolerated and all SMA patients who participated completed the study. In the high dose treated patients, the SMN protein levels in the CSF more than doubled in the two highest dose cohorts and that those children continued to show increases in muscle function scores up to 14 months after a single injection of the MOE-

modified AON (Rigo *et al.*, 2012). Currently a phase II trial is ongoing with 6 mg or 12 mg doses of MOE-modified AON administered intrathecally on days 1, 15 and 85. The interim results reported that the MOE-modified AON was well tolerated (ClinicalTrials.gov, 2012).

1.8. Drug delivery to the brain, how to cross the blood brain barrier?

One major challenge of AON-mediated therapies for neurodegenerative disorders is delivery of the AON to the brain. In this paragraph I will describe in short the BBB function and how this impairs the uptake of peripherally administered drugs. I will focus in particular on the limitations and possibilities of AON delivery to the brain and specifically neurons, and will speculate on future clinical applications.

Blood Brain Barrier

A unique feature of the brain is that it is separated from the blood by the BBB. This is a monolayer of endothelial cells forming tight junctions through the interaction of cell adhesion molecules (Palmer, 2010). Astrocytes with their processes surrounding the endothelial cells, pericytes located between the endothelial cells and astrocytes, macrophages, and the basement membrane, form the other structural components of the BBB. Endothelial cells of the BBB are characterized by only few fenestrae and pinocytic vesicles, limiting transport to and from the brain. In this respect, it should be noted that the BBB also largely separates the immune system from the brain. Despite this gate-controlling system, essential nutrients, such as glucose, are permitted to pass (Bernacki *et al.*, 2008). In neurodegenerative diseases, including HD, disruption of the BBB is common (Tomkins *et al.*, 2007; Palmer, 2010). Interestingly, in animal models, this can even lead to neurodegenerative changes itself (Tomkins *et al.*, 2007).

The BBB has been already noticed in the work of Paul Ehrlich, Nobel Prize winning bacteriologist in the late 19th century. Injected dyes stained all organs except the brain and spinal cord. However, he did not attribute this phenomenon to the presence of a barrier but to dye characteristics. His student showed later that staining of the brain was possible when the dye was injected directly into the brain (Palmer, 2010). Subsequent studies using electron microscopy allowed to directly visualize the BBB.

While essential to protect the brain, the BBB is a major challenge in CNS drug development. When a drug is administered to the body, a fraction will be bound to proteins (e.g. serum albumin, lipoprotein etc.) and a fraction will be free. The free fraction is the pharmacologically relevant fraction, since it is, in principle, available to cross the BBB (Palmer, 2010), depending on its physiochemical properties. After crossing the BBB, the drug will enter the interstitial fluid and go to the target (proteins, receptors, transporters etc.). Subsequently, the interstitial fluid drains to the CSF, which is produced at a rate of 500 ml/day in humans, while the ventricle system can house only 100-150 ml. This means that there is a continuous dehydration as well, making up for at least a threefold CSF circulation, allowing a continuous drainage of the brain's interstitial fluid.

In the process of drug discovery, the aim is to find a substance which is potent, selective and preferably bioavailable. In addition, it needs to be able to cross the BBB, and reach the target at a sufficient concentration (Alavijeh *et al.*, 2005). The following mechanisms are available

to cross the BBB. The first one is simple diffusion. Small lipophilic substances which have a hydrogen bond are more likely to pass the BBB (Gerebtzoff and Seelig, 2006). The second mechanism is via active transport mediated by transporter molecules. The most well-known is glucose with its glucose transporter 1 (GLUT1), which is the most widely expressed of the GLUT family (13 isoforms) (Guo *et al.*, 2005; Palmer, 2010). Other carriers are for instance lactate and amino acids. A well-known drug transported via this way is levodopa (Cotzias *et al.*, 1967). The third mechanism to cross the BBB is via receptor-mediation. Receptor-mediated endocytosis allows macromolecules to enter the brain, such as transferrin, insulin, leptin, and insulin-like growth factor 1 (Pardridge, 2007).

Besides systemic mechanisms to cross the BBB, there are also techniques to bypass the BBB by direct infusions into the subdural space, the brain's ventricle system, or the brain parenchyma. These infusions can be single, repeated, or continuous depending on the methodology, using either simple or sophisticated pump systems. It is possible to use one probe or more probes for infusion. Using the subdural and ventricle compartments, diffuse delivery of the drug into the brain can be achieved, while using intraparenchymal delivery, a local, but well-targeted delivery can be realized.

When a substance has successfully entered the brain, there are mechanisms preventing adequate functioning. One mechanism is active transport to remove the substance, also known as resistance. A superfamily of multidrug resistance proteins, belonging to the adenosine triphosphate (ATP)-binding cassette transporters, drives substances out by an ATP-dependent process (Palmer, 2010). One of the most abundant proteins is the P-glycoprotein. This mechanism is responsible for the failure of some anticancer drugs. Another relevant family of egress transporters is the organic anion transporting proteins.

In the field of HD, efforts are ongoing to deliver innovative drugs to the brain via the systemic route and drugs are designed to use any of the three mechanisms to cross the BBB, as explained earlier. For instance, Lee and associates described the use of a peptide nucleic acid as an antisense which was able to access endogenous transferrin transport pathways (receptor mediated endocytosis) and reach the brain in a transgenic mouse model (Lee *et al.*, 2002). However, there are also efforts to bypass the BBB, and to deliver the drug using either the ventricle system or intraparenchymally.

Cellular delivery and associated safety of oligonucleotide-mediated therapeutics

In all instances of oligonucleotide-mediated therapeutics targeting the brain, delivery is an issue. *In vivo* manipulation of gene expression with shRNA very often depends on the use of viral vectors (Di Benedetto *et al.*, 2009; Ehlert *et al.*, 2010; Kubo *et al.*, 2010), as do cre-recombinase mediated gene excision (Kolber *et al.*, 2008) or gene overexpression models (Ulusoy *et al.*, 2010; Woldbye *et al.*, 2010). However, after reaching the brain, AONs are readily taken up by neurons, and are therefore independent of viral transduction of neurons (Kordasiewicz *et al.*, 2012). The ease of delivery of the present day modified AONs seems to be linked with a lack of any major adverse side effects, making AONs suitable candidates as potential treatment for the polyQ disorders.

Associated safety of oligonucleotide-mediated therapeutics

Delivery of viral vectors has been associated with toxicity in the brain, mainly depending on viral type used. For example, adeno-associated virus (AAV) vectors have been shown to induce neurotoxicity when delivered to the CNS (Ehlert *et al.*, 2010; Jayandharan *et al.*, 2011), although serotypes may differ in that aspect (Sanchez *et al.*, 2011). Other viral types, such as retrovirus, show milder toxicity, but they are not suitable for investigation of long term effects and due to their tropism for mitotically active cells have limits in the applicability to postmitotic neurons (Kaplitt *et al.*, 1998). Lentivirus causes less inflammatory and immune response, but still share the disadvantage that pre-existing immunity to parental wild-type virus may cause an accentuated immune response. Furthermore, toxicity could also be triggered due to the lack of dosage regulation of virally-mediated shRNAs since they tend to produce an all-or-nothing effect, particularly when cre-recombinase systems are used (Kolber *et al.*, 2008; Pfeifer *et al.*, 2001).

Although AONs have a longer half-life than, for instance, siRNAs (Smith *et al.*, 2006), eventually they are degraded allowing gene expression to return to basal levels, offering the possibility to discontinue treatment (Smith *et al.*, 2006). Obviously, in instances where long-term manipulation is the goal, viral delivery may be desirable (Hua *et al.*, 2010). The lack of viral vectors makes that AON administration allows better dosage control while reducing potential toxic effects (Smith *et al.*, 2006; Heemskerk *et al.*, 2010; Hua *et al.*, 2010). For 2′-O-modified-PS AONs only very mild toxicity has been reported, which did not interfere with their desired effects after delivery in the brain via the ventricles (Liebsch *et al.*, 1999; Hua *et al.*, 2010), or in cultured neuronal cells (Muller *et al.*, 2000). Although it has been shown that PS AONs can have an immunostimulatory effect via toll-like receptors, appropriate 2′-O modifications, such as 2OMe can suppress these effects (Robbins *et al.*, 2007; Hamm *et al.*, 2010; Ma *et al.*, 2011). It is important to mention that possible toxic and immunostimulatory effects of 2OMePS AONs may also be a function of dosage, concentration, or duration of treatment (Hua *et al.*, 2010).

Cellular delivery of AONs

Single stranded AONs have a very rapid uptake within minutes to hours (Pitts *et al.*, 2009; Ma *et al.*, 2011). A typical AON used to modulate splicing is negatively charged and has a PS backbone. There are diverse chemical modifications to strengthen binding to the target mRNA and to improve pharmacokinetics by reducing nuclease-induced degradation. Most chemistries have modifications of the 2′O sugar ribose (such as 2OMePS and MOE), which is the target cleavage site of the RNase H enzyme, and thus have increased resistance to degradation. Other oligonucleotide chemistries, such as PNAs, LNAs, PMOs, are even more resistant to nuclease degradation.

Conjugating arginine-rich peptides to 2OMePS and PMOs (PPMO) have been shown to improve cellular uptake (Moulton *et al.*, 2009; Jirka *et al.*, 2014). This is not required for neurodegenerative disorders when locally administered, since 2OMePS and MOE AONs are readily taken up by neurons and translocate to the nucleus where splicing events take place

(Kordasiewicz *et al.*, 2012; Zalachoras *et al.*, 2013). Furthermore, ICV injected PMOs resulted in increased SMN protein expression in the spinal cord and total brain of severe SMA mice (Mitrpant *et al.*, 2013). Nevertheless, these "naked" AONs do not cross the BBB and therefore need to be administered into the CSF.

Interestingly, a PPMO against ataxia-telangiecatasia causing out-of-frame splicing mutations did cross the BBB after intravenous injections (Du *et al.*, 2011). The PPMOs were widely distributed throughout the brain of wild-type mice (Du *et al.*, 2011). Although remarkable, thus far no follow-up studies have been published showing an *in vivo* restoration of normal splicing and protein production in ataxia-telangiecatasia mice. Unfortunately, two PPMOs are abandoned as therapeutic agent since repetitive intravenous bolus injections of PPMOs caused lethargy and weight loss in rats (Amantana *et al.*, 2007) and tubular degeneration in the kidneys of monkeys (Moulton and Moulton, 2010).

To conclude, most *in vivo* data on splicing modulation or protein reduction in brain disorders make use of MOE PS and as described in chapter 3 to 5, 2OMePS AONs. While AONs for use in the CNS cannot be administered systemically, they have excellent entry into cells once they passed the BBB. For several chemistries, it has been shown that local injection and distribution via the CSF seem to be devoid of any major toxicity, making these oligonucleotide chemistries suitable candidates as potential treatment for the polyQ disorders.

1.9. Scope and outline of the thesis

Although polyQ disorders are caused by CAG triplet repeat expansions in different genes, they all result in gain of toxic polyQ protein function and subsequently neurodegeneration. The polyQ disorders have a monogenic cause and thus far no therapies are available to delay the age of onset or slow the disease progression. Because of the well-defined nature of the primary mutation and its direct consequence on toxic polyQ protein function, reducing the expression of the CAG repeat expansion-containing gene should in principle contribute significantly to halting the disease progression. Therefore, much effort has been put in reducing the expression of the mutant gene and thereby inhibiting all downstream toxic polyQ effects. Preclinical results during the course of this PhD research using oligonucleotide-mediated therapies for polyQ disorders, particularly HD, look promising. Despite the fact that for several neurodegenerative disorders oligonucleotide-mediated therapies moved from preclinical to clinical testing, for polyQ disorders we are not there yet.

While much research has been done on the underlying polyQ disease mechanisms, knowledge on mRNA and protein regulation and expression levels are limited. In **Chapter 2**, htt expression levels in adult-onset HD and juvenile HD patient-derived fibroblasts and *post-mortem* brain are studied. Subtle differences in htt mRNA and protein expression between adult-onset and juvenile HD are described.

By targeting the polyQ-encoding transcripts, translation of mutant polyQ protein is reduced, inhibiting all downstream toxic polyQ effects. **Chapter 3** describes the reduction of polyQ disease-causing proteins by specifically targeting expanded CAG repeat transcripts. By targeting the common denominator of all polyQ disorders, using CUG triplet-repeat AONs, mutant polyQ transcript and protein levels in several polyQ disorders were found to be reduced.

Chapter 4 describes a novel therapeutic approach for HD through removal of cleavage motifs that are implicated in the formation of toxic htt polyQ fragments. In HD, expanded polyQ htt is known to undergo proteolytic processing, which results in toxic polyQ-containing htt protein fragments. Preventing the formation of these toxic polyQ htt fragments is achieved by AONs that induce exon skipping of HTT pre-mRNA. Thus by modifying the htt protein, cleavage motifs are removed and less toxic polyQ htt fragments are formed.

Chapter 5 describes the removal of the CAG repeat-encoding exon from SCA3-causing mutant ATXN3 pre-mRNA. This AON-mediated skipping results in the removal of the toxic polyQ repeat from the ataxin-3 protein. A modified ataxin-3 protein is formed that lacks the toxic polyQ repeat, but maintains important wild-type functions of the protein.

Chapter 6 provides a general discussion of the thesis, reviewing the main findings, followed by recent developments and its implications for the genetic therapies proposed in this thesis and finally discussing future perspective.

Melvin M. Evers [1,#]
Menno H. Schut [1,#]
Barry A. Pepers [1]
Melek Atalar [2]
Martine van Belzen [3]
Richard L. Faull [4]
Raymund A.C. Roos [5]
Willeke M.C. van Roon-Mom [1]

[#] Contributed equally to this work

[1] Department of Human Genetics, Leiden University Medical Center
[2] Galapagos B.V., Leiden
[3] Department of Clinical Genetics, Leiden University Medical Center
[4] Centre for Brain Research and Department of Anatomy with Radiology, University of Auckland, New Zealand
[5] Department of Neurology, Leiden University Medical Center

2

Making (anti-) sense out of huntingtin levels in Huntington disease

Neurobiology of Disease 2014, under review

2.1. Abstract

Huntington disease (HD) is an autosomal dominant neurodegenerative disorder, characterized by motor, psychiatric and cognitive symptoms. HD is caused by a CAG repeat expansion in the first exon of the *HTT* gene, resulting in an expanded polyglutamine tract at the N-terminus of the huntingtin protein. Typical disease onset is around mid-life (adult-onset HD) whereas onset below 21 years is classified as juvenile HD. While much research has been done on the underlying HD disease mechanisms, little is known about regulation and expression levels of huntingtin RNA and protein.

In this study we used a unique collection of human *post-mortem* HD brain tissue and fibroblast cells to investigate huntingtin mRNA and protein expression, as well as huntingtin antisense isoforms. In adult-onset HD brain samples, there was only a small but significant lower expression of mutant huntingtin mRNA compared to wild-type huntingtin mRNA, while protein expression levels were equal. Juvenile HD subjects did show a lower protein expression of mutant huntingtin compared to wild-type huntingtin protein. Additionally, in brain tissue we did not find any evidence for a reduced expression of huntingtin antisense with an expanded CTG repeat, as we showed HTTAS_v1 expression in a homozygous HD patient. Finally, we have identified a novel huntingtin antisense isoform and named it HTTAS_v2.2.

Our results highlight subtle differences in huntingtin RNA and protein expression with less mutant huntingtin mRNA, but equal wild-type and mutant huntingtin protein levels in adult-onset HD. In juvenile HD mutant huntingtin protein levels were lower compared with wild-type huntingtin. This indicates subtle differences in huntingtin protein expression between adult-onset and juvenile HD.

2.2. Introduction

Huntington disease (HD) is an autosomal dominant neurodegenerative disorder, characterized by motor, psychiatric and cognitive symptoms (Roos, 2010). HD is caused by a CAG repeat expansion in the first exon of the *HTT* gene on chromosome 4p16, resulting in an expanded polyglutamine (polyQ) tract at the N-terminus of the huntingtin (htt) protein. Carriers of 40 or more CAG repeats will develop HD, whereas people with 36 to 39 repeats show reduced penetrance (Kremer *et al.*, 1992; Losekoot *et al.*, 2013). The mean disease onset lies between 30 and 50 years of age (adult-onset HD). HD patients with onset below 21 years of age (juvenile HD), typically carry more than 55 polyQs (Roos, 2010). The major neuropathology in HD occurs in the striatum and cerebral cortex but degeneration is seen throughout the brain as the disease progresses (Vonsattel and Difiglia, 1998) and insoluble protein aggregates in the nucleus and cytoplasm of cells are a hallmark of the disease (Difiglia *et al.*, 1997).

Knowledge on regulation of htt RNA and protein expression is limited and inconsistent. Upregulation of mutant HTT mRNA translation in HD was suggested by interaction of the expanded CAG repeat with the MID1-PP2A complex (Krauss *et al.*, 2013). Upregulation of mutant HTT mRNA translation was also suggested by HTT antisense transcript regulation (Chung *et al.*, 2011). Two natural HTT antisense transcripts (HTTAS_v1 and v2) were identified at the HTT locus, of which HTTAS_v1 contains a CTG repeat. Overexpression of HTTAS_v1 resulted in reduced HTT transcript levels, whereas HTTAS_v1 knockdown increased HTT transcript levels (Chung *et al.*, 2011). Furthermore, in *post-mortem* HD brain no HTTAS_v1 with expanded CTG repeat could be detected. From these observations, it was suggested that HTTAS_v1 negatively regulated HTT transcript expression (Chung *et al.*, 2011). Contrasting, in patient-derived lymphoblasts, no CAG repeat-related effect on total HTT mRNA was observed (Lee *et al.*, 2013), suggesting that there is no difference in wild-type and mutant HTT RNA expression. To our knowledge, levels of wild-type and mutant htt RNA and protein in human HD tissue have not been assessed systematically.

In this study we have investigated htt mRNA and protein levels in a unique collection of human *post-mortem* HD brain tissue and fibroblasts. For *post-mortem* adult-onset HD brain tissue we detected a small, but significant, decrease in mutant HTT mRNA levels compared to wild-type HTT mRNA. Moreover, both brain tissue and fibroblasts from adult-onset HD patients did not show difference in wild-type and mutant htt protein expression levels. In contrast, juvenile HD fibroblasts and brain tissue showed a small, but significant, lower level of mutant htt protein compared to wild-type htt protein. Furthermore, similar HTTAS levels in (homozygous) HD and controls were found. Additionally, we identified a novel HTTAS isoform and named it HTTAS_v2.2.

2.3. Materials & Methods

Patient-derived fibroblasts and human brain samples

Fibroblasts derived from HD patients and controls were purchased from Coriell Cell Repositories, Camden, USA (**Table 1**). Fibroblasts were cultured at 37°C and 5% CO2 in Minimal Essential Medium (Gibco Invitrogen, Carlsbad, USA) with 15% heat inactivated fetal bovine serum (Clontech, Palo Alto USA), 1% Glutamax (Gibco) and 100 U/ml penicillin/streptomycin (Gibco).

Post-mortem human brain tissue was obtained from the Neurological Foundation of New Zealand Human Brain Bank in the Centre for Brain Research, University of Auckland, and the brain bank from the department of Neurology, Leiden University Medical Center. Tissue was obtained with the families full consent and with the ethical approval of the various institutional Ethics Committees. For a complete list of samples and corresponding clinical information, see **Table 2**.

Table 1. Patient-derived fibroblasts.

Name	CAG 1	CAG 2	Type	Age at Sampling	Age of Onset	Sex
GM02173	44	17	HD	52	NA	F
GM04022	44	18	HD	28	NA	F
GM04855	48	20	HD	11	26	M
GM04857	50	40	homozygous HD	23	28	F
GM04281	71	17	juvenile HD	20	14	F
GM05539	97	22	juvenile HD	10	2	M
GM09197	179	18	juvenile HD	6	NA	M
GM04204	18	17	control	81	NA	M

Samples ranked on CAG repeat size of the longest allele.
M: male, F: female, NA: not assessed.

CAG repeat sizing

Genomic DNA samples were isolated from patient-derived fibroblasts and human brain using the Wizard Genomic DNA Purification Kit (Promega) according to manufacturer's instructions and diluted to 50 µg/ml. The number of CAG repeats in the *HTT* gene was determined by PCR using primers "HD-1" and "HD-3" as described previously (Warner *et al.*, 1993), followed by fragment analysis on an ABI 3130 Automated Capillary DNA Sequencer (Applied Biosystems, Life Technologies Corporation, Carlsbad, USA). The exact PCR conditions are available on request. The 3' CAA and following CAG are not counted. For the polyQ repeat the CAA and CAG triplet are counted and the polyQ repeat is therefore 2 units longer than the CAG repeat size.

RNA and genomic DNA analysis

Post-mortem brain tissue was homogenized using ceramic MagNA Lyser beads (Roche, Mannheim, Germany) by grinding in a Bullet Blender (Next Advance, Averill Park, USA) according

Table 2. *Post-mortem* human brain tissue.

Name	CAG 1	CAG 2	Tissue	PMD	Grade	Age of Death	Age of Onset	Sex
HC103	40	19	MTG	11	1	41	35	M
HC105	42	15	MTG	9	1	67	47	F
HD166	42	17	FC	32	2	80	> 70	M
HC102	43	17	MTG	10	3	64	40	M
HC107	43	19	MTG	3	3	75	58	M
HD193	44	9	FC	18	3	68	44	M
HD188	44	16	FC	NA	3	64	44	M
HD195	44	22	FC	8.5	3	61	NA	F
HD159	47	17	FC	42	3	41	26	F
HC114	47	21	MTG	12	NA	53	30	F
HD192	52	18	FC	62	4	37	NA	M
HC104	53	18	MTG	15	3	40	15	M
HD86	84	17	FC/STR	20	3	20	16	F
HD29	84	20	FC	11	NA	11	8	F
H121	23	18	MTG	6	control	64	control	F

Samples ranked on CAG repeat size of the longest allele. MTG: middle temporal gyrus, FC: frontal cortex, STR: striatum, PMD: post-mortem delay (hours), Grade: neuropathological classification, M: male, F: female, NA: not assessed.

to manufacturer's instructions.

Total RNA was isolated from fibroblast cells and brain tissue using the Aurum Total RNA Mini Kit (BioRad, Hercules, USA), with an on-column DNase treatment for 30 min. RNA was eluted in 40 µl elution buffer and cDNA was synthesized from 1 µg total RNA using the Transcriptor First Strand cDNA Synthesis Kit with oligo (dT) primers at 55°C for 90 min (Roche).

PCR was performed using 1 µl cDNA or genomic DNA, 10x Expand High Fidelity buffer with 15 mM $MgCl_2$ (Roche), 200 µM dNTPs (Roche), 1 M Betaine (Sigma-Aldrich, St. Louis, USA), 15 pmol of both forward primer HttCAGFw: 5'- ATG GCG ACC CTG GAA AAG CTG AT -3' and reverse primer HttCAGRev: 5'- TGA GGC AGC AGC GGC TG -3' (Eurogentec, Liege, Belgium), 3 U Expand High Fidelity enzyme mix (Roche), and PCR grade water to a final volume of 30 µl. The PCR program started with a 2 min initial denaturation at 94°C, followed by 35 cycles of 15 sec denaturation at 94°C, 30 sec annealing at 60°C, 1 min elongation at 72°C, after which a final elongation step was performed at 72°C for 7 min.

PCR products were loaded on a 2% agarose gel diluted in Tris/Borate/EDTA buffer (TBE). DNA gel electrophoresis was performed for 1 hour at 100 V. Intensities of DNA bands were quantified using ImageJ software. Intensity of the HTT mRNA band was divided by the corresponding genomic DNA band to normalize for differences in PCR efficiency between wild-type and mutant HTT due to CAG repeat length.

SNP genotyping and SNP linkage by circularization (SLiC)

The procedure for SNPs rs362273 genotyping and SNP linkage by circularization on human brain tissue was adapted from Liu *et al.* (Liu *et al.*, 2008). One µg of DNase-treated total RNA, together with oligo (dT) primers, was used for cDNA synthesis using SuperScript III First-Strand Synthesis System (Invitrogen). To improve reverse transcription of long cDNA templates, 2 M Betaine and 0.6 M Trehalose (both Sigma-Aldrich) were added to the reaction mixture (Spiess

and Ivell, 2002). cDNA synthesis was performed at 42°C for 2.5 hours, followed by RNase H treatment at 37°C for 20 min. Next, 5 µl cDNA was used as template for long-range PCR and SLiC.

Taqman SNP assay

Quantitative PCR was performed using the LightCycler 480 II (Roche), according to manufacturer's instructions, using a mixture containing 45 ng cDNA, 1xTaqMan® Universal PCR Master Mix, no AmpErase®UNG (Applied Biosystems), 1xTaqMan® SNP Genotyping Assay (Applied Biosystems), and nuclease-free water (Ambion) in a 20µl reaction volume. ACTB (Applied Biosystems, cat#Hs99999903_m1) was included as reference gene. A standard curve was generated using pooled equal amounts of cDNA from all samples. Quantification of the dual-color hydrolysis of both allele-specific fluorescent reporter dyes, FAM ("G" allele) and VIC ("A" allele), was performed with the LightCycler® 480 SW 1.5.1 software using the 2nd derivative method, according to manufacturer's instructions.

HTT antisense determination

RNA isolation as described above. PCR was performed using 1.5 µl cDNA, 10x PCR buffer with 20 mM $MgCl_2$ (Roche), 200 µM dNTPs (Roche), 6 pmol primer, for HTTAS_v1, forward: 5'-CAC CGG GGC AAT GAA TGG-3', reverse: 5'- GTG CGG ATG GCA AGG ACA G -3'; and for HTTAS_v2.1/2.2, forward: 5'-GAA GGC GCG GGG CTC AAC-3', reverse: 5'- TGC AGT GCG GAT GGC AAG GA -3', 2 U FastStart Taq DNA Polymerase (Roche), 1 M ethylene glycol (Sigma-Aldrich, St. Louis, USA), and PCR grade water to a final volume of 30 µl. The PCR program started with a 3 min initial denaturation at 95°C, followed by 40 cycles of 10 sec denaturation at 95°C, 10 sec annealing at 60°C, 10 sec elongation at 72°C, after which a final elongation step was performed at 72°C for 7 min.

PCR products were loaded on a 3% TBE agarose gel and bands were extracted using the NucleoSpin Gel & PCR Clean-up kit (Machery Nagel, Düren, Germany). To identify the sequence of the novel HTTAS isoform, PCR products were cloned into a pGEM-T Easy vector (Promega) and analyzed by Sanger sequencing using a T7-specific forward primer.

Protein isolation

Fibroblasts were detached from the culture surface with a 0.5% Trypsin/EDTA solution. After washing twice with HBSS, cells were resuspended in 200 µl ice cold lysis buffer, containing 15 mM HEPES, pH 7.9, 200 mM KCl, 10 mM $MgCl_2$, 1% NP40, 10% glycerol, 20 µg/ml BSA, and 1 tablet Complete mini protease inhibitor EDTA free (Roche) per 10 ml buffer. Next, samples were sonicated 3 times 5 sec using ultrasound with amplitude 60 at 4°C. After 1 hour head-over-head incubation at 4°C, extracts were centrifuged for 15 min at 10,000 x g and 4°C and supernatant was isolated.

For brain homogenates, slices from frozen unfixed human brain tissue were collected using a sliding microtome (Leica SM 2010 R.). Tissue was homogenized using ceramic MagNA Lyser beads (Roche) by grinding in a Bullet Blender (Next Advance) for 3 min at strength 8 in lysis

buffer as described previously (Hu *et al.*, 2009). Homogenates were incubated for 1 hour in a head-over-head rotator at 4ºC, and centrifuged for 15 min at 10,000 x g at 4ºC.

Protein concentrations were determined with the bicinchoninic acid kit (BCA) (Thermo Fisher Scientific, Waltham, USA) using Bovine Serum Albumin (BSA) as a standard. After addition of 5% glycerol, samples were aliquotted, snap frozen and stored at -80°C.

Western blotting

SDS-PAGE separation of proteins was performed according to the "shorter CAG repeats" protocol as described previously (Hu *et al.*, 2009). Proteins were transferred to a 0.2 µm nitrocellulose membrane (Bio-Rad, #170-4159.) using the Trans-blot Turbo (BioRad) at 2.5A (constant)/25V for 10 min. Membranes were blocked for 15 min in tris buffered saline (TBS) containing 5% non-fat milk (Nutricia, Schiphol, the Netherlands). Next, membranes were incubated with primary rabbit antibody EPR5526 (Abcam, Cambridge, UK) that recognizes the N-terminus of the htt protein, diluted 1:5000 in blocking buffer, followed by secondary incubation with rabbit IRDye800 (LI-COR, Lincoln, USA) diluted 1:5000 in blocking buffer. Blots were analyzed on an Odyssey reader (LI-COR). Protein bands corresponding to wild-type and mutant htt were quantified using the Odyssey software version 3.0 (LI-COR). Background correction was performed by sampling an empty area of the blot of the same size as the area that contained the positive protein band. Wild-type and mutant htt protein expression levels relative to total htt protein expression were calculated by dividing wild-type and mutant htt band intensities with total htt band intensity (wild-type + mutant).

Dot blot assay

Brain homogenates were prepared in 150 mM sucrose, 15 mM HEPES pH 7.9, 60 mM KCl, 5 mM EDTA, 1 mM EGTA and 1 tablet Complete mini protease inhibitor EDTA free (Roche) per 10 ml buffer. Tissue was homogenized using ceramic MagNA Lyser beads (Roche) by grinding in a Bullet Blender (Next Advance) for 3 min at strength 8. Next, Triton X-100 (Sigma) was added to a final concentration of 1%. Homogenates were incubated in a head-over-head rotator for 1 hour at 4ºC and extracts were centrifuged for 10 min at 10,000 x g. Protein pellets were washed three times in 60 mM Tris and centrifuged for 10 min at 10,000 x g. Next, pellets were resuspended in 15% SDS and incubated overnight at 95ºC. Protein concentrations of the resulting pellet suspensions were determined by BCA. Per well, 100 µg of pellet suspension was applied to in 0.2% SDS pre-wetted cellulose acetate pore size 0.2 µm (Schleicher and Schuell, St. Louis, USA) membranes by vacuum application using the Bio-dot manifold (Bio-Rad). Wells were washed twice with 0.2% SDS and membrane was fixed in 0.5% glutaraldehyde for 20 min. The fixed membrane was blocked in TBS containing Tween-20 (TBST) and 5% non-fat milk (Nutricia). First incubation was performed with rabbit EPR5526 antibody diluted1:5,000 in TBST containing 5% non-fat milk. Secondary incubation was performed with mouse anti rabbit antibody conjugated with horse radish peroxidase (Santa Cruz, Dallas, USA), diluted 1:10,000 in TBST containing 5% non-fat milk. Membranes were incubated with enhanced chemiluminescence (ECL) (GE Healthcare, Cleveland, USA) and exposed to light sensitive film.

Statistical analyses

GraphPad Prism version 6.02 was used for statistical analysis. Typically, significance was determined using the two-tailed paired Student's t-test after testing for normal distribution. Data presented as bar graphs (means + standard deviation (SD)), whisker boxplots (whiskers = 10-90 percentile), or scatter dot plot (line = mean).

2.4. Results

No difference in wild-type and mutant HTT mRNA levels in HD patient-derived fibroblasts

To measure both wild-type and mutant HTT mRNA levels we performed a PCR with primers flanking the CAG repeat that separated on gel electrophoresis due to differences in their CAG repeat length (**Figure 1a**). In total four HD patient-derived fibroblasts of which 1, GM04857, contained a homozygous CAG repeat expansion were analyzed. For more information, see **Table 1**. Genomic DNA (gDNA) was taken along to control for differences in PCR amplification efficiencies across the CAG repeat. Furthermore, reverse transcription without reverse transcription enzyme was taken along, verifying that there was no gDNA contamination in our RT-PCR (**Figure 1b**). The two PCR products for each cell line were quantified and individual wild-type versus mutant HTT mRNA expression ratios were calculated. Next, the average expression levels of wild-type and mutant HTT mRNA in the adult-onset HD fibroblasts were calculated. No significant difference (P = 0.5168) between wild-type and mutant HTT mRNA expression was observed (**Figure 1c**).

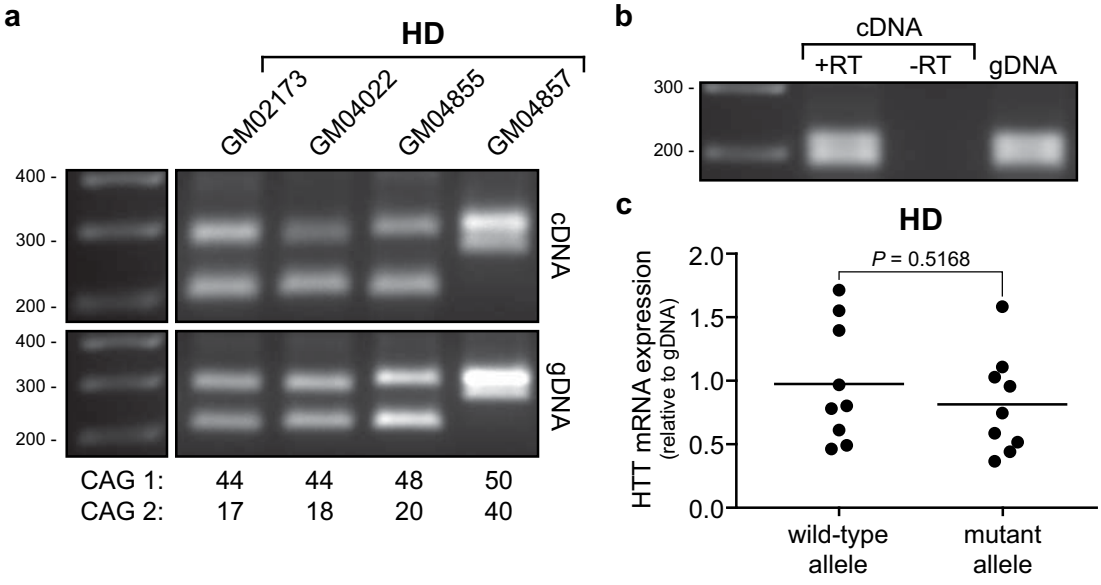

Figure 1. Wild-type and mutant HTT mRNA levels in HD patient-derived fibroblasts. Wild-type and mutant HTT mRNA PCR products were separated on gel electrophoresis by differences in their CAG repeat length. **(a)** RT-PCR products from 3 HD (GM02173, GM04022, GM04855) and one homozygous HD (GM04857) fibroblasts. Allelic CAG repeat sizes are indicated below each lane. gDNA was taken along to control for differences in PCR amplification efficiencies across the CAG repeat. **(b)** RT-PCR products with input: cDNA (+RT), cDNA lacking reverse transcriptase (-RT) and gDNA of 1 control (GM04204). **(c)** Scatter boxplot of RT-PCR from HD patient-derived fibroblasts, comparing wild-type and mutant HTT mRNA expression levels, relative to gDNA. Line = mean, data were evaluated using two-tailed student-t test, n = 3.

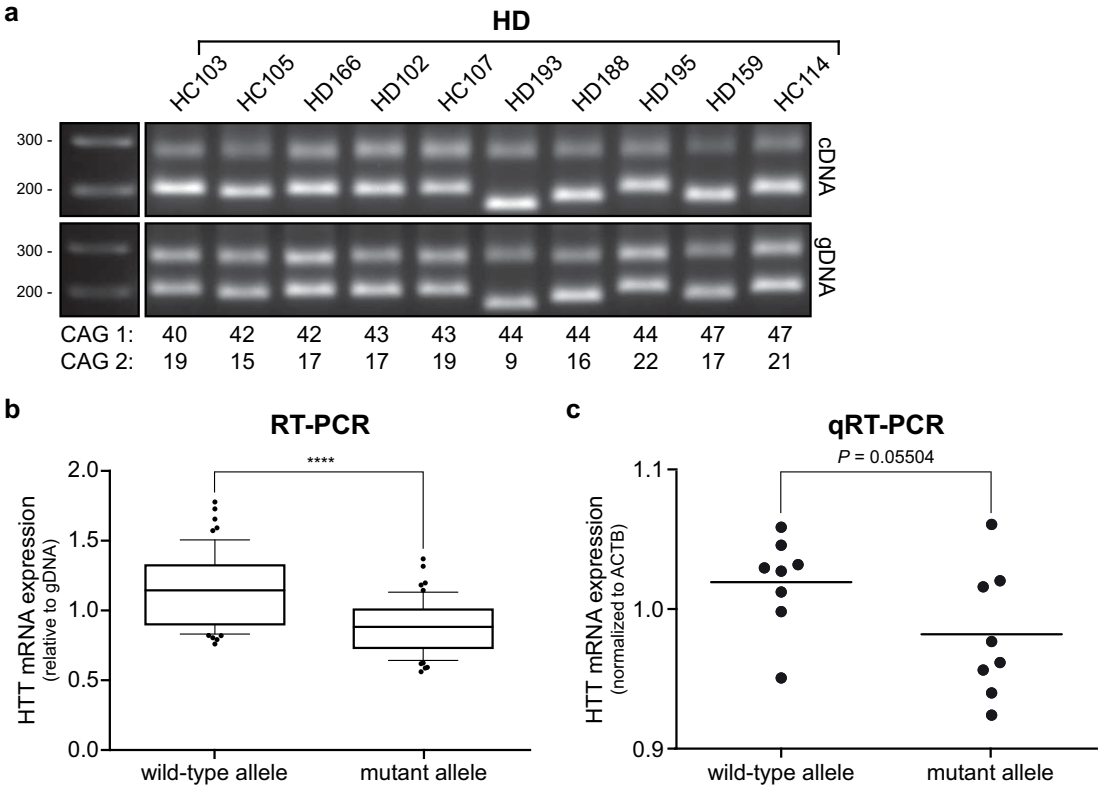

Figure 2. Wild-type and mutant HTT mRNA levels in HD human *post-mortem* brain material. Wild-type and mutant HTT mRNA PCR products were separated on gel electrophoresis by differences in their CAG repeat length. **(A)** RT-PCR products from brain tissue derived from 10 HD patients. Allelic CAG repeat sizes are indicated below each lane. gDNA was taken along to control for differences in PCR amplification efficiencies across the CAG repeat. **(B)** Whisker boxplot of HD RT-PCR data, comparing wild-type and mutant HTT mRNA expression levels, relative to gDNA. Whiskers = 10-90 percentile, data were evaluated using a two-tailed student t-test, **** $P < 0.0001$, n = 10. **(C)** Scatter boxplot of SNP rs362273-specific quantitative RT-PCR on HD *post-mortem* brain material, comparing wild-type and mutant HTT mRNA expression levels, normalized to β-actin (ACTB). Line = mean, data were evaluated using a two-tailed student t-test, n = 4.

More wild-type than mutant HTT mRNA in human *post-mortem* HD brain material

Next, we investigated HTT mRNA expression levels in *post-mortem* brain tissue from HD patients with a wide range of repeat lengths. RNA was isolated and PCR was performed with primers flanking the CAG repeat. PCR products were separated by gel electrophoresis due to differences in their CAG repeat length (**Figure 2a**). Individual bands were quantified and normalized against PCR products from gDNA (**Figure S1**).

After calculating average expression, wild-type and mutant HTT mRNA levels were compared (**Figure 2b**). Although the PCR approached the plateau phase, we still found a small, but significant, lower average mutant HTT mRNA expression 0.89 (±0.19) versus 1.15 (±0.25) of wild-type mRNA in *post-mortem* brain tissue from HD patients.

To validate the semi-quantitative RT-PCR gel electrophoresis analysis, we performed a SNP-

specific TaqMan quantitative PCR, using probes for SNP rs362273 located at exon 57 of HTT. Of our *post-mortem* brain samples, 6 out of 14 were heterozygous for SNP rs362273. Next, SNP linkage by circularization (SLiC) was successfully performed to determine which allele has the guanine and which allele the adenine in exon 57 (Liu *et al.*, 2008). Due to the variable RNA quality of brain tissue, SLiC was only possible in 4 out of 6 samples. The SNP-specific TaqMan quantitative (q)RT-PCR showed a consistent trend towards wild-type HTT. Due to the smaller number of brain samples that we could use for this SNP-specific TaqMan assay, the difference did not reach significance. However, it confirmed the higher expression of wild-type HTT mRNA compared to mutant HTT mRNA in HD *post-mortem* brain (**Figure 2c**).

No difference in wild-type and mutant htt protein levels in HD fibroblast and *post-mortem* brain

We examined levels of SDS-soluble wild-type and mutant htt protein levels in patient-derived fibroblasts by Western blot (**Figure 3a**). In the homozygous HD fibroblast GM04857, only one protein band was visible because the difference in protein size between the htt protein expressed from the two alleles is too small to separate by Western blot. For the other samples, the separated wild-type and mutant htt protein bands were quantified and individual wild-type versus mutant htt protein ratios were calculated (**Figure S2**). Next, we averaged all data from individual measurements and compared wild-type and mutant htt protein levels. No significant difference between wild-type and mutant htt protein levels in patient-derived fibroblasts was found (**Figure 3c**).

We then analyzed SDS-soluble wild-type and mutant htt protein levels in *post-mortem* human HD brain homogenates (**Figure 3b**). As with the HD fibroblasts, there was no difference in wild-type and mutant htt levels in HD brains (**Figure 3d** and **Figure S2**). We also examined aggregation of mutant htt in our *post-mortem* human HD brain tissue by investigating SDS-insoluble htt using a dot blot assay. We found comparable levels of SDS-insoluble htt for subjects HC105 and HD166, which had the same polyQ stretch of 44, and more insoluble htt for subject HC107 which had a slightly longer polyQ stretch of 45 (**Figure 3e**).

Soluble wild-type and mutant htt protein levels are similar in both fibroblasts and brain, while in fibroblasts it is known that mutant htt protein does not aggregate (Sathasivam *et al.*, 2001). We found more htt protein aggregation in the brain sample with the longer polyQ repeat, but there was no decrease in mutant htt protein levels on Western blot.

More wild-type than mutant htt protein in juvenile HD fibroblasts and *post-mortem* brain

Next, we used Western blot to analyze SDS-soluble levels of wild-type and mutant htt protein in juvenile HD samples. Analysis of juvenile HD fibroblast cell lines showed a significant higher level of wild-type htt protein compared to mutant htt (0.55 versus 0.45 (±0.05)) (**Figure 4a and c**). Western blot analysis of *post-mortem* juvenile HD brain lysates also showed a significantly higher level of wild-type htt protein with respect to mutant htt (0.53 versus 0.47 (± 0.06)) (**Figure 4b and d**).

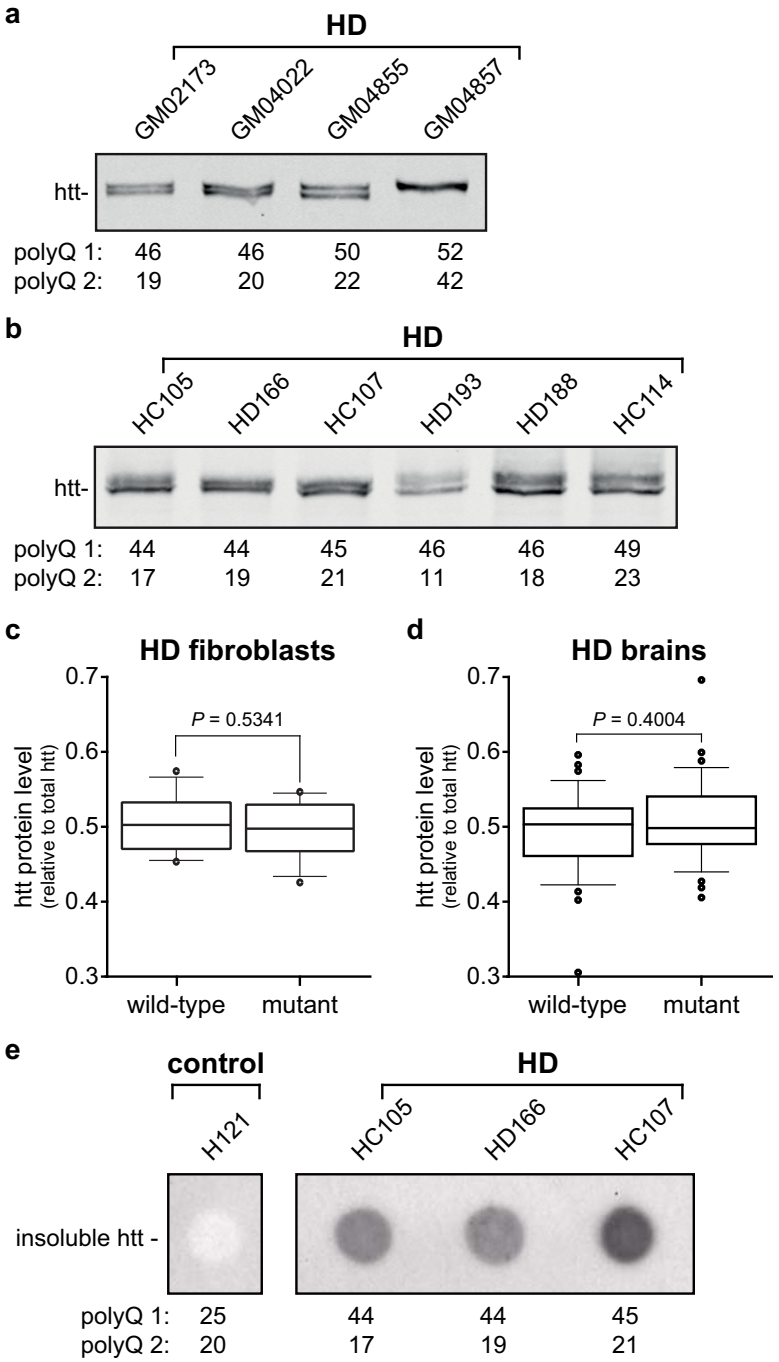

Figure 3. Wild-type and mutant htt protein levels in HD fibroblasts and *post-mortem* brain tissue. PolyQ repeat lengths are indicated below each lane. The lower band represents wild-type htt protein, the upper band mutant htt protein. **(a)** Western blot analysis of total protein lysates from human fibroblasts from three heterozygous HD (GM02173, GM04022, GM04855) and one homozygous HD subject (GM04857). **(b)** Western blot analysis of cortical brain homogenates from six HD subjects. **(c)** Whisker box plots comparing wild-type and mutant htt levels normalized against total htt in HD fibroblasts (n = 3) and **(d)** HD *post-mortem* brain tissue (n = 6). Whiskers = 10-90 percentile, data were evaluated using a two-tailed student t-test. **(e)** Dot blot assay of SDS-insoluble htt protein fractions of human control (H121) and HD brain (HC105, HD166, HC107). Dot intensity indicates level of insoluble htt protein.

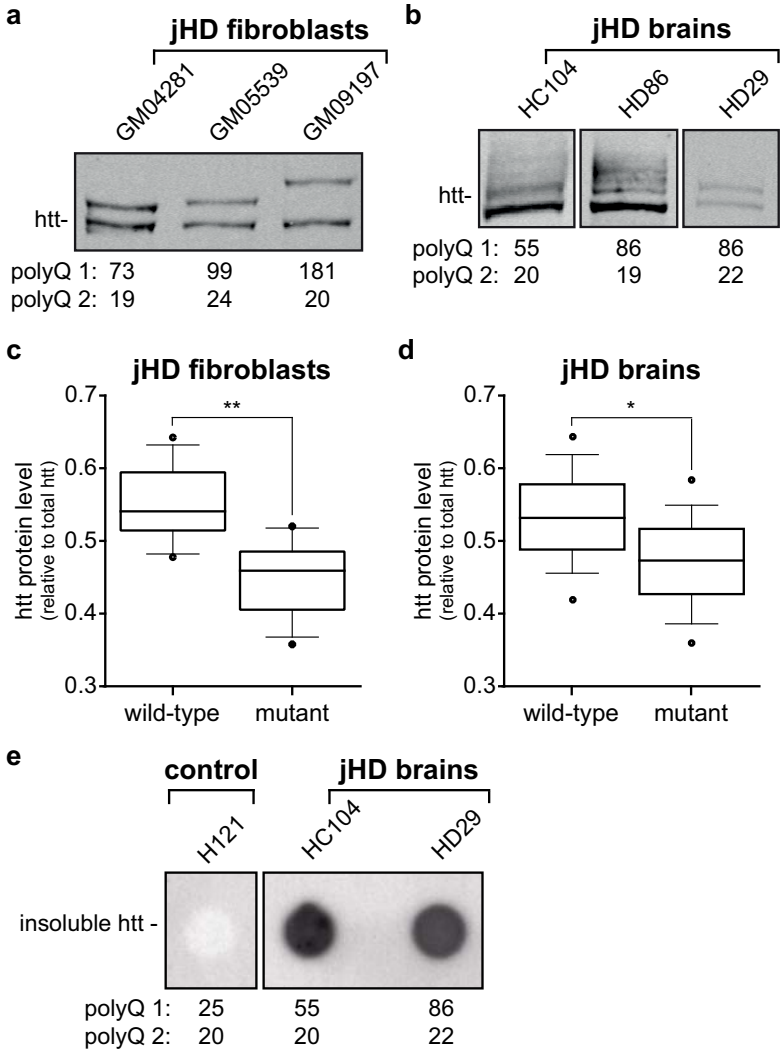

Figure 4. Wild-type and mutant htt protein levels in patient-derived juvenile HD fibroblasts and *post-mortem* brain tissue. (a) Western blot analysis of total protein lysates from human fibroblasts derived from three juvenile HD subjects. PolyQ repeat lengths are indicated below each lane. **(b)** *Post-mortem* cortical brain tissue from three juvenile HD subjects (GM04281, GM05539, GM09197). The lower band represents wild-type htt, the upper band mutant htt. **(c)** Whisker box plots comparing wild-type and mutant htt levels normalized against total htt in juvenile HD fibroblasts and **(d)** juvenile HD *post-mortem* brain tissue. Whiskers = 10-90 percentile, data were evaluated using a two-tailed student t-test, n = 3, * $P > 0.05$, ** $P > 0.01$. **(e)** Dot blot assay of SDS-insoluble htt protein fractions of human control (H121) and juvenile HD brain homogenates (HC104 and HD29). Dot intensity indicates level of insoluble htt protein. PolyQ repeat lengths are indicated below each lane.

We also looked at aggregation of *post-mortem* juvenile HD brain lysates from subjects HC104 and HD29 using the dot blot assay (**Figure 4e**). As expected, when compared with the HD brain lysates, juvenile HD brain lysates clearly showed more aggregated SDS-insoluble mutant htt protein.

To conclude, in adult-onset HD samples, wild-type and mutant htt protein levels are equal, regardless of mutant htt protein aggregation. In juvenile HD there is a consistent lower level of mutant htt protein expression, in both brain and fibroblast samples.

Identification of novel HTT antisense isoform in patient-derived fibroblasts and brain tissue

In previous studies in *post-mortem* HD brain it was suggested that the HTTAS_v1 with an expanded CTG repeat was not expressed (Chung *et al.*, 2011). To validate this a homozygous HD patient-derived fibroblast GM04857 was included since it has two expanded CAG repeats and therefore should not have any HTTAS_v1 expression. Unexpectedly, we also found HTTAS_v1 in fibroblasts obtained from an HD patient homozygous for the CAG repeat expansion (**Figure 5a**). The HTTAS_v1 expression level of the homozygous HD patient was comparable to that of the heterozygous patient samples, suggesting that there is expression of HTTAS_v1 with the expanded CTG repeat.

Next, we designed HTTAS isoform-specific primers to examine the expression of HTTAS_v1 and v2 in: (I) fibroblasts derived from a control, (II) an HD patient, and (III) a juvenile HD patient (**Figure 5a**), as well as *post-mortem* (juvenile) HD brain tissue (**Figure 5b**). Similar levels of HTTAS_v1 in all brain and fibroblasts samples were shown. Interestingly, the primers specific for HTTAS_v2 gave an additional band, slightly bigger than the expected PCR amplicon. Sanger sequencing confirmed that this was a novel HTTAS isoform, which we named HTTAS_v2.2 (**Figure 5c**). This HTTAS_v2.2 has an additional 69 nucleotides at the 3'end of HTTAS exon 2.

In sum, similar HTTAS expression levels in (homozygous) HD and controls were found, suggesting that the observed variations in wild-type and control HTT transcript levels in *post-mortem* brain are probably not caused by changes in HTTAS expression levels. Furthermore, we have identified a novel HTTAS isoform, which we named HTTAS_v2.2.

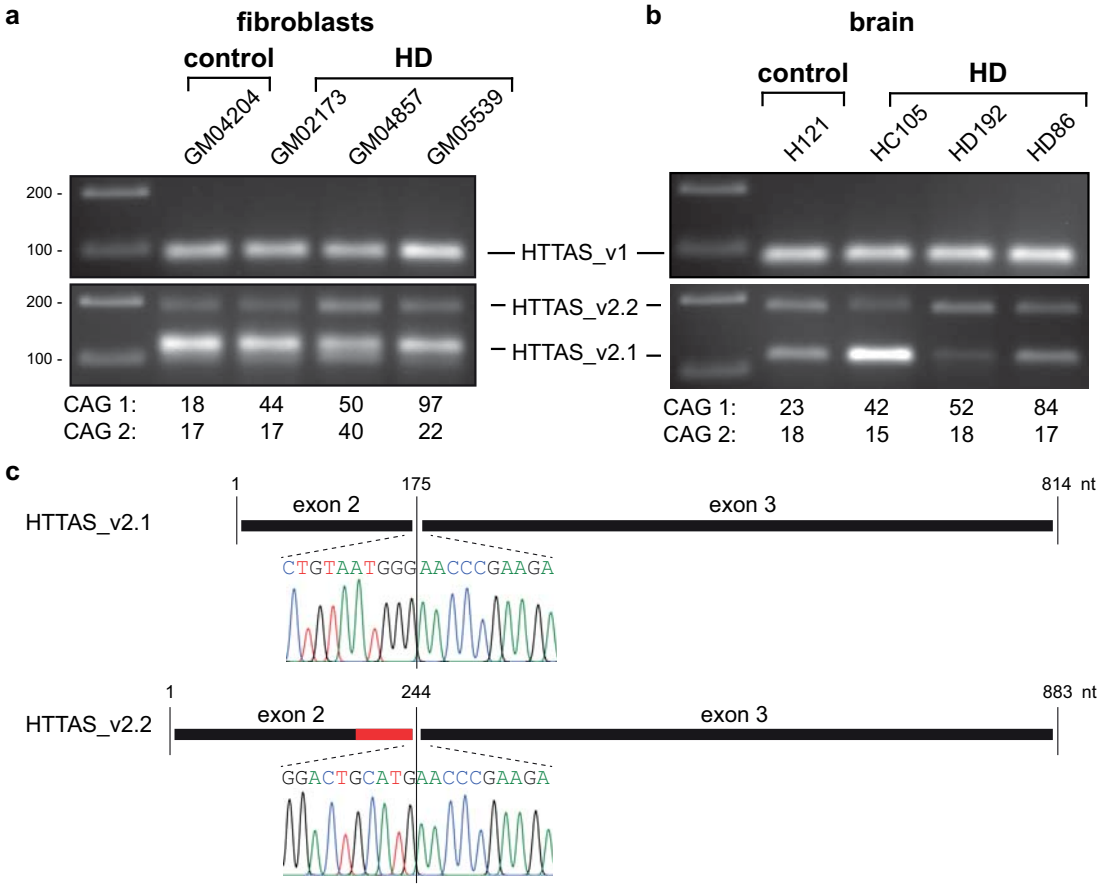

Figure 5. HTT antisense (HTTAS) identification in HD patient-derived fibroblasts and *post-mortem* brain tissue. HTTAS_v1 and HTTAS_v2 were amplified using strand- and HTTAS isoform-specific primers. **(a)** Gel electrophoresis of HTTAS_v1 and HTTAS_v2 RT-PCR of patient-derived fibroblasts from a control (GM04204), an HD patient (GM02173), an HD patient homozygous for the CAG repeat expansion (GM04857) and a juvenile HD patient (GM05539). **(b)** Gel electrophoresis of HTTAS_v1 and HTTAS_v2 RT-PCR of *post-mortem* brain tissue from a control (H121), an HD patient (HC105), and 2 juvenile HD patients (HD192 and HD86). Allelic CAG repeat sizes below each lane. **(c)** Schematic representation of HTTAS_v2.1 and the novel identified HTTAS_v2.2. Sanger sequencing of the exon 2 - exon 3 boundaries of both HTTAS_v2 isoforms are shown. The novel HTTAS_v2.2 has an additional 69 nucleotides at the 3'end of HTTAS exon 2.

2.5. Discussion

In the current study we found that in adult-onset HD patient-derived fibroblasts, the levels of wild-type and mutant HTT mRNA did not significantly differ. This is in concordance with results found in patient-derived HD lymphoblasts (Lee *et al.*, 2013). By analyzing microarray probes that detect both wild-type and mutant HTT mRNA, it was shown that the expanded CAG repeat did not affect HTT mRNA expression (Lee *et al.*, 2013). CAG repeat-induced RNA toxicity has recently also been proposed to be involved in the HD pathogenesis (Wojciechowska and Krzyzosiak, 2011). The size of the CAG repeat is thought to be critical for the contribution of RNA toxicity (Wang *et al.*, 2011). Juvenile fibroblast cells with mutant htt alleles containing either 68 or 151 CAGs exhibited aggregation of mutant HTT mRNA (de Mezer *et al.*, 2011). Our results show that there is no difference in wild-type and mutant HTT mRNA levels in fibroblasts, suggesting that there is no detectable effect of mRNA aggregation on mRNA levels in adult-onset fibroblast samples. However, in *post-mortem* brain tissue we did find a small but significant lower level of mutant than wild-type HTT mRNA, highlighting subtle differences between *post-mortem* brain tissue and patient-derived fibroblasts.

Wild-type and mutant htt protein levels did not significantly differ in either patient-derived fibroblasts or *post-mortem* brain samples. Soluble htt has a half-life of approximately 24 hours (Persichetti *et al.*, 1996) and we hypothesize that with Western blot analysis we detect soluble htt that is present in the cells. Aggregated htt is less efficiently cleared (Gutekunst *et al.*, 1999). This SDS-insoluble accumulated htt protein is detected by dot blot assay. Since protein aggregation is an important feature in HD brain tissue, but does not occur in HD fibroblasts (Sathasivam *et al.*, 2001), our results show that protein aggregation does not affect the levels of soluble htt protein. Although htt protein levels did not differ, in human brain samples we did find less mutant HTT mRNA. A possible explanation could be an enhanced translation of mutant HTT, resulting in equal htt protein levels. Recently, increased translation of mutant htt by binding of the MID1-PP2A translational complex was shown (Krauss *et al.*, 2013). Cells overexpressing N-terminal htt fragments with a normal and mutant polyQ repeat showed an enhanced protein synthesis of htt fragments with an expanded polyQ repeat. This more efficient translation of mutant HTT mRNA was proposed to be caused by enhanced binding of the MID1-complex to the expanded CAG repeat and mediated by mTOR and S6K kinases (Krauss *et al.*, 2013). However, this cannot be a general expanded polyQ mechanism, since we only found a difference in wild-type and mutant HTT mRNA in brain tissue samples and not in fibroblast cells. Another possible explanation for the differences in HTT mRNA levels between human fibroblasts and brain could be the nature of the tissue where RNA was isolated from; dividing living cells versus brain material with *post-mortem* delay and subsequently autolysis. Nevertheless, our results show subtle differences in htt protein levels between *post-mortem* brain tissue and patient-derived fibroblasts. This has to be considered when interpreting results obtained from patient-derived HD fibroblasts or other peripheral tissue with respect to disease processes in HD.

In juvenile HD samples we consistently found that the levels of wild-type htt protein were higher than mutant htt protein in both patient-derived fibroblasts and *post-mortem* brain tissue. This is in contradiction with previous studies in knock-in HD mice carrying one or two repeats with 111 CAGs (Krauss *et al.*, 2013), which showed increased mutant htt protein levels. It is known that reverse transcriptase and polymerase chain reactions across CG-rich regions are notoriously difficult (Stine *et al.*, 1995), this combined with a reduced RNA quality in our juvenile HD samples, is why we could not reliably quantify mutant HTT mRNA levels in juvenile HD subjects. It is conceivable that the lower mutant htt protein level in juvenile HD is caused by an equivalent lower level of mutant HTT mRNA. Clearly, our results indicate that expression of wild-type and mutant htt in juvenile HD are different compared to that of adult-onset HD.

Recently it has been suggested that in polyQ disorders bidirectional RNA transcription could play a role in the disease pathology by deregulation of the sense transcript (Chung *et al.*, 2011; Sopher *et al.*, 2011). In HD, two natural HTTAS transcripts (HTTAS_v1 and v2) were identified at the HTT locus, of which HTTAS_v1 contained the CTG repeat (Chung *et al.*, 2011). It was shown that overexpression of HTTAS_v1with an wild-type repeat resulted in reduced HTT sense transcript levels, whereas knockdown of HTTAS_v1 increased HTT sense transcript levels. Based on these findings, it was hypothesized that HTTAS_v1 negatively regulated htt transcript expression (Chung *et al.*, 2011). Also, when the CTG repeat in HTTAS_v1 was expanded, expression was strongly reduced in HD brains. However, our results show expression of HTTAS_v1 in human-derived fibroblasts homozygous for the CAG repeat expansion, suggesting that there is an HTTAS_v1 with expanded CTG repeat transcribed. Unfortunately we did not have *post-mortem* material from a homozygous HD patient to validate this HTTAS_v1 expression in human homozygous HD brain. Furthermore, we have identified a novel HTTAS_v2 isoform, which has an additional 69 nucleotides at the 3'end of HTTAS exon 2, which we named HTTAS_v2.2. Future research will have to determine the role of these antisense transcripts in HTT expression.

Recent advances have shown the potential of reducing mutant htt levels with oligonucleotide-based therapeutics. Reduction of both wild-type and mutant htt up to 70% was well tolerated in HD rodent models and non-human primates (Kordasiewicz *et al.*, 2012). Long-term suppression of wild-type and mutant htt might not be desirable because of htt's anti-apoptotic function (Rigamonti *et al.*, 2000) and importance for cell survival in the adult brain (Dragatsis *et al.*, 2000; Zhang *et al.*, 2003). A different approach would be an allele-specific reduction of mutant htt. This could be achieved with oligonucleotides directed against SNPs unique to the mutant htt transcript, or by targeting the expanded CAG repeat directly (Appl *et al.*, 2012). Showing that the basal levels of mutant HTT mRNA and mutant htt protein are equal or lower when compared to wild-type, provides feasibility for oligonucleotide therapeutics that are not completely specific for the mutant HTT allele.

Our results highlight subtle differences in htt RNA and protein expression with less mutant HTT mRNA, but equal wild-type and mutant htt protein levels in adult-onset HD. In juvenile HD mutant htt protein levels were lower compared with wild-type htt, indicating subtle differences in htt protein expression between adult-onset and juvenile HD. Differences between *post-mortem* brain tissue and patient-derived fibroblasts have to be taken into account when

interpreting results obtained from HD patient-derived fibroblasts. Furthermore, differences in htt levels between adult-onset HD and juvenile HD samples should be taken into account when using HD tissue and animal models with juvenile polyQ repeat lengths.

2.6. Acknowledgements

We thank David F. Fischer (BioFocus, a Galapagos company, Leiden, The Netherlands) and Michela A. Tessari (Galapagos B.V., Leiden, The Netherlands) for the TaqMan SNP assay. We thank Marika Eszes and Ingrid Hegeman for providing us with the relevant clinical information.

This work was supported by the Center for Biomedical Genetics (the Netherlands), the Prinses Beatrix Spierfonds (the Netherlands), and Integrated European Project in Omics Research of Rare Neuromuscular and Neurodegenerative Diseases (Neuromics). The funders had no role in study design, data collection and analysis, decision to publish, or preparation of the manuscript.

2.7. Supplementary Material

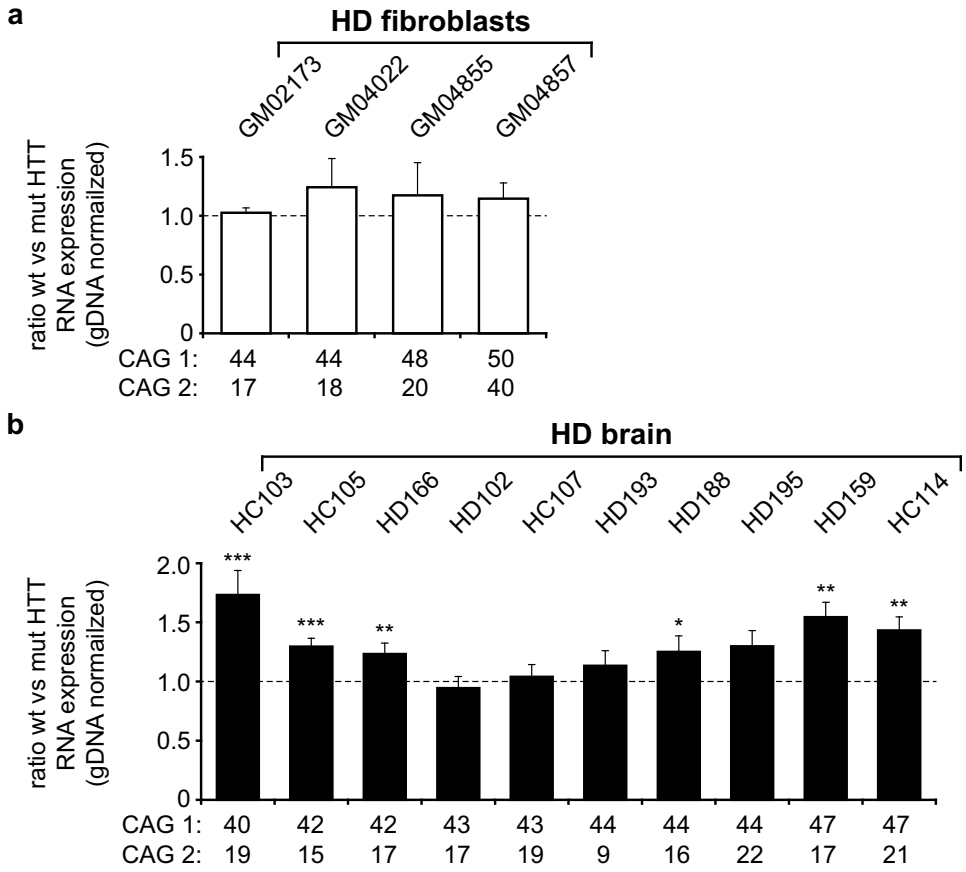

Figure S1. Wild-type and mutant HTT mRNA levels in individual HD patient-derived fibroblasts and post-mortem brain material. Wild-type and mutant HTT alleles were separated by differences in CAG repeat length. Allelic CAG repeat sizes below each bar. gDNA was taken along to control for the PCR reaction over the CAG repeat. Wild-type and mutant HTT RNA expression levels were calculated by dividing the intensity of the gDNA normalized wild-type HTT band by the mutant HTT band. **(a)** Gel electrophoresis quantification of 4 HD fibroblasts. Bars represent mean values with standard deviation (n = 3). **(b)** Gel electrophoresis quantification of brain tissue derived from 10 HD patients. Bars represent mean values with standard deviation. Data were evaluated using two-tailed student-t test, * $P > 0.05$, ** $P > 0.01$, *** $P > 0.001$, n = 5.

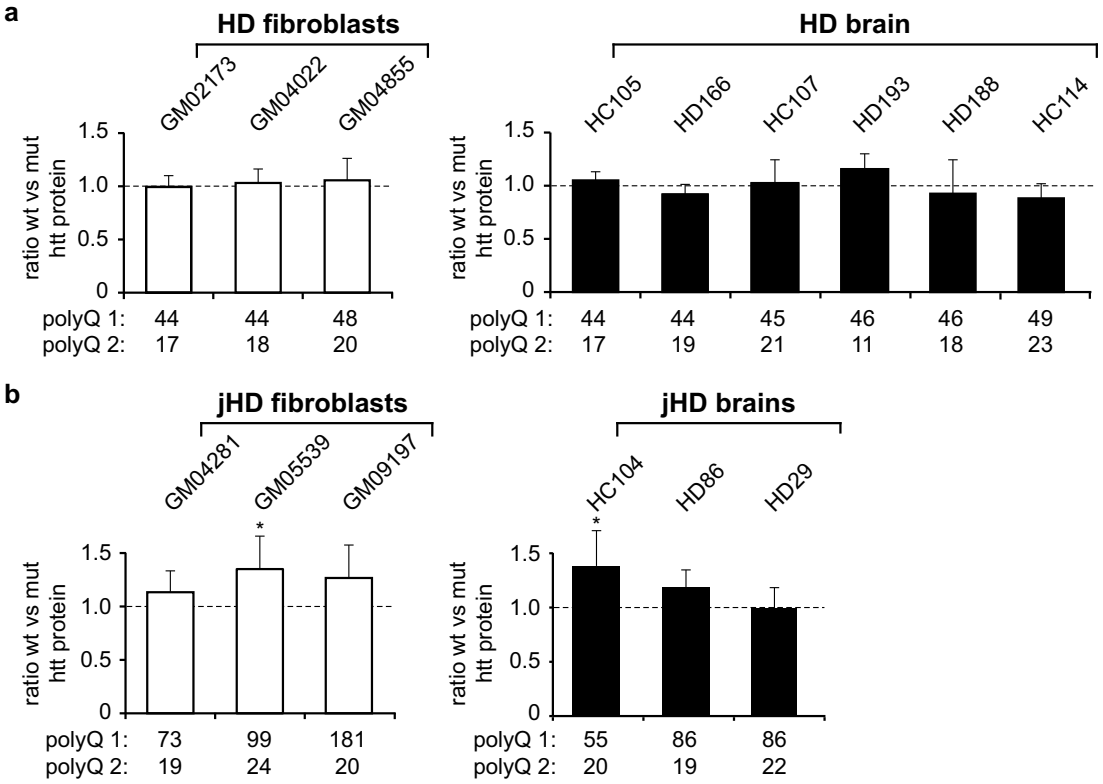

Figure S2. Analysis of wild-type and mutant htt ratio's in individual subjects. Wild-type versus mutant htt ratio for individual subjects was calculated by dividing wild-type htt band intensity with mutant htt band intensity. Individual polyQ tracts are indicated below each subject. **(a)** Individual patient-derived HD fibroblast cell lines (left), or individual post-mortem cortical brain lysates (right). **(b)** Individual patient-derived juvenile HD fibroblast cell lines (left), or individual post-mortem cortical juvenile HD brain lysates (right). Bars represent mean values with standard deviation (n ≥ 3). Data were evaluated using two-tailed student-t test, * $P < 0.05$.

Melvin M. Evers [1]
Barry A. Pepers [1]
Judith C.T. van Deutekom [2]
Susan A.M. Mulders [2]
Johan T. den Dunnen [1,3,4]
Annemieke Aartsma-Rus [1]
Gert-Jan B. van Ommen [1]
Willeke M.C. van Roon-Mom [1]

[1] Department of Human Genetics, Leiden University Medical Center
[2] Prosensa Therapeutics B.V., Leiden
[3] Leiden Genome Technology Center, Leiden University Medical Center
[4] Department of Clinical Genetics, Leiden University Medical Center

3

Targeting several CAG expansion diseases by a single antisense oligonucleotide

PLoS One 2011, 6(9):e24308

3.1. Abstract

To date there are 9 known diseases caused by an expanded polyglutamine repeat, with the most prevalent being Huntington's disease. Huntington's disease is a progressive autosomal dominant neurodegenerative disorder for which currently no therapy is available. It is caused by a CAG repeat expansion in the *HTT* gene, which results in an expansion of a glutamine stretch at the N-terminal end of the huntingtin protein. This polyglutamine expansion plays a central role in the disease and results in the accumulation of cytoplasmic and nuclear aggregates. Here, we make use of modified 2'-O-methyl phosphorothioate $(CUG)_n$ triplet-repeat antisense oligonucleotides to effectively reduce mutant huntingtin transcript and protein levels in patient-derived Huntington's disease fibroblasts and lymphoblasts. The most effective antisense oligonucleotide, $(CUG)_7$, also reduced mutant ataxin-1 and ataxin-3 mRNA levels in spinocerebellar ataxia 1 and 3, respectively, and atrophin-1 in dentatorubral-pallidoluysian atrophy patient derived fibroblasts. This antisense oligonucleotide is not only a promising therapeutic tool to reduce mutant huntingtin levels in Huntington's disease but our results in spinocerebellar ataxia and dentatorubral-pallidoluysian atrophy cells suggest that this could also be applicable to other polyglutamine expansion disorders as well.

3.2. Introduction

Polyglutamine (polyQ) diseases are a group of disorders caused by CAG triplet repeat expansions in the coding region of the genome. The disease causing proteins in these polyQ diseases are very different, but in each case the expanded stretch of glutamines results in a toxic-gain-of function of the protein and this leads to neurodegeneration. To date, a total of 9 polyQ disorders have been described: dentatorubral-pallidoluysian atrophy (DRPLA), Huntington's disease (HD), spinal bulbar muscular atrophy (SBMA), and spinocerebellar ataxias (SCA1, 2, 3, 6, 7, and 17) (Cummings and Zoghbi, 2000; Nakamura *et al.*, 2001). Of these polyQ disorders, HD and SCA3 have the highest prevalence worldwide (Bauer and Nukina, 2009). The expanded repeats in these polyQ diseases are unstable resulting in anticipation; a more severe and earlier onset of disease in following generations (Ranen *et al.*, 1995). There is an inverse correlation of disease onset and polyQ length in the protein; the longer the CAG repeat, the earlier the age of onset of the disease (Cummings and Zoghbi, 2000). Protein aggregates are found in the nucleus and cytoplasm of cells, indicating that protein misfolding is a common feature of these disorders. Currently no treatment is available to delay onset or even slow progression of polyQ diseases.

In HD, the expanded CAG repeat is located in the first exon of the *HTT* gene on chromosome 4p16. The expanded CAG transcript is translated into a mutant huntingtin (htt) protein with an expanded polyQ tract at the N-terminus. Patients with 40 or more CAG repeats will develop the disease, whereas people with 35 to 39 repeats show reduced penetrance (Mcneil *et al.*, 1997). The disease is characterized by motor, psychiatric and cognitive impairments and the typical age of onset lies between 30 and 50 years (Andrew *et al.*, 1993). The major neuropathology occurs in the striatum but degeneration is seen throughout the brain when the disease progresses. Various other proteins have been found to co-localize with htt aggregates, i.e. TATA box binding protein (TBP), CREB binding protein (CBP) and several molecular chaperones (Huang *et al.*, 1998; Steffan *et al.*, 2000; Muchowski *et al.*, 2002; Roon-Mom *et al.*, 2002). When the mutation for HD was found, htt was a protein of unknown function but extensive research over the past decade has revealed numerous functions for htt. Also many affected cellular processes have been identified in HD, such as transcriptional de-regulation, mitochondrial dysfunction, and impaired vesicle transport (Bauer and Nukina, 2009; Ross and Tabrizi, 2011).

SCAs are genetically and clinically distinct autosomal dominant CAG-expansion diseases, numbered by the order of gene description. Patients with SCA exhibit cerebellar degeneration resulting in ataxia and oculomotor deficits, often followed by general brain atrophy (Manto, 2005; Schols *et al.*, 2004). The first SCA identified, SCA1, is caused by a CAG repeat expansion of 41 or more in exon 8 of the *ATXN1* gene (Bauer and Nukina, 2009). *ATXN1* is translated into the 98 kDa protein ataxin-1, which is involved in transcriptional regulation and RNA metabolism (Matilla-Duenas *et al.*, 2008). Mutated ataxin-1, by entering the nucleus, causes cellular dysfunction (Klement *et al.*, 1998). In SCA3, the expanded CAG repeat is located in exon 10 of the *ATXN3* gene which is translated into mutant ataxin-3 (Kawaguchi *et al.*, 1994).

Patients develop the disease when the number of CAGs exceed 51, while there is reduced penetrance when the number of repeats is between 45 and 51 (Padiath *et al.*, 2005). The 42 kDa ataxin-3 protein is suggested to be involved in proteasomal degradation and transport of ubiquitinated proteins (Riess *et al.*, 2008). DRPLA is a rare autosomal dominant disorder, characterized by dementia, ataxia, chorea, myoclonic epilepsy, and psychiatric disturbances. The disease is caused by a CAG repeat expansion in exon 5 of the *ATN1* gene, which encodes the 200 kDa atrophin-1 protein. Atrophin-1 is a known transcriptional co-regulator although its exact function is not well understood (Shen and Peterson, 2009). Patients with a repeat of 49 or more glutamines will develop the disease (Nagafuchi *et al.*, 1994).

Most therapeutic strategies under investigation for polyQ disorders are aimed at counteracting one of the many cellular processes that are altered due to expression of the mutant protein. For instance, in all of these neurodegenerative diseases the formation of fragmented protein products by proteolytic cleavage is an important step in the pathogenic process (Bauer and Nukina, 2009). It has been shown that altering proteolysis of the mutant htt protein can be beneficial, as an HD mouse model lacking the caspase 6 cleavage site had reduced neuronal dysfunction and neurodegeneration (Graham *et al.*, 2006). Reducing mutant polyQ protein levels and thereby inhibiting all downstream toxic effects would be much more effective than targeting a single cellular process. One way to achieve this would be to enhance the degradation of mutant polyQ proteins through activation of the proteasome (Seo *et al.*, 2007) or through upregulation of the autophagic pathway (Metcalf *et al.*, 2010). Another strategy would be to inhibit the formation of mutant polyQ proteins by gene silencing or transcript degradation (Scholefield and Wood, 2010). RNAi is increasingly used as a potential therapeutic tool to reduce expression of target transcripts (Rao *et al.*, 2009). RNAi is an endogenous cellular defense mechanism against exogenous viral components and is also involved in transcriptional regulation (Ding and Voinnet, 2007). Specific knock down of target sequences is achieved by introducing exogenously modified oligonucleotides (e.g. short hairpin RNA (shRNA) and short interfering RNA (siRNA)) that bind to the target transcript, which is subsequently degraded or its translation blocked. Recently an siRNA targeting both normal and mutant htt was found to be well-tolerated in wild-type rats (Drouet *et al.*, 2009). However, endogenous htt expression is important for normal cellular function, as underlined by the finding that conditional knockout of murine htt in forebrain and testis resulted in loss of function and progressive neurodegeneration (Dragatsis *et al.*, 2000). Total loss of the endogenous htt homolog in a Drosophila HD model expressing the human first exon of the *HTT* gene with 93 Qs enhanced the HD pathogenesis (Zhang *et al.*, 2009a). These studies show that a specific reduction of mutant htt levels, leaving as much wild-type htt protein as possible, would be the optimal outcome of a therapy aimed at htt knockdown. Specific reduction of the mutant htt transcript was shown by allele-specific siRNAs directed against a single nucleotide polymorphism (SNP) in htt exon 50 (van Bilsen *et al.*, 2008). In a recent study on the cleavage of triplet repeat hairpins by ribonuclease dicer it was shown that an siRNA with 7 consecutive CUG nucleotides specifically reduced the expression of the mutant htt transcript containing 44 CAG repeats in HD human fibroblasts (Krol *et al.*, 2007). Although off-target effects and

interference with endogenous RNAi processes remains to be assessed (McBride *et al.*, 2008), these results are encouraging.

Another RNA based therapy approach to knock down gene or protein expression is the use of single stranded antisense oligonucleotides (AON). One of the most promising examples of AON treatment in a neurodegenerative disease is aimed at amyotrophic lateral sclerosis (ALS). In ~2% of ALS patients, the disease is caused by a mutation in superoxide dismutase 1 (SOD1) (Robberecht, 2000). Continuous intraventricular infusion of AONs successfully down regulated SOD1 mRNA and protein levels in the brain and significantly slowed disease progression in an animal model of ALS (Smith *et al.*, 2006). A clinical trial is currently ongoing in ALS patients with SOD1 mutations and results are expected this year (ClinicalTrials.gov, 2009).

For glutamine-expansion disorders, peptide nucleic acid (PNA) and locked nucleic acid (LNA) antisense oligomers targeting CAG repeats have been used to reduce expanded HD and SCA3 transcripts *in vitro* (Hu *et al.*, 2009a; Hu *et al.*, 2009b; Gagnon *et al.*, 2010; Hu *et al.*, 2011). However, although PNA transfection efficiently reduced mutant protein levels with very long glutamine expansions, the reductions on polyQ lengths that occur most frequently in the HD patient population were less pronounced (Hu *et al.*, 2009a; Hu *et al.*, 2009b). In the current we make use of 2'-O-methyl (2OMe) modified RNA AONs with a phosphorothioate (PS) backbone carrying different CUG numbers. We examine the effect of (CUG)n AONs on mRNA level in cell lines derived from HD, SCA1, SCA3, and DRPLA patients with CAG expansions that occur most frequently in the patient population. A significant reduction in expanded transcript levels was found in patient derived fibroblast from HD, SCA1, SCA3, and DRPLA. Furthermore a significant reduction of mutant htt protein was seen in the HD cells. For htt, a reduction in wild-type htt transcript levels was observed as well, but this reduction was less pronounced than for the mutant transcript. Lowering the AON concentration increased the specificity for the mutant transcript. These results show that one single antisense oligonucleotide could be a promising therapeutic treatment for all polyQ disorders.

3.3. Materials & Methods

Cell culture and transfection

Patient derived fibroblasts from HD (GM04022), SCA3 (GM06151), SCA1 (GM06927), and DRPLA (GM13716) (purchased from Coriell Cell Repositories, Camden, USA); and control fibroblasts FLB73 (kind gift from Dr. M.P.G. Vreeswijk, LUMC) were cultured at 37°C and 5% CO_2 in Minimal Essential Medium (Gibco Invitrogen, Carlsbad, USA) with 15% heat inactivated fetal bovine serum (Clontech, Palo Alto USA), 1% Glutamax (Gibco) and 100 U/ml penicillin/ streptomycin (Gibco). Human Epstein Barr Virus transformed lymphoblasts HL2.42 and HL2.93 were a kind gift from Prof. E. Bakker (Laboratory of Diagnostic Genome Analysis (LDGA), LUMC). Cells were cultured at 37°C and 5% CO_2 in RPMI 1640 medium (Gibco), containing 15% FBS, 1% glutamax and 100 U/ml P/S.

AON transfection was performed with 3.3 µl ExGen 500 polyethylenimine (PEI) (MBI Fermentas, Vilnius, Lithuania) per µg AON. AON and PEI were diluted in 150 mM NaCl to a total volume of 100 µl and mixtures were prepared according to the manufacturer's instruction. Four different transfection conditions were used: 1) transfection with 1-100nM $(CUG)_7$, 100nM $(CUG)_3$, 100nM $(CUG)_{12}$, 2) transfection with 10-100nM h40AON2 directed against exon 40 of the *DMD* gene (5'- UCC UUU CAU CUC UGG GCU C -3') (Control AON) (Aartsma-Rus *et al.*, 2002), 3) transfection without AON (Mock II), and 4) NaCl only (Mock I). Mixtures were added to a total volume of 2 ml of medium with 5% FBS. Four hours after transfection, medium was replaced with fresh medium and a second identical transfection was performed 24 hours after the first transfection. All AONs consist of 2'-O-methyl RNA and contain a full-length phosphorothioate backbone (Prosensa B.V. Leiden, the Netherlands).

RNA Isolation and RT-PCR

Forty eight hours after the first transfection cells were harvested by trypsinization and washed twice with Hanks buffered salt solution (HBSS) (Gibco). Total RNA was isolated from the cells using an RNeasy Mini Kit (QIAgen, Venlo, The Netherlands), with an on-column DNase treatment for approximately 30 minutes. RNA was eluted in 50 µl elution buffer and cDNA was synthesized from total RNA using the Transcriptor First Strand cDNA Synthesis Kit with Random Hexamer primers at 65°C (Roche, Mannheim, Germany).

PCR was performed using 1 µl cDNA, 10x PCR buffer with 1.5 mM $MgCl_2$ (Roche), 2mM dNTPs, 10 pmol forward primer, 10 pmol reverse primer, 1U FastStart Taq DNA Polymerase (Roche), 1M Betaine (Sigma-Aldrich, St. Louis, USA), and PCR grade water to a final volume of 20 µl. PCR was performed with primers for HTT, ATXN1, ATXN3, and ATN1 (all flanking the CAG repeat), ACTB, and RPL22 (for sequences, see **Table S1**). The PCR program started with a 4 min initial denaturation at 95°C, followed by 35 cycles of 30 sec denaturation at 95°C, 30 sec annealing at 60°C (56°C for ATXN3), 45 sec elongation at 72°C, after which a final elongation step was performed at 72°C for 7 min.

Lab-on-a-Chip was performed on the Agilent 2100 Bioanalyzer (Agilent Technologies, Waldbronn, Germany), using the Agilent DNA 1000 Kit. Expression levels were normalized for β-actin levels and relative to transcript levels without transfection (Mock I). The relative mutant transcript levels were analyzed using a paired two-sided Student t test. Differences were considered significant when $P < 0.05$.

qPCR, Calculations and Sequencing. The qPCR was performed using 1 µl of 5x diluted cDNA, 2x FastStart Universal SYBR Green Master mix (Roche), 2.5 pmol forward primer, 2.5 pmol reverse primer and PCR grade water to a total volume of 10 µl. Primer pairs for 6 transcripts containing long uninterrupted CAG repeats were selected for qPCR by BLAST analysis and ACTB and RPL22 were used as reference genes. (For primer list, see **Table S1**). The qPCR was performed using the LightCycler 480 (Roche). Initial denaturation was 10 min. at 95°C, followed by 45 cycles of 10 sec. denaturation at 95°C, 30 sec. annealing at 59°C and 20 sec. elongation at 72°C. The final elongation was performed 5 min. at 72°C. Next, we performed a melting curve analysis of all samples from 60°C to 98°C with a ramp rate of 0.02°C per sec.

Relative expression of the transcript levels was calculated as described previously (Pfaffl, 2001). All samples were run in triplicate on a plate and two independent experiments were performed for each sample. On all plates both reference genes were included to correct for inter-plate variance.

Primer efficiencies were determined using LinRegPCR v11.1 (Ruijter *et al.*, 2009) with the raw data amplification curves as input and Mock II was used as reference. Values from the mock water transfected cells (Mock I) were set on 100%. The relative transcript levels were analyzed using a paired two-sided Student t test. Differences between groups were considered significant when $P < 0.05$.

CAG repeats of the CAG enclosing transcripts were amplified using primers flanking the CAG repeat (see **Table S1**). PCR products were loaded on an agarose gel and bands were extracted using the QIAquick Gel Extraction Kit (QIAgen). The purified products were sequenced by Sanger sequencing, using the Applied Biosystems 96-capillary 3730XL system (Life Technologies Corporation, Carlsbad, USA) with the Applied Biosystems BigDyeTerminator v3.1 kit.

Protein isolation and Western blotting

Cells were detached from the culture surface with a 0.5% Trypsin/EDTA solution. After washing twice with 1x HBSS, cells were resuspended in 200 µl ice cold lysis buffer, containing 1x PBS, 0.4% Triton-X100, and 1 tablet Complete mini protease inhibitor EDTA free (Roche) per 10 ml buffer. Next, samples were sonicated 3 times for 5 seconds using ultrasound with an amplitude of 60 at 4°C. After incubation in a head-over-head rotor at 4°C for 1 hour, the extract was centrifuged for 15 min at 10,000g and 4°C and supernatant was isolated. Protein concentrations were determined by the bicinchoninic acid kit (Thermo Fisher Scientific, Waltham, USA) using Bovine Serum Albumin as a standard. Samples were snap frozen and stored at -80°C.

Protein extracts were separated by SDS-PAGE, with 4-15% acryl/bisacrylamide 1:37.5 separating gels and 30 µg (human fibroblasts) of protein lysate loaded. For each sample the Spectra Multicolor High Range Protein Ladder (Fermentas) was used as a marker. Electrophoresis was performed for 30 min at 100V through the stacking gel and 5 hours at 150V through the running gel. Gels were blotted onto a polyvinylidene fluoride (PVDF) membrane for 3 hours at 300mA. Membranes were blocked with 1x Tris Buffered Saline + 0.5% Tween 20 (TBST) containing 5% non-fat milk powder (Profitar Plus, Nutricia, Zoetermeer, the Netherlands). The antibodies used for detection were mouse 4C8 for htt (Eurogentec, Liege, Belgium) dilution 1:1000, mouse 1C2 specific for expanded poly glutamine stretches (Eurogentec) dilution 1:500, mouse ataxin-3 (Eurogentec) 1:1000, rabbit TBP (Santa Cruz Biotechnology, USA) 1:1000, and mouse β-actin, diluted 1:5000. Secondary antibodies were goat α-mouse-horseradish peroxidase (Santa Cruz) and goat α-rabbit-horseradish peroxidase (Santa Cruz), both diluted 1:10.000 in 1x TBST. Horseradish peroxidase was activated by ECL+ reagent (GE Healthcare, Buckinghamshire, United Kingdom) to visualize positive staining on film.

Protein bands were quantified using ImageJ software. The percentage of inhibition was calculated as a relative value to a non-treated control sample and was normalized using β-actin.

3.4. Results

$(CUG)_7$ AON shows most pronounced reduction of HTT transcript levels

Patient-derived human fibroblasts were transfected with AONs with 3, 7 and 12 consecutive CUGs ($(CUG)_3$, $(CUG)_7$, and $(CUG)_{12}$, respectively) and total RNA was isolated after 48 hours. In the *HTT* gene the glutamine repeat consists of a CAG stretch, followed by one CAA and a final CAG triplet. The HD cell line GM04022 contained a $(CAG)_n$ CAA CAG repeat with n = 18 and 44. As a control fibroblasts cell line FLB73 was used where n = 17 and 21. To avoid influences of CAG repeat length, reductions in total HTT mRNA levels were measured by quantitative PCR (qPCR) with primers within the CAG containing exon but amplifying a transcript fragment upstream of the repeat (**Table S1**). The most significant reduction in total HTT transcript of 81% (± 4%) in the HD and 76% (± 4%) in the control fibroblasts was found after $(CUG)_7$ treatment (**Figure 1**). $(CUG)_{12}$ transfection resulted in a significant reduction of total HTT transcript of 78% (± 5%) in the HD and 61% (± 18%) in the control cell line. The (CUG)3 did not show significant reduction of HTT mRNA levels. The $(CUG)_7$ AON was selected for further testing since it was the shortest AON resulting in the most significant reduction in HTT mRNA levels.

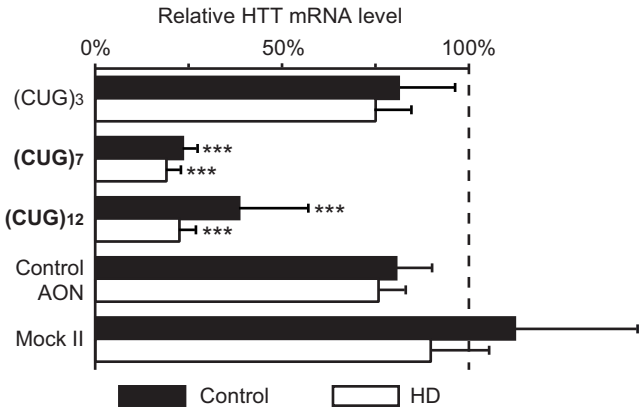

Figure 1. Number of CUGs of AON influences the reduction of HTT transcript levels. Total RNA was isolated 48 hours after transfection. Quantitative RT-PCR was used to measure HTT mRNA levels in control and HD fibroblasts after treatment with 100nM $(CUG)_3$, $(CUG)_7$, $(CUG)_{12}$ AON, 100nM non-htt specific h40AON2 (Control AON), transfection agent only (Mock II), or non-transfected cells (Mock I, not included in this figure). ACTB and RPL22 are used as reference genes. The expression level of Mock I transfections are set to 100%. For all transfections n = 6 and *** $P < 0.001$.

Reduction of mutant HTT mRNA levels in HD cells after $(CUG)_7$ treatment

Since regular htt expression is important for normal cellular function, our approach is to lower mutant htt protein levels, while maintaining sufficient levels of normal protein. To examine the effect of $(CUG)_7$ treatment on both HTT transcripts an allele-specific PCR with primers flanking the CAG repeat was performed in quadruplo (**Figure 2a**). The mutant transcript was decreased by 83% (± 13%, measured by Lab-on-a-Chip analysis) in $(CUG)_7$ treated cells compared to controls, while normal transcript was reduced to a lesser extent with 43% (± 32%) (**Figure 2b**). Treatment of the control cell line with $(CUG)_7$ showed a reduction for both alleles of 21% (± 38%) and 40% (± 38%) respectively.

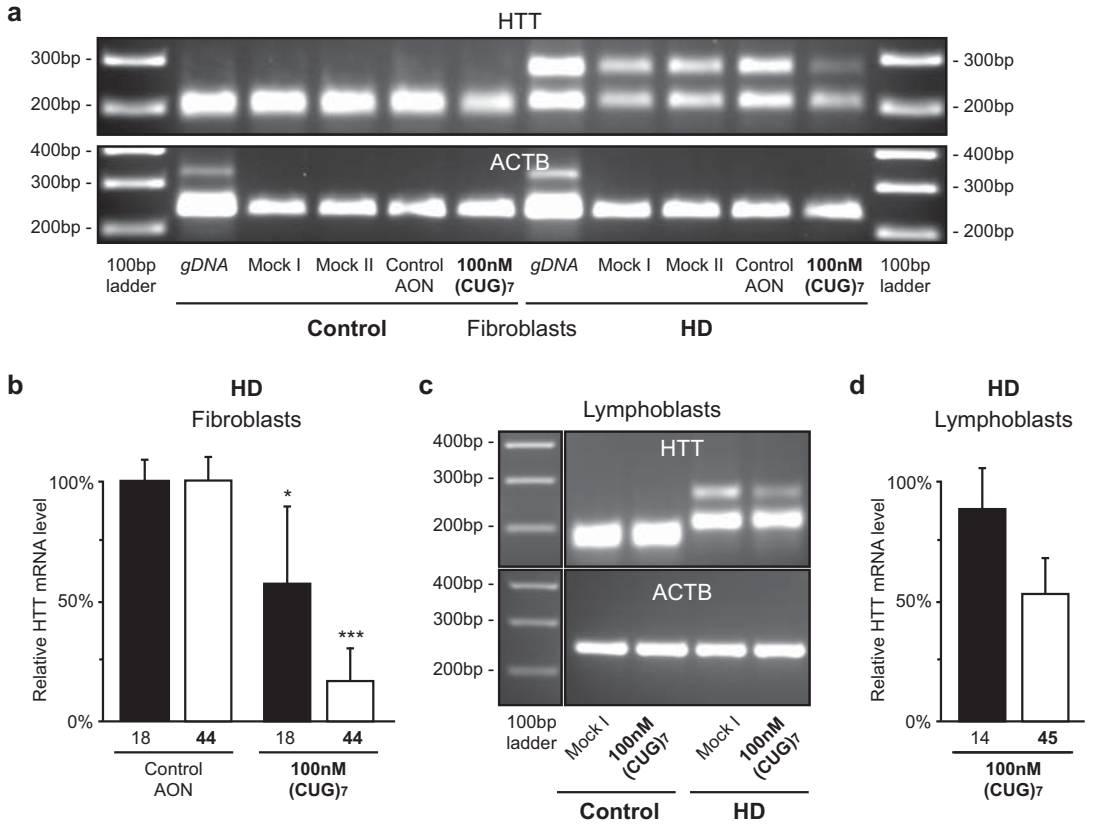

Figure 2. Effect of $(CUG)_7$ AON on HTT mRNA levels in HD patient derived cell lines 48 hours after transfection. Cells were transfected with 100nM $(CUG)_7$, non-htt specific h40AON2 (Control AON), transfection agent only (Mock II), or non-transfected cells (Mock I). **(a)** Agarose gel analysis of the HTT transcript with primers flanking the CAG repeat of control (FLB73) and HD (GM04022) fibroblasts treated with various AONs. Transfection with $(CUG)_7$ shows a decrease of the upper band, representing the transcript from the mutant allele. The lower band, representing the normal HTT transcript, is also reduced, but to a lesser extent. Control cells treated with $(CUG)_7$ only show a slight reduction compared to the control transfections. PCR products with primers for ACTB were used as loading control. gDNA was taken along to control for the PCR reaction over the CAG repeat. **(b)** Lab-on-a-Chip analysis of HTT transcripts after $(CUG)_7$ treatment in a HD fibroblast cell line. The mutant transcript, with 44 CAGs, is significantly reduced by 83% after $(CUG)_7$ treatment, compared to transfection controls. The normal HTT transcript with 18 CAGs is reduced by 43%. Expression levels are corrected for loading differences with ACTB. The mRNA level of the Mock I transfection was set on 100% (* $P < 0.05$, *** $P < 0.001$, n = 4). **(c)** Agarose gel analysis of HTT transcripts after $(CUG)_7$ treatment in EBV transformed control and HD human lymphoblasts. After transfection with $(CUG)_7$ the mutant HTT transcript with 45 CAGs is decreased compared to the Mock transfection. No changes in intensity of the HTT transcripts from the control lymphoblasts are seen after $(CUG)_7$ treatment. **(d)** Lab-on-a-Chip analysis of HTT transcripts after PS57 treatment of human HD lymphoblasts. Mutant HTT transcript is reduced by 46% after $(CUG)_7$ treatment, whereas the normal HTT allele shows an 11% reduction. (n = 2)

We repeated this experiment in duplo in patient-derived Epstein Barr Virus transformed control and HD lymphoblasts (**Figure 2c**). $(CUG)_7$ transfection of the HD cell line gave a reduction of the mutant transcript of 53% (± 10%), while only a small decrease of 22% (± 11%) for the normal transcript was detected (**Figure 2d**). No apparent reduction in the control cell line was found (data not shown).

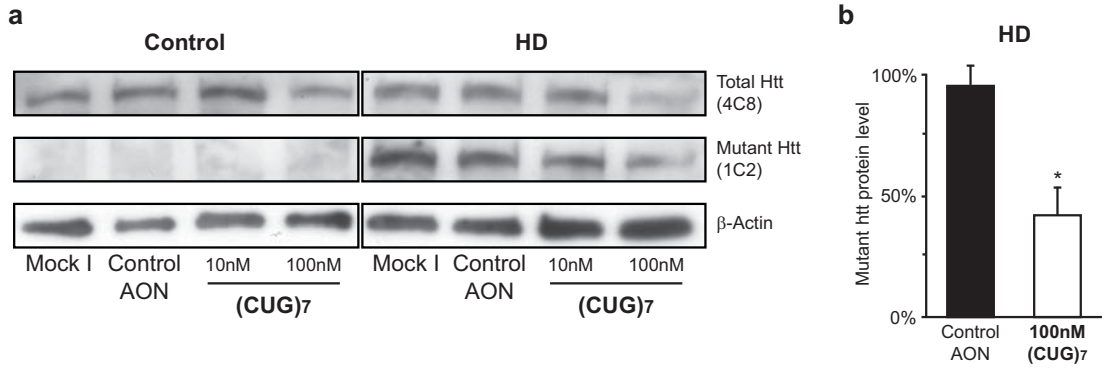

Figure 3. $(CUG)_7$ AON reduces mutant htt protein levels in HD patient fibroblast cell lines. Cells were transfected with 10nM and 100nM $(CUG)_7$, non-htt specific h40AON2 (Control AON), or non-transfected cells (Mock I). **(a)** Western blot of control (FLB73) and HD (GM04022) fibroblasts treated with $(CUG)_7$ and controls. Total (4C8) and mutant (1C2) htt protein expression is reduced 72 hours after treatment with $(CUG)_7$. No mutant htt could be detected in the control fibroblasts with 1C2. β-actin is used as loading control. **(b)** Mutant htt protein levels in HD (GM04022) fibroblasts after 100nM $(CUG)_7$ transfection were quantified by ImageJ software. A significant reduction of 58% of mutant htt protein was seen after $(CUG)_7$ transfection as compared to control transfections (* $P < 0.05$, n = 2). Mutant protein levels of Mock I transfection were set to 100%.

Reduction of mutant htt protein levels in a HD cell line after $(CUG)_7$ treatment

Since mRNA levels of the HTT transcript were substantially reduced after treatment with $(CUG)_7$, in both experiments, we investigated htt protein levels (**Figure 3a**). Antibody 4C8 can be used to detect total htt protein (Trottier *et al.*, 1995a), while antibody 1C2 specifically recognizes the expanded polyQ tract (Trottier *et al.*, 1995b). Patient-derived human fibroblasts were transfected and protein isolated (see Materials and Methods). 96 hours after first treatment of HD fibroblasts with 100nM $(CUG)_7$ 4C8 antibody showed a clear reduction of 54% (± 34%) in htt protein level, while a less pronounced reduction of 16% (± 28%) was observed in the control fibroblasts (**Figure 3a** and data not shown). With 1C2 antibody a significant reduction of 58% (± 16%) of mutant htt protein was seen in the HD fibroblasts following 100nM $(CUG)_7$ treatment (**Figure 3b**). Thus, reduction of mutant htt protein was more pronounced than normal htt.

$(CUG)_7$ AON efficiency is concentration dependent

To test if $(CUG)_7$ AON concentration is related to efficacy, various AON concentrations were used to transfect HD and control fibroblasts. Lab-on-a-Chip analysis (**Figure 4a and b**) showed a reduction of mutant HTT with an IC50 value between 2.5nM and 5nM (**Figure 4b**). At 10nM $(CUG)_7$ the mRNA expression of mutant HTT was reduced by 89% (± 5%), whereas normal HTT transcript was reduced by 38% (± 9%) in the HD fibroblasts. HTT mRNA reduction was less pronounced for both alleles (16% (± 6%) and 36% (± 5%)) in the control cells, suggesting that at lower concentrations the $(CUG)_7$ AON is more specific at reducing HTT transcripts with expanded CAG repeats (**Figure 4a**).

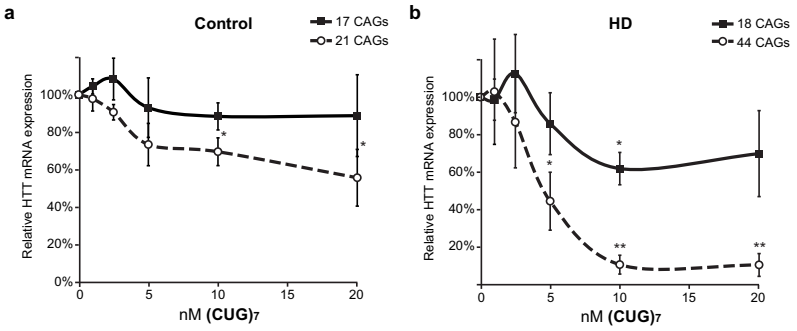

Figure 4. Effect of various $(CUG)_7$ AON concentrations on HTT mRNA expression. Cells were transfected with 1-20nM $(CUG)_7$. PCR products with primers flanking the CAG repeat of HTT were quantified by Lab on a Chip. **(a)** In the control cell line (FLB73) both alleles (17 and 21 CAGs) show a comparable concentration dependent reduction of HTT mRNA quantification after $(CUG)_7$ transfection. **(b)** In HD fibroblasts (GM04022) the mutant transcript, with 44 CAGs, shows a strong reduction of mutant HTT mRNA expression with increasing $(CUG)_7$ AON concentrations, whereas the normal HTT transcript with 18 CAGs is reduced to a lesser degree. Expression levels are corrected for loading differences with ACTB and mRNA levels of the Mock I transfections were set on 100% (* $P < 0.05$, ** $P < 0.01$, n = 4).

AON directed against the CAG repeat reduces mutant ataxin-3 levels

Since CAG repeat expansions are a hallmark of several neurodegenerative disorders, we tested the molecular efficacy of our AON approach to reduce the expression of other genes as well. SCA3 patients have a CAG triplet repeat expansion in the ATXN3 gene, we examined the effect of $(CUG)_7$ treatment in patient-derived SCA3 fibroblasts with a CAG CAA $(CAG)_n$ repeat where n = 18 and 72. As for htt, the $(CUG)_7$ treatment reduced the transcript from the expanded ataxin-3 allele, while reduction in transcript levels from the normal allele was less pronounced (**Figure 5a**).

PCR with primers amplifying a product containing the CAG repeat in ATXN3 showed a significant 97% (± 1%) down regulation of mutant ATXN3 after both 10nM and 100nM $(CUG)_7$ AON transfection (**Figure 5b**). The wild-type allele was reduced by respectively 27% (± 17%) and 33% (± 6%) by 10nM and 100nM after $(CUG)_7$ AON treatment.

Reduction on other expanded CAG transcripts by $(CUG)_7$ treatment

We next tested SCA1 and DRPLA fibroblasts. Allele-specific PCRs with primers flanking the CAG repeat were performed to examine the effect of $(CUG)_7$ treatment in both the normal and mutant allele. The mutant ataxin-1 (ATXN1) transcript was decreased by 89% (± 14%) in 100nM $(CUG)_7$ treated SCA1 cells compared to control transfections (**Figure 6a and c**), while the normal transcript was not reduced. (The SCA1 and DRPLA cell lines served as each other's control.) Mutant atrophin-1 (ATN1) in DRPLA was also reduced after 100nM $(CUG)_7$ treatment by 98% (± 2%), whereas there was only a 30% (± 6%) reduction in the normal allele (**Figure 6b and d**).

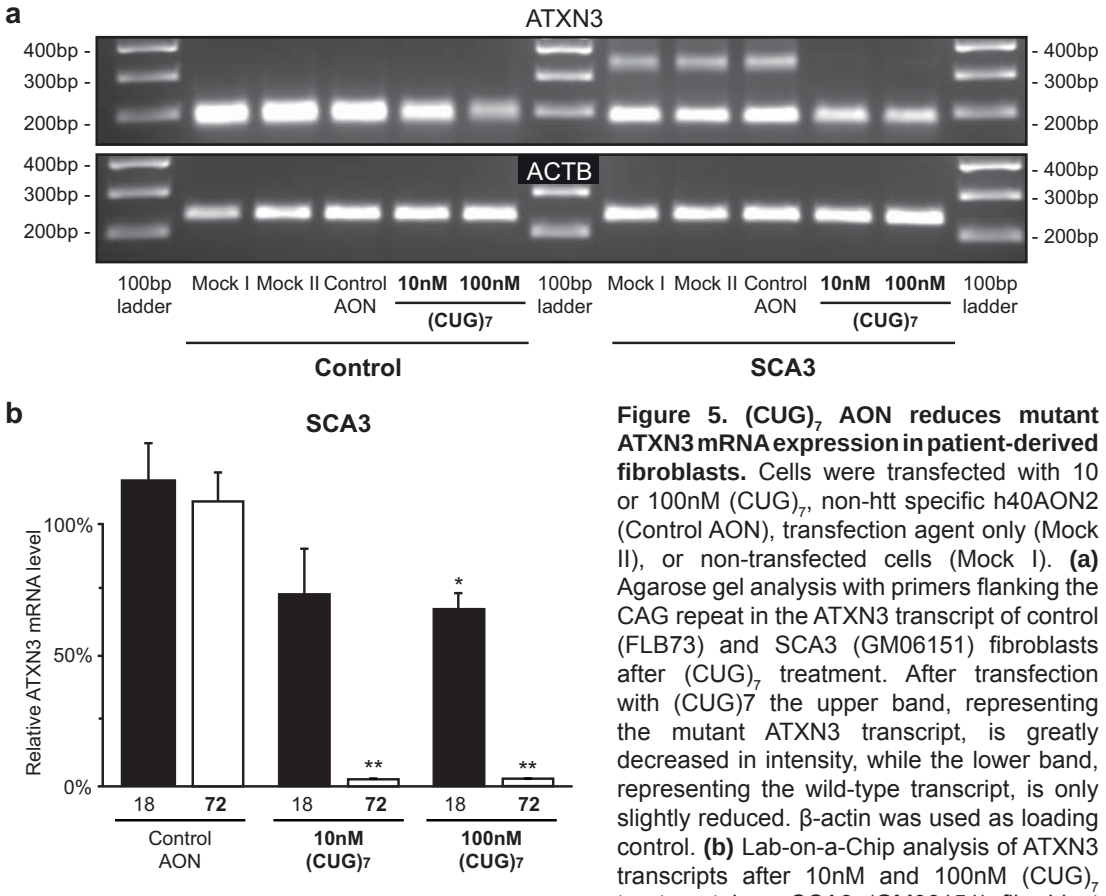

Figure 5. $(CUG)_7$ AON reduces mutant ATXN3 mRNA expression in patient-derived fibroblasts. Cells were transfected with 10 or 100nM $(CUG)_7$, non-htt specific h40AON2 (Control AON), transfection agent only (Mock II), or non-transfected cells (Mock I). **(a)** Agarose gel analysis with primers flanking the CAG repeat in the ATXN3 transcript of control (FLB73) and SCA3 (GM06151) fibroblasts after $(CUG)_7$ treatment. After transfection with (CUG)7 the upper band, representing the mutant ATXN3 transcript, is greatly decreased in intensity, while the lower band, representing the wild-type transcript, is only slightly reduced. β-actin was used as loading control. **(b)** Lab-on-a-Chip analysis of ATXN3 transcripts after 10nM and 100nM $(CUG)_7$ treatment in a SCA3 (GM06151) fibroblast cell line. The mutant transcript, with 72 CAGs, is significantly reduced by 97% after $(CUG)_7$ treatment, compared to transfection controls. The normal ATXN3 transcript with 18 CAGs is reduced by 27% and 33% after 10nM and 100nM $(CUG)_7$ AON treatment, respectively. Expression levels are corrected for loading differences with β-actin. The mRNA level of the Mock I transfection was set on 100% (* $P < 0.05$, ** $P < 0.01$, n = 2).

$(CUG)_7$ does not affect other endogenous CAG-enclosing transcripts

The human genome contains several proteins that contain polyQ tracts, usually encoded by a combination of CAG and CAA triplets. Most of these transcripts are essential for normal cellular function (Molla *et al.*, 2009) so reducing those transcripts could impair normal cellular function. To verify whether other uninterrupted CAG repeat containing transcripts were affected, 5 other transcripts were selected after a BLAST search: androgen receptor (AR), ataxin-2 (ATXN2), glutaminase (GLS), TBP, and zinc finger protein 384 (ZNF384). For the cells used in the present study the exact CAG tract length of these 5 transcripts was first determined by Sanger sequencing (**Table 1**). Primers for qPCR were designed within the CAG containing exon but amplifying a fragment downstream of the CAG repeat in the transcript (**Table S1**). For technical reasons primers for ATXN2 were designed upstream of the CAG repeat.

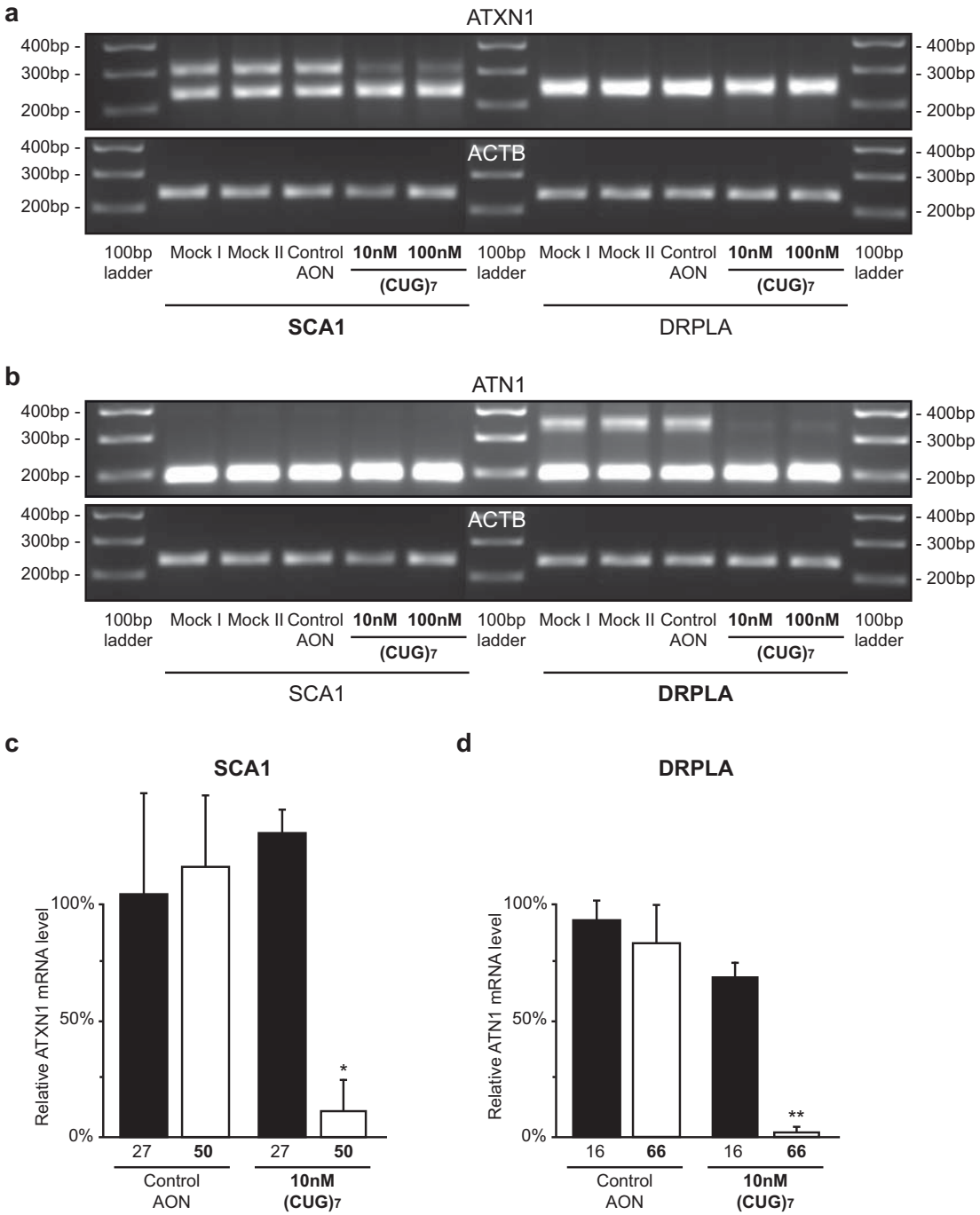

Figure 6. $(CUG)_7$ AON reduces mutant ATXN1 and ATN1 transcripts in SCA1 and DRPLA fibroblasts. SCA1 (GM06927) and DRPLA (GM13716) patient derived fibroblasts were transfected with 10 and 100nM $(CUG)_7$, 10nM non-htt specific h40 AON2 (Control AON), transfection agent only (Mock II), or non-transfected cells (Mock I). **(a)** Agarose gel analysis with primers flanking the CAG repeat in the ATXN1 transcript. After transfection with both 10nm and 100nM $(CUG)_7$ the upper band, representing the mutant ATXN1 transcript, is greatly decreased in intensity, while the lower band, representing the wild-type transcript, is not reduced. β-actin was used as loading control. **(b)** Agarose gel analysis with

primers flanking the CAG repeat in the ATN1 transcript. After transfection with both 10nM and 100nM $(CUG)_7$, the upper band representing the mutant ATN1 transcript, is greatly decreased in intensity, while the lower band representing the wild-type transcript, is not reduced. β-actin was used as loading control. **(c)** Lab-on-a-Chip analysis of ATXN1 transcripts in SCA1 cells after control AON and 10nM $(CUG)_7$ treatment. The mutant transcript, with 72 CAGs, is significantly reduced by 89% after $(CUG)_7$ treatment, compared to transfection controls. The normal ATXN1 transcript with 27 CAGs is not reduced. **(d)** ImageJ analysis of ATN1 transcripts in DRPLA cells after control AON and 10nM $(CUG)_7$ treatment. The 66 CAGs containing mutant ATN1 transcript is significantly reduced by 98% after $(CUG)_7$ treatment, while normal ATN1 transcript with 16 CAGs is not significantly reduced by 30%. Expression levels are corrected for loading differences with β-actin. The mRNA level of the Mock I transfection was set on 100% (* $P < 0.05$, ** $P < 0.01$, n = 3).

All tested CAG-enclosing transcripts were unaffected by 100nM $(CUG)_7$ treatment (**Figure 7**), including the AR transcript that contained CAG repeats of 21 and 23 CAGs. Endogenous ataxin-3 (with 17:18 Qs) and TBP (37:38 Qs) protein levels were unaffected by 100nM $(CUG)_7$ treatment (**Figure 8**). From the above results we can conclude that $(CUG)_7$ does not significantly reduce endogenous CAG containing transcripts and does not decrease endogenous polyQ-containing protein levels.

3.5. Discussion

The present study shows that an AON targeting CAG repeats and consisting of 7 CUGs significantly reduces protein and RNA levels of mutant htt in patient-derived fibroblast cell lines. This reduction was also seen, but to a lesser extends with $(CUG)_{12}$ but not with $(CUG)_3$. Although there was also a reduction of normal HTT transcript levels, the results show a preferential allele-specific reduction of mutant HTT in patient derived HD cells and this allele specificity was improved when AON concentration was lowered from 100nM to 10nM.

Furthermore, other non-expanded CAG-containing transcripts that were investigated were not affected by $(CUG)_7$ treatment. There was no reduction after $(CUG)_7$ treatment of the AR transcript that contained the longest tested uninterrupted CAG repeat, namely 21 and 23 CAGs. Normal HTT that contained 17 and 21 CAG repeats did show a reduction after $(CUG)_7$ treatment, suggesting that there are other factors besides the number of consecutive CAG triplets that determine $(CUG)_7$ efficacy.

The results with mutant ATXN1, ATXN3, and ATN1 confirmed the specificity of $(CUG)_7$ for transcripts with an expanded CAG tract in SCA1, 3, and DRPLA patient derived cells, respectively. Our results suggest that $(CUG)_7$ could

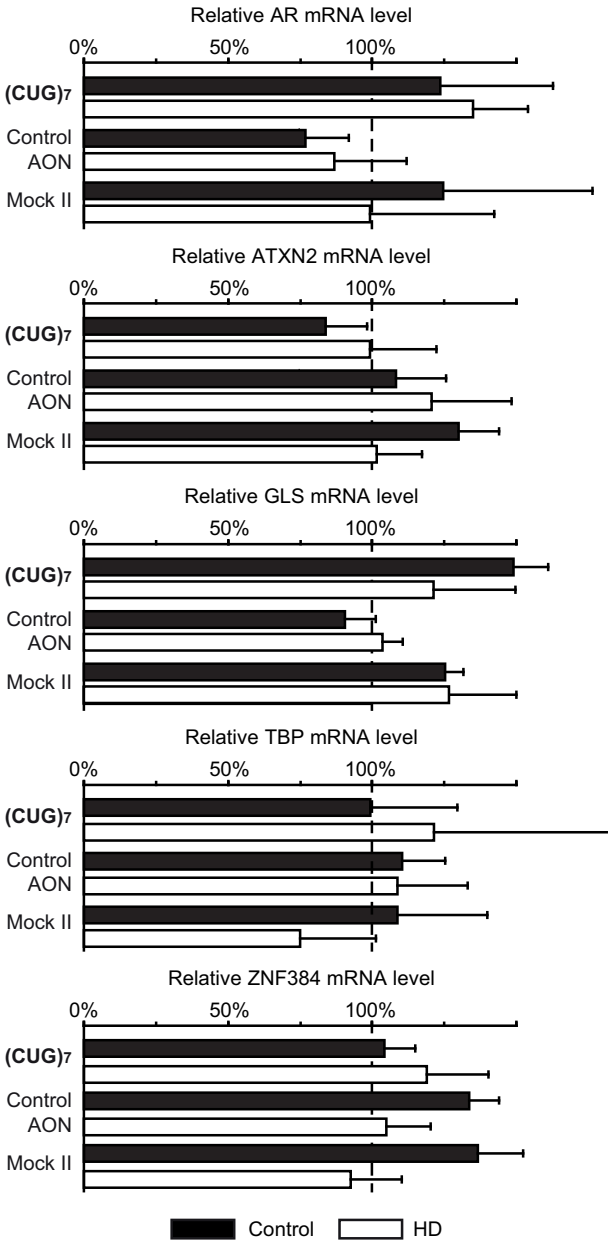

Figure 7. $(CUG)_7$ AON does not affect other CAG-containing transcripts. Quantitative real-time PCR was used to measure androgen receptor (AR), ataxin-2 (ATXN2), glutaminase (GLS), TATA box binding protein (TBP), and zinc finger protein 384 (ZNF384) mRNA levels in control and HD fibroblasts after treatment with 100nM $(CUG)_7$, non-htt specific h40AON2 (Control AON), transfection agent only (Mock II), or non-transfected cells (Mock I). All tested CAG-enclosing transcripts were unaffected by $(CUG)_7$ treatment. ACTB and RPL22 are used as reference genes. The expression level of Mock I transfections were set on 100% (n= 6)

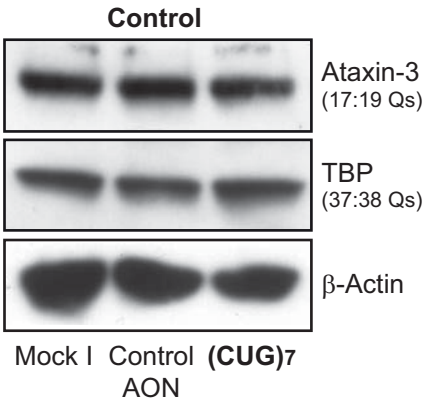

Figure 8. $(CUG)_7$ AON does not reduce other polyQ-containing proteins. Western blot of control (FLB73) fibroblasts treated with 100nM $(CUG)_7$, non-htt specific h40AON2 (Control AON), and non-transfected (Mock I). TATA box binding protein (TBP) and ataxin-3 are not reduced 72 hours after treatment with $(CUG)_7$. β-actin is used as loading control.

be effective in reducing expanded CAG repeat containing transcripts in all polyQ diseases.

In HD there is a gain of toxic function of the mutant htt protein, while regular htt expression is important for normal cellular function. Knockout of the homologous *htt* mouse gene was found to be early embryonic lethal (Zeitlin *et al.*, 1995) and previous studies have shown that approximately 50% of htt protein level is required to maintain cell functionality (Dragatsis *et al.*, 2000; Rigamonti *et al.*, 2000; Cattaneo *et al.*, 2001; Cattaneo *et al.*, 2005). In addition, increased clearance of mutant htt protein by autophagy in a Drosophila model and blockage of mutant htt in a conditional knock-out mouse model of HD resulted in a reduction in aggregates and an ameliorated phenotype (Yamamoto *et al.*, 2000; Sarkar *et al.*, 2007). Reduction of mutant protein levels will therefore most likely result in amelioration of the toxic HD phenotype but total knockdown of htt protein expression would not be advantageous (Sah and Aronin, 2011).

For other polyQ disorders the role of wild-type polyQ proteins in adult brain is still poorly understood. In a SCA3 Drosophila model expressing normal and mutant human ataxin-3, loss of normal ataxin-3 contributed to neurodegeneration (Warrick *et al.*, 2005). In contrast, non-allele-specific reduction of endogenous ataxin-3 was not found to be detrimental in rodents (Schmitt *et al.*, 2007; Alves *et al.*, 2010). Ataxin-1 knockout mice resulted in cerebellar transcriptional changes resembling SCA1 pathology, suggesting a neuroprotective role of normal ataxin-1 (Crespo-Barreto *et al.*, 2010). In contrast, atrophin-1 knockout mice were viable and did not show a clear phenotype (Shen *et al.*, 2007), suggesting that non-allele-specific reduction of both alleles in DRPLA is not harmful. Future research is necessary to determine the significance of wild-type polyQ protein levels for normal cellular function and the importance of AON-mediated allele-specific transcript reduction.

Several papers have shown allele-specific silencing of mutant htt with SNP-specific siRNAs (van Bilsen *et al.*, 2008; Zhang *et al.*, 2009b). Indeed HD patients carry different SNPs, requiring the development of at least five different siRNAs, to target 75% of the European and United States HD population (Lombardi *et al.*, 2009; Pfister *et al.*, 2009). However, the advantage of the approach described in the current paper is that it requires only 1 AON to treat all HD patients and would be applicable in other polyQ diseases. Furthermore, siRNAs are double stranded oligonucleotides and these have been described to cause off-target effects by the sense strand, (Fedorov *et al.*, 2006) as well as striatal toxicity (Grimm *et al.*, 2006; McBride *et al.*, 2008). In addition, RNA interference is an endogenous process; addition of siRNAs might cause toxicity due to an overload of the endogenous system. Recently, nucleic acids conjugates, with

Table 1. Number of uninterrupted CAGs and codons that encode for glutamine in CAG repeat enclosing transcripts as determined by Sanger sequencing and a summary of the effect of $(CUG)_7$ treatment in those transcripts.

Transcript Name	Cell Line	Glutamine stretch		Uninterrupted CAGs		Significant reduction after 100nM $(CUG)_7$ AON
		Allele 1	Allele 2	Allele 1	Allele 2	
AR	Control	22	24	21	23	No
	HD	23	24	22	23	No
ATN1	Control	19	20	15	16	No
	HD	12	19	8	15	No
	DRPLA	**20**	**70**	**16**	**66**	**Yes**
	SCA1	20	20	16	16	No
ATXN1	DRPLA	29	31	14	15	No
	SCA1	**29**	**52**	**14**	**37**	**Yes**
ATXN2	Control	20	20	8	8	No
	HD	20	20	8	8	No
ATXN3	**Control**	**17**	**19**	**15**	**17**	**Yes**
	HD	19	23	17	21	No
	SCA3	**20**	**74**	**18**	**72**	**Yes**
GLS	Control	8	14	8	14	No
	HD	7	18	7	18	No
HTT	**Control**	**19**	**23**	**17**	**21**	**Yes**
	HD	**20**	**46**	**18**	**44**	**Yes**
TBP	Control	37	38	17	18	No
	HD	35	36	16	17	No
ZNF384	Control	15	16	14	15	No
	HD	15	16	14	15	No

Abbreviations: AR, androgen receptor; ATN1, atrophin-1; ATXN1, ataxin-1; ATXN2, ataxin-2; ATXN3, ataxin-3; GLS, glutaminase; HTT, huntingtin; TBP, TATA box binding protein; ZNF384, zinc finger protein 384. Reduced transcripts after $(CUG)_7$ treatment are depicted in bold.

different chemistries than the AONs used in the current study, were used for allele-specific silencing of mutant htt. PNAs consisting of 1 guanine, followed by 6 CTGs, complementary to the CAG repeat, were found to specifically reduce mutant htt and ataxin-3 protein levels in patient-derived cells (Hu *et al.*, 2009a; Hu *et al.*, 2011). Although the reduction in protein levels by PNA transfection was highly efficient with very long stretches of CAGs, there was only a minor decrease when the number of CAG repeats that occur most frequently in the patient population was targeted (Hu *et al.*, 2009a; Hu *et al.*, 2009b). Testing a variety of modifications resulted in oligonucleotides with a thymine (T) LNA nucleotide at every third base (LNA(T)) and 2'O,4'O-C-ethyl nucleic acid (cET) which show higher selectivity (2.9 and 3.7 fold) for mutant alleles with 41 CAG repeats (Gagnon *et al.*, 2010).

AONs are a promising therapeutic tool, as was recently shown by phase I and phase I/II clinical trials in Duchenne muscular dystrophy (DMD) boys carrying specific deletions in the DMD gene (Goemans *et al.*, 2011). Local and systemic (subcutaneous) delivery of a specific 2OMe modified AON induced exon 51 skipping in the *DMD* gene on transcript level allowing the synthesis of novel, internally deleted, but likely (semi-) functional, dystrophin proteins without clinically apparent adverse events (van Deutekom *et al.*, 2007). AONs have also been used for the treatment of neurodegenerative disorders and are found to be taken up by neurons when delivered into the cerebral lateral ventricles. As treatment for ALS 2'-O-methoxyethyl modified deoxynucleotides infused intraventricularly were found to reduce both SOD1 transcript and protein levels in rats and rhesus monkeys, which resulted in a slower disease progression (Smith *et al.*, 2006). Similarly modified oligonucleotides for spinal muscular atrophy (SMA) resulted in putative therapeutic levels in all regions of the spinal cord after intrathecal infusion in non-human primates (Passini *et al.*, 2011).

The exact mechanism by which the AONs are used in the current study to reduce transcript levels and why they show both an allele and gene preference is not known. This selective repeat-length dependent reduction was also seen in myotonic dystrophy type 1 after $(CAG)_7$ AON treatment (Mulders *et al.*, 2009). Since 2OMe PS modified AONs are nuclease and RNase H resistant, RNase H-induced cleavage or RISC mediated degradation of dsRNA is not likely to be involved (Mulders *et al.*, 2009). Another explanation could be RNase H-independent translational blocking by $(CUG)_7$ AON binding to the transcript, preventing binding or steric blockage of the ribosomal units. However, translational blocking is not likely to be involved since htt transcript levels are also reduced (Hu *et al.*, 2009a). Reduction of transcript levels are not thought to be caused by interference of the $(CUG)_7$ AON during cDNA synthesis. Addition of $(CUG)_7$ AON just prior to the mRNA before cDNA synthesis did not result in reduced htt transcript levels (data not shown). A more likely explanation for the allele-specific effect of the $(CUG)_7$ AON shown in the current paper could be caused by structural differences in transcripts with normal and expanded repeats. Expanded CAG repeats are known to from hairpin structures (de Mezer *et al.*, 2011). $(CUG)_7$ AON binding could stabilize this CAG RNA hairpin, resulting in selective breakdown of the mutant transcripts. Another explanation could be that the expanded CAG repeats have a more open structure, making them more accessible for AON binding, thereby leading to induction of selective breakdown, resulting in a lower mRNA expression. These two models are not mutually exclusive and other mechanisms may as well be involved.

However, these results show that reduction of the mutant mRNA and/or its translation are promising generic routes towards therapy of triplet expansion diseases. Our future plans would be unraveling the exact mechanism of the reduction of HTT transcripts by the AON and *in vivo* testing of the toxicity and delivery of the $(CUG)_7$ in animal models of polyQ diseases.

Here we show the first evidence of a specific reduction of mutant huntingtin, ataxin-1 and -3, and atrophin-1 transcript levels using 2OMe PS modified AONs that recognizes pure CAG repeat stretches, suggesting that a single AON is potentially applicable to polyQ neurodegenerative diseases with an expanded pure CAG repeat.

3.6. Acknowledgments

Judith C.T. van Deutekom and Susan A.M. Mulders are employed by Prosensa Therapeutics B.V. (Leiden, The Netherlands). Prosensa Therapeutics B.V. holds a patent on the use of AONs to reduce CAG and GTG repeat containing transcripts and may (ultimately) benefit from the application of the submitted information. The LUMC does not have any patents on the reported area and has no financial relationship with Prosensa in the field of triplet expansion diseases, nor foresees to benefit otherwise from the use of the reported information.

This work was supported by the Center for Biomedical Genetics (The Netherlands); and Agentschap NL - IOP Genomics IGE07001 (The Netherlands).

3.7. Supplementary Material

Table S1. Used primers for Sanger sequencing and (quantitative) RT-PCR.

Transcript	Direction	Amplifying the CAG repeat	Without CAG repeat
HTT	Forward	ATGGCGACCCTGGAAAAGCTGAT	ATGGCGACCCTGGAAAAG
	Reverse	TGAGGCAGCAGCGGCTG	CTGCTGCTGGAAGGACTTG
AR	Forward	GACCTACCGAGGAGCTTTCC	TGCAACTCCTTCAGCAACAG
	Reverse	CTCATCCAGGACCAGGTAGC	TCGAAGTGCCCCCTAAGTAA
ATXN1	Forward	TGGAGGCCTATTCCACTCTG	
	Reverse	TGGACGTACTGGTTCTGCTG	
ATXN2	Forward	CCTCACCATGTCGCTGAAG	CTCCGCCTCAGACTGTTTTG
	Reverse	GGAGACCGAGGACGAGGAC	GAGAAGGAGGACGACGAAGG
ATXN3	Forward	GAGCTTCGGAAGAGACGAGA	GGGGACCTATCAGGACAGAG
	Reverse	GATCACTCCCAAGTGCTCCT	CAAGTGCTCCTGAACTGGTG
ATN1	Forward	CACCCACCAGTCTCAACACA	TCACAGCCAGGTGTCCTACA
	Reverse	GAGACATGGCGTAAGGGTGT	GTAGCCGAAGAGGTGGTGAC
GLS	Forward	TAGGCGGAGCGAAGAGAAC	ACCCAAGTAGCTGCCCTTTC
	Reverse	GCTCAACAGGGGAGGATG	GCTCAACAGGGGAGGATG
TBP	Forward	GACCCCACAGCCTATTCAGA	CCACAGCTCTTCCACTCACA
	Reverse	TTGACTGCTGAACGGCTGCA	GCGGTACAATCCCAGAACTC
ZNF384	Forward	ACATATGCGCAAACACAACC	CCACCACACTTCCAGTCTCC
	Reverse	CCAGGAGACTGGAAGTGTGG	TGACAGTGAGGCAGATGTCC
ACTB	Forward		GGACTTCGAGCAAGAGATGG
	Reverse		AGCACTGTGTTGGCGTACAG
RPL22	Forward		TCGCTCACCTCCCTTTCTAA
	Reverse		TCACGGTGATCTTGCTCTTG

All primer sequences are from 5' - 3'. Abbreviations are as follows: AR, androgen receptor; ATN1, atrophin-1; ATXN1, ataxin-1; ATXN2, ataxin-2; ATXN3, ataxin-3; GLS, glutaminase; HTT, huntingtin; TBP, TATA box binding protein; ZNF384, zinc finger protein 384; ACTB, β-actin; RPL22: ribosomal protein L22.

Melvin M. Evers [1]
Hoang-Dai Tran [1]
Ioannis Zalachoras [2]
Onno C. Meijer [2]
Johan T. den Dunnen [1,3,4]
Gert-Jan B. van Ommen [1]
Annemieke Aartsma-Rus [1]
Willeke M.C. van Roon-Mom [1]

[1] Department of Human Genetics, Leiden University Medical Center
[2] Department of Endocrinology, Leiden University Medical Center
[3] Leiden Genome Technology Center, Leiden University Medical Center
[4] Department of Clinical Genetics, Leiden University Medical Center

4

Preventing formation of toxic N-terminal huntingtin fragments through antisense oligonucleotide-mediated protein modification

Nucleic Acid Therapeutics 2014, 24(1):4-12

4.1. Abstract

Huntington's disease (HD) is a progressive autosomal dominant disorder, caused by a CAG repeat expansion in the HTT gene, which results in expansion of a polyglutamine stretch at the N-terminal end of the huntingtin protein. Several studies have implicated the importance of proteolytic cleavage of mutant huntingtin in HD pathogenesis and it is generally accepted that N-terminal huntingtin fragments are more toxic than full-length protein. Important cleavage sites are encoded by exon 12 of HTT. Here we report proof of concept using antisense oligonucleotides to induce skipping of exon 12 in huntingtin pre-mRNA, thereby preventing the formation of a 586 amino acid N-terminal huntingtin fragment implicated in HD toxicity. *In vitro* studies showed successful exon skipping and appearance of a shorter huntingtin protein. Cleavage assays showed reduced 586 amino acid N-terminal huntingtin fragments in the treated samples. *In vivo* studies revealed exon skipping after a single injection of antisense oligonucleotides in the mouse striatum. Recent advances to inhibit the formation of mutant huntingtin using oligonucleotides seem promising therapeutic strategies for HD. Nevertheless, huntingtin is an essential protein and total removal has been shown to result in progressive neurodegeneration *in vivo*. Our proof of concept shows a completely novel approach to reduce mutant huntingtin toxicity not by reducing its expressing levels, but by modifying the huntingtin protein.

4.2. Introduction

Polyglutamine (polyQ) diseases are a group of autosomal dominant neurodegenerative disorders caused by a CAG triplet repeat expansion in protein coding regions of the genome. The most prevalent polyQ disorder, Huntington's disease (HD), is caused by a CAG repeat expansion in the first exon of the *HTT* gene on chromosome 4p16. The expanded CAG transcript is translated into a mutant huntingtin (htt) protein with an expanded polyQ tract at the N-terminus. Carriers of 40 or more CAG repeats will develop HD, whereas people with 35 to 39 repeats show reduced penetrance (Mcneil *et al.*, 1997). The disease is characterized by motor, psychiatric and cognitive impairments and the typical age of onset lies between 30 and 50 years and is inversely correlated to the number of CAGs (Andrew *et al.*, 1993).

In HD, insoluble protein aggregates are found in the nucleus and cytoplasm of cells, indicating that htt protein misfolding is a common feature (Ross and Tabrizi, 2011). Major neuropathology occurs in the striatum but degeneration is seen throughout the brain when the disease progresses (Vonsattel and Difiglia, 1998). Many cellular processes are affected in HD, as is evident from transcriptional de-regulation, mitochondrial dysfunction, and impaired vesicle transport (Ross and Tabrizi, 2011). Several studies have implicated the importance of apoptosis and specifically proteolytic cleavage of mutant htt in HD pathogenesis (Ehrnhoefer *et al.*, 2011). Exon 1 of the *HTT* gene with an expanded CAG repeat is sufficient to induce symptoms in the R6/2 mouse model of HD (Mangiarini *et al.*, 1996), also shorter htt fragments seems to be more pathogenic than longer htt fragments (Crook and Housman, 2011). Aggregates in brains of HD patients can be stained with antibodies directed at N-terminal epitopes but not C-terminal epitopes of htt (Lunkes *et al.*, 2002), suggesting that aggregates contain truncated N-terminal htt fragments. In apoptotic cells, htt is cleaved by cysteine aspartic acid proteases, called caspases (Goldberg *et al.*, 1996). Mutations in caspase-3 at amino acid positions 513 and 552 and caspase-6 motifs at position 586 in mutant htt resulted in cleavage-resistant neuronal and non-neuronal cells with reduced toxicity and less aggregates *in vitro* (Wellington *et al.*, 2000). *In vivo* it was also shown that mutation of amino acid position 586 in the caspase-6 cleavage motif resulted in reversal of the HD phenotype in a YAC128 mouse model (Graham *et al.*, 2006; Pouladi *et al.*, 2009). These mice express the full human genomic HTT, which is translated into a mutant htt protein with 128 glutamines. Using the same YAC128 model, no improvement of HD phenotype was seen after mutations in the caspase-3 cleavage sites at amino acid positions 513 and 552. This suggests that cleavage at position 586 is an important step in HD neuropathology and results in neuronal dysfunction and neurodegeneration (Graham *et al.*, 2006).

Recent advances to inhibit the formation of mutant htt using oligonucleotides seem promising therapeutic strategies for HD (Sah and Aronin, 2011). These approaches make use of RNA interference (RNAi), RNAi-like mechanisms using single-stranded RNAs (ssRNAs) or antisense oligonucleotides (AONs) (Sah and Aronin, 2011; Yu *et al.*, 2012). Lowering mutant htt protein levels would prevent all downstream toxic effects, but complete suppression of

htt may not be desirable since wild-type htt has numerous cellular functions. Htt is reported to act as protector of brain cells from apoptotic stimuli (Rigamonti *et al.*, 2000) and is required in adult neurons and testis (Dragatsis *et al.*, 2000). Knock-out of the homologous htt mouse gene was found to be early embryonic lethal (Zeitlin *et al.*, 1995) and htt inactivation in adult mice was shown to result in progressive neurodegeneration (Dragatsis *et al.*, 2000). However, non-allele-specific reduction of both normal and mutant htt transcripts up to 75% was found to be well tolerated in HD rodents and non-human primates (Boudreau *et al.*, 2009; Drouet *et al.*, 2009; McBride *et al.*, 2011; Kordasiewicz *et al.*, 2012) and resulted in phenotypic reversal up to 4 months post treatment (Kordasiewicz *et al.*, 2012). Although studies so far have shown that lowering of htt levels can be well tolerated, safety and specificity of htt transcript lowering drugs after long-term exposure need to be assessed.

Allele-specific reduction would be preferred since this would leave the wild-type htt protein levels unchanged. This was achieved with oligonucleotides directed against single nucleotide polymorphisms (SNPs) unique to the mutant htt transcript (van Bilsen *et al.*, 2008; Lombardi *et al.*, 2009; Pfister *et al.*, 2009; Warby *et al.*, 2009; Zhang *et al.*, 2009; Carroll *et al.*, 2011). Another approach for an allele-specific reduction of mutant htt is targeting the expanded CAG repeat. Oligonucleotides complementary to the CAG repeat were found to result in allele-specific reduction of htt transcript and protein levels in patient derived cells (Krol *et al.*, 2007; Hu *et al.*, 2009; Gagnon *et al.*, 2010; Yu *et al.*, 2012; Chapter 3).

A novel way to alter toxicity of the mutant htt protein is through protein modification. The major advantage of this approach is that htt transcript and protein levels are unchanged. Using AONs it is possible to mask exons from the splicing machinery resulting in exclusion of the targeted exon (Spitali and Aartsma-Rus, 2012). When the reading frame is intact or restored after exon skipping there is subsequent translation of a modified protein. This exon skipping is a promising therapeutic tool that is already in phase II/III clinical trial for Duchenne muscular dystrophy (DMD) (Cirak *et al.*, 2011; van Putten and Aartsma-Rus, 2011).

In this study we use 2'O-methyl modified AONs with a phosphorothioate backbone to induce an in-frame partial exon 12 skip in human htt pre-mRNA. This resulted in a shorter htt protein lacking the 552 caspase-3 and 586 caspase-6 cleavage site, while total htt protein levels were unaltered. Using *in vitro* caspase-6 cleavage assay, AON treated samples showed less 586 N-terminal htt fragments implied in expanded htt toxicity. Injection of a single dose of AONs in the mouse striatum also resulted in removal of the same 552 caspase-3 and 586 caspase-6 cleavage sites, further supporting the concept that proteolytic site removal by exon skipping could be a potential therapeutic approach to prevent formation of toxic N-terminal htt fragments.

4.3. Materials and Methods

Antisense oligonucleotide design

Our AONs were designed following the guidelines described by Aartsma-Rus (Aartsma-Rus, 2012). In short, the AONs were designed to anneal to in silico predictions of potential exonic splicing enhancer sites (ESEs) (Desmet *et al.*, 2009), which have been shown to be an efficient modulator of splicing (Aartsma-Rus *et al.*, 2005; Wilton *et al.*, 2007). Primarily, AON design was based on targeting an open region in the secondary structure of the target exon as predicted by m-fold (Zuker, 2003) and ensuring favorable thermodynamic properties (Aartsma-Rus *et al.*, 2009). Furthermore, cytosine-phosphate-guanine (CpG) dinucleotides were avoided in the AON design, as these potentially activate the Toll-like receptor-9 inflammatory response (Bauer *et al.*, 2001). Finally, sequences were BLAST-verified using megablast general algorithm parameters and short input sequence for the absence of stretches more than 15 homologous nucleotides to the entire genomic sequence of the relevant species.

Table 1. Antisense oligonucleotides sequences used for transfection and injection.

AON Name	Sequence (5' - 3')
AON12.1	GUCCCAUCAUUCAGGUCCAU
Control AON	UCCUUUCAUCUCUGGGCUC
mAON12.1	GGCUCAAGAUGUCCUCCUCAUCC
mAON12.2	UUUCAGAACUGUCCGAAGGAGUC
mAON13	GGCUGUCCUAUCUGCAUG
Scrambled AON	CUGAACUGGUCUACAGCUC

Cell culture and transfection

Patient derived fibroblasts from HD patients (GM04022, purchased from Coriell Cell Repositories, Camden, USA) and controls (FLB73, a kind gift from Dr. M.P.G. Vreeswijk, LUMC) were cultured at 37°C and 5% CO2 in Minimal Essential Medium (MEM) (Gibco Invitrogen, Carlsbad, USA) with 15% heat inactivated fetal bovine serum (FBS) (Clontech, Palo Alto USA), 1% Glutamax (Gibco) and 100 U/ml penicillin/streptomycin (Gibco).

AON transfection was performed in a 6-wells plate with 3 µl of Lipofectamine 2000 (Life Technologies, Paisley, UK) per well. AON and Lipofectamine 2000 were diluted in MEM to a total volume of 500 µl and mixtures were prepared according to the manufacturer's instruction. Four different transfection variables were used: 1) transfection with 1-200 nM AON12.1, 2) transfection with h40AON2 directed against exon 40 of the *DMD* gene (Control AON) (Aartsma-Rus *et al.*, 2002), 3) transfection without AON (Mock). For AON sequences, see **Table 1**. Mixtures were added to a total volume of 1 ml of MEM. Four hours after transfection, medium was replaced with fresh medium containing 5% FBS. A control AON with a 5' fluorescein label was used to ascertain optimal transfection efficiencies by counting the number of fluorescent nuclei (in general, over 80% of all nuclei). All AONs consist of 2'-O-methyl RNA and contain a full-length phosphorothioate backbone (Eurogentec, Liege, Belgium).

RNA analysis

Twenty four hours after the first transfection total RNA was isolated from cells using the Aurum Total RNA Mini Kit (BioRad, Hercules, USA), with an on-column DNase treatment for 30 minutes. RNA was eluted in 40 µl elution buffer and cDNA was synthesized from 500ng total RNA using the Transcriptor First Strand cDNA Synthesis Kit with Random Hexamer primers at 65°C (Roche, Mannheim, Germany).

PCR was performed using 2 µl cDNA, 10x PCR buffer with 1.5 mM $MgCl_2$ (Roche), 0.25 mM dNTPs, 10 pmol of both forward and reverse primer (Eurogentec), 1U FastStart Taq DNA Polymerase (Roche), and PCR grade water to a final volume of 20 µl. PCR was performed with primers flanking exon 9 to 16 of the human sequence (see **Table 2**). The PCR program started with a 4 min initial denaturation at 95°C, followed by 35 cycles of 30 sec denaturation at 95°C, 30 sec annealing at 59°C, 70 sec elongation at 72°C, after which a final elongation step was performed at 72°C for 7 min.

Lab-on-a-Chip was performed on the Agilent 2100 Bioanalyzer (Agilent Technologies, Waldbronn, Germany), using the Agilent DNA 1000 Kit.

The qPCR was performed on RNA extracted from striatal tissue isolated from mouse brain, using 2 µl of 5x diluted cDNA, 20x EvaGreen-qPCR dye (Biotium, Hayward, USA), 10x PCR buffer with 1 mM $MgCl_2$ (Roche), 0.25 mM dNTPs (Roche), 2.5 pmol forward primer, 2.5 pmol reverse primer, 0.35U FastStart Taq DNA Polymerase (Roche), and PCR grade water to a total volume of 10 µl. Primer pairs located in various exons of htt were selected for qPCR using Primer3 software (Rozen and Skaletsky, 2000) and tyrosine 3-monooxygenase/tryptophan 5-monooxygenase activation protein, zeta polypeptide (Ywhaz) and ribosomal protein L22 (Rpl22) were used as reference genes. (For primer list, see **Table 2**). The qPCR was performed using the LightCycler 480 (Roche). Initial denaturation was 10 min. at 95°C, followed by 45 cycles of 10 sec. denaturation at 95°C, 30 sec. annealing at 59°C and 20 sec. elongation at 72°C. The final elongation was performed 5 min. at 72°C.

Primer efficiencies were determined using LinRegPCR v2012.0 with the raw data amplification curves as input. The raw data were baseline corrected and absolute transcript level expressions (N0) were calculated as described previously (Ruijter *et al.*, 2009). All samples were run in triplicate on a plate. On all plates both reference genes were included to correct for inter-plate variance.

Sanger sequencing

Full-length and skipped products were amplified using exon 9 forward or htt exon 16 reverse primer (see **Table 2**). PCR products were loaded on agarose gel and bands were extracted using the QIAquick Gel Extraction Kit (QIAgen). The purified products were re-amplified, purified, and analyzed by Sanger sequencing, using the Applied Biosystems 96-capillary 3730XL system (Life Technologies Corporation, Carlsbad, USA) with the Applied Biosystems BigDyeTerminator v3.1 kit.

Table 2. Primer sequences used for Sanger sequencing and (quantitative) RT-PCR.

Target gene	Species	Primer Name	Application	Sequence (5' - 3')
HTT	Human	hHttEx9Fw1	RT-PCR	GAGCTTCTGCAAACCCTGAC
HTT	Human	hHttEx16Rev1	RT-PCR	CTTCACGCTGACCCTCACAT
Htt	Mouse	mHttEx11Fw1	RT-PCR	TCCAGGTCAGATGTCAGCAG
Htt	Mouse	mHttEx14Rev1	RT-PCR	CTATGGCCCATTCTTTCCAA
Htt	Mouse	mHttEx12Fw1	qRT-PCR	CCACTCCTGGTTCTGTTGGT
Htt	Mouse	mHttEx12Rev1	qRT-PCR	TGGGATCTAGGCTGCTCAGT
Htt	Mouse	mHttEx13Fw1	qRT-PCR	GTTAGATGGTGCCGATAGCC
Htt	Mouse	mHttEx13Rev1	qRT-PCR	GTCCTCCTGTGGCTGTCCTA
Htt	Mouse	mHttEx27Fw1	qRT-PCR	ACGGAAAGGGAAGGAGAAAG
Htt	Mouse	mHttEx27Rev1	qRT-PCR	CACCAACTTTCTTGGGACTCA
Rpl22	Mouse	mRpl22Ex3Fw1	qRT-PCR	AGGAGTCGTGACCATCGAAC
Rpl22	Mouse	mRpl22Ex3Rev1	qRT-PCR	TTTGGAGAAAGGCACCTCTG
Ywhaz	Mouse	mYwhazEx4Fw1	qRT-PCR	TCTGGCCCTCAACTTCTCTG
Ywhaz	Mouse	mYwhazEx4Rev1	qRT-PCR	AGGCTTTCTCTGGGGAGTTC

Abbreviations: HTT, huntingtin; Rpl22, ribosomal protein L22; Ywhaz, tyrosine 3-monooxygenase/tryptophan 5-monooxygenase activation protein, zeta polypeptide.

Protein isolation, caspase-6 assay and Western blotting

Cells were detached from the culture surface with a 0.5% Trypsin/EDTA solution three days after transfection. After washing twice with HBSS, cells were resuspended in 200 µl ice cold caspase lysis buffer, containing 50 mM Hepes, 50 mM NaCl, 10 mM EDTA, 10 mM DTT, 0.1% CHAPS. Next, samples were sonicated 3 times for 5 seconds using ultrasound with an amplitude of 60 at 4°C. After 1 hour incubation in a head-over-head rotor at 4°C, the extract was centrifuged for 15 min at 10,000 g and 4°C and supernatant was isolated. Protein concentrations were determined by the bicinchoninic acid kit (Thermo Fisher Scientific, Waltham, USA) using Bovine Serum Albumin as a standard. Samples were snap frozen and stored at -80°C.

For *in vitro* caspase cleavage, 30 µg protein lysate was incubated with 0.5 to 1.5 U human recombinant caspase-6 (Calbiochem, Darmstadt, Germany) for 5 hours at 37°C.

Protein extracts were separated by Criterion XT Tris-Acetate Gel, 3–8%, 12-wells (BioRad). For each sample both the PageRuler prestained and Spectra Multicolor High Range protein ladders (Thermo Fisher Scientific) were used as markers. Gels were blotted onto a nitrocellulose membrane using the Transblot Turbo (BioRad) for 30 min at 2.5 A. Membranes were blocked with Tris Buffered Saline (TBS) containing 5% non-fat milk powder (Profitar Plus, Nutricia, Zoetermeer, the Netherlands). The antibodies used for detection of htt were 4C8 (MAB2166) for htt (Millipore, Billerica, USA) dilution 1:1,000. A β-actin antibody (mouse AC-15 (Abcam,Cambridge, UK) , dilution 1:2000) was used as loading control. Secondary antibody was goat α-mouse-IRDye800 (LI-COR Biosciences, Lincoln, USA), diluted 1:5,000 in block buffer. Odyssey scanner (LI-COR) was used to visualize infrared bands. Intensities of protein

bands were quantified using Odyssey software. The skipping efficiencies were calculated as described in calculations and statistical analysis paragraph.

In vivo injection into mice

Mouse htt specific AONs (mAON12.1, mAON12.2, and mAON13) and scrambled control AONs were injected in anesthetized C57bl/6j male mice between the ages of 12-14 weeks (Janvier SAS, France). For AON list, see **Table 1**. Animals were singly housed in individually ventilated cages (IVC) at a 12 hour light cycle with lights on at 7 am. Food and water were available ad libitum. All animal experiments were carried out in accordance with European Communities Council Directive 86/609/EEC and the Dutch law on animal experiments and were approved by the Leiden University animal ethical committee (protocol number: 11203). Animals were anesthetized with a cocktail of Hypnorm-Dormicum-demineralized water in a volume ratio of 1.33:1:3. The depth of anesthesia was confirmed by examining the paw and tail reflexes. When mice were deeply anesthetized they were mounted on a Kopf stereotact (David Kopf instruments, Tujunga, USA). A total of 30 µg AON mix diluted in 2.5 µl sterile saline was bilaterally injected at the exact locations 0.50mm frontal from bregma, ±2.0mm medio-lateral, and -3.5mm dorso-ventral. For injections, customized borosilicate glass micro-capillary tips of approximately 100 µm in diameter, connected to a Hamilton needle (5 µl, 30 gauge) were used. The Hamilton syringe was connected to an injection pump (Harvard apparatus, Holliston, MA, USA) which controlled the injection rate set at 0.5 µl/min. After surgery the animals were returned to the home cage and remained undisturbed until sacrifice, with the exception of daily weighing in order to monitor their recovery from surgery. After 7 days the mice were sacrificed by intraperitoneal injection of overdose Euthasol (ASTfarma, Oudewater, the Netherlands) and brain tissue isolated and snap frozen till further analysis.

Calculations and statistical analysis

RNA and protein skipping percentages were calculated using the following formula: Skipping % = (Molarity skipped product / (Total molarity full length product + skipped product)) * 100%. The 586 N-terminal htt fragment levels were calculated using β-actin as reference. The skipping percentages were analyzed using a paired two-sided Student t test. Differences were considered significant when $P < 0.05$.

4.4. Results

Exon 12 skipping resulted in a shorter htt protein resistant to caspase-6 cleavage

The first amino acid of the 586 caspase-6 site previously implicated in disease pathology (Graham *et al.*, 2006), is encoded in exon 12 and the last three amino acids are encoded in exon 13. Exon 12 also encodes two caspase-3 sites at amino acids 513 and 552 (Wellington *et al.*, 1998; Wellington *et al.*, 2000). Our initial aim was to generate a shorter htt protein lacking these 3 caspase sites by skipping both exon 12 and 13. This double exon skip would be necessary to maintain the open reading frame and subsequently protein translation. Therefore, we transfected various AONs (**Table 1**) in patient derived fibroblasts, total RNA was isolated after 24 hours and cDNA was amplified using htt primers flanking the skipped exon to examine skipping efficiencies.

However, after transfection of one of the exon 12 AONs, AON12.1, that targets an ESE in the 3' part of exon 12, a 135 base pair partial skip of exon 12 was observed (**Figure 1a**). This in-frame skip was confirmed by Sanger sequencing (**Figure 1b**). The highest skipping percentage of AON12.1 in patient derived fibroblasts was 59.9% (±0.7%) at a concentration of 50 nM (**Figure 1c**). The partial exclusion of the 3' part of htt exon 12 can be explained by activation of a cryptic 5' splice site present in exon 12 (AG|GTCAG (Zhang, 1998)) (**Figure 1d**). A thus modified htt protein also lacks the active caspase-3 site at amino acid 552 (DLND), and the isoleucine (I) of the active caspase-6 site at amino acid 586 (IVLD) is replaced by a glutamine (Q).

Western blot analysis using the 4C8 antibody indeed revealed a 5 kDa shorter htt protein (**Figure 2a**), which is in concordance with the predicted 45 amino acid skip. Three days after a single AON12.1 transfection, 27.7% (±5.4%) of total htt protein levels consisted of this shorter htt protein (**Figure 2b**). There was no decreased cell viability after AON transfection *in vitro* (**Figure S1**).

To show a reduction in the amount of the 586 N-terminal htt protein fragments that are normally formed after caspase-6 cleavage, we performed an *in vitro* caspase-6 assay. Protein was isolated from human fibroblasts three days after treatment with 50 nM of AON12.1. After samples were incubated with recombinant active caspase-6, the 586 N-terminal htt protein fragment was detected at 98 kDa by Western blot (**Figure 2a**). Samples treated with AON12.1 resulted in a 48.9% (±11.2%) reduction of these 586 N-terminal htt protein fragments (**Figure 2c**). Furthermore, changing the first amino acid of the amino acid 583 to 586 caspase-6 motif is sufficient to prevent the formation of the toxic 586 N-terminal htt protein fragments.

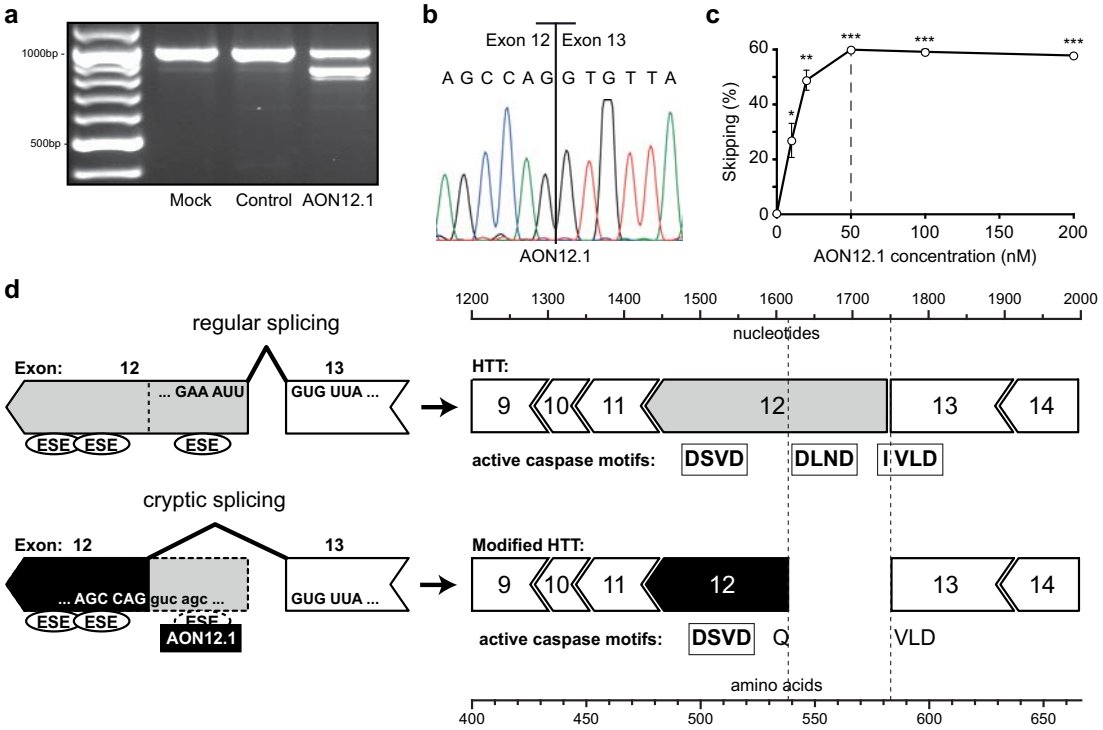

Figure 1. In-frame partial skip of human htt exon 12. Patient-derived fibroblasts were transfected with a htt AON targeting exon 12 (AON12.1), control AON, and non-transfected cells (Mock) and RNA was isolated after 24 hours. **(a)** Agarose gel analysis of the htt transcript with primers flanking exon 12 and 13. Transfection with 100 nM AON12.1 resulted in a product lacking the 3' part of exon 12. **(b)** Partial skip of exon 12 by AON12.1 was confirmed by Sanger sequencing. **(c)** Lab-on-a-Chip analysis was performed to calculate skip levels with AON12.1 concentrations ranging from 10 to 200 nM. Mean ± SD, data were analyzed using paired student t-test, * $P < 0.05$, ** $P < 0.01$, *** $P < 0.001$, relative to mock transfection, n = 4. **(d)** Schematic representation of partial htt exon 12 skipping and subsequent changes in the 552 and 586 caspase cleavage motifs on the htt protein. AON12.1 targets an exonic splicing enhancer site (ESE) cluster in the 3' part of htt exon 12, activating a 5' cryptic splice site and an in-frame exclusion of the 3' part of exon 12. Skipping of the distal part of exon 12 results in the translation of a modified htt protein, lacking the caspase-3 site at amino acid 552 (DLND), and the isoleucine **(I)** of the active caspase-6 site at amino acid 586 (IVLD) is replaced by a glutamine **(Q)**.

In vivo htt exon 12 skipping

To investigate the potential of htt exon skipping *in vivo* and to test if removal of the amino acid sequence surrounding the 586 caspase-6 cleavage site could be harmful *in vivo*, we designed AONs homologous to the mouse sequence. Since mice do not exhibit the cryptic splice site responsible for the partial skip in human cells, we could only investigate the in-frame full skip of both exon 12 and 13. This required the combined application of three AONs: mAON12.1, mAON12.2, and mAON13.

As proof of principle, murine C2C12 cells were transfected with 200nM of mAON12.1, mAON12.2, and mAON13. This resulted in a skip of both exons with an efficiency of 86.8% (±5.6) (**Figure S2**).

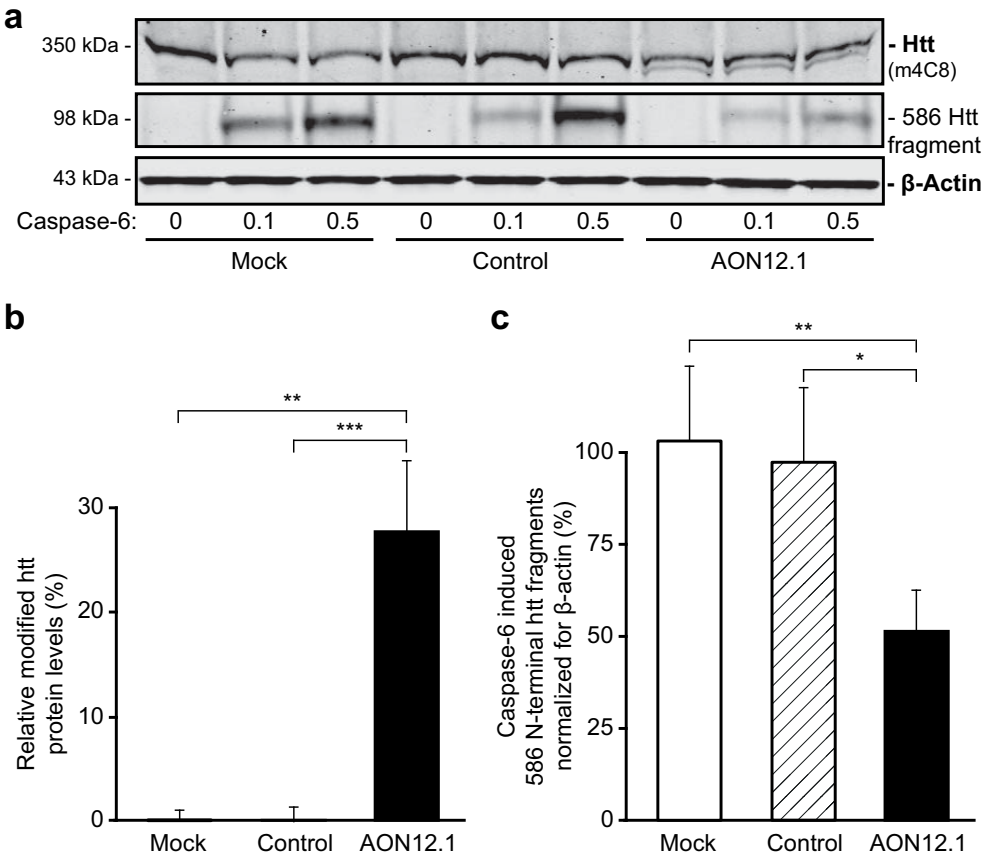

Figure 2. Modified htt protein after partial exon 12 skipping is resistant to caspase-6 cleavage. Patient-derived fibroblasts were transfected with 50nM AON12.1 and control AONs. **(a)** Transfection with AON12.1 resulted in the appearance of a modified htt protein of approximately 343 kDa. *In vitro* caspase-6 cleavage assay shows that the 586 N-terminal htt fragment (98 kDa) increases with increasing concentration of caspase-6. In samples from cells treated with AON12.1 this 586 N-terminal htt fragment is reduced, while the loading control β-actin remains unchanged. **(b)** Levels of modified htt protein after transfection with AON12.1 determined by Odyssey software quantification, normalized for β-actin. **(c)** Quantification of the 586 N-terminal htt fragment, determined by Odyssey software, normalized for β-actin. Mean ± SD, data were evaluated using paired student t-test, * $P < 0.05$, ** $P < 0.01$, *** $P < 0.001$, n = 6.

Next, a single dose of 30 µg scrambled AON or 30 µg mAON12.1, mAON12.2, and mAON13 (10 µg per AON) was injected bilaterally into the mouse striatum. After 7 days the mice were sacrificed and expression levels of exon 12 and 13 in the mouse htt transcript were assessed by qRT-PCR (**Figure 3**). Exon 12 was significantly reduced by 21.5% (±8.5%) and exon 13 was significantly reduced by 23.1% (±8.3%). Exon 27, downstream of the area targeted for skipping, was not reduced.

This reduction in htt exon 12 and 13 after single injection in the mouse striatum further supports the concept that exon skipping could be a potential therapeutic approach to prevent formation of toxic 586 N-terminal htt fragments.

4.5. Discussion

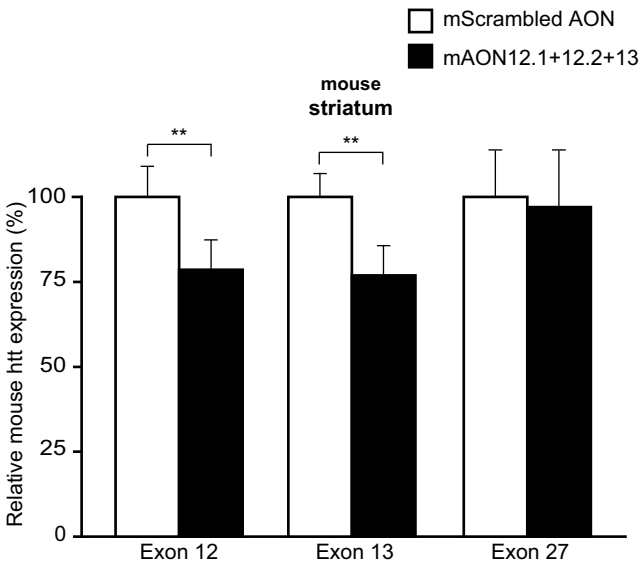

Figure 3. Reduction of mouse htt exon 12 and 13 after a single local injection into the mouse striatum. A single injection consisting of mAON12.1, mAON12.2 and mAON13 (10 µg each) or 30 µg scrambled AON was injected bilaterally into the mouse striatum. After 7 days the mice were sacrificed and the presence of exon 12, 13 and 27 in the htt transcript was examined by qRT-PCR. Mean + SD, data were evaluated using paired student t-test, * $P < 0.05$, n = 5.

Our results provide proof of concept that AON-mediated exon skipping can remove the caspase-3 and caspase-6 motifs from the htt protein, both *in vitro* and *in vivo*. *In vitro* skipping, at least in the human transcript, counteracted the formation of the 586 N-terminal htt protein fragment implicated in toxicity of expanded htt. This htt protein modification is therefore a novel potential therapeutic approach. Our results in patient-derived fibroblasts show that a single AON can remove the 3' part of exon 12 from the human htt mRNA through activation of a cryptic splice site in exon 12. This results in the formation of a shorter htt protein resistant to caspase-6 cleavage. A single injection of AONs targeting htt exon 12 and 13 into the striatum of control mice already resulted in a 22% reduction of htt exon 12 and 13. *In vivo* skipping efficiencies are known to be lower than *in vitro* and 20 to 25% AON-induced splicing already has been shown to result in phenotypic improvements in DMD (Tanganyika-de Winter *et al.*, 2012) and Usher syndrome mice (Lentz *et al.*, 2013).

Possibly, not only this 586 N-terminal htt fragment, but smaller fragments may be toxic entities (Sathasivam *et al.*, 2013; Lunkes *et al.*, 2002; Waldron-Roby *et al.*, 2012). However, the formation of the 586 N-terminal mutant htt protein fragments by caspase-6 cleavage was found to be crucial in the pathogenesis of HD (Graham *et al.*, 2006; Wellington *et al.*, 2000). Notably, caspase-6 is activated in the striatum and frontal cortex of (pre-symptomatic) HD patients and this activation inversely correlates with the age of disease onset, as well as with the CAG repeat size (Graham *et al.*, 2010). Mice expressing the 586 N-terminal htt expanded polyQ fragment develop symptoms similar to mouse models with shorter N-terminal polyQ fragments (Warby *et al.*, 2008; Tebbenkamp *et al.*, 2011; Waldron-Roby *et al.*, 2012) and removal of the 586 caspase-6 site from the full-length mutant htt protein, prevents this phenotype (Graham *et al.*, 2006; Pouladi *et al.*, 2009), underscoring the significance of this particular htt protein fragment, and suggesting that modifying the htt protein using AONs to prevent the formation of the N-terminal 586 htt fragment would be beneficial. That caspase-6 is not exclusively responsible

for the formation of the 586 N-terminal htt fragment was concluded from experiments where a transgenic HD mouse model was crossed with a caspase-6 knock-out mouse. These mice did show the same 586 amino acid N-terminal htt fragment, suggesting that other proteases can also cleave the caspase-6 motif (Gafni *et al.*, 2012). Our exon skip approach does not target the proteases, but removes the proteolytic motif proper, implicated in enhanced toxicity from the htt protein (Warby *et al.*, 2008; Tebbenkamp *et al.*, 2011; Waldron-Roby *et al.*, 2012).

A key question for translating genetic therapies into clinical applications for neurodegenerative disorders is how to administer AONs into the human brain. Since AONs do not cross the blood-brain-barrier, a more invasive delivery method was applied by intracranial injection (Miller *et al.*, 2013). AONs thus infused have been shown to diffuse throughout the non-human primate brain and could be detected in the nuclei and cell bodies of neurons and glial fibrillary acidic protein (GFAP)-positive astrocytes in the striatum, hippocampus, cerebellum, cortex, and spinal cord (Kordasiewicz *et al.*, 2012). The stability, potency, and broad distribution of AONs in the brain marks them as good candidate for potential htt lowering therapeutic for HD.

In our approach, AON-mediated reduction of the toxic N-terminal htt fragment is achieved without lowering of overall htt expression. This would be an advantage over non-allele-specific htt reduction approaches. In HD there is a gain of toxic function of the mutant htt protein, but regular htt is important for normal cellular function (Dragatsis *et al.*, 2000) and is essential during development (Zeitlin *et al.*, 1995). Kordasiewicz *et al.* showed that 4 months repression of total htt of around 50% to 75% did not produce side effects in rats and non-human primates (Kordasiewicz *et al.*, 2012). However, the effects of non-allele-specific lowering of htt over longer time periods has not yet been studied. This is important since HD carriers or patients probably have to be treated lifelong.

For this AON-mediated htt protein modification a single AON would be applicable to the entire HD patient population. Furthermore, by specifically removing critical caspase motifs in htt, there is less chance of unwanted side effects that could result from pharmacological inhibition of overall caspase-6 activity. On the other hand, while it is plausible to expect that the removal of a small stretch of 45 internal amino acids from htt will not, or only modestly, affect htt function - and only after the start of treatment - the extent of this remains to be established. We aim to study this further, as well as the effect on the HD-phenotype, by sustained intraventricular infusion of exon skipping AONs in HD animal models.

In conclusion, in the current manuscript we provide proof of principle for a novel approach to reduce mutant htt toxicity by modifying the protein proper, without changing its protein level. This would provide a valuable addition to the emerging field of AON treatment strategies for neurodegenerative disorders.

4.6. Acknowledgements

This work was supported by the Center for Biomedical Genetics (the Netherlands), Center for Medical Systems Biology (OCM/IZ), and Integrated European Project in Omics Research of Rare Neuromuscular and Neurodegenerative Diseases (Neuromics). The authors would like to thank Neil MacCallum, and Astrid Coolen for technical assistance.

4.7. Supplementary Material

Supplementary Materials and Methods

Cell culture mouse cells

Mouse myoblasts C2C12 (ATCC, Teddington, UK) were cultured in Dulbecco's Modified Eagle Medium (DMEM) (Gibco) with 10% FBS, 1% glucose, 2% Glutamax and 100 U/ml P/S. For AON sequences, see **Table 1**.

PCR mouse huntingtin

PCR was performed with forward and reverse primer in respectively exon 9 and 14 of the mouse htt sequence (see **Table 2**).

Cell viability assay

Two days after transfection in a 96-wells plate, cells were prepared for Cellomics multiparameter cytotoxicity version 3 (Thermo Fisher Scientific) measurements, according to manufacturer's instructions. Cell viability was analyzed on the Array Scan VTI reader (Thermo Fisher Scientific) using the following absorption/emission filter sets: (1) total nuclear intensity: 350/461 nm, (2) lysosomal mass: 646/674 nm, and (3) cell permeability: 491/509 nm. All transfections were performed in triplicates on one plate.

Supplementary Figures

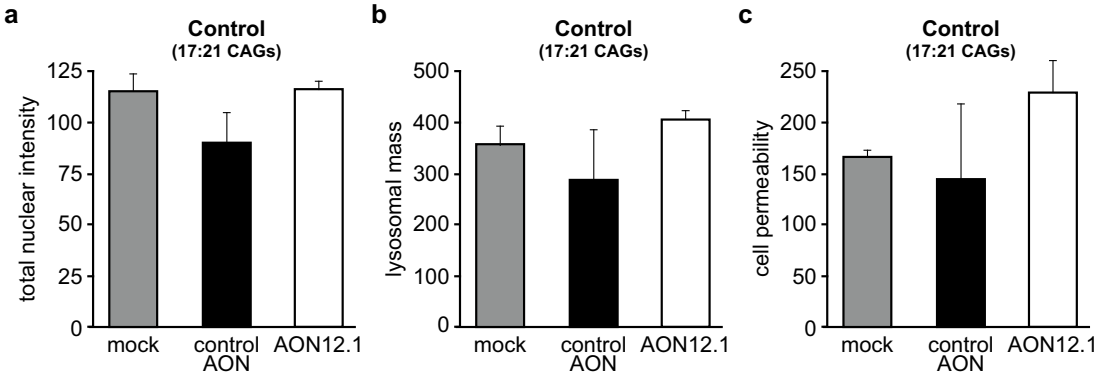

Figure S1. No negative effect htt AON treatment on cell viability *in vitro*. Control fibroblasts were transfected with htt AONs inducing partial skip of exon 12 (AON12.1), control AON, and non-transfected (mock). Mean ± SD, n = 2. The **(a)** total nuclear intensity, **(b)** lysosomal mass, and **(c)** cell permeability were measured. Mean ± SD, n = 2.

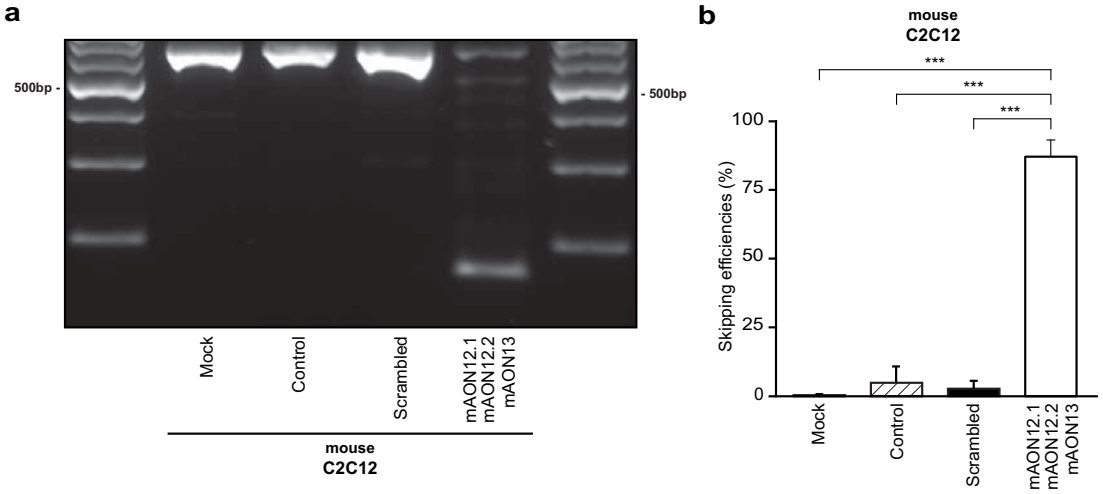

Figure S2. Skipping murine htt exon 12 and 13 *in vitro*. Mouse C2C12 cells were transfected with murine htt AONs, control AON, scrambled AON, and not transfected (Mock). **(a)** Agarose gel analysis of the htt transcript with primers flanking exon 12 and 13. Skipping of htt exon 12 and 13 is seen after transfection with mAON12.1, mAON12.2, and mAON13. **(b)** Lab-on-a-Chip analysis of double-exon skipping after AON treatment. Mean ± SD, data were evaluated using paired student t-test, *** P<0.001, relative to mock transfection, n = 4.

Melvin M. Evers [1]
Hoang-Dai Tran [1]
Ioannis Zalachoras [2]
Barry A. Pepers [1]
Onno C. Meijer [2]
Johan T. den Dunnen [1,3,4]
Gert-Jan B. van Ommen [1]
Annemieke Aartsma-Rus [1]
Willeke M.C. van Roon-Mom [1]

[1] Department of Human Genetics, Leiden University Medical Center
[2] Department of Endocrinology, Leiden University Medical Center
[3] Leiden Genome Technology Center, Leiden University Medical Center
[4] Department of Clinical Genetics, Leiden University Medical Center

5

Ataxin-3 protein modification as a treatment strategy for spinocerebellar ataxia type 3: Removal of the CAG containing exon

Neurobiology of Disease 2013, 58:49-56

5.1. Abstract

Spinocerebellar ataxia type 3 is caused by a polyglutamine expansion in the ataxin-3 protein, resulting in gain of toxic function of the mutant protein. The expanded glutamine stretch in the protein is the result of a CAG triplet repeat expansion in the penultimate exon of the *ATXN3* gene. Several gene silencing approaches to reduce mutant ataxin-3 toxicity in this disease aim to lower ataxin-3 protein levels but since this protein is involved in deubiquitination and proteasomal protein degradation, its long-term silencing might not be desirable. Here, we propose a novel antisense oligonucleotide-based protein modification approach to reduce mutant atxin-3 toxicity by removing the toxic polyglutamine repeat from the ataxin-3 protein through antisense mediated exon skipping and maintaining important wild-type functions of the protein. *In vitro* studies showed that the ubiquitin binding capacity of ataxin-3 was unaffected after exon skipping and *in vitro*. Our *in vivo* studies showed no toxic properties of the novel truncated ataxin-3 protein. These results suggest a novel therapeutic approach to reduce polyglutamine-induced toxicity in spinocerebellar ataxia type 3.

5.2. Introduction

Spinocerebellar ataxia type 3 (SCA3), also known as Machado-Joseph disease (MJD), is one of nine known polyglutamine (polyQ) disorders. PolyQ disorders are autosomal dominant neurodegenerative disorders caused by expansion of a CAG triplet in the coding region of a gene. This CAG repeat is translated into an extended glutamine stretch in the mutant protein, which causes a gain of toxic function inducing neuronal loss in various regions throughout the brain (Bauer and Nukina, 2009). A hallmark of all polyQ disorders is the formation of large insoluble protein aggregates containing the expanded disease protein. Whether these large aggregates are neurotoxic or neuroprotective is still under debate (Takahashi *et al.*, 2010).

In SCA3, the CAG repeat is located in the penultimate exon of the *ATXN3* gene on chromosome 14q32.1. Healthy individuals have a CAG repeat ranging from 10 to 51, whereas SCA3 patients have an expansion of 52 repeats or more (Cummings and Zoghbi, 2000). Transgenic mice expressing either a mutant ataxin-3 cDNA fragment (Ikeda *et al.*, 1996) or the mutated full-length genomic sequence (Cemal *et al.*, 2002; Goti *et al.*, 2004), showed a clear ataxic phenotype with a more severe phenotype in the animals carrying larger repeats (Bichelmeier *et al.*, 2007), demonstrating a relationship between CAG repeat length and disease severity. The *ATXN3* gene codes for the ataxin-3 protein of 45 kDa, which acts as an isopeptidase and is thought to be involved in deubiquitination and proteasomal protein degradation (Burnett *et al.*, 2003; Scheel *et al.*, 2003; Schmitt *et al.*, 2007). The ataxin-3 protein contains an N-terminal Josephin domain that displays ubiquitin protease activity and a C-terminal tail with 2 or 3 ubiquitin interacting motifs (UIMs), depending on the isoform (Goto *et al.*, 1997). Although in the past decade there has been extensive research into the SCA3 disease mechanisms (Matos *et al.*, 2011), it is still not completely understood how the ataxin-3 polyQ expansion results in the observed pathology.

The most promising recent therapeutic strategy under development for polyQ disorders is reducing levels of mutant polyQ proteins using RNA interference (RNAi) and antisense oligonucleotides (AONs). As potential gene silencing treatment for SCA3, non-allele-specific reduction of ataxin-3 has been tested in both mice (Schmitt *et al.*, 2007) and rats (Alves *et al.*, 2010). The treated rodents were viable and displayed no overt phenotype, suggesting that ataxin-3 is a non-essential protein. However, ataxin-3 might also have a protective role, since in flies ataxin-3 was found to alleviate neurodegeneration induced by mutant polyQ proteins (Warrick *et al.*, 2005). Whether this is also true in humans is not known. The results in flies favors selective inhibition of mutant ataxin-3 protein levels over a total reduction of ataxin-3 protein levels. Successful allele-specific reduction of the mutant ataxin-3 transcript was shown using lentiviral small hairpin RNAs directed against a single nucleotide polymorphism (SNP) in the *ATXN3* gene *in vitro* (Miller *et al.*, 2003) and *in vivo* (Alves *et al.*, 2008; Nobrega *et al.*, 2013). However, this approach is limited to SCA3 patients carrying a heterozygous SNP in the ATXN3 gene. Semi-allele-specific reduction of mutant ataxin-3 has also been achieved by targeting the expanded CAG repeat using single stranded AONs *in vitro* (Hu *et al.*, 2009; Hu *et al.*, 2011;

Chapter 3).

We here introduce a novel way to reduce toxicity of the ataxin-3 protein through protein modification. Using AONs it is possible to mask exons in the pre-mRNA from the splicing machinery resulting in exclusion of the targeted exon (Spitali and Aartsma-Rus, 2012). If the reading frame remains intact, subsequent translation yields an internally truncated protein. This has the major advantage that the polyQ-containing part of the protein is removed, while maintaining global ataxin-3 protein levels. AON-mediated exon skipping is a promising therapeutic tool that is already in phase II/III clinical trial for Duchenne muscular dystrophy (DMD) (Cirak *et al.*, 2011; van Putten and Aartsma-Rus, 2011).

In this study we used 2'O-methyl modified AONs with a phosphorothioate backbone to induce an in-frame exon skip in the ataxin-3 pre-mRNA. This resulted in a modified ataxin-3 protein lacking the polyQ repeat, while total ataxin-3 protein levels were unaltered and its functional domains remained intact. We showed that this modified protein retains its ubiquitin binding capacity. No cell death was seen after exon skipping, suggesting this modified protein did not induce *in vitro* toxicity. Injection of a single dose of AONs in the mouse cerebral ventricle resulted in exon skipping in the cerebellum, the brain area most affected in SCA3. These results suggest exon skipping could be a promising novel therapeutic approach to reduce polyglutamine-induced toxicity in SCA3.

5.3. Materials and Methods

Cell culture and transfection

Patient derived fibroblasts from SCA3 patients (GM06151, purchased from Coriell Cell Repositories, Camden, USA) and controls (FLB73, a kind gift from Dr. M.P.G. Vreeswijk, LUMC) were cultured at 37°C and 5% CO2 in Minimal Essential Medium (MEM) (Gibco Invitrogen, Carlsbad, USA) with 15% heat inactivated fetal bovine serum (FBS) (Clontech, Palo Alto USA), 1% Glutamax (Gibco) and 100 U/ml penicillin/streptomycin (Gibco). Mouse myoblasts C2C12 (ATCC, Teddington, UK) were cultured in Dulbecco's Modified Eagle Medium (DMEM) (Gibco) with 10% FBS, 1% glucose, 2% Glutamax and 100 U/ml P/S.

AON transfection was performed in a 6-well plate with 3 µl of Lipofectamine 2000 (Life Technologies, Paisley, UK) per well. AON and Lipofectamine 2000 were diluted in MEM to a total volume of 500 µl and mixtures were prepared according to the manufacturer's instruction. Four different transfection conditions were used: 1) transfection with 1-200 nM AONs, 2) transfection with non-relevant h40AON2 directed against exon 40 of the *DMD* gene (Control AON) (Aartsma-Rus *et al.*, 2002), 3) transfection with scrambled AON (Scrambled), and 4) transfection without AON (Mock). For AON sequences, see **Table 1**. Mixtures were added to a total volume of 1 ml of MEM. Four hours after transfection, medium was replaced with fresh medium containing 5% FBS. All AONs consisted of 2'-O-methyl RNA and contained a full-length phosphorothioate modified backbone (Eurogentec, Liege, Belgium).

Table 1. Antisense oligonucleotides sequences used for transfection and injection.

AON Name	Sequence (5' - 3')
AON9.1	GAGAUAUGUUUCUGGAACUACC
AON9.2	GCUUCUCGUCUCUUCCGAAGC
AON10	GCUGUUGCUGCUUUUGCUGCUG
Control AON	UCCUUUCAUCUCUGGGCUC
mAON9.1	GCUUCUCGUCUCCUCCGCAGC
mAON10	GAACUUGUGGUCGGUCUUUCAC
Scrambled AON	CUGAACUGGUCUACAGCUC

Plasmids and mutations

Full length as well as AON9.2 and AON10 induced skipped ataxin-3 fragments were PCR-amplified with ATXN3-specific primers (see **Table 2**) and cloned into pIVEX 1.4 WG vector that contained 6 His tags (His6-ataxin-3 full length and His6-ataxin-3Δ59aa, respectively). Three µg of vector DNA was used as template for cell free protein production using the RTS 100 kit together with the RTS ProteoMaster (Roche). His6-tagged beta-glucuronidase (GUS) (5 Prime) was taken along as control vector.

Leucine to alanine mutations in the UIMs were performed using the QuickChange II Site-Directed Mutagenesis kit (Agilent Technologies, Waldbronn, Germany) following manufacturer's instructions, using forward and reverse primers containing the desired mutation (see **Table 2**).

RNA analysis

Twenty four hours after the first transfection, total RNA was isolated from cells using the Aurum Total RNA Mini Kit (BioRad, Hercules, USA), with an on-column DNase treatment for 30 minutes. Brain tissue was homogenized using ceramic MagNA Lyser beads (Roche, Mannheim, Germany) by grinding in a Bullet Blender (Next Advance, Averill Park, USA) according to manufacturer's instructions. RNA was eluted in 40 µl elution buffer and cDNA was synthesized from 1 µg total RNA using the Transcriptor First Strand cDNA Synthesis Kit with Random Hexamer primers at 65°C (Roche).

PCR was performed using 2 µl cDNA, 10x PCR buffer with 1.5 mM $MgCl_2$ (Roche), 0.25 mM dNTPs, 10 pmol of both forward and reverse primer (Eurogentec), 1U FastStart Taq DNA Polymerase (Roche), and PCR grade water to a final volume of 20 µl. PCR was performed with primers for human and mouse ataxin-3 (see **Table 2**). The PCR program started with a 4 min initial denaturation at 95°C, followed by 35 cycles of 30 sec denaturation at 95°C, 30 sec annealing at 59°C, 45 sec elongation at 72°C, after which a final elongation step was performed at 72°C for 7 min. Lab-on-a-Chip was performed on the Agilent 2100 Bioanalyzer (Agilent Technologies), using the Agilent DNA 1000 Kit.

The qPCR was performed on RNA extracted from tissue isolated from mouse brain, using 2 µl of 5 times diluted cDNA, 20 times EvaGreen-qPCR dye (Biotium, Hayward, USA), 10 times PCR buffer with 1 mM $MgCl_2$ (Roche), 0.25 mM dNTPs (Roche), 2.5 pmol forward primer, 2.5 pmol reverse primer, 0.35U FastStart Taq DNA Polymerase (Roche), and PCR grade water to a total volume of 10 µl. Primer pairs located in various exons of ataxin-3 were selected for qRT-PCR using Primer3 software (Rozen and Skaletsky, 2000) and tyrosine 3-monooxygenase/tryptophan 5-monooxygenase activation protein, zeta polypeptide (Ywhaz) and ribosomal protein L22 (Rpl22) were used as reference genes. (For primer list, see **Table 2**). The qRT-PCR was performed using the LightCycler 480 (Roche). Initial denaturation was 10 min. at 95°C, followed by 45 cycles of 10 sec. denaturation at 95°C, 30 sec. annealing at 60°C and 20 sec. elongation at 72°C. The final elongation was performed 5 min. at 72°C.

Primer efficiencies were determined using LinRegPCR v2012.0 with the raw data amplification curves as input. The raw data were baseline corrected and absolute transcript level expressions (N0) were calculated as described previously (Ruijter *et al.*, 2009). All samples were run in triplicate on a plate. On all plates both reference genes were included to correct for inter-plate variance.

Sanger sequencing

Full length and skipped products were amplified using primers flanking ataxin-3 exon 9 and 10 (see **Table 2**). PCR products were loaded on agarose gel and bands were extracted using the QIAquick Gel Extraction Kit (QIAgen, Valencia, USA). The purified products were re-amplified, purified, and analyzed by Sanger sequencing, using the Applied Biosystems 96-capillary 3730XL system (Life Technologies Corporation, Carlsbad, USA) with the Applied Biosystems BigDyeTerminator v3.1 kit.

Table 2. Primer sequences used for Sanger sequencing, mutagenesis, and (quantitative) RT-PCR.

Target gene	Species	Primer Name	Application	Sequence (5' - 3')
ATXN3	Human	hATXN3Ex8Fw1	RT-PCR	CCATAAAACAGACCTGGAACG
ATXN3	Human	hATXN3Ex11Rev1	RT-PCR	ACAGCTGCCTGAAGCATGTC
ATXN3	Human	hATXN3_SDM_L229AFw	Mutagenesis	ACGAAGATGAGGAGGATGCGCAGAGGGCTCTGGC
ATXN3	Human	hATXN3_SDM_L229ARev	Mutagenesis	GCCAGAGCCCTCTGCGCATCCTCCTCATCTTCGT
ATXN3	Human	hATXN3_SDM_L249AFw	Mutagenesis	ACATGGAAGATGAGGAAGCAGATGCCCGCAGGGCTAT
ATXN3	Human	hATXN3_SDM_L249ARev	Mutagenesis	ATAGCCCTGCGGGCATCTGCTTCCTCATCTTCCATGT
Atxn3	Mouse	mAtxn3Ex7Fw1	RT-PCR	AAGAGCAGAGTGCCCTCAAA
Atxn3	Mouse	mAtxn3Ex11Rev1	RT-PCR	TTTCTAAAGACATGGTCACAGC
Atxn3	Mouse	mAtxn3Ex4Fw1	qRT-PCR	TGCTTTGAAAGTTTGGGGTTT
Atxn3	Mouse	mAtxn3Ex4Rev1	qRT-PCR	CTGAGCCTCTGGTACTCTGGA
Atxn3	Mouse	mAtxn3Ex9Fw1	qRT-PCR	GTCCACAGACATCAAGTCCAGA
Atxn3	Mouse	mAtxn3Ex9Rev1	qRT-PCR	GTCTCCTCCGCAGCTCTTC
Atxn3	Mouse	mAtxn3Ex10Fw1	qRT-PCR	AGCAGCAGCAGGAGGTAGAC
Atxn3	Mouse	mAtxn3Ex10Rev1	qRT-PCR	CGTCCTCCTGAACTTGTGGT
Atxn3	Mouse	mAtxn3Ex11Fw1	qRT-PCR	ACCGACCACAAGTTCAGGAG
Atxn3	Mouse	mAtxn3Ex11Rev2	qRT-PCR	CCGAAGCATGTCCTCTTCAC
Rpl22	Mouse	mRpl22Ex3Fw1	qRT-PCR	AGGAGTCGTGACCATCGAAC
Rpl22	Mouse	mRpl22Ex3Rev1	qRT-PCR	TTTGGAGAAAGGCACCTCTG
Ywhaz	Mouse	mYwhazEx4Fw1	qRT-PCR	TCAGCAAAAAGGAGATGCAG
Ywhaz	Mouse	mYwhazEx4Rev1	qRT-PCR	TTTCTCTGGGGAGTTCAGGA

Abbreviations: ATXN3, ataxin-3; Rpl22, ribosomal protein L22; Ywhaz, tyrosine 3-monooxygenase/tryptophan 5-monooxygenase activation protein, zeta polypeptide.

Protein isolation, ubiquitin binding assay and Western blotting

Cells were detached from the culture surface with a 0.5% Trypsin/EDTA solution. After washing twice with HBSS, cells were resuspended in 200 µl ice cold lysis buffer, containing 15 mM Hepes, pH 7.9, 200 mM KCl, 10 mM $MgCl_2$, 1% NP40, 10% glycerol, 20 µg/ml BSA, and 1 tablet Complete mini protease inhibitor EDTA free (Roche) per 10 ml buffer. Next, samples were sonicated 3 times for 5 seconds using ultrasound with an amplitude of 60 at 4°C. After 1 hour incubation in a head-over-head rotor at 4°C, the extract was centrifuged for 15 min at 10,000 g and 4°C and supernatant was isolated. Protein concentrations were determined by the bicinchoninic acid kit (Thermo Fisher Scientific, Waltham, USA) using Bovine Serum Albumin (BSA) as a standard. Samples were snap frozen and stored at -80°C.

His6-ataxin-full length and His6-ataxin-3Δ59aa proteins were bound to TALON metal affinity beads (Clontech) for 30 minutes. The ataxin-3-bound beads were incubated at 4°C with 5 µg poly-ubiquitin chains (Enzo Life Sciences, Farmingdale, USA). Binding reactions contained 15 mM Hepes, pH 7.9, 200 mM KCl, 10 mM $MgCl_2$, 1% NP40, 10% glycerol, and 20 µg/ml BSA. Beads were washed extensively and bound proteins were removed from the beads by 2

hours incubation at 23°C with 2 µg Factor Xa Protease (New England Biolabs, Ipswich, United Kingdom) per reaction.

Protein extracts were separated by SDS-PAGE, with 10% acryl/bisacrylamide 1:37.5 separating gels, or Any kD precast TGX gels (BioRad). For each gel the PageRuler prestained protein ladder (Thermo Fisher Scientific) was used as marker. Electrophoresis was performed until the lowest marker reached the bottom of the gel. Gels were blotted onto nitrocellulose membranes using the Transblot Turbo (BioRad) for 30 min at 2.5 A. Membranes were blocked with Tris Buffered Saline (TBS) containing 5% non-fat milk powder (Profitar Plus, Nutricia, Zoetermeer, the Netherlands).

The mouse SCA3-1H9 antibody was used for detecting ataxin-3 (Millipore, Billerica, USA), dilution 1:1000, or rabbit His-tag 2365 (Cell Signaling Technology, Danvers, USA). To detect expanded polyQ stretches we used mouse 1C2 (Eurogentec), dilution 1:500. To detect ubiquitin chains, we used rabbit ubiquitin-protein conjugates (Enzo Life Sciences), diluted 1:2000. Secondary antibodies were goat α-mouse-IRDye800, goat α-rabbit-IRDye800 (LI-COR Biosciences, Lincoln, USA), or goat α-mouse-horseradish peroxidase (HRP) (Santa Cruz Biotechnology, USA), diluted 1:5,000 in block buffer. Horseradish peroxidase was activated by ECL+ reagent (GE Healthcare, Buckinghamshire, United Kingdom) to visualize positive staining on film or Odyssey scanner (LI-COR) was used to visualize infrared bands. Intensities of protein bands were quantified using Odyssey software. The skipping efficiencies were calculated as described in the calculations and statistical analysis paragraph.

AON injection into mice

Mouse ataxin-3 specific AONs (mAON9.1 and mAON10) and scrambled control AONs (**Table 1**) were injected in anesthetized 12-14 week old C57bl/6j male mice (Janvier SAS, France). Animals were singly housed in individually ventilated cages (IVC) at a 12 hour light cycle with lights on at 7 am. Food and water were available ad libitum. All animal experiments were carried out in accordance with European Communities Council Directive 86/609/EEC and the Dutch law on animal experiments and were approved by the Leiden University animal ethical committee (protocol number: 12186). A total of 40 µg AON mix diluted in 5 µl sterile saline was injected into the left lateral ventricle at 0.22 mm anterior-posterior, 1.5 mm medio-lateral, and -2.5 mm dorso-ventral relative to bregma, using borosilicate glass micro-capillary tips connected to a Hamilton syringe (5 µl, 30 gauge). The Hamilton syringe was connected to an injection pump (Harvard apparatus, Holliston, MA, USA), which controlled the injection rate set at 0.5 µl/min. After 7 days the mice were sacrificed and brain isolated and frozen for qRT-PCR analysis.

Calculations and statistical analysis

RNA and protein skipping percentages were calculated using the following formula: Skipping% = (Molarity skipped product / (Total molarity full length product + skipped product)) * 100%. The skipping percentages were analyzed using a paired two-sided Student t test. Differences were considered significant when $P < 0.05$.

5.4. Results

AON mediated skipping of ataxin-3 exon 9 and 10 *in vitro*

The CAG repeat in the *ATXN3* gene is located in exon 10, which is 119 nucleotides in length. Thus skipping will disrupt the reading frame. To preserve the reading frame exon 9 (97 nucleotides) and 10 need to be skipped simultaneously. Various AONs were designed targeting exon internal sequences of ataxin-3 exon 9 and 10 and transfected in human fibroblasts (**Table 1**). PCR analysis revealed a 97 nucleotide skip after transfection with 100nM of AON9.1 (efficiency = 59.2% ±1.0%) (**Figure 1a and b**). Sanger sequencing confirmed that this was a skip of exon 9. Transfection with 100 nM AON9.2 resulted in a skip of 55 nucleotides (efficiency = 62.3% ±3.7%) instead of the anticipated 97 nucleotides (**Figure 1a and c**). Sanger sequencing revealed that this fragment was a partial skip product that still contained the 5′ part of exon 9. In silico analysis showed the existence of a cryptic 5′ splice site AG|GTCCA in exon 9 that could explain the occurrence of this shorter fragment (Zhang, 1998). Successful skipping of exon 10 was achieved with 50 nM AON10 (efficiency = 96.3% ±0.3%) (**Figure 1a and d**), as confirmed by Sanger sequencing.

Co-transfection of AON9.1 and AON10 and AON9.2 and AON10 resulted in a skip of respectively 216 and 174 nucleotides (**Figure 2**). The efficiency of the AON9.1 and AON10 induced double skip was 77.0% (±0.9%) in control fibroblasts (**Figure 2d and e**). The efficiency of AON9.2 and AON10 co-transfection was 97.8% (±0.8%) in control fibroblasts (**Figure 2d and e**). The unexpected in-frame partial skip of exon 9 with AON9.2 resulted in an alternative approach to remove the CAG repeat containing exon from the ataxin-3 transcript (**Figure 2**).

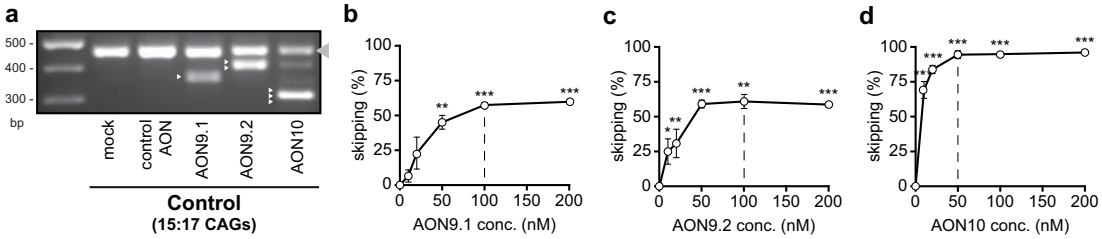

Figure 1. Single exon skipping of ataxin-3 pre-mRNA *in vitro*. Control fibroblasts were transfected with ataxin-3 AONs, control AON, and non-transfected (mock) and RNA was isolated after 24 hours. **(a)** Agarose gel analysis of the ataxin-3 transcript with primers flanking exon 9 and 10 (full-length, grey arrowhead). Transfection with 50 nM AON against exon 9 resulted in a product lacking the entire exon 9 (AON9.1, white arrowhead) or lacking the 3' part of exon 9 (AON9.2, two white arrowheads). Transfection with 50 nM AON10 resulted in a product lacking exon 10 (three white arrowheads). Fibroblasts were transfected with concentrations ranging from 10 to 200 nM per ataxin-3 AON and Lab-on-a-Chip analysis was performed to calculate exon skip levels for **(b)** AON9.1, **(c)** AON9.2, and **(d)** AON10. Mean ± SD, data were evaluated using paired student t-test, * $P < 0.05$, ** $P < 0.01$, *** $P < 0.001$, relative to mock transfection, n = 4.

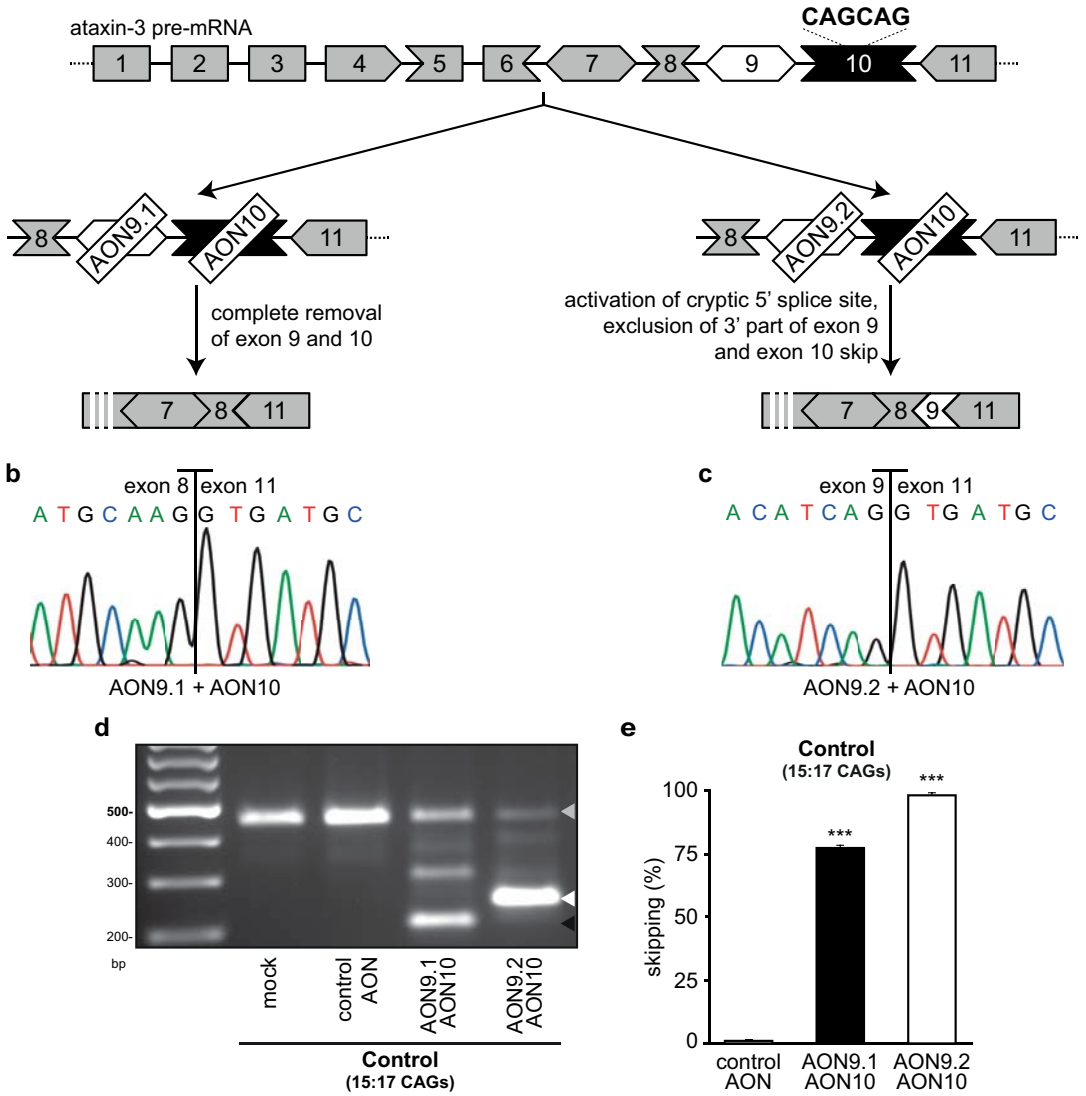

Figure 2. Double exon skipping of ataxin-3 pre-mRNA *in vitro*. (a) Schematic representation of two approaches to induce in-frame skipping of the CAG repeat-containing exon. **(b)** Skip of exon 9 and 10 (AON9.1 + AON10) confirmed by Sanger sequencing. **(c)** Partial skip of exon 9 and complete skip of exon 10 (AON9.2 + AON10) confirmed by Sanger sequencing. **(d)** Agarose gel analysis of the ataxin-3 transcript with primers flanking exon 9 and 10. Transfection of control fibroblasts resulted in a product lacking both exon 9 and 10 (AON9.1 + AON10, black arrowhead) or lacking the 3' part of exon 9 and exon 10 (AON9.2 + AON10, white arrowhead). **(e)** Lab-on-a-Chip analysis was performed to calculate exon skip levels in control cells. Mean + SD, data were evaluated using paired student t-test, ** P <0.01, *** P < 0.001, relative to mock, n = 4.

Modified ataxin-3 protein maintains its ubiquitin binding capacity

To investigate if AON transfection resulted in a modified ataxin-3 protein, control and SCA3 fibroblasts were transfected with AONs targeting exon 9 and 10 and protein was isolated three days after transfection. We did not see a negative effect on cell viability after AON treatment in

either control or SCA3 fibroblasts (**Figure S1**). Western blot analysis using an ataxin-3-specific antibody revealed a modified band of approximately 35 kDa after the complete skip of exon 9 and 10 (ataxin-3 Δ72aa) (**Figure 3a**); 11.4% (±5.1%) and 6.2% (±1.9%) of total ataxin-3 protein levels consisted of this modified ataxin-3 Δ72aa protein , in respectively control and SCA3 fibroblasts (**Figure 3b and c**).

The partial exon skip resulted in a novel 37 kDa protein (ataxin-3 Δ59aa) (**Figure 3a**). 27.1% (±9.0%) and 15.9% (±3.2%) of total ataxin-3 protein levels consisted of this 59 amino acids shorter ataxin-3 protein, in respectively control and SCA3 cells (**Figure 3b and c**). The ataxin-3 Δ72aa protein was also formed, suggesting that AON9.2 and AON10 transfection also resulted in some ataxin-3 Δ72aa protein. The consistent lower percentage of exon skipping in SCA3 cells were caused by the lower AON transfection efficiencies in the diseased cells as compared to control cells.

A significant reduction in expanded polyQ containing ataxin-3 was shown using the 1C2 antibody, that recognizes long glutamine stretches (Trottier *et al.*, 1995) (**Figure 3a**) in the

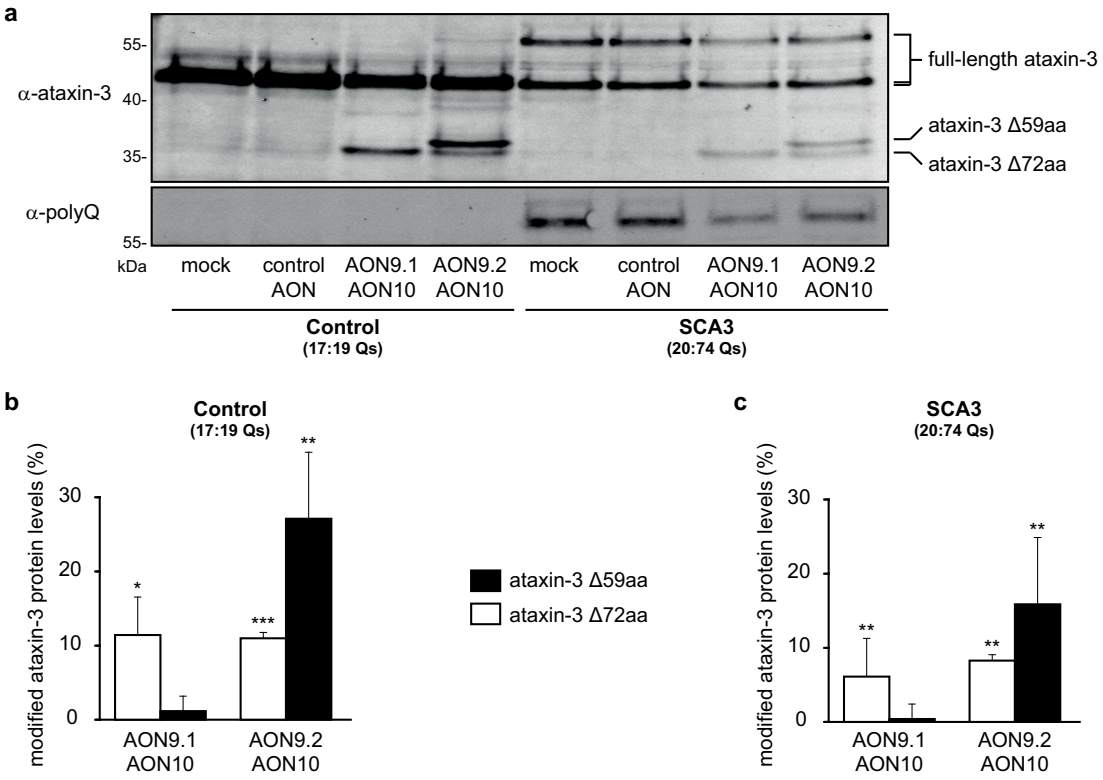

Figure 3. Modified ataxin-3 protein after exon 9 and 10 skipping. Human control and SCA3 fibroblasts were transfected with 50nM of each AON. **(a)** Transfection with AON9.1 and AON10, or AON9.2 and AON10 resulted in modified ataxin-3 proteins of 35 kDa (ataxin-3 Δ72aa) and 37 kDa (ataxin-3 Δ59aa), respectively. The modified protein products were shown using an ataxin-3 specific antibody. The reduction in polyQ-containing mutant ataxin-3 was shown with the polyQ antibody 1C2. Densitometric analysis was used after transfection with AONs. Ataxin-3 Δ72aa (white bars) and ataxin-3 Δ59aa (black bars) in **(b)** control and **(c)** SCA3 cells. Mean + SD, data were evaluated using paired student t-test, * $P < 0.05$, ** $P < 0.01$, *** $P < 0.001$, relative to mock, n = 5.

samples with the full and partial exon skip approaches. This indicates a reduction of expanded polyQ-containing ataxin-3 in SCA3 patient derived fibroblasts after AON transfection.

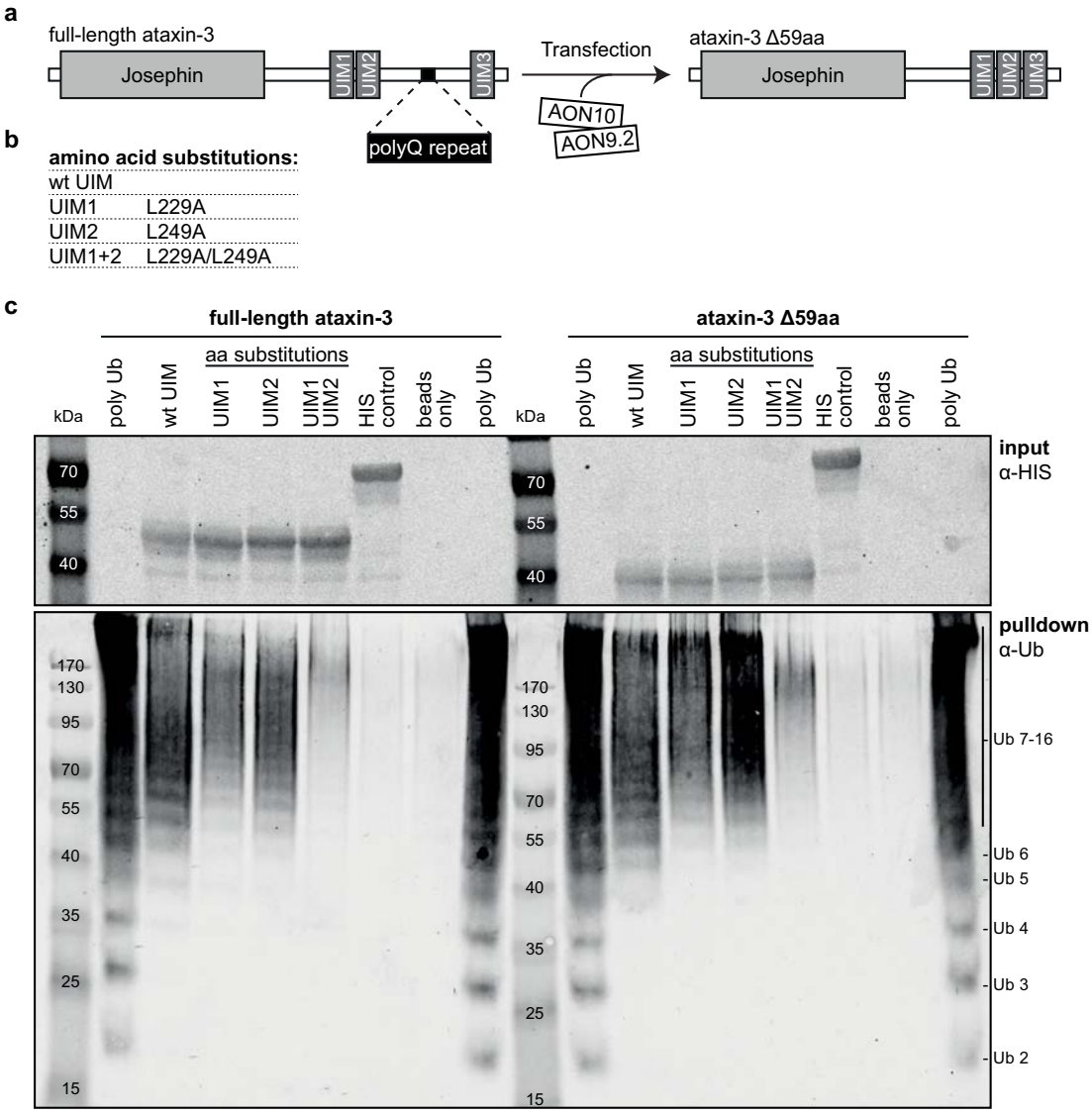

Figure 4. Full-length and modified ataxin-3 protein displays identical ubiquitin binding. **(a)** Schematic representation of the known functional domains of the ataxin-3 protein involved in deubiquitination. The ataxin-3 protein consists of an N-terminal (Josephin) domain with ubiquitin protease activity and a C-terminal tail with the polyQ repeat and 3 ubiquitin interacting motifs (UIMs). After exon skipping (ataxin-3 Δ59aa), the polyQ repeat is removed, leaving the Josephin domain and UIMs intact. **(b)** Overview of a leucine **(L)** to alanine **(A)** substitution in UIM 1 (L229A), UIM 2 (L249A) or both (L229A/L249A) in full-length ataxin-3 and ataxin-3 Δ59aa. **(c)** Ubiquitin binding assay. HIS-tagged full-length ataxin-3 and ataxin-3 Δ59aa-bound ubiquitylated proteins were analyzed by Western blot. HIS control and beads only were taken along as negative control. The modified ataxin-3 Δ59aa lacking the polyQ repeat showed identical ubiquitylated protein binding as unmodified ataxin-3. (n = 3)

The polyQ repeat in the ataxin-3 protein is located between the second and third UIM (**Figure 4A**). Both full and partial exon skip approaches resulted in removal of the polyQ repeat, preserving the Josephin domain, nuclear export signal (NES), and UIMs. To investigate whether the ubiquitin binding capacities of the UIMs in ataxin-3 are still intact after protein modification, poly-ubiquitin chains were incubated with purified cell free produced full-length ataxin-3 and ataxin-3 Δ59aa protein. As negative controls, we produced 3 different ataxin-3 protein products containing 1 amino acid substitutions from leucine (L) to alanine (A) in UIM 1 (L229A), UIM 2 (L249A), or both (L229A/L249A) (**Figure 4b**). Single amino acid changes in UIM 1 (L229A) already showed reduced binding of ataxin-3 to poly-ubiquitin chains, whereas double UIM mutated ataxin-3 (L229A/L249A) resulted in a nearly complete elimination poly-ubiquitin binding (**Figure 4c**). This is consistent with previously described data (Burnett *et al.*, 2003). The negative HIS control protein did not bind ubiquitylated proteins as expected. Ataxin-3 Δ59aa bound poly-ubiquitin chains comparable to full-length ataxin-3, indicating that its ubiquitin binding capacity after protein modification is still intact (**Figure 4c**).

AON mediated skipping of ataxin-3 exon 9 and 10 in mouse

To examine ataxin-3 exon skipping in the mouse brain and to determine if the modified protein is not harmful, we designed AONs specific to the mouse sequence. Since mice do not exhibit the cryptic splice site that is responsible for the partial exon 9 skip in the human transcript, we only investigated the full skip of exon 9 and 10. Transfection of 200 nM of each murine AON9 (mAON9) and AON10 (mAON10) in mouse C2C12 cells showed a skip of both exons with an efficiency of 31.7% (±2.4%) (**Figure 5a**). Sanger sequencing confirmed this in-frame double exon skip (**Figure 5b**). Transfection with mAON9 and mAON10 resulted in formation of a modified protein of 34 kDa (**Figure 5c**).

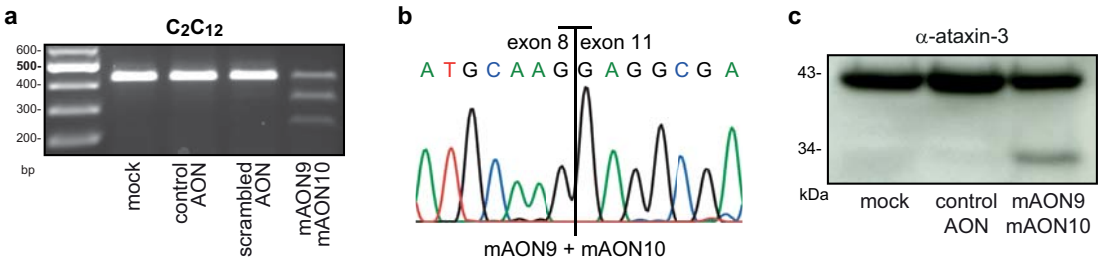

Figure 5. Double exon skipping of murine ataxin-3 pre-mRNA *in vitro*. Mouse C2C12 cells were transfected with murine ataxin-3 AONs, control AON, scrambled AON, and not transfected (Mock). **(a)** Agarose gel analysis of the ataxin-3 transcript with primers flanking exon 9 and 10. Skipping of ataxin-3 exon 9 and 10 was seen after transfection with mAON9.1 and mAON10. **(b)** Sanger sequencing confirmed the precise skipping of exon 9 and 10. **(c)** Transfection with mouse AON9.1 and AON10 resulted in the appearance of a modified ataxin-3 protein of 34 kDa.

Next, a single intra-cerebral ventricular (ICV) injection was administered of 40 µg ataxin-3 AON mix (20 µg per AON) or 40 µg scrambled AON. After 7 days the mice were sacrificed and skipping efficiency in the cerebellum was assessed by qRT-PCR (**Figure 6**). Exon 9 was found significantly reduced by 44.5% (±7.6%) and exon 10 was reduced by 35.9% (±14.1%) after a single ICV injection of AONs as compared to scrambled AON. Exon 4, upstream, and exon 11, downstream of the area targeted for skipping were not reduced, demonstrating a specific skip of ataxin-3 exon 9 and 10 *in vivo*.

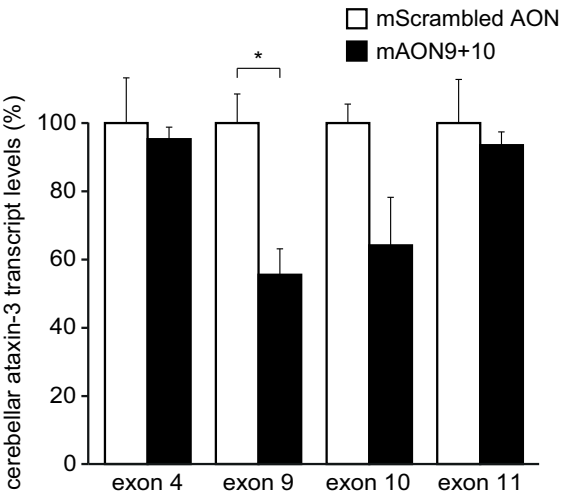

Figure 6. Reduction of mouse ataxin-3 exon 9 *in vivo*. Seven days after a single injection consisting of mAON9 and mAON10 (20 µg each) into the mouse cerebral ventricle. qRT-PCR analysis of cerebellar tissue showed reduced exon 9 and 10 transcript levels, whereas exon 4 and 11 levels were not affected. Mean + SD, data were evaluated using paired student t-test, * $P < 0.05$, n = 3.

5.5. Discussion

In the current study we show a novel approach to reduce toxicity of the mutant ataxin-3 protein through skipping of the CAG repeat containing exon in the ataxin-3 transcript. The resulting modified ataxin-3 protein lacks the polyQ repeat that is toxic when expanded, but maintains its ubiquitin binding properties. ICV administration of these AONs in mice resulted in skipping of the CAG repeat-containing exon in the cerebellum of control mice, proving distribution and efficiency of ataxin-3 exon skipping after ICV injection *in vivo*.

There was no negative effect on cell viability after AON treatment in both control and SCA3 fibroblasts and also no overt toxicity *in vivo*. There are several known important functional domains in ataxin-3 that have been implicated to be involved in the SCA3 pathogenesis. Skipping of exon 9 and 10 described here resulted in removal of sequences encoding the calcium-dependent calpain cleavage and nuclear localization signal (NLS), both located in exon 9. Following to the weak NLS located in the C-terminus (Macedo-Ribeiro *et al.*, 2009), the ataxin-3 protein has two strong NES located at the N-terminal part (Macedo-Ribeiro *et al.*, 2009). In SCA3 it is thought that proteolytic cleavage of mutant ataxin-3 results in C-terminal fragments lacking the NES but containing the polyglutamine stretch, resulting in localization of the toxic C-terminal fragments into the nucleus and formation of nuclear inclusion bodies (Bichelmeier *et al.*, 2007; Colomer Gould *et al.*, 2007). Recent studies in a mutant N-terminal ataxin-3 mouse model showed that N-terminal fragments, lacking the NLS, reside in the cytosol and form cytoplasmic inclusion bodies with subsequent neuronal degeneration (Hubener *et al.*, 2011). Both above described mutant C- and N-terminal ataxin-3 fragments could be the result of calpain cleavage at amino acid 260 (Haacke *et al.*, 2007). Skipping of exon 9 and 10 will also result in removal of an arginine/lysine-rich motif around amino acid 285 that was found to be a potential valosin containing protein (VCP) binding domain (Doss-Pepe *et al.*, 2003; Boeddrich *et al.*, 2006). The ataxin-3-VCP complex is thought to be involved in assisting targeted proteins to the proteasome (Wang *et al.*, 2006). In flies, co-expression of mutant ataxin-3 and VCP, resulted in alleviation of ataxin-3 aggregation and neurotoxicity in photoreceptor neurons (Boeddrich *et al.*, 2006). Whether removal of the VCP binding domain by exon skipping causes impaired degradation of target substrates needs to be assessed in future studies.

As potential gene silencing treatment for SCA3, both non-allele and allele-specific reduction of (mutant) ataxin-3 have been tested. The main advantage of the AON-based protein modification approach compared to existing gene silencing approaches is the preservation of overall ataxin-3 transcript and protein levels. Only the polyQ stretch and a small portion of the surrounding amino acids of the protein are removed and the N-terminal Josephine domain and C-terminal ubiquitin binding motifs are preserved. We validated this by showing that the modified ataxin-3 protein retains its normal ubiquitin binding function. Furthermore, the exon skipping approach described here has the advantage that one set of AONs can be applied to all SCA3 patients. This in contrast with a previously described SNP-specific approach (Miller *et al.*, 2003; Alves *et al.*, 2008) that is only applicable for 70% of the patients who have the

targeted SNP in their *ATXN3* gene (Gaspar *et al.*, 2001).

That AONs are a promising therapeutic tool was recently shown in phase I and phase I/II clinical trials in DMD (Cirak *et al.*, 2011; Goemans *et al.*, 2011). As treatment for neurodegenerative disorders, AONs with a phosphorothioate backbone are very promising and are currently tested in phase I and phase I/II clinical trials for amyotrophic lateral sclerosis (ClinicalTrials.gov, 2009) and, more recently, a phase I trial has been initiated for spinal muscular atrophy (Rigo *et al.*, 2012). After injection into the cerebrospinal fluid in non-human primates, AONs diffuse to the brain areas affected most in SCA3, which are the cerebellum, basal ganglia, and pons (Kordasiewicz *et al.*, 2012). In transgenic HD mice, the most pronounced mutant huntingtin protein reduction was seen after AON infusion for a limited period of time. Furthermore, several months after the last AON infusions there were sustained phenotypic improvements (Kordasiewicz *et al.*, 2012).

The above results are very promising but future experiments will have to determine the best route of administration to the brain, optimal dosage, and treatment regime. Future experiments are required to evaluate whether polyQ skipping improves the SCA3 induced phenotype using transgenic SCA3 mice. Furthermore, it will also be necessary to assess whether the modified ataxin-3 protein is not toxic *in vitro* and *in vivo* and whether exon skipping results in altered localization, function, or aggregation.

In conclusion, we show that it is possible to remove the toxic polyQ repeat from a polyQ disease-causing protein and that this modified ataxin-3 protein exhibits regular ubiquitin binding. We also show the *in vivo* potential of this approach as CAG repeat-containing exon skip in the cerebellum was seen after a single ICV injection.

5.6. Acknowledgements

The authors would like to thank Lodewijk Toonen and Nisha Verwey for technical assistance. This work was supported by AtaxiaUK (United Kingdom), patiëntenvereniging Autosomaal Dominante Cerebellaire Ataxia (ADCA) (the Netherlands), the Center for Biomedical Genetics (the Netherlands), and Center for Medical Systems Biology (OCM/IZ).

5.7. Supplementary material

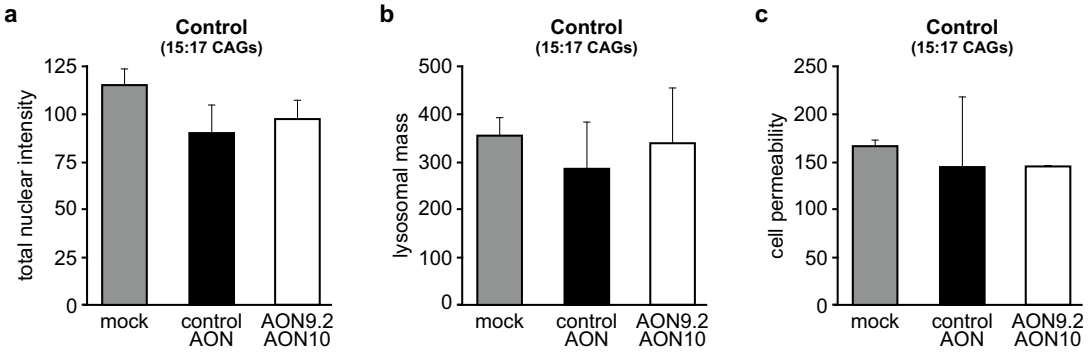

Figure S1. No negative effect on cell viability after ataxin-3 AON treatment in control fibroblasts. Control fibroblasts were transfected in a 96-wells plate with ataxin-3 AONs inducing partial skip of exon 9 and complete skip of exon 10 (AON9.2 + AON10), control AON, and non-transfected (mock). Two days after transfection cells were prepared for Cellomics multiparameter cytotoxicity version 3 (Thermo Fisher Scientific) measurements, according to manufacturer's instructions. Cell viability was analysed on the Array Scan VTI reader (Thermo Fisher Scientific) using the following absorption/emission filter sets: **(a)** total nuclear intensity: 350/461 nm, **(b)** lysosomal mass: 646/674 nm, and **(c)** cell permeability: 491/509 nm. All transfections were performed in triplicates on one plate. Mean ± SD, n = 2.

6

General discussion & Future perspective

6.1. Introduction

In this thesis I have discussed various AON-mediated therapies to reduce polyQ-induced toxicity, particularly in HD and SCA3. These expanded polyQ proteins are known to undergo proteolytic processing and this results in polyQ-containing protein fragments that are considered to be the main toxic entities in polyQ disorders. By targeting the polyQ-encoding transcripts, translation of mutant polyQ protein is reduced or the polyQ protein is modified. This is achieved by targeting the CAG repeat directly (chapter 3), removing the motifs that are implicated in the formation of polyQ fragments (chapter 4), or by removal of the CAG repeat-encoding exon (chapter 5).

Recently however, it has also been suggested that the polyQ pathogenesis is not only caused by polyQ protein toxicity. The significance of these novel findings will be assessed together with implication for the AON-mediated treatments proposed in this thesis. Subsequently, I will discuss the prospect of applying similar AON-mediated therapies to other polyQ disorders. Finally, using existing knowledge from preclinical studies with AONs in rodents and clinical trials with disease-modifying drugs, I will discuss what is required for the enrolment of future clinical trials of genetic therapies in polyQ diseased patients.

6.2. Main findings

In this thesis I propose various novel genetic therapies for polyQ disorders, aiming at reducing and/or modifying polyQ disease-causing proteins. While much research has been done on the underlying polyQ disease mechanisms, knowledge on mRNA and protein regulation and expression levels are limited. Chapter 2 describes differences in HTT RNA and htt protein expression in adult-onset HD with less mutant HTT mRNA, but equal wild-type and mutant htt protein levels. Juvenile HD subjects did show less mutant htt protein expression compared to wild-type, indicating subtle differences in htt protein expression between adult-onset and juvenile HD.

In chapter 3, CUG triplet-repeat AONs are used to reduce mutant polyQ transcript and protein levels in several polyQ disorders. A slight reduction in wild-type CAG transcript levels was observed as well, showing that the $(CUG)_7$ AON is not completely specific for the mutant allele. However, several other non-expanded CAG-containing transcripts investigated were not affected by $(CUG)_7$ AON treatment, implying the preference of the $(CUG)_7$ AON for the expanded transcript. Furthermore, chapter 2 describes that the basal levels of mutant HTT mRNA and protein are equal or lower than wild-type, providing feasibility for AONs such as the $(CUG)_7$ AON described in chapter 3, that are not completely specific for the mutant HTT allele.

Next to specifically targeting the expanded CAG repeat transcripts to reduce the translation of mutant polyQ protein, chapter 4 reports on removing motifs that are implicated in the formation of toxic polyQ fragments. Preventing the formation of a 586 amino acid N-terminal htt fragment, implicated in HD toxicity, is achieved by AONs that induce skipping of exon 12 in HTT pre-mRNA. This resulted in a shorter protein lacking the caspase-6 cleavage motif with subsequently reduced 586 amino acid N-terminal htt fragments. This proof of concept shows a completely novel approach to reduce mutant htt toxicity not by reducing its expression levels, but by modifying the protein.

A more direct genetic approach to reduce polyQ-induced toxicity is shown in chapter 5, where the toxic polyQ repeat is removed from the ataxin-3 protein through AON-mediated skipping of the CAG repeat-enclosing ATXN3 exon 10. A modified ataxin-3 protein is formed that lacks the toxic polyQ repeat, but may well maintain many important wild-type functions of the protein.

In chapter 4 and 5 the feasibility of the AONs is shown *in vivo* by ICV injections of the murine AONs into control mice. Above described results suggest that both targeting the CAG repeat directly, or AON-mediated exon skipping may be suitable therapeutic approaches to reduce polyQ-induced toxicity in HD, SCA3 and other polyQ disorders.

6.3. Recent developments

Until recently it was believed that polyQ disorders are solely the result of gain of toxic protein function and to a lesser extent, loss of wild-type protein function. Recent findings have shown that the molecular pathogenesis of these disorders is more complex. More and more observations suggest that next to polyQ protein toxicity, RNA toxicity and bidirectional transcription are also involved in the polyQ disease pathogenesis. These potential novel toxic mechanisms have to be taken into account when designing an AON-mediated disease-modifying treatment.

CAG repeat-induced RNA toxicity

Recently, in patient-derived juvenile HD fibroblasts expanded CAG repeat-induced RNA foci were shown (de Mezer *et al.*, 2011), suggesting a RNA toxicity component in HD. Furthermore, overexpression of untranslated repeats with 200 CAGs showed clear nuclear RNA foci, progressive neural dysfunction, reduced breeding efficiency, and premature death in various transgenes (Li *et al.*, 2008; Hsu *et al.*, 2011; Wang *et al.*, 2011). Although the exact mechanism of this expanded CAG repeat-induced toxicity remains elusive, there is some evidence that RNA toxicity may result from stable CAG hairpin structures which can sequester RNA binding proteins in nuclear foci, resulting in misregulation of alternative splicing (Li *et al.*, 2008; Mykowska *et al.*, 2011; Wang *et al.*, 2011). Next to CAG repeat-induced deregulation of splicing, short CAG repeat-containing RNAs of around 21 nucleotides, originating from mutant CAG repeat-containing RNAs were found to induce cell death (Banez-Coronel *et al.*, 2012). The toxicity was CAG repeat dependent, since toxicity was blocked by AONs against the CAG repeat sequence, similar to the $(CUG)_7$ AON described in chapter 3 (Banez-Coronel *et al.*, 2012).

The size of the CAG repeat is probably critical for the contribution of mRNA aggregation from the expanded CAG repeat because overexpression of untranslated repeats with 83 and 93 CAGs did not appear to result in a phenotype (McLeod *et al.*, 2005; Wang *et al.*, 2011). Likewise, in chapter 2 the levels of wild-type and mutant HTT mRNA and htt protein did not differ in adult-onset HD fibroblasts, suggesting that there is no mutant CAG repeat-induced mRNA aggregation in HD fibroblasts. To note, the repeat sizes of the adult-onset HD patients described in chapter 2 are shorter compared to the juvenile HD fibroblasts (with 68 and 151 CAGs repeats) in which RNA foci were observed (de Mezer *et al.*, 2011), and therefore CAG repeat-induced RNA toxicity could still play a role in patients with extremely expanded CAG repeat lengths.

In chapter 5 a novel protein modification approach is proposed to reduce mutant ataxin-3 toxicity by removing the toxic polyQ repeat from the ataxin-3 protein. In case of CAG repeat-induced RNA toxicity, this AON-mediated exon skipping is still applicable, since the toxic CAG repeat is removed from the mRNA. In the same way the RNA toxicity component in polyQ disorders will be prevented by the $(CUG)_7$ AON described in chapter 3, through direct binding of the $(CUG)_7$ AON to the expanded CAG repeat. The potential RNA toxicity is not targeted by

the AON-mediated htt protein modification described in chapter 4. This potential therapeutic approach prevents the formation of toxic N-terminal htt fragments and leaves the hypothetical toxic RNA entities intact. However, removal of the 586 caspase-6 site from the full-length mutant htt protein was shown to alleviate the phenotype in transgenic HD mice (Graham *et al.*, 2006; Pouladi *et al.*, 2009), supporting the significance of this particular htt protein fragment. Therefore the role of RNA toxicity in the disease pathology remains to be assessed.

Bidirectional transcription in polyQ disorders

For many genes in the genome transcription occurs from both DNA strands (Katayama *et al.*, 2005; He *et al.*, 2008). Several studies have shown that bidirectional transcription occurs from triplet repeat disorder genes (Cho *et al.*, 2005; Moseley *et al.*, 2006; Wilburn *et al.*, 2011). Although bidirectional transcriptional tags have been identified for all nine polyQ disease-causing loci (He *et al.*, 2008), only for HD and SCA7 antisense transcripts have been studied in more detail (Chung *et al.*, 2011; Sopher *et al.*, 2011). The SCA7 antisense noncoding transcript 1 (SCAANT1) and HTT antisense (HTTAS) transcripts are thought to be involved in downregulation of the corresponding sense *ATNX7* and *HTT* gene expression (Chung *et al.*, 2011; Sopher *et al.*, 2011). In total 3 HTTAS versions have been identified, of which one, HTTAS_v1 contained the CTG repeat whereas two other, HTTAS_v2.1 (Chung *et al.*, 2011) and HTTAS_v2.2 (chapter 2), did not. It was hypothesized that HTTAS_v1 was downregulated in HD patients since HTTAS_v1 with an expanded CTG repeat was not detected in HD brains (Chung *et al.*, 2011). However, in chapter 2 we did show HTTAS_v1 expression in human-derived fibroblasts homozygous for the CAG repeat expansion, suggesting that there is bidirectional transcription from the expanded CAG repeat, questioning the role of HTTAS in HTT regulation.

Altogether, these novel findings suggest that in some triplet repeat disorders bidirectional transcription could potentially play a role in the disease pathology. On the other hand, for only two out of nine polyQ disorders antisense transcripts have been characterized thus far, questioning the significance of bidirectional transcription in deregulation of sense transcripts and disease manifestation.

Other potential toxic entities in polyQ disorders

A major line of thinking with regard to polyQ disorder pathogenesis termed the 'toxic fragment hypothesis' concerns the proteolytic cleavage of polyQ expanded protein. This proteolytic cleavage is thought to lead to generation of short cytotoxic and aggregation-prone fragments containing the expanded polyQ repeat. Most research on the formation of toxic entities has been performed on HD, for which various rodent models expressing full-length or N-terminal mutant htt fragments have been generated (Heng *et al.*, 2008).

Recently, it was shown in various knock-in and transgenic HD mouse models that alternative splicing of HTT pre-mRNA results in a short HTT transcript with a stop codon in the beginning of intron 1 and a polyA tail 700 nucleotides into intron 1. This HTT exon 1-intron 1 transcript was shown to be translated into a short polyQ-containing htt protein of 216 amino acids (with 150Qs) (Sathasivam *et al.*, 2013). Interestingly, this aberrantly spliced transcript occurred in a

repeat-dependent manner, probably by altered binding of splicing factors to the expanded CAG repeat (Sathasivam *et al.*, 2013). While this alternative splicing of HTT pre-mRNA is interesting, it is difficult to assess the importance of this finding. Although the authors showed the aberrantly spliced transcript in patient-derived fibroblasts, they could only detect this HTT exon 1-intron transcript in two out of four *post-mortem* HD brain tissues. Neither did they show protein data from human brain samples, suggesting low abundance of this short N-terminal polyQ fragment in HD brain tissue. Still, these results show that not only posttranslational modification, but also gene expression alteration can generate short toxic N-terminal htt fragments. If this would be the main or sole pathogenic mechanism, this would mean that the removal of the 586 caspase-6 site from the full-length mutant htt protein as proposed in in chapter 4 would not be therapeutically beneficial. On the other hand, the $(CUG)_7$ AON described in chapter 3 would still prevent the formation of these short polyQ-containing htt protein fragments.

Other toxic entities resulting from reading frame shifting have been suggested to be involved in the polyQ disease pathogeneses. Next to expanded polyQ repeats, also polyA stretches occur in cells derived from HD and SCA3 patients (Gaspar *et al.*, 2000; Davies and Rubinsztein, 2006). These polyA stretches in the full-length ataxin-3 protein were toxic when overexpressed in *D. melanogaster* and neuronal cell models (Stochmanski *et al.*, 2012). Next to reading frame shifting, repeat associated non-ATG translation was recently also proposed as a novel class of protein toxicity, in which coding RNA transcripts with mutant CAG repeats are translated in the absence of an ATG start codon (Zu *et al.*, 2011). This repeat associated non-ATG translation was found in all three possible CAG repeat reading frames, resulting in the translation of proteins with polyQ, polyA, and polyserine (polyS) repeats (Zu *et al.*, 2011). However, these non-ATG translated htt and ataxin-3 proteins were only shown in artificial overexpression systems with low expression levels and their contribution to the polyQ disease pathology is as yet unclear.

To conclude, although most evidence points towards a toxic gain of polyQ protein fragments, novel toxic entities have been described that are potentially involved in the pathogenesis of polyQ disorders. These toxic proteins could be the result of aberrant splicing, proteolytic cleavage, reading frame shifting, or repeat associated non-ATG translation. On transcriptional level bidirectional transcription and CAG repeat-induced RNA toxicity could also be involved. Although extensive research is necessary to assess the relevance of these novel toxic entities, in many cases AON-mediated protein lowering approaches would still have an effect as they interfere with mRNA levels and compositions.

6.4. Future directions

There are several neurodegenerative disorders where AON-mediated therapies moved from preclinical to clinical testing during the course of this PhD research. All completed clinical trials on AON-mediated therapies into the CSF reported thus far have been successful and no major adverse events were reported (Rigo *et al.*, 2012; Miller *et al.*, 2013). Although recent preclinical results using non-allele-specific, SNP-specific and CAG repeat-targeting oligonucleotides look promising (Graham *et al.*, 2006; Alves *et al.*, 2008; Hu *et al.*, 2009b; Kordasiewicz *et al.*, 2012; Ostergaard *et al.*, 2013), no trials of genetic therapies in polyQ patients have been done thus far.

Modulating splicing in polyQ disorders

In chapter 3 an allele-specific silencing is achieved based on the common denominator of al polyQ patients, being their expanded CAG repeat. A reduction of the mutant transcript is shown in fibroblasts derived from patients with DRPLA, HD, SCA1, and SCA3. Unfortunately for the other 5 polyQ disorders the allele-specific effect of the $(CUG)_7$ AON could not be investigated, because no fibroblasts were available. Still, based on the mutant CAG repeat sizes of SBMA, SCA2, SCA7 and SCA17, it is expected that these can also be targeted by the $(CUG)_7$ AON. For SCA6 this could be more complicated since the pathogenic repeat size starts at already 19 CAGs.

Next to targeting the mutant CAG repeat directly, chapter 5 describes removal of the CAG repeat-containing exon 10 from ATXN3 pre-mRNA in SCA3. Recently, it was also shown that a $(CUG)_7$ single-stranded silencing RNA (ss-siRNA), comparable to the $(CUG)_7$ AON described in chapter 3, resulted in exon skipping of ataxin-3 exon 10 (Liu *et al.*, 2013). The $(CUG)_7$ ss-siRNA was found to mask exon 10 from the splicing machinery, resulting in the activation of a downstream stop codon and subsequently the formation of a shorter, C-terminus-lacking ataxin-3 protein. CAG repeat-containing exon skipping could hypothetically also be used for other polyQ disorders, except for HD, SBMA, SCA2 and SCA6, where the CAG repeat is located in the first or last exon of the transcript. In SCA7 the CAG repeat is located in the third exon of ATXN7, which is the first coding exon. In this case therefore, the activation of an alternative start 3'of the CAG repeat codon would be necessary for the translation of a polyQ lacking ataxin-7 protein. In SCA1 the CAG repeat is also located in the first coding exon, however, the ATXN1 transcript only consists of 2 coding exons, making exon skipping unsuitable. As explained in chapter 4 and 5, it could be necessary to use more AONs to remove additional exons to preserve the reading frame. To remove the CAG repeat in DRPLA and SCA17 this would mean skipping of two exons to induce translation of a modified polyQ-lacking atrophin-1 and TBP.

Chapter 4 describes a proof of concept for AON-mediated exon skipping to remove proteolytic cleavage motifs from the htt protein. Proteolytically processed polyQ fragments are implicated in toxicity of HD and other polyQ disorders (Shao and Diamond, 2007). Removal of these coding regions that code for the proteolytic cleavage site would ideally reduce the formation of toxic fragments. For SCA3 this would mean removal of ATXN3 exon 8 and 9 to

subsequently remove calpain and caspase cleavage sites from the ataxin-3 protein (Wellington *et al.*, 1998; Berke *et al.*, 2004; Hubener *et al.*, 2012). For DRPLA, it is preferred that the caspase-3 cleavage site near the N-terminus of the protein is removed from the protein. This is encoded by exon 5 of the *ATN1* gene (Wellington *et al.*, 1998; Ellerby *et al.*, 1999a). Skipping of exon 5, and exon 6 to maintain the reading frame, would result in the removal of both the proteolytic cleavage encoding region as well as the CAG repeat. The known caspase-3 cleavage motif in the AR is encoded by the first exon (Ellerby *et al.*, 1999b) and therefore AON-mediated skipping of this caspase-3 motif-encoding exon is not an option as treatment for SBMA. For the remaining polyQ disorders proteolytic processing has been implicated in disease pathogenesis, but the exact proteases and motifs are thus far unknown and therefore no AON-mediated therapy to remove proteolytic cleavage motifs can be designed for those disorders.

Towards clinical trials of genetic therapies for polyQ disorders

Some disease-modifying drugs were successful in small studies to prevent or even slow down the progression of polyQ disorders. But none of them were shown to be effective in larger, randomised, double-blind, placebo-controlled trials. For example, drugs aiming at correcting mitochondrial dysfunction, such as coenzyme Q10, ethyl-eicosapentaenoic acid, and antihistamine latrepirdine, were shown not to improve cognition or global function in HD patients in phase III placebo-controlled trials (Huntington Study Group, 2001; Huntington Study Group TREND-HD Investigators, 2008; HORIZON *et al.*, 2013). Likewise, the dopamine neurotransmission-stabilizing molecule pridopidine, which was promising in phase II, did not result in improved motor score in HD patients in a phase III clinical trial (de Yebenes *et al.*, 2011). A phase II/III clinical trial with lithium carbonate was recently carried out in SCA3 patients. The mechanism of lithium is thought to rely on upregulation of autophagy, though anti-apoptotic effects have also been implicated (Jia *et al.*, 2013). Due to the limited group size, this did not show a significant effect on disease progression as determined by the neurological examination score for spinocerebellar ataxia (Saute *et al.*, 2013).

For potential genetic therapies it would be best to start treatment before onset of clinical symptoms, before irreversible brain atrophy has occurred. Indeed, in symptomatic transgenic HD mice, AON treatment did not lead to a significant phenotypical improvement, whereas treatment of younger mice did show disease reversal (Kordasiewicz *et al.*, 2012). Yet after disease onset there seems to be a window of opportunity for AON treatments. In a conditional knockout model of SCA1 it was shown that removal of mutant ataxin-1 in 6 week old mice with mild motor deficits and some aggregation in Purkinje cells resulted in complete disease reversal (Zu *et al.*, 2004). Likewise, knockdown of mutant ataxin-1 in more severe 12 week old transgenic SCA1 mice with clear signs of ataxia and Purkinje cell atrophy a partial recovery was seen (Zu *et al.*, 2004), suggesting (partial) disease reversal in later stages.

The full penetrance of the polyQ mutation in combination with the availability of predictive genetic testing at the age of 18 provides the opportunity to start treatment in presymptomatic polyQ patients. The disease stage prior to onset of (typically motor) symptoms is variably called the presymptomatic, premanifest, preclinical or prodromal stage. The stage in which

subtle symptoms can be identified upon refined comparisons is called the prodromal stage. To assess the therapeutic benefit of disease-modifying compounds in polyQ patients who do not yet manifest signs of illness, there is a need for sensitive and stable clinical endpoints, such as subtle cognitive or motor improvement, brain imaging, or disease-specific biomarkers. As example, for HD the unified HD rating scale (UHDRS) is thus far used in clinical trials to show improvements on disease phenotype after disease-modifying drugs (Huntington Study Group, 1996), whereas for ataxias, the scale for the assessment and rating of ataxia (SARA) clinical scale has been developed as clinical measurement for trials (Schmitz-Hubsch *et al.*, 2006). However, available rating scales can only be reliably employed after onset of clinical symptoms and are therefore inadequate to assess therapeutic potency in presymptomatic polyQ patients. Likewise, both scales require a large number of patients to show a possible significant effect of treatment, which is not always feasible for the rare polyQ disorders.

Recently, much effort has been put into characterizing the polyQ disease stage before onset of symptoms. For HD, two extensive longitudinal observational studies are ongoing (Tabrizi *et al.*, 2013; Biglan *et al.*, 2013). Half-term reports showed that various motor and cognitive task scores were significantly decreased over 3 year period in presymptomatic HD individuals (Tabrizi *et al.*, 2013). Combining these individual measurements into a multidimensional diagnosis may result in a more sensitive diagnosis of presymptomatic HD (Biglan *et al.*, 2013). For the SCAs 1, 2, 3, and 6 a prospective observational study has also been enrolled to define presymptomatic disease stage. The first baseline data from the RISCA showed mild coordination deficits in SCA1 and SCA2 patients respectively 10 to 20 years before age of onset (Jacobi *et al.*, 2013). Follow-up studies of this cohort will hopefully gain more biological and clinical characteristics for SCA patients.

In summary, polyQ pathology can be measured long before the onset of clinical symptoms and preferably disease-modifying drugs such as AON-mediated therapeutics need to be administered in the presymptomatic stage to prevent polyQ-induced toxicity and with best prospect of reversal of disease.

6.5. In conclusion

This thesis proposes various novel genetic therapies for polyQ disorders, aiming at reducing and/or modifying polyQ disease-causing proteins. Since AONs are never 100% effective, it is likely that a combination of lowering mutant polyQ protein levels and modifying the remaining mutant polyQ protein will be the most optimal therapy for polyQ disorders. Future experiments in small rodents are required to evaluate whether AON-mediated treatment improves the polyQ induced phenotype. Furthermore, it will also be necessary to assess (1) whether the novel modified normal proteins retain their function and localization, and (2) whether the novel modified mutant proteins are less toxic and less aggregation-prone. Also the best route of administration to the brain, optimal dosage, and treatment regime needs to be determined.

The ultimate aim should of course be to cure patients, but a more realistic short-term objective would be to delay the age of onset or reduce the progression and thereby increase the quality of life for both polyQ patients and their families. Although extensive *in vitro* and *in vivo* research is required to rule out toxic off-target effects of the various AONs and the resulting modified proteins, these preclinical AON-mediated treatments look promising. Hopefully this thesis will help in the quest to develop treatments for individuals with one of the polyQ disorders.

7

References

Aartsma-Rus,A., Bremmer-Bout,M., Janson,A.A., den Dunnen,J.T., van Ommen,G.J., and van Deutekom,J.C. (2002). Targeted exon skipping as a potential gene correction therapy for Duchenne muscular dystrophy. Neuromuscular Disord. 12, S71-S77.

Aartsma-Rus,A., de Winter,C.L., Janson,A.A., Kaman,W.E., van Ommen,G.J., den Dunnen,J.T., and van Deutekom,J.C. (2005). Functional analysis of 114 exon-internal AONs for targeted DMD exon skipping: indication for steric hindrance of SR protein binding sites. Oligonucleotides. 15, 284-297.

Aartsma-Rus,A., van Vliet,L., Hirschi,M., Janson,A.A., Heemskerk,H., de Winter,C.L., de Kimpe,S., van Deutekom,J.C., 't Hoen,P.A., and van Ommen,G.J. (2009). Guidelines for antisense oligonucleotide design and insight into splice-modulating mechanisms. Mol. Ther. 17, 548-553.

Aartsma-Rus,A. (2012). Overview on AON design. Methods Mol. Biol. 867, 117-129.

Ajayi,A., Yu,X., Lindberg,S., Langel,U., and Strom,A.L. (2012). Expanded ataxin-7 cause toxicity by inducing ROS production from NADPH oxidase complexes in a stable inducible Spinocerebellar ataxia type 7 (SCA7) model. BMC. Neurosci. 13, 86.

Alavijeh,M.S., Chishty,M., Qaiser,M.Z., and Palmer,A.M. (2005). Drug metabolism and pharmacokinetics, the blood-brain barrier, and central nervous system drug discovery. NeuroRx. 2, 554-571.

Albrecht,M., Hoffmann,D., Evert,B.O., Schmitt,I., Wullner,U., and Lengauer,T. (2003). Structural modeling of ataxin-3 reveals distant homology to adaptins. Proteins 50, 355-370.

Albrecht,M., Golatta,M., Wullner,U., and Lengauer,T. (2004). Structural and functional analysis of ataxin-2 and ataxin-3. Eur. J. Biochem. 271, 3155-3170.

Alves,S., Nascimento-Ferreira,I., Auregan,G., Hassig,R., Dufour,N., Brouillet,E., Pedroso de Lima,M.C., Hantraye,P., Pereira de,A.L., and Deglon,N. (2008). Allele-specific RNA silencing of mutant ataxin-3 mediates neuroprotection in a rat model of Machado-Joseph disease. PLoS One 3, e3341.

Alves,S., Nascimento-Ferreira,I., Dufour,N., Hassig,R., Auregan,G., Nobrega,C., Brouillet,E., Hantraye,P., Pedroso de Lima,M.C., Deglon,N., and de Almeida,L.P. (2010). Silencing ataxin-3 mitigates degeneration in a rat model of Machado-Joseph disease: no role for wild-type ataxin-3? Hum. Mol. Genet. 19, 2380-2394.

Amantana,A., Moulton,H.M., Cate,M.L., Reddy,M.T., Whitehead,T., Hassinger,J.N., Youngblood,D.S., and Iversen,P.L. (2007). Pharmacokinetics, biodistribution, stability and toxicity of a cell-penetrating peptide-morpholino oligomer conjugate. Bioconjug. Chem. 18, 1325-1331.

Andresen,J.M., Gayan,J., Djousse,L., Roberts,S., Brocklebank,D., Cherny,S.S., Cardon,L.R., Gusella,J.F., MacDonald,M.E., Myers,R.H., Housman,D.E., and Wexler,N.S. (2007). The relationship between CAG repeat length and age of onset differs for Huntington's disease patients with juvenile onset or adult onset. Ann Hum. Genet. 71, 295-301.

Andrew,S.E., Goldberg,Y.P., Kremer,B., Telenius,H., Theilmann,J., Adam,S., Starr,E., Squitieri,F., Lin,B., Kalchman,M.A., Graham,R.K., and Hayden,M.R. (1993). The relationship between trinucleotide (CAG) repeat length and clinical features of Huntington disease. Am. J. Hum. Gen. 53, 1118.

Antony,P.M., Mantele,S., Mollenkopf,P., Boy,J., Kehlenbach,R.H., Riess,O., and Schmidt,T. (2009). Identification and functional dissection of localization signals within ataxin-3. Neurobiol. Dis. 36, 280-292.

Appl,T., Kaltenbach,L., Lo,D.C., and Terstappen,G.C. (2012). Targeting mutant huntingtin for the development of disease-modifying therapy. Drug Discov. Today 17, 1217-1223.

Araujo,J., Breuer,P., Dieringer,S., Krauss,S., Dorn,S., Zimmermann,K., Pfeifer,A., Klockgether,T., Wuellner,U., and Evert,B.O. (2011). FOXO4-dependent upregulation of superoxide dismutase-2 in response to oxidative stress is impaired in spinocerebellar ataxia type 3. Hum. Mol. Genet. 20, 2928-2941.

Arrasate,M., Mitra,S., Schweitzer,E.S., Segal,M.R., and Finkbeiner,S. (2004). Inclusion body formation reduces levels of mutant huntingtin and the risk of neuronal death. Nature 431, 805-810.

Atwal,R.S., Xia,J., Pinchev,D., Taylor,J., Epand,R.M., and Truant,R. (2007). Huntingtin has a membrane association signal that can modulate huntingtin aggregation, nuclear entry and toxicity. Hum. Mol. Genet. 16, 2600-2615.

Banez-Coronel,M., Porta,S., Kagerbauer,B., Mateu-Huertas,E., Pantano,L., Ferrer,I., Guzman,M., Estivill,X., and Marti,E. (2012). A pathogenic mechanism in Huntington's disease involves small CAG-repeated RNAs with neurotoxic activity. PLoS Genet. 8, e1002481.

Banno,H., Katsuno,M., Suzuki,K., Tanaka,F., and Sobue,G. (2012). Pathogenesis and molecular targeted therapy of spinal and bulbar muscular atrophy (SBMA). Cell Tissue Res. 349, 313-320.

Bauer,P.O. and Nukina,N. (2009). The pathogenic mechanisms of polyglutamine diseases and current therapeutic strategies. J. Neurochem. 110, 1737-1765.

Bauer,S., Kirschning,C.J., Hacker,H., Redecke,V., Hausmann,S., Akira,S., Wagner,H., and Lipford,G.B. (2001). Human TLR9 confers responsiveness to bacterial DNA via species-specific CpG motif recognition. Proc. Natl. Acad. Sci. U. S. A. 98, 9237-9242.

Beitel,L.K., Alvarado,C., Mokhtar,S., Paliouras,M., and Trifiro,M. (2013). Mechanisms mediating spinal and bulbar muscular atrophy: investigations into polyglutamine-expanded androgen receptor function and dysfunction. Front. Neurol. 4, 53.

Bence,N.F., Sampat,R.M., and Kopito,R.R. (2001). Impairment of the ubiquitin-proteasome system by protein aggregation. Science 292, 1552-1555.

Berke,S.J., Schmied,F.A., Brunt,E.R., Ellerby,L.M., and Paulson,H.L. (2004). Caspase-mediated proteolysis of the polyglutamine disease protein ataxin-3. J. Neurochem. 89, 908-918.

Berke,S.J., Chai,Y., Marrs,G.L., Wen,H., and Paulson,H.L. (2005). Defining the role of ubiquitin-interacting motifs in the polyglutamine disease protein, ataxin-3. J. Biol. Chem. 280, 32026-32034.

Bernacki,J., Dobrowolska,A., Nierwinska,K., and Malecki,A. (2008). Physiology and pharmacological role of the blood-brain barrier. Pharmacol. Rep. 60, 600-622.

Bett,J.S., Cook,C., Petrucelli,L., and Bates,G.P. (2009). The ubiquitin-proteasome reporter GFPu does not accumulate in neurons of the R6/2 transgenic mouse model of Huntington's disease. PLoS One 4, e5128.

Bettencourt,C., Santos,C., Montiel,R., Costa,M.C., Cruz-Morales,P., Santos,L.R., Simoes,N., Kay,T., Vasconcelos,J., Maciel,P., and Lima,M. (2010). Increased transcript diversity: novel splicing variants of Machado-Joseph disease gene (ATXN3). Neurogenetics 11, 193-202.

Bettencourt,C. and Lima,M. (2011). Machado-Joseph Disease: from first descriptions to new perspectives. Orphanet. J. Rare. Dis. 6, 35.

Bichelmeier,U., Schmidt,T., Hubener,J., Boy,J., Ruttiger,L., Habig,K., Poths,S., Bonin,M., Knipper,M., Schmidt,W.J., Wilbertz,J., Wolburg,H., Laccone,F., and Riess,O. (2007). Nuclear localization of ataxin-3 is required for the manifestation of symptoms in SCA3: in vivo evidence. J. Neurosci. 27, 7418-7428.

Biglan,K.M., Zhang,Y., Long,J.D., Geschwind,M., Kang,G.A., Killoran,A., Lu,W., McCusker,E., Mills,J.A., Raymond,L.A., Testa,C., Wojcieszek,J., and Paulsen,J.S. (2013). Refining the diagnosis of Huntington disease: the PREDICT-HD study. Front. Aging Neurosci. 5, 12.

Boeddrich,A., Gaumer,S., Haacke,A., Tzvetkov,N., Albrecht,M., Evert,B.O., Muller,E.C., Lurz,R., Breuer,P., Schugardt,N., Plassmann,S., Xu,K., Warrick,J.M., Suopanki,J., Wullner,U., Frank,R., Hartl,U.F., Bonini,N.M., and Wanker,E.E. (2006). An arginine/lysine-rich motif is crucial for VCP/p97-mediated modulation of ataxin-3 fibrillogenesis. EMBO J. 25, 1547-1558.

Bossy-Wetzel,E., Schwarzenbacher,R., and Lipton,S.A. (2004). Molecular pathways to neurodegeneration. Nat. Med. 10 Suppl, S2-S9.

Boudreau,R.L., McBride,J.L., Martins,I., Shen,S., Xing,Y., Carter,B.J., and Davidson,B.L. (2009). Nonallele-specific silencing of mutant and wild-type huntingtin demonstrates therapeutic efficacy in Huntington's disease mice. Mol. Ther. 17, 1053-1063.

Boy,J., Schmidt,T., Wolburg,H., Mack,A., Nuber,S., Bottcher,M., Schmitt,I., Holzmann,C., Zimmermann,F., Servadio,A., and Riess,O. (2009). Reversibility of symptoms in a conditional mouse model of spinocerebellar ataxia type 3. Hum. Mol. Genet. 18, 4282-4295.

Breuer,P., Haacke,A., Evert,B.O., and Wullner,U. (2010). Nuclear aggregation of polyglutamine-expanded ataxin-3: fragments escape the cytoplasmic quality control. J. Biol. Chem. 285, 6532-6537.

Brinkmann,A.O. (2011). Molecular mechanisms of androgen action--a historical perspective. Methods Mol. Biol. 776, 3-24.

Brook,J.D., McCurrach,M.E., Harley,H.G., Buckler,A.J., Church,D., Aburatani,H., Hunter,K., Stanton,V.P., Thirion,J.P., Hudson,T., and . (1992). Molecular basis of myotonic dystrophy: expansion of a trinucleotide (CTG) repeat at the 3' end of a transcript encoding a protein kinase family member. Cell 68, 799-808.

Burnett,B., Li,F., and Pittman,R.N. (2003). The polyglutamine neurodegenerative protein ataxin-3 binds polyubiquitylated proteins and has ubiquitin protease activity. Hum. Mol. Genet. 12, 3195-3205.

Burnett,B.G. (2005). The polyglutamine neurodegenerative protein ataxin 3 regulates aggresome formation. Proc. Natl. Acad. Sci. U. S. A. 102, 4330-4335.

Burright,E.N., Clark,H.B., Servadio,A., Matilla,T., Feddersen,R.M., Yunis,W.S., Duvick,L.A., Zoghbi,H.Y., and Orr,H.T. (1995). SCA1 transgenic mice: a model for neurodegeneration caused by an expanded CAG trinucleotide repeat. Cell 82, 937-948.

Busch,A., Engemann,S., Lurz,R., Okazawa,H., Lehrach,H., and Wanker,E.E. (2003). Mutant huntingtin promotes the fibrillogenesis of wild-type huntingtin: a potential mechanism for loss of huntingtin function in Huntington's disease. J. Biol. Chem. 278, 41452-41461.

Caplen,N.J., Taylor,J.P., Statham,V.S., Tanaka,F., Fire,A., and Morgan,R.A. (2002). Rescue of polyglutamine-mediated cytotoxicity by double-stranded RNA-mediated RNA interference. Hum. Mol. Genet. 11, 175-184.

Carroll,J.B., Warby,S.C., Southwell,A.L., Doty,C.N., Greenlee,S., Skotte,N., Hung,G., Bennett,C.F., Freier,S.M., and Hayden,M.R. (2011). Potent and selective antisense oligonucleotides targeting single-nucleotide polymorphisms in the Huntington disease gene / allele-specific silencing of mutant huntingtin. Mol. Ther. 19, 2178-2185.

Carvalho,D.R., La Rocque-Ferreira,A., Rizzo,I.M., Imamura,E.U., and Speck-Martins,C.E. (2008). Homozygosity enhances severity in spinocerebellar ataxia type 3. Pediatr. Neurol. 38, 296-299.

Cattaneo,E., Rigamonti,D., Goffredo,D., Zuccato,C., Squitieri,F., and Sipione,S. (2001). Loss of normal huntingtin function: new developments in Huntington's disease research. Trends Neurosci. 24, 182-188.

Cattaneo,E., Zuccato,C., and Tartari,M. (2005). Normal huntingtin function: An alternative approach to Huntington's disease. Nat. Rev. Neurosci. 6, 919-930.

Caviston,J.P., Zajac,A.L., Tokito,M., and Holzbaur,E.L. (2011). Huntingtin coordinates the dynein-mediated dynamic positioning of endosomes and lysosomes. Mol. Biol. Cell 22, 478-492.

Cemal,C.K., Carroll,C.J., Lawrence,L., Lowrie,M.B., Ruddle,P., Al-Mahdawi,S., King,R.H., Pook,M.A., Huxley,C., and Chamberlain,S. (2002). YAC transgenic mice carrying pathological alleles of the MJD1 locus exhibit a mild and slowly progressive cerebellar deficit. Hum. Mol. Genet. 11, 1075-1094.

Cha,J.H. (2007). Transcriptional signatures in Huntington's disease. Prog. Neurobiol. 83, 228-248.

Chai,Y., Koppenhafer,S.L., Shoesmith,S.J., Perez,M.K., and Paulson,H.L. (1999). Evidence for proteasome involvement in polyglutamine disease: localization to nuclear inclusions in SCA3/MJD and suppression of polyglutamine aggregation in vitro. Hum. Mol. Genet. 8, 673-682.

Chai,Y., Shao,J., Miller,V.M., Williams,A., and Paulson,H.L. (2002). Live-cell imaging reveals divergent intracellular dynamics of polyglutamine disease proteins and supports a sequestration model of pathogenesis. Proc. Natl. Acad. Sci. U. S. A. 99, 9310-9315.

Chang,D.T., Rintoul,G.L., Pandipati,S., and Reynolds,I.J. (2006). Mutant huntingtin aggregates impair mitochondrial movement and trafficking in cortical neurons. Neurobiol. Dis. 22, 388-400.

Chauhan,N.B. and Siegel,G.J. (2007). Antisense inhibition at the [beta]-secretase-site of [beta]-amyloid precursor protein reduces cerebral amyloid and acetyl cholinesterase activity in Tg2576. Neuroscience 146, 143-151.

Chen,H.K., Fernandez-Funez,P., Acevedo,S.F., Lam,Y.C., Kaytor,M.D., Fernandez,M.H., Aitken,A., Skoulakis,E.M., Orr,H.T., Botas,J., and Zoghbi,H.Y. (2003). Interaction of Akt-phosphorylated ataxin-1 with 14-3-3 mediates neurodegeneration in spinocerebellar ataxia type 1. Cell 113, 457-468.

Cho,D.H., Thienes,C.P., Mahoney,S.E., Analau,E., Filippova,G.N., and Tapscott,S.J. (2005). Antisense transcription and heterochromatin at the DM1 CTG repeats are constrained by CTCF. Mol. Cell 20, 483-489.

Choo,Y.S., Johnson,G.V., MacDonald,M., Detloff,P.J., and Lesort,M. (2004). Mutant huntingtin directly increases susceptibility of mitochondria to the calcium-induced permeability transition and cytochrome c release. Hum. Mol. Genet. 13, 1407-1420.

Chou,A.H., Yeh,T.H., Ouyang,P., Chen,Y.L., Chen,S.Y., and Wang,H.L. (2008). Polyglutamine-expanded ataxin-3 causes cerebellar dysfunction of SCA3 transgenic mice by inducing transcriptional dysregulation. Neurobiol. Dis. 31, 89-101.

Chung,D.W., Rudnicki,D.D., Yu,L., and Margolis,R.L. (2011). A natural antisense transcript at the Huntington's disease repeat locus regulates HTT expression. Hum. Mol. Genet. 20, 3467-3477.

Cirak,S., Arechavala-Gomeza,V., Guglieri,M., Feng,L., Torelli,S., Anthony,K., Abbs,S., Garralda,M.E., Bourke,J., Wells,D.J., Dickson,G., Wood,M.J., Wilton,S.D., Straub,V., Kole,R., Shrewsbury,S.B., Sewry,C., Morgan,J.E., Bushby,K., and Muntoni,F. (2011). Exon skipping and dystrophin restoration in patients with Duchenne muscular dystrophy after systemic phosphorodiamidate morpholino oligomer treatment: an open-label, phase 2, dose-escalation study. Lancet 378, 595-605.

ClinicalTrials.gov. (2009) Safety,Tolerability,and Activity Study of ISIS SOD1Rx to Treat Familial Amyotrophic Lateral Sclerosis (ALS) Caused by SOD1 Gene Mutations (SOD-1). NCT01041222.

ClinicalTrials.gov. (2011). An Open-label Safety, Tolerability, and Dose-range Finding Study of ISIS SMNRx in Patients With Spinal Muscular Atrophy. NCT01494701.

ClinicalTrials.gov. (2012). An Open-label Safety, Tolerability and Dose-range Finding Study of Multiple Doses of ISIS SMNRx in Patient With Spinal Muscular Atrophy (SMNRx - CS2). NCT01703988.

Cloud,L.J. and Wilmot,G. (2012). Other spinocerebellar ataxias. Handb. Clin. Neurol. 103, 581-586.

Colomer Gould,V.F., Goti,D., Pearce,D., Gonzalez,G.A., Gao,H., Bermudez de,L.M., Jenkins,N.A., Copeland,N.G., Ross,C.A., and Brown,D.R. (2007). A mutant ataxin-3 fragment results from processing at a site N-terminal to amino acid 190 in brain of Machado-Joseph disease-like transgenic mice. Neurobiol. Dis. 27, 362-369.

Cooper,J.K., Schilling,G., Peters,M.F., Herring,W.J., Sharp,A.H., Kaminsky,Z., Masone,J., Khan,F.A., Delanoy,M., Borchelt,D.R., Dawson,V.L., Dawson,T.M., and Ross,C.A. (1998). Truncated N-terminal fragments of huntingtin with expanded glutamine repeats form nuclear and cytoplasmic aggregates in cell culture. Hum. Mol. Genet. 7, 783-790.

Cortes,C.J. and La Spada,A.R. (2014). The many faces of autophagy dysfunction in Huntington's disease: from mechanistic pathways to therapeutic opportunities. Drug Discov. Today.

Cotzias,G.C., Van Woert,M.H., and Schiffer,L.M. (1967). Aromatic amino acids and modification of parkinsonism. N. Engl. J. Med. 276, 374-379.

Coutinho,P. and Andrade,C. (1978). Autosomal dominant system degeneration in Portuguese families of the Azores Islands. A new genetic disorder involving cerebellar, pyramidal, extrapyramidal and spinal cord motor functions. Neurology 28, 703-709.

Crespo-Barreto,J., Fryer,J.D., Shaw,C.A., Orr,H.T., and Zoghbi,H.Y. (2010). Partial loss of ataxin-1 function contributes to transcriptional dysregulation in spinocerebellar ataxia type 1 pathogenesis. PLoS Genet. 6, e1001021.

Crook,Z.R. and Housman,D. (2011). Huntington's disease: can mice lead the way to treatment? Neuron 69, 423-435.

Cummings,C.J. and Zoghbi,H.Y. (2000a). Fourteen and counting: unraveling trinucleotide repeat diseases. Hum. Mol. Genet. 9, 909-916.

Cummings,C.J. and Zoghbi,H.Y. (2000b). Trinucleotide repeats: mechanisms and pathophysiology. Annu. Rev. Genomics Hum. Genet. 1, 281-328.

David,G., Abbas,N., Stevanin,G., Durr,A., Yvert,G., Cancel,G., Weber,C., Imbert,G., Saudou,F., Antoniou,E., Drabkin,H., Gemmill,R., Giunti,P., Benomar,A., Wood,N., Ruberg,M., Agid,Y., Mandel,J.L., and Brice,A. (1997). Cloning of the SCA7 gene reveals a highly unstable CAG repeat expansion. Nat. Genet. 17, 65-70.

Davies,J.E. and Rubinsztein,D.C. (2006). Polyalanine and polyserine frameshift products in Huntington's disease. J. Med. Genet. 43, 893-896.

Davies,S.W., Turmaine,M., Cozens,B.A., Difiglia,M., Sharp,A.H., Ross,C.A., Scherzinger,E., Wanker,E.E., Mangiarini,L., and Bates,G.P. (1997). Formation of neuronal intranuclear inclusions underlies the neurological dysfunction in mice transgenic for the HD mutation. Cell 90, 537-548.

Davis,B.M., McCurrach,M.E., Taneja,K.L., Singer,R.H., and Housman,D.E. (1997). Expansion of a CUG trinucleotide repeat in the 3' untranslated region of myotonic dystrophy protein kinase transcripts results in nuclear retention of transcripts. Proc. Natl. Acad. Sci. U. S. A. 94, 7388-7393.

de Mezer,M., Wojciechowska,M., Napierala,M., Sobczak,K., and Krzyzosiak,W.J. (2011). Mutant CAG repeats of Huntingtin transcript fold into hairpins, form nuclear foci and are targets for RNA interference. Nucleic Acids Res. 39, 3852-3863.

de Rooij,K.E., Dorsman,J.C., Smoor,M.A., Den Dunnen,J.T., and Van Ommen,G.J. (1996). Subcellular localization of the Huntington's disease gene product in cell lines by immunofluorescence and biochemical subcellular fractionation. Hum. Mol. Genet. 5, 1093-1099.

de Yebenes,J.G., Landwehrmeyer,B., Squitieri,F., Reilmann,R., Rosser,A., Barker,R.A., Saft,C., Magnet,M.K., Sword,A., Rembratt,A., and Tedroff,J. (2011). Pridopidine for the treatment of motor function in patients with Huntington's disease (MermaiHD): a phase 3, randomised, double-blind, placebo-controlled trial. Lancet Neurol. 10, 1049-1057.

Desmet,F.O., Hamroun,D., Lalande,M., Collod-Beroud,G., Claustres,M., and Beroud,C. (2009). Human Splicing Finder: an online bioinformatics tool to predict splicing signals. Nucleic Acids Res. 37, e67.

Di Benedetto,B., Wefers,B., Wurst,W., and Kuhn,R. (2009). Local knockdown of ERK2 in the adult mouse brain via adeno-associated virus-mediated RNA interference. Mol. Biotechnol. 41, 263-269.

Diaz-Hernandez,M., Valera,A.G., Moran,M.A., Gomez-Ramos,P., Alvarez-Castelao,B., Castano,J.G., Hernandez,F., and Lucas,J.J. (2006). Inhibition of 26S proteasome activity by huntingtin filaments but not inclusion bodies isolated from mouse and human brain. J. Neurochem. 98, 1585-1596.

Difiglia,M., Sapp,E., Chase,K.O., Davies,S.W., Bates,G.P., Vonsattel,J.P., and Aronin,N. (1997). Aggregation of huntingtin in neuronal intranuclear inclusions and dystrophic neurites in brain. Science 277, 1990-1993.

Ding,S.W. and Voinnet,O. (2007). Antiviral immunity directed by small RNAs. Cell 130, 413-426.

do Carmo,C.M., Bajanca,F., Rodrigues,A.J., Tome,R.J., Corthals,G., Macedo-Ribeiro,S., Paulson,H.L., Logarinho,E., and Maciel,P. (2010). Ataxin-3 plays a role in mouse myogenic differentiation through regulation of integrin subunit levels. PLoS One 5, e11728.

Donato,S.D., Mariotti,C., and Taroni,F. (2012). Spinocerebellar ataxia type 1. Handb. Clin. Neurol. 103, 399-421.

Doss-Pepe,E.W., Stenroos,E.S., Johnson,W.G., and Madura,K. (2003). Ataxin-3 interactions with rad23 and valosin-containing protein and its associations with ubiquitin chains and the proteasome are consistent with a role in ubiquitin-mediated proteolysis. Mol. Cell Biol. 23, 6469-6483.

Doyu,M., Sobue,G., Mukai,E., Kachi,T., Yasuda,T., Mitsuma,T., and Takahashi,A. (1992). Severity of X-linked recessive bulbospinal neuronopathy correlates with size of the tandem CAG repeat in androgen receptor gene. Ann. Neurol. 32, 707-710.

Dragatsis,I., Levine,M.S., and Zeitlin,S. (2000). Inactivation of Hdh in the brain and testis results in progressive neurodegeneration and sterility in mice. Nat. Genet. 26, 300-306.

Drouet,V., Perrin,V., Hassig,R., Dufour,N., Auregan,G., Alves,S., Bonvento,G., Brouillet,E., Luthi-Carter,R., Hantraye,P., and Deglon,N. (2009). Sustained effects of nonallele-specific Huntingtin silencing. Ann. Neurol. 65, 276-285.

Du,L., Kayali,R., Bertoni,C., Fike,F., Hu,H., Iversen,P.L., and Gatti,R.A. (2011). Arginine-rich cell-penetrating peptide dramatically enhances AMO-mediated ATM aberrant splicing correction and enables delivery to brain and cerebellum. Hum. Mol. Genet. 20, 3151-3160.

Duennwald,M.L. and Lindquist,S. (2008). Impaired ERAD and ER stress are early and specific events in polyglutamine toxicity. Genes Dev. 22, 3308-3319.

Durr,A., Stevanin,G., Cancel,G., Duyckaerts,C., Abbas,N., Didierjean,O., Chneiweiss,H., Benomar,A., Lyon-Caen,O., Julien,J., Serdaru,M., Penet,C., Agid,Y., and Brice,A. (1996). Spinocerebellar ataxia 3 and Machado-Joseph disease: clinical, molecular, and neuropathological features. Ann. Neurol. 39, 490-499.

Duyao,M.P., Auerbach,A.B., Ryan,A., Persichetti,F., Barnes,G.T., McNeil,S.M., Ge,P., Vonsattel,J.P., Gusella,J.F., and Joyner,A.L. (1995). Inactivation of the mouse Huntington's disease gene homolog Hdh. Science 269, 407-410.

Ehlert,E.M., Eggers,R., Niclou,S.P., and Verhaagen,J. (2010). Cellular toxicity following application of adeno-associated viral vector-mediated RNA interference in the nervous system. BMC. Neurosci. 11, 20.

Ehrnhoefer,D.E., Sutton,L., and Hayden,M.R. (2011). Small changes, big impact: posttranslational modifications and function of huntingtin in Huntington disease. Neuroscientist. 17, 475-492.

Elden,A.C., Kim,H.J., Hart,M.P., Chen-Plotkin,A.S., Johnson,B.S., Fang,X., Armakola,M., Geser,F., Greene,R., Lu,M.M., Padmanabhan,A., Clay-Falcone,D., McCluskey,L., Elman,L., Juhr,D., Gruber,P.J., Rub,U., Auburger,G., Trojanowski,J.Q., Lee,V.M., Van Deerlin,V.M., Bonini,N.M., and Gitler,A.D. (2010). Ataxin-2 intermediate-length polyglutamine expansions are associated with increased risk for ALS. Nature 466, 1069-1075.

Ellerby,L.M., Andrusiak,R.L., Wellington,C.L., Hackam,A.S., Propp,S.S., Wood,J.D., Sharp,A.H., Margolis,R.L., Ross,C.A., Salvesen,G.S., Hayden,M.R., and Bredesen,D.E. (1999a). Cleavage of atrophin-1 at caspase site aspartic acid 109 modulates cytotoxicity. J. Biol. Chem. 274, 8730-8736.

Ellerby,L.M., Hackam,A.S., Propp,S.S., Ellerby,H.M., Rabizadeh,S., Cashman,N.R., Trifiro,M.A., Pinsky,L., Wellington,C.L., Salvesen,G.S., Hayden,M.R., and Bredesen,D.E. (1999b). Kennedy's disease: caspase cleavage of the androgen receptor is a crucial event in cytotoxicity. J. Neurochem. 72, 185-195.

Emerit,J., Edeas,M., and Bricaire,F. (2004). Neurodegenerative diseases and oxidative stress. Biomed. Pharmacother. 58, 39-46.

Enevoldson,T.P., Sanders,M.D., and Harding,A.E. (1994). Autosomal dominant cerebellar ataxia with pigmentary macular dystrophy. A clinical and genetic study of eight families. Brain 117 (Pt 3), 445-460.

Evert,B.O., Wullner,U., Schulz,J.B., Weller,M., Groscurth,P., Trottier,Y., Brice,A., and Klockgether,T. (1999). High level expression of expanded full-length ataxin-3 in vitro causes cell death and formation of intranuclear inclusions in neuronal cells. Hum. Mol. Genet. 8, 1169-1176.

Evert,B.O., Vogt,I.R., Kindermann,C., Ozimek,L., de Vos,R.A., Brunt,E.R., Schmitt,I., Klockgether,T., and Wullner,U. (2001). Inflammatory genes are upregulated in expanded ataxin-3-expressing cell lines and spinocerebellar ataxia type 3 brains. J. Neurosci. 21, 5389-5396.

Evert,B.O., Vogt,I.R., Vieira-Saecker,A.M., Ozimek,L., de Vos,R.A., Brunt,E.R., Klockgether,T., and Wullner,U. (2003). Gene expression profiling in ataxin-3 expressing cell lines reveals distinct effects of normal and mutant ataxin-3. J. Neuropathol. Exp. Neurol. 62, 1006-1018.

Evert,B.O., Araujo,J., Vieira-Saecker,A.M., de Vos,R.A., Harendza,S., Klockgether,T., and Wullner,U. (2006). Ataxin-3 represses transcription via chromatin binding, interaction with histone deacetylase 3, and histone deacetylation. J. Neurosci. 26, 11474-11486.

Fang,S. and Weissman,A.M. (2004). A field guide to ubiquitylation. Cell Mol. Life Sci. 61, 1546-1561.

Fardaei,M., Larkin,K., Brook,J.D., and Hamshere,M.G. (2001). In vivo co-localisation of MBNL protein with DMPK expanded-repeat transcripts. Nucleic Acids Res. 29, 2766-2771.

Fedorov,Y., Anderson,E.M., Birmingham,A., Reynolds,A., Karpilow,J., Robinson,K., Leake,D., Marshall,W.S., and Khvorova,A. (2006). Off-target effects by siRNA can induce toxic phenotype. RNA 12, 1188-1196.

Fei,E., Jia,N., Zhang,T., Ma,X., Wang,H., Liu,C., Zhang,W., Ding,L., Nukina,N., and Wang,G. (2007). Phosphorylation of ataxin-3 by glycogen synthase kinase 3beta at serine 256 regulates the aggregation of ataxin-3. Biochem. Biophys. Res. Commun. 357, 487-492.

Fischbeck,K.H. (2001). Polyglutamine expansion neurodegenerative disease. Brain Res. Bull. 56, 161-163.

Fiszer,A., Olejniczak,M., Switonski,P.M., Wroblewska,J.P., Wisniewska-Kruk,J., Mykowska,A., and Krzyzosiak,W.J. (2012). An evaluation of oligonucleotide-based therapeutic strategies for polyQ diseases. BMC. Mol. Biol. 13, 6.

Flanigan,K.M., Voit,T., Rosales,X.Q., Servais,L., Kraus,J.E., Wardell,C., Morgan,A., Dorricott,S., Nakielny,J., Quarcoo,N., Liefaard,L., Drury,T., Campion,G., and Wright,P. (2014). Pharmacokinetics and safety of single doses of drisapersen in non-ambulant subjects with Duchenne muscular dystrophy: Results of a double-blind randomized clinical trial. Neuromuscul. Disord. 24, 16-24.

Fletcher,C.F., Tottene,A., Lennon,V.A., Wilson,S.M., Dubel,S.J., Paylor,R., Hosford,D.A., Tessarollo,L., McEnery,M.W., Pietrobon,D., Copeland,N.G., and Jenkins,N.A. (2001). Dystonia and cerebellar atrophy in Cacna1a null mice lacking P/Q calcium channel activity. FASEB J. 15, 1288-1290.

Friedman,M.J., Wang,C.E., Li,X.J., and Li,S. (2008). Polyglutamine expansion reduces the association of TATA-binding protein with DNA and induces DNA binding-independent neurotoxicity. J. Biol. Chem. 283, 8283-8290.

Frontali,M., Novelletto,A., Annesi,G., and Jodice,C. (1999). CAG repeat instability, cryptic sequence variation and pathogeneticity: evidence from different loci. Philos. Trans. R. Soc. Lond. B. Biol. Sci. 354, 1089-1094.

Fu,Y.H., Kuhl,D.P., Pizzuti,A., Pieretti,M., Sutcliffe,J.S., Richards,S., Verkerk,A.J., Holden,J.J., Fenwick,R.G., Jr., Warren,S.T., Oostra,B.A., Nelson,D.L., and Caskey,C.T. (1991). Variation of the CGG repeat at the fragile X site results in genetic instability: resolution of the Sherman paradox. Cell 67, 1047-1058.

Fu,Y.H., Pizzuti,A., Fenwick,R.G., Jr., King,J., Rajnarayan,S., Dunne,P.W., Dubel,J., Nasser,G.A., Ashizawa,T., de Jong,P., Wieringa,B., Korneluk,R. Perryman,M.B., Epstein,H.F., and Caskey,C.T. (1992). An unstable triplet repeat in a gene related to myotonic muscular dystrophy. Science 255, 1256-1258.

Furrer,S.A., Waldherr,S.M., Mohanachandran,M.S., Baughn,T.D., Nguyen,K.T., Sopher,B.L., Damian,V.A., Garden,G.A., and La Spada,A.R. (2013). Reduction of mutant ataxin-7 expression restores motor function and prevents cerebellar synaptic reorganization in a conditional mouse model of SCA7. Hum. Mol. Genet. 22, 890-903.

Gafni,J. and Ellerby,L.M. (2002). Calpain activation in Huntington's disease. J. Neurosci. 22, 4842-4849.

Gafni,J., Papanikolaou,T., Degiacomo,F., Holcomb,J., Chen,S., Menalled,L., Kudwa,A., Fitzpatrick,J., Miller,S., Ramboz,S., Tuunanen,P.I., Lehtimaki,K.K., Yang,X.W., Park,L., Kwak,S., Howland,D., Park,H., and Ellerby,L.M. (2012). Caspase-6 activity in a BACHD mouse modulates steady-state levels of mutant huntingtin protein but is not necessary for production of a 586 amino acid proteolytic fragment. J. Neurosci. 32, 7454-7465.

Gagnon,K.T., Pendergraff,H.M., Deleavey,G.F., Swayze,E.E., Potier,P., Randolph,J., Roesch,E.B., Chattopadhyaya,J., Damha,M.J., Bennett,C.F., Montaillier,C., Lemaitre,M., and Corey,D.R. (2010). Allele-Selective Inhibition of Mutant Huntingtin Expression with Antisense Oligonucleotides Targeting the Expanded CAG Repeat. Biochemistry 49, 10166-10178.

Garden,G.A., Libby,R.T., Fu,Y.H., Kinoshita,Y., Huang,J., Possin,D.E., Smith,A.C., Martinez,R.A., Fine,G.C., Grote,S.K., Ware,C.B., Einum,D.D., Morrison,R.S., Ptacek,L.J., Sopher,B.L., and La Spada,A.R. (2002). Polyglutamine-expanded ataxin-7 promotes non-cell-autonomous purkinje cell degeneration and displays proteolytic cleavage in ataxic transgenic mice. J. Neurosci. 22, 4897-4905.

Gaspar,C., Jannatipour,M., Dion,P., Laganiere,J., Sequeiros,J., Brais,B., and Rouleau,G.A. (2000). CAG tract of MJD-1 may be prone to frameshifts causing polyalanine accumulation. Hum. Mol. Genet. 9, 1957-1966.

Gaspar,C., Lopes-Cendes,I., Hayes,S., Goto,J., Arvidsson,K., Dias,A., Silveira,I., Maciel,P., Coutinho,P., Lima,M., Zhou,Y.X., Soong,B.W., Watanabe,M., Giunti,P., Stevanin,G., Riess,O., Sasaki,H., Hsieh,M., Nicholson,G.A., Brunt,E., Higgins,J.J., Lauritzen,M., Tranebjaerg,L., Volpini,V., Wood,N., Ranum,L., Tsuji,S., Brice,A., Sequeiros,J., and Rouleau,G.A. (2001). Ancestral origins of the Machado-Joseph disease mutation: a worldwide haplotype study. Am. J. Hum. Genet. 68, 523-528.

Gauthier,L.R., Charrin,B.C., Borrell-Pages,M., Dompierre,J.P., Rangone,H., Cordelieres,F.P., De,M.J., MacDonald,M.E., Lessmann,V., Humbert,S., and Saudou,F. (2004). Huntingtin controls neurotrophic support and survival of neurons by enhancing BDNF vesicular transport along microtubules. Cell 118, 127-138.

Gerebtzoff,G. and Seelig,A. (2006). In silico prediction of blood-brain barrier permeation using the calculated molecular cross-sectional area as main parameter. J. Chem. Inf. Model 46, 2638-2650.

Geschwind,D.H., Perlman,S., Figueroa,C.P., Treiman,L.J., and Pulst,S.M. (1997a). The prevalence and wide clinical spectrum of the spinocerebellar ataxia type 2 trinucleotide repeat in patients with autosomal dominant cerebellar ataxia. Am. J. Hum. Genet. 60, 842-850.

Geschwind,D.H., Perlman,S., Figueroa,K.P., Karrim,J., Baloh,R.W., and Pulst,S.M. (1997b). Spinocerebellar ataxia type 6. Frequency of the mutation and genotype-phenotype correlations. Neurology 49, 1247-1251.

Giunti,P., Sabbadini,G., Sweeney,M.G., Davis,M.B., Veneziano,L., Mantuano,E., Federico,A., Plasmati,R., Frontali,M., and Wood,N.W. (1998). The role of the SCA2 trinucleotide repeat expansion in 89 autosomal dominant cerebellar ataxia families. Frequency, clinical and genetic correlates. Brain 121 (Pt 3), 459-467.

Goemans,N.M., Tulinius,M., van den Akker,J.T., Burm,B.E., Ekhart,P.F., Heuvelmans,N., Holling,T., Janson,A.A., Platenburg,G.J., Sipkens,J.A., Sitsen,J.M., Aartsma-Rus,A., van Ommen,G.J., Buyse,G., Darin,N., Verschuuren,J.J., Campion,G.V., de Kimpe,S.J., and van Deutekom,J.C. (2011). Systemic administration of PRO051 in Duchenne's muscular dystrophy. N. Engl. J. Med. 364, 1513-1522.

Goldberg,Y.P., Nicholson,D.W., Rasper,D.M., Kalchman,M.A., Koide,H.B., Graham,R.K., Bromm,M., Kazemi-Esfarjani,P., Thornberry,N.A., Vaillancourt,J.P., and Hayden,M.R. (1996). Cleavage of huntingtin by apopain, a proapoptotic cysteine protease, is modulated by the polyglutamine tract. Nat. Genet. 13, 442-449.

Goswami,A., Dikshit,P., Mishra,A., Mulherkar,S., Nukina,N., and Jana,N.R. (2006). Oxidative stress promotes mutant huntingtin aggregation and mutant huntingtin-dependent cell death by mimicking proteasomal malfunction. Biochem. Biophys. Res. Commun. 342, 184-190.

Goti,D., Katzen,S.M., Mez,J., Kurtis,N., Kiluk,J., Ben-Haiem,L., Jenkins,N.A., Copeland,N.G., Kakizuka,A., Sharp,A.H., Ross,C.A., Mouton,P.R., and Colomer,V. (2004). A mutant ataxin-3 putative-cleavage fragment in brains of Machado-Joseph disease patients and transgenic mice is cytotoxic above a critical concentration. J. Neurosci. 24, 10266-10279.

Goto,J., Watanabe,M., Ichikawa,Y., Yee,S.B., Ihara,N., Endo,K., Igarashi,S., Takiyama,Y., Gaspar,C., Maciel,P., Tsuji,S., Rouleau,G.A., and Kanazawa,I. (1997). Machado-Joseph disease gene products carrying different carboxyl termini. Neurosci. Res. 28, 373-377.

Graham,R.K., Deng,Y., Slow,E.J., Haigh,B., Bissada,N., Lu,G., Pearson,J., Shehadeh,J., Bertram,L., Murphy,Z., Warby,S.C., Doty,C.N., Roy,S., Wellington,C.L., Leavitt,B.R., Raymond,L.A., Nicholson,D.W., and Hayden,M.R. (2006). Cleavage at the caspase-6 site is required for neuronal dysfunction and degeneration due to mutant huntingtin. Cell 125, 1179-1191.

Graham,R.K., Deng,Y., Carroll,J., Vaid,K., Cowan,C., Pouladi,M.A., Metzler,M., Bissada,N., Wang,L., Faull,R.L., Gray,M., Yang,X.W., Raymond,L.A., and Hayden,M.R. (2010). Cleavage at the 586 amino acid caspase-6 site in mutant huntingtin influences caspase-6 activation in vivo. J. Neurosci. 30, 15019-15029.

Grimm,D., Streetz,K.L., Jopling,C.L., Storm,T.A., Pandey,K., Davis,C.R., Marion,P., Salazar,F., and Kay,M.A. (2006). Fatality in mice due to oversaturation of cellular microRNA/short hairpin RNA pathways. Nature 441, 537-541.

Grondin,R., Kaytor,M.D., Ai,Y., Nelson,P.T., Thakker,D.R., Heisel,J., Weatherspoon,M.R., Blum,J.L., Burright,E.N., Zhang,Z., and Kaemmerer,W.F. (2012). Six-month partial suppression of Huntingtin is well tolerated in the adult rhesus striatum. Brain 135, 1197-1209.

Gunawardena,S., Her,L.S., Brusch,R.G., Laymon,R.A., Niesman,I.R., Gordesky-Gold,B., Sintasath,L., Bonini,N.M., and Goldstein,L.S. (2003). Disruption of axonal transport by loss of huntingtin or expression of pathogenic polyQ proteins in Drosophila. Neuron 40, 25-40.

Guo,X., Geng,M., and Du,G. (2005). Glucose transporter 1, distribution in the brain and in neural disorders: its relationship with transport of neuroactive drugs through the blood-brain barrier. Biochem. Genet. 43, 175-187.

Gusella,J.F., Wexler,N.S., Conneally,P.M., Naylor,S.L., Anderson,M.A., Tanzi,R.E., Watkins,P.C., Ottina,K., Wallace,M.R., and Sakaguchi,A.Y. (1983). A polymorphic DNA marker genetically linked to Huntington's disease. Nature 306, 234-238.

Gutekunst,C.A., Li,S.H., Yi,H., Mulroy,J.S., Kuemmerle,S., Jones,R., Rye,D., Ferrante,R.J., Hersch,S.M., and Li,X.J. (1999). Nuclear and neuropil aggregates in Huntington's disease: relationship to neuropathology. J. Neurosci. 19, 2522-2534.

Haacke,A., Broadley,S.A., Boteva,R., Tzvetkov,N., Hartl,F.U., and Breuer,P. (2006). Proteolytic cleavage of polyglutamine-expanded ataxin-3 is critical for aggregation and sequestration of non-expanded ataxin-3. Hum. Mol. Genet. 15, 555-568.

Haacke,A., Hartl,F.U., and Breuer,P. (2007). Calpain inhibition is sufficient to suppress aggregation of polyglutamine-expanded ataxin-3. J. Biol. Chem. 282, 18851-18856.

Haberhausen,G., Damian,M.S., Leweke,F., and Muller,U. (1995). Spinocerebellar ataxia, type 3 (SCA3) is genetically identical to Machado-Joseph disease (MJD). J. Neurol. Sci. 132, 71-75.

Hagerman,R.J., Leehey,M., Heinrichs,W., Tassone,F., Wilson,R., Hills,J., Grigsby,J., Gage,B., and Hagerman,P.J. (2001). Intention tremor, parkinsonism, and generalized brain atrophy in male carriers of fragile X. Neurology 57, 127-130.

Halliday,G.M., McRitchie,D.A., Macdonald,V., Double,K.L., Trent,R.J., and McCusker,E. (1998). Regional specificity of brain atrophy in Huntington's disease. Exp. Neurol. 154, 663-672.

Hamm,S., Latz,E., Hangel,D., Muller,T., Yu,P., Golenbock,D., Sparwasser,T., Wagner,H., and Bauer,S. (2010). Alternating 2'-O-ribose methylation is a universal approach for generating non-stimulatory siRNA by acting as TLR7 antagonist. Immunobiology 215, 559-569.

Harjes,P. and Wanker,E.E. (2003). The hunt for huntingtin function: interaction partners tell many different stories. Trends Biochem. Sci. 28, 425-433.

Harper,S.Q., Staber,P.D., He,X., Eliason,S.L., Martins,I.H., Mao,Q., Yang,L., Kotin,R.M., Paulson,H.L., and Davidson,B.L. (2005). RNA interference improves motor and neuropathological abnormalities in a Huntington's disease mouse model. Proc. Natl. Acad Sci U. S. A. 102, 5820-5825.

Harris,G.M., Dodelzon,K., Gong,L., Gonzalez-Alegre,P., and Paulson,H.L. (2010). Splice isoforms of the polyglutamine disease protein ataxin-3 exhibit similar enzymatic yet different aggregation properties. PLoS One 5, e13695.

He,Y., Vogelstein,B., Velculescu,V.E., Papadopoulos,N., and Kinzler,K.W. (2008). The antisense transcriptomes of human cells. Science 322, 1855-1857.

Heemskerk,H., de Winter,C., van Kuik,P., Heuvelmans,N., Sabatelli,P., Rimessi,P., Braghetta,P., van Ommen,G.J., de Kimpe,S., Ferlini,A., Aartsma-Rus,A., and van Deutekom,J.C. (2010). Preclinical PK and PD studies on 2'-O-methyl-phosphorothioate RNA antisense oligonucleotides in the mdx mouse model. Mol. Ther. 18, 1210-1217.

Heng,M.Y., Detloff,P.J., and Albin,R.L. (2008). Rodent genetic models of Huntington disease. Neurobiol. Dis. 32, 1-9.

Hirabayashi,M., Inoue,K., Tanaka,K., Nakadate,K., Ohsawa,Y., Kamei,Y., Popiel,A.H., Sinohara,A., Iwamatsu,A., Kimura,Y., Uchiyama,Y., Hori,S., and Kakizuka,A. (2001). VCP/p97 in abnormal protein aggregates, cytoplasmic vacuoles, and cell death, phenotypes relevant to neurodegeneration. Cell Death Differ. 8, 977-984.

Hirayama,K., Takayanagi,T., Nakamura,R., Yanagisawa,N., Hattori,T., Kita,K., Yanagimoto,S., Fujita,M., Nagaoka,M., and Satomura,Y. (1994). Spinocerebellar degenerations in Japan: a nationwide epidemiological and clinical study. Acta Neurol. Scand. Suppl 153, 1-22.

Hodges,A., Strand,A.D., Aragaki,A.K., Kuhn,A., Sengstag,T., Hughes,G., Elliston,L.A., Hartog,C., Goldstein,D.R., Thu,D., Hollingsworth,Z.R., Collin,F., Synek,B., Holmans,P.A., Young,A.B., Wexler,N.S., Delorenzi,M., Kooperberg,C., Augood,S.J., Faull,R.L., Olson,J.M., Jones,L., and Luthi-Carter,R. (2006). Regional and cellular gene expression changes in human Huntington's disease brain. Hum. Mol. Genet. 15, 965-977.

Holmberg,M., Duyckaerts,C., Durr,A., Cancel,G., Gourfinkel-An,I., Damier,P., Faucheux,B., Trottier,Y., Hirsch,E.C., Agid,Y., and Brice,A. (1998). Spinocerebellar ataxia type 7 (SCA7): a neurodegenerative disorder with neuronal intranuclear inclusions. Hum. Mol. Genet. 7, 913-918.

Hoogeveen,A.T., Willemsen,R., Meyer,N., de Rooij,K.E., Roos,R.A.,van Ommen,G.J., and Galjaard,H. (1993). Characterization and localization of the Huntington disease gene product. Hum. Mol. Genet. 2, 2069-2073.

HORIZON, Huntington Study Group, and European Huntington's Disease Network (2013). A randomized, double-blind, placebo-controlled study of latrepirdine in patients with mild to moderate Huntington disease. JAMA Neurol. 70, 25-33.

Howeler,C.J., Busch,H.F., Geraedts,J.P., Niermeijer,M.F., and Staal,A. (1989). Anticipation in myotonic dystrophy: fact or fiction? Brain 112 (Pt 3), 779-797.

Hsu,R.J., Hsiao,K.M., Lin,M.J., Li,C.Y., Wang,L.C., Chen,L.K., and Pan,H. (2011). Long tract of untranslated CAG repeats is deleterious in transgenic mice. PLoS One 6, e16417.

Hu,J., Matsui,M., and Corey,D.R. (2009a). Allele-selective inhibition of mutant huntingtin by peptide nucleic acid-peptide conjugates, locked nucleic acid, and small interfering RNA. Ann. N. Y. Acad. Sci. 1175, 24-31.

Hu,J., Matsui,M., Gagnon,K.T., Schwartz,J.C., Gabillet,S., Arar,K., Wu,J., Bezprozvanny,I., and Corey,D.R. (2009b). Allele-specific silencing of mutant huntingtin and ataxin-3 genes by targeting expanded CAG repeats in mRNAs. Nat. Biotechnol. 27, 478-484.

Hu,J., Gagnon,K.T., Liu,J., Watts,J.K., Syeda-Nawaz,J., Bennett,C.F., Swayze,E.E., Randolph,J., Chattopadhyaya,J., and Corey,D.R. (2011). Allele-selective inhibition of ataxin-3 (ATX3) expression by antisense oligomers and duplex RNAs. Biol. Chem. 392, 315-325.

Hua,Y., Sahashi,K., Hung,G., Rigo,F., Passini,M.A., Bennett,C.F., and Krainer,A.R. (2010). Antisense correction of SMN2 splicing in the CNS rescues necrosis in a type III SMA mouse model. Genes Dev. 24, 1634-1644.

Huang,C.C., Faber,P.W., Persichetti,F., Mittal,V., Vonsattel,J.P., MacDonald,M.E., and Gusella,J.F. (1998). Amyloid formation by mutant huntingtin: Threshold, progressivity and recruitment of normal polyglutamine proteins. Somat. Cell Molec. Gen. 24, 217-233.

Huang,E.J. and Reichardt,L.F. (2001). Neurotrophins: roles in neuronal development and function. Annu. Rev. Neurosci. 24, 677-736.

Huang,K., Yanai,A., Kang,R., Arstikaitis,P., Singaraja,R.R., Metzler,M., Mullard,A., Haigh,B., Gauthier-Campbell,C., Gutekunst,C.A., Hayden,M.R., and El-Husseini,A. (2004). Huntingtin-interacting protein HIP14 is a palmitoyl transferase involved in palmitoylation and trafficking of multiple neuronal proteins. Neuron 44, 977-986.

Hubener,J. and Riess,O. (2010). Polyglutamine-induced neurodegeneration in SCA3 is not mitigated by non-expanded ataxin-3: conclusions from double-transgenic mouse models. Neurobiol. Dis. 38, 116-124.

Hubener,J., Vauti,F., Funke,C., Wolburg,H., Ye,Y., Schmidt,T., Wolburg-Buchholz,K., Schmitt,I., Gardyan,A., Driessen,S., Arnold,H.H., Nguyen,H.P., and Riess,O. (2011). N-terminal ataxin-3 causes neurological symptoms with inclusions, endoplasmic reticulum stress and ribosomal dislocation. Brain 134, 1925-1942.

Hubener,J., Weber,J.J., Richter,C., Honold,L., Weiss,A., Murad,F., Breuer,P., Wullner,U., Bellstedt,P., Paquet-Durand,F., Takano,J., Saido,T.C., Riess,O., and Nguyen,H.P. (2012). Calpain-mediated ataxin-3 cleavage in the molecular pathogenesis of spinocerebellar ataxia type 3 (SCA3). Hum. Mol. Genet.

Huntington Study Group (1996). Unified Huntington's Disease Rating Scale: reliability and consistency. Mov. Disord. 11, 136-142.

Huntington Study Group (2001). A randomized, placebo-controlled trial of coenzyme Q10 and remacemide in Huntington's disease. Neurology 57, 397-404.

Huntington Study Group TREND-HD Investigators (2008). Randomized controlled trial of ethyl-eicosapentaenoic acid in Huntington disease: the TREND-HD study. Arch. Neurol. 65, 1582-1589.

Ikeda,H., Yamaguchi,M., Sugai,S., Aze,Y., Narumiya,S., and Kakizuka,A. (1996). Expanded polyglutamine in the Machado-Joseph disease protein induces cell death in vitro and in vivo. Nat. Genet. 13, 196-202.

Ikeuchi,T., Koide,R., Tanaka,H., Onodera,O., Igarashi,S., Takahashi,H., Kondo,R., Ishikawa,A., Tomoda,A., and Miike,T. (1995). Dentatorubral-pallidoluysian atrophy: clinical features are closely related to unstable expansions of trinucleotide (CAG) repeat. Ann. Neurol. 37, 769-775.

Imbert,G., Saudou,F., Yvert,G., Devys,D., Trottier,Y., Garnier,J.M., Weber,C., Mandel,J.L., Cancel,G., Abbas,N., Durr,A., Didierjean,O., Stevanin,G., Agid,Y., and Brice,A. (1996). Cloning of the gene for spinocerebellar ataxia 2 reveals a locus with high sensitivity to expanded CAG/glutamine repeats. Nat. Genet. 14, 285-291.

Irwin,S., Vandelft,M., Pinchev,D., Howell,J.L., Graczyk,J., Orr,H.T., and Truant,R. (2005). RNA association and nucleocytoplasmic shuttling by ataxin-1. J. Cell Sci. 118, 233-242.

Ishikawa,K., Fujigasaki,H., Saegusa,H., Ohwada,K., Fujita,T., Iwamoto,H., Komatsuzaki,Y., Toru,S., Toriyama,H., Watanabe,M., Ohkoshi,N., Shoji,S., Kanazawa,I., Tanabe,T., and Mizusawa,H. (1999). Abundant expression and cytoplasmic aggregations of [alpha]1A voltage-dependent calcium channel protein associated with neurodegeneration in spinocerebellar ataxia type 6. Hum. Mol. Genet. 8, 1185-1193.

Jacobi,H., Reetz,K., du Montcel,S.T., Bauer,P., Mariotti,C., Nanetti,L., Rakowicz,M., Sulek,A., Durr,A., Charles,P., Filla,A., Antenora,A., Schols,L., Schicks,J., Infante,J., Kang,J.S., Timmann,D., Di,F.R., Masciullo,M., Baliko,L., Melegh,B., Boesch,S., Burk,K., Peltz,A., Schulz,J.B., Dufaure-Gare,I., and Klockgether,T. (2013). Biological and clinical characteristics of individuals at risk for spinocerebellar ataxia types 1, 2, 3, and 6 in the longitudinal RISCA study: analysis of baseline data. Lancet Neurol. 12, 650-658.

Jacquemont,S., Hagerman,R.J., Leehey,M., Grigsby,J., Zhang,L., Brunberg,J.A., Greco,C., Des,P., V, Jardini,T., Levine,R., Berry-Kravis,E., Brown,W.T., Schaeffer,S., Kissel,J., Tassone,F., and Hagerman,P.J. (2003). Fragile X premutation tremor/ataxia syndrome: molecular, clinical, and neuroimaging correlates. Am. J. Hum. Genet. 72, 869-878.

Jacquemont,S., Hagerman,R.J., Hagerman,P.J., and Leehey,M.A. (2007). Fragile-X syndrome and fragile X-associated tremor/ataxia syndrome: two faces of FMR1. Lancet Neurol. 6, 45-55.

Jacquemont,S., Leehey,M.A., Hagerman,R.J., Beckett,L.A., and Hagerman,P.J. (2006). Size bias of fragile X premutation alleles in late-onset movement disorders. J. Med. Genet. 43, 804-809.

Jana,N.R. and Nukina,N. (2004). Misfolding promotes the ubiquitination of polyglutamine-expanded ataxin-3, the defective gene product in SCA3/MJD. Neurotox. Res. 6, 523-533.

Jayandharan,G.R., Aslanidi,G., Martino,A.T., Jahn,S.C., Perrin,G.Q., Herzog,R.W., and Srivastava,A. (2011). Activation of the NF-kappaB pathway by adeno-associated virus (AAV) vectors and its implications in immune response and gene therapy. Proc. Natl. Acad. Sci. U. S. A. 108, 3743-3748.

Jia,D.D., Zhang,L., Chen,Z., Wang,C.R., Huang,F.Z., Duan,R.H., Xia,K., Tang,B.S., and Jiang,H. (2013). Lithium Chloride Alleviates Neurodegeneration Partly by Inhibiting Activity of GSK3beta in a SCA3 Drosophila Model. Cerebellum.

Jirka,S.M., Heemskerk,H., Tanganyika-de Winter,C.L., Muilwijk,D., Pang,K.H., de Visser,P.C., Janson,A., Karnaoukh,T.G., Vermue,R., 't Hoen,P.A., van Deutekom,J.C., Aguilera,B., and Aartsma-Rus,A. (2014). Peptide Conjugation of 2'-O-methyl Phosphorothioate Antisense Oligonucleotides Enhances Cardiac Uptake and Exon Skipping in mdx Mice. Nucleic Acid Ther. 24, 25-36.

Juenemann,K., Schipper-Krom,S., Wiemhoefer,A., Kloss,A., Sanz,S.A., and Reits,E.A. (2013). Expanded polyglutamine-containing N-terminal huntingtin fragments are entirely degraded by mammalian proteasomes. J. Biol. Chem. 288, 27068-27084.

Kalchman,M.A., Graham,R.K., Xia,G., Koide,H.B., Hodgson,J.G., Graham,K.C., Goldberg,Y.P., Gietz,R.D., Pickart,C.M., and Hayden,M.R. (1996). Huntingtin is ubiquitinated and interacts with a specific ubiquitin-conjugating enzyme. J. Biol. Chem. 271, 19385-19394.

Kaplitt,M.G., Darakchiev,B., and During,M.J. (1998). Prospects for gene therapy in pediatric neurosurgery. Pediatr. Neurosurg. 28, 3-14.

Katayama,S., Tomaru,Y., Kasukawa,T., Waki,K., Nakanishi,M., Nakamura,M., Nishida,H., Yap,C.C., Suzuki,M., Kawai,J., Suzuki,H., Carninci,P., Hayashizaki,Y., Wells,C., Frith,M., Ravasi,T., Pang,K.C., Hallinan,J., Mattick,J., Hume,D.A., Lipovich,L., Batalov,S., Engstrom,P.G., Mizuno,Y., Faghihi,M.A., Sandelin,A., Chalk,A.M., Mottagui-Tabar,S., Liang,Z., Lenhard,B., and Wahlestedt,C. (2005). Antisense transcription in the mammalian transcriptome. Science 309, 1564-1566.

Katsuno,M., Tanaka,F., Adachi,H., Banno,H., Suzuki,K., Watanabe,H., and Sobue,G. (2012). Pathogenesis and therapy of spinal and bulbar muscular atrophy (SBMA). Prog. Neurobiol. 99, 246-256.

Kaushik,S., Massey,A.C., Mizushima,N., and Cuervo,A.M. (2008). Constitutive activation of chaperone-mediated autophagy in cells with impaired macroautophagy. Mol. Biol. Cell 19, 2179-2192.

Kawaguchi,Y., Okamoto,T., Taniwaki,M., Aizawa,M., Inoue,M., Katayama,S., Kawakami,H., Nakamura,S., Nishimura,M., and Akiguchi,I. (1994). CAG expansions in a novel gene for Machado-Joseph disease at chromosome 14q32.1. Nat. Genet. 8, 221-228.

Kazachkova,N., Raposo,M., Montiel,R., Cymbron,T., Bettencourt,C., Silva-Fernandes,A., Silva,S., Maciel,P., and Lima,M. (2013). Patterns of mitochondrial DNA damage in blood and brain tissues of a transgenic mouse model of Machado-Joseph disease. Neurodegener. Dis. 11, 206-214.

Kazantsev,A., Preisinger,E., Dranovsky,A., Goldgaber,D., and Housman,D. (1999). Insoluble detergent-resistant aggregates form between pathological and nonpathological lengths of polyglutamine in mammalian cells. Proc. Natl. Acad. Sci. U. S. A. 96, 11404-11409.

Kegel,K.B., Meloni,A.R., Yi,Y., Kim,Y.J., Doyle,E., Cuiffo,B.G., Sapp,E., Wang,Y., Qin,Z.H., Chen,J.D., Nevins,J.R., Aronin,N., and Difiglia,M. (2002). Huntingtin is present in the nucleus, interacts with the transcriptional corepressor C-terminal binding protein, and represses transcription. J. Biol. Chem. 277, 7466-7476.

Kegel,K.B., Sapp,E., Yoder,J., Cuiffo,B., Sobin,L., Kim,Y.J., Qin,Z.H., Hayden,M.R., Aronin,N., Scott,D.L., Isenberg,G., Goldmann,W.H., and Difiglia,M. (2005). Huntingtin associates with acidic phospholipids at the plasma membrane. J. Biol. Chem. 280, 36464-36473.

Keiser,M.S., Geoghegan,J.C., Boudreau,R.L., Lennox,K.A., and Davidson,B.L. (2013). RNAi or overexpression: alternative therapies for Spinocerebellar Ataxia Type 1. Neurobiol. Dis. 56, 6-13.

Kelp,A., Koeppen,A.H., Petrasch-Parwez,E., Calaminus,C., Bauer,C., Portal,E., Yu-Taeger,L., Pichler,B., Bauer,P., Riess,O., and Nguyen,H.P. (2013). A novel transgenic rat model for spinocerebellar ataxia type 17 recapitulates neuropathological changes and supplies in vivo imaging biomarkers. J. Neurosci. 33, 9068-9081.

Kenneson,A., Zhang,F., Hagedorn,C.H., and Warren,S.T. (2001). Reduced FMRP and increased FMR1 transcription is proportionally associated with CGG repeat number in intermediate-length and premutation carriers. Hum. Mol. Genet. 10, 1449-1454.

Kim,S.J., Kim,T.S., Hong,S., Rhim,H., Kim,I.Y., and Kang,S. (2003). Oxidative stimuli affect polyglutamine aggregation and cell death in human mutant ataxin-1-expressing cells. Neurosci. Lett. 348, 21-24.

Kim,Y.J., Sapp,E., Cuiffo,B.G., Sobin,L., Yoder,J., Kegel,K.B., Qin,Z.H., Detloff,P., Aronin,N., and Difiglia,M. (2006). Lysosomal proteases are involved in generation of N-terminal huntingtin fragments. Neurobiol. Dis. 22, 346-356.

Klement,I.A., Skinner,P.J., Kaytor,M.D., Yi,H., Hersch,S.M., Clark,H.B., Zoghbi,H.Y., and Orr,H.T. (1998). Ataxin-1 nuclear localization and aggregation: role in polyglutamine-induced disease in SCA1 transgenic mice. Cell 95, 41-53.

Koch,P., Breuer,P., Peitz,M., Jungverdorben,J., Kesavan,J., Poppe,D., Doerr,J., Ladewig,J., Mertens,J., Tuting,T., Hoffmann,P., Klockgether,T., Evert,B.O., Wullner,U., and Brustle,O. (2011). Excitation-induced ataxin-3 aggregation in neurons from patients with Machado-Joseph disease. Nature 480, 543-546.

Kolber,B.J., Roberts,M.S., Howell,M.P., Wozniak,D.F., Sands,M.S., and Muglia,L.J. (2008). Central amygdala glucocorticoid receptor action promotes fear-associated CRH activation and conditioning. Proc. Natl. Acad. Sci. U. S. A. 105, 12004-12009.

Kole,R., Krainer,A.R., and Altman,S. (2012). RNA therapeutics: beyond RNA interference and antisense oligonucleotides. Nat. Rev. Drug Discov. 11, 125-140.

Kordasiewicz,H.B., Stanek,L.M., Wancewicz,E.V., Mazur,C., McAlonis,M.M., Pytel,K.A., Artates,J.W., Weiss,A., Cheng,S.H., Shihabuddin,L.S., Hung,G., Bennett,C.F., and Cleveland,D.W. (2012). Sustained Therapeutic Reversal of Huntington's Disease by Transient Repression of Huntingtin Synthesis. Neuron 74, 1031-1044.

Krauss,S., Griesche,N., Jastrzebska,E., Chen,C., Rutschow,D., Achmuller,C., Dorn,S., Boesch,S.M., Lalowski,M., Wanker,E., Schneider,R., and Schweiger,S. (2013). Translation of HTT mRNA with expanded CAG repeats is regulated by the MID1-PP2A protein complex. Nat. Commun. 4, 1511.

Kremer,B., Weber,B., and Hayden,M.R. (1992). New insights into the clinical features, pathogenesis and molecular genetics of Huntington disease. Brain Pathol. 2, 321-335.

Kremer,B., Almqvist,E., Theilmann,J., Spence,N., Telenius,H., Goldberg,Y.P., and Hayden,M.R. (1995). Sex-dependent mechanisms for expansions and contractions of the CAG repeat on affected Huntington disease chromosomes. Am. J. Hum. Genet. 57, 343-350.

Kremer,E.J., Pritchard,M., Lynch,M., Yu,S., Holman,K., Baker,E., Warren,S.T., Schlessinger,D., Sutherland,G.R., and Richards,R.I. (1991). Mapping of DNA instability at the fragile X to a trinucleotide repeat sequence p(CCG)n. Science 252, 1711-1714.

Krol,J., Fiszer,A., Mykowska,A., Sobczak,K., de,M.M., and Krzyzosiak,W.J. (2007). Ribonuclease dicer cleaves triplet repeat hairpins into shorter repeats that silence specific targets. Mol. Cell 25, 575-586.

Kubo,K., Tomita,K., Uto,A., Kuroda,K., Seshadri,S., Cohen,J., Kaibuchi,K., Kamiya,A., and Nakajima,K. (2010). Migration defects by DISC1 knockdown in C57BL/6, 129X1/SvJ, and ICR strains via in utero gene transfer and virus-mediated RNAi. Biochem. Biophys. Res. Commun. 400, 631-637.

Kubodera,T., Yokota,T., Ohwada,K., Ishikawa,K., Miura,H., Matsuoka,T., and Mizusawa,H. (2003). Proteolytic cleavage and cellular toxicity of the human alpha1A calcium channel in spinocerebellar ataxia type 6. Neurosci. Lett. 341, 74-78.

La Spada,A.R., Wilson,E.M., Lubahn,D.B., Harding,A.E., and Fischbeck,K.H. (1991). Androgen receptor gene mutations in X-linked spinal and bulbar muscular atrophy. Nature 352, 77-79.

La Spada,A.R. and Taylor,J.P. (2010). Repeat expansion disease: progress and puzzles in disease pathogenesis. Nat. Rev. Genet. 11, 247-258.

Laco,M.N., Cortes,L., Travis,S.M., Paulson,H.L., and Rego,A.C. (2012a). Valosin-containing protein (VCP/p97) is an activator of wild-type ataxin-3. PLoS One 7, e43563.

Laco,M.N., Oliveira,C.R., Paulson,H.L., and Rego,A.C. (2012b). Compromised mitochondrial complex II in models of Machado-Joseph disease. Biochim. Biophys. Acta 1822, 139-149.

Landschulz,W.H., Johnson,P.F., and McKnight,S.L. (1988). The leucine zipper: a hypothetical structure common to a new class of DNA binding proteins. Science 240, 1759-1764.

Lee,H.J., Boado,R.J., Braasch,D.A., Corey,D.R., and Pardridge,W.M. (2002). Imaging gene expression in the brain in vivo in a transgenic mouse model of Huntington's disease with an antisense radiopharmaceutical and drug-targeting technology. J. Nucl. Med. 43, 948-956.

Lee,J.M., Galkina,E.I., Levantovsky,R.M., Fossale,E., Anne,A.M., Gillis,T., Srinidhi,M.J., Coser,K.R., Shioda,T., Zhang,B., Furia,M.D., Derry,J., Kohane,I.S., Seong,I.S., Wheeler,V.C., Gusella,J.F., and MacDonald,M.E. (2013). Dominant effects of the Huntington's disease HTT CAG repeat length are captured in gene-expression data sets by a continuous analysis mathematical modeling strategy. Hum. Mol. Genet. 22, 3227-3238.

Legleiter,J., Mitchell,E., Lotz,G.P., Sapp,E., Ng,C., Difiglia,M., Thompson,L.M., and Muchowski,P.J. (2010). Mutant huntingtin fragments form oligomers in a polyglutamine length-dependent manner in vitro and in vivo. J. Biol. Chem. 285, 14777-14790.

Lentz,J.J., Jodelka,F.M., Hinrich,A.J., McCaffrey,K.E., Farris,H.E., Spalitta,M.J., Bazan,N.G., Duelli,D.M., Rigo,F., and Hastings,M.L. (2013). Rescue of hearing and vestibular function by antisense oligonucleotides in a mouse model of human deafness. Nat. Med. 19, 345-350.

Levesque,M., Bedard,A., Cossette,M., and Parent,A. (2003). Novel aspects of the chemical anatomy of the striatum and its efferents projections. J. Chem. Neuroanat. 26, 271-281.

Li,F., Macfarlan,T., Pittman,R.N., and Chakravarti,D. (2002). Ataxin-3 is a histone-binding protein with two independent transcriptional corepressor activities. J. Biol. Chem. 277, 45004-45012.

Li,L.B., Yu,Z., Teng,X., and Bonini,N.M. (2008). RNA toxicity is a component of ataxin-3 degeneration in Drosophila. Nature 453, 1107-1111.

Li,W., Serpell,L.C., Carter,W.J., Rubinsztein,D.C., and Huntington,J.A. (2006). Expression and characterization of full-length human huntingtin, an elongated HEAT repeat protein. J. Biol. Chem. 281, 15916-15922.

Li,X., Standley,C., Sapp,E., Valencia,A., Qin,Z.H., Kegel,K.B., Yoder,J., Comer-Tierney,L.A., Esteves,M., Chase,K., Alexander,J., Masso,N., Sobin,L., Bellve,K., Tuft,R., Lifshitz,L., Fogarty,K., Aronin,N., and Difiglia,M. (2009). Mutant huntingtin impairs vesicle formation from recycling endosomes by interfering with Rab11 activity. Mol. Cell Biol. 29, 6106-6116.

Liebsch,G., Landgraf,R., Engelmann,M., Lorscher,P., and Holsboer,F. (1999). Differential behavioural effects of chronic infusion of CRH 1 and CRH 2 receptor antisense oligonucleotides into the rat brain. J. Psychiatr. Res. 33, 153-163.

Lim,K.L. and Lim,G.G. (2011). K63-linked ubiquitination and neurodegeneration. Neurobiol. Dis. 43, 9-16.

Liu,J., Yu,D., Aiba,Y., Pendergraff,H., Swayze,E.E., Lima,W.F., Hu,J., Prakash,T.P., and Corey,D.R. (2013). ss-siRNAs allele selectively inhibit ataxin-3 expression: multiple mechanisms for an alternative gene silencing strategy. Nucleic Acids Res.

Liu,W., Kennington,L.A., Rosas,H.D., Hersch,S., Cha,J.H., Zamore,P.D., and Aronin,N. (2008). Linking SNPs to CAG repeat length in Huntington's disease patients. Nat. Methods 5, 951-953.

Liu,Y. and Ye,Y. (2012). Roles of p97-associated deubiquitinases in protein quality control at the endoplasmic reticulum. Curr. Protein Pept. Sci. 13, 436-446.

Lombardi,M.S., Jaspers,L., Spronkmans,C., Gellera,C., Taroni,F., Di,M.E., Donato,S.D., and Kaemmerer,W.F. (2009). A majority of Huntington's disease patients may be treatable by individualized allele-specific RNA interference. Exp. Neurol. 217, 312-319.

Losekoot,M., van Belzen,M.J., Seneca,S., Bauer,P., Stenhouse,S.A., and Barton,D.E. (2013). EMQN/CMGS best practice guidelines for the molecular genetic testing of Huntington disease. Eur. J. Hum. Genet. 21, 480-486.

Lund,A., Udd,B., Juvonen,V., Andersen,P.M., Cederquist,K., Davis,M., Gellera,C., Kolmel,C., Ronnevi,L.O., Sperfeld,A.D., Sorensen,S.A., Tranebjaerg,L., Van,M.L., Watanabe,M., Weber,M., Yeung,L., and Savontaus,M.L. (2001). Multiple founder effects in spinal and bulbar muscular atrophy (SBMA, Kennedy disease) around the world. Eur. J. Hum. Genet. 9, 431-436.

Lunkes,A., Lindenberg,K.S., Ben-Haiem,L., Weber,C., Devys,D., Landwehrmeyer,G.B., Mandel,J.L., and Trottier,Y. (2002). Proteases acting on mutant huntingtin generate cleaved products that differentially build up cytoplasmic and nuclear inclusions. Mol. Cell 10, 259-269.

Ma,L., Wang,D.D., Zhang,T.Y., Yu,H., Wang,Y., Huang,S.H., Lee,F.S., and Chen,Z.Y. (2011). Region-specific involvement of BDNF secretion and synthesis in conditioned taste aversion memory formation. J. Neurosci. 31, 2079-2090.

Macedo-Ribeiro,S., Cortes,L., Maciel,P., and Carvalho,A.L. (2009). Nucleocytoplasmic shuttling activity of ataxin-3. PLoS One 4, e5834.

Maciel,P., Gaspar,C., DeStefano,A.L., Silveira,I., Coutinho,P., Radvany,J., Dawson,D.M., Sudarsky,L., Guimaraes,J., and Loureiro,J.E. (1995). Correlation between CAG repeat length and clinical features in Machado-Joseph disease. Am. J. Hum. Genet. 57, 54-61.

Magana,J.J., Velazquez-Perez,L., and Cisneros,B. (2013). Spinocerebellar ataxia type 2: clinical presentation, molecular mechanisms, and therapeutic perspectives. Mol. Neurobiol. 47, 90-104.

Mahadevan,M., Tsilfidis,C., Sabourin,L., Shutler,G., Amemiya,C., Jansen,G., Neville,C., Narang,M., Barcelo,J., O'Hoy,K., LeBlond,S., Earle-Macdonald,J. de Jong,P.J., Wieringa,B, and Korneluk,R.G. (1992). Myotonic dystrophy mutation: an unstable CTG repeat in the 3' untranslated region of the gene. Science 255, 1253-1255.

Mangiarini,L., Sathasivam,K., Seller,M., Cozens,B., Harper,A., Hetherington,C., Lawton,M., Trottier,Y., Lehrach,H., Davies,S.W., and Bates,G.P. (1996). Exon 1 of the HD gene with an expanded CAG repeat is sufficient to cause a progressive neurological phenotype in transgenic mice. Cell 87, 493-506.

Manto,M.U. (2005). The wide spectrum of spinocerebellar ataxias (SCAs). Cerebellum 4, 2-6.

Mao,Y., Senic-Matuglia,F., Di Fiore,P.P., Polo,S., Hodsdon,M.E., and De Camilli,P. (2005). Deubiquitinating function of ataxin-3: insights from the solution structure of the Josephin domain. Proc. Natl. Acad. Sci. U. S. A. 102, 12700-12705.

Martin,J.J. (2012). Spinocerebellar ataxia type 7. Handb. Clin. Neurol. 103, 475-491.

Martinez-Vicente,M., Talloczy,Z., Wong,E., Tang,G., Koga,H., Kaushik,S., de,V.R., Arias,E., Harris,S., Sulzer,D., and Cuervo,A.M. (2010). Cargo recognition failure is responsible for inefficient autophagy in Huntington's disease. Nat. Neurosci. 13, 567-576.

Matilla,A., Roberson,E.D., Banfi,S., Morales,J., Armstrong,D.L., Burright,E.N., Orr,H.T., Sweatt,J.D., Zoghbi,H.Y., and Matzuk,M.M. (1998). Mice lacking ataxin-1 display learning deficits and decreased hippocampal paired-pulse facilitation. J. Neurosci. 18, 5508-5516.

Matilla-Duenas,A., Goold,R., and Giunti,P. (2008). Clinical, genetic, molecular, and pathophysiological insights into spinocerebellar ataxia type 1. Cerebellum 7, 106-114.

Matos,C.A., de Macedo-Ribeiro,S., and Carvalho,A.L. (2011). Polyglutamine diseases: the special case of ataxin-3 and Machado-Joseph disease. Prog. Neurobiol. 95, 26-48.

Maxwell,M.M. (2009). RNAi applications in therapy development for neurodegenerative disease. Curr. Pharm. Des 15, 3977-3991.

Maynard,C.J., Bottcher,C., Ortega,Z., Smith,R., Florea,B.I., Diaz-Hernandez,M., Brundin,P., Overkleeft,H.S., Li,J.Y., Lucas,J.J., and Dantuma,N.P. (2009). Accumulation of ubiquitin conjugates in a polyglutamine disease model occurs without global ubiquitin/proteasome system impairment. Proc. Natl. Acad. Sci. U. S. A. 106, 13986-13991.

McBride,J.L., Boudreau,R.L., Harper,S.Q., Staber,P.D., Monteys,A.M., Martins,I., Gilmore,B.L., Burstein,H., Peluso,R.W., Polisky,B., Carter,B.J., and Davidson,B.L. (2008). Artificial miRNAs mitigate shRNA-mediated toxicity in the brain: implications for the therapeutic development of RNAi. Proc. Natl. Acad Sci U. S. A. 105, 5868-5873.

McBride,J.L., Pitzer,M.R., Boudreau,R.L., Dufour,B., Hobbs,T., Ojeda,S.R., and Davidson,B.L. (2011). Preclinical safety of RNAi-mediated HTT suppression in the rhesus macaque as a potential therapy for Huntington's disease. Mol. Ther. 19, 2152-2162.

McCampbell,A., Taylor,J.P., Taye,A.A., Robitschek,J., Li,M., Walcott,J., Merry,D., Chai,Y., Paulson,H., Sobue,G., and Fischbeck,K.H. (2000). CREB-binding protein sequestration by expanded polyglutamine. Hum. Mol. Genet. 9, 2197-2202.

McLeod,C.J., O'Keefe,L.V., and Richards,R.I. (2005). The pathogenic agent in Drosophila models of 'polyglutamine' diseases. Hum. Mol. Genet. 14, 1041-1048.

McNeil,S.M., Novelletto,A., Srinidhi,J., Barnes,G., Kornbluth,I., Altherr,M.R., Wasmuth,J.J., Gusella,J.F., MacDonald,M.E., and Myers,R.H. (1997). Reduced penetrance of the Huntington's disease mutation. Hum. Mol Genet 6, 775-779.

Meijer,H., de,G.E., Merckx,D.M., Jongbloed,R.J., de Die-Smulders,C.E., Engelen,J.J., Fryns,J.P., Curfs,P.M., and Oostra,B.A. (1994). A deletion of 1.6 kb proximal to the CGG repeat of the FMR1 gene causes the clinical phenotype of the fragile X syndrome. Hum. Mol. Genet. 3, 615-620.

Mende-Mueller,L.M., Toneff,T., Hwang,S.R., Chesselet,M.F., and Hook,V.Y. (2001). Tissue-specific proteolysis of Huntingtin (htt) in human brain: evidence of enhanced levels of N- and C-terminal htt fragments in Huntington's disease striatum. J. Neurosci. 21, 1830-1837.

Menon,R.P., Nethisinghe,S., Faggiano,S., Vannocci,T., Rezaei,H., Pemble,S., Sweeney,M.G., Wood,N.W., Davis,M.B., Pastore,A., and Giunti,P. (2013). The role of interruptions in polyQ in the pathology of SCA1. PLoS Genet. 9, e1003648.

Metcalf,D.J., Garcia-Arencibia,M., Hochfeld,W.E., and Rubinsztein,D.C. (2010). Autophagy and misfolded proteins in neurodegeneration. Exp. Neurol.

Milakovic,T. and Johnson,G.V. (2005). Mitochondrial respiration and ATP production are significantly impaired in striatal cells expressing mutant huntingtin. J. Biol. Chem. 280, 30773-30782.

Miller,J.W., Urbinati,C.R., Teng-Umnuay,P., Stenberg,M.G., Byrne,B.J., Thornton,C.A., and Swanson,M.S. (2000). Recruitment of human muscleblind proteins to (CUG)(n) expansions associated with myotonic dystrophy. EMBO J. 19, 4439-4448.

Miller,T.M., Pestronk,A., David,W., Rothstein,J., Simpson,E., Appel,S.H., Andres,P.L., Mahoney,K., Allred,P., Alexander,K., Ostrow,L.W., Schoenfeld,D., Macklin,E.A., Norris,D.A., Manousakis,G., Crisp,M., Smith,R., Bennett,C.F., Bishop,K.M., and Cudkowicz,M.E. (2013). An antisense oligonucleotide against SOD1 delivered intrathecally for patients with SOD1 familial amyotrophic lateral sclerosis: a phase 1, randomised, first-in-man study. Lancet Neurol. 12, 435-442.

Miller,V.M., Xia,H., Marrs,G.L., Gouvion,C.M., Lee,G., Davidson,B.L., and Paulson,H.L. (2003). Allele-specific silencing of dominant disease genes. Proc. Natl. Acad Sci U. S. A. 100, 7195-7200.

Mirkin,S.M. (2007). Expandable DNA repeats and human disease. Nature 447, 932-940.

Mitrpant,C., Porensky,P., Zhou,H., Price,L., Muntoni,F., Fletcher,S., Wilton,S.D., and Burghes,A.H. (2013). Improved antisense oligonucleotide design to suppress aberrant SMN2 gene transcript processing: towards a treatment for spinal muscular atrophy. PLoS One 8, e62114.

Miyata,R., Hayashi,M., Tanuma,N., Shioda,K., Fukatsu,R., and Mizutani,S. (2008). Oxidative stress in neurodegeneration in dentatorubral-pallidoluysian atrophy. J. Neurol. Sci. 264, 133-139.

Miyazaki,Y., Adachi,H., Katsuno,M., Minamiyama,M., Jiang,Y.M., Huang,Z., Doi,H., Matsumoto,S., Kondo,N., Iida,M., Tohnai,G., Tanaka,F., Muramatsu,S., and Sobue,G. (2012). Viral delivery of miR-196a ameliorates the SBMA phenotype via the silencing of CELF2. Nat. Med. 18, 1136-1141.

Modregger,J., DiProspero,N.A., Charles,V., Tagle,D.A., and Plomann,M. (2002). PACSIN 1 interacts with huntingtin and is absent from synaptic varicosities in presymptomatic Huntington's disease brains. Hum. Mol. Genet. 11, 2547-2558.

Mohan,R.D., Dialynas,G., Weake,V.M., Liu,J., Martin-Brown,S., Florens,L., Washburn,M.P., Workman,J.L., and Abmayr,S.M. (2014). Loss of Drosophila Ataxin-7, a SAGA subunit, reduces H2B ubiquitination and leads to neural and retinal degeneration. Genes Dev. 28, 259-272.

Molla,M., Delcher,A., Sunyaev,S., Cantor,C., and Kasif,S. (2009). Triplet repeat length bias and variation in the human transcriptome. Proc. Natl. Acad. Sci. U. S. A. 106, 17095-17100.

Moseley,M.L., Zu,T., Ikeda,Y., Gao,W., Mosemiller,A.K., Daughters,R.S., Chen,G., Weatherspoon,M.R., Clark,H.B., Ebner,T.J., Day,J.W., and Ranum,L.P. (2006). Bidirectional expression of CUG and CAG expansion transcripts and intranuclear polyglutamine inclusions in spinocerebellar ataxia type 8. Nat. Genet. 38, 758-769.

Moulton,H.M., Wu,B., Jearawiriyapaisarn,N., Sazani,P., Lu,Q.L., and Kole,R. (2009). Peptide-morpholino conjugate: a promising therapeutic for Duchenne muscular dystrophy. Ann. N. Y. Acad. Sci. 1175, 55-60.

Moulton,H.M. and Moulton,J.D. (2010). Morpholinos and their peptide conjugates: therapeutic promise and challenge for Duchenne muscular dystrophy. Biochim. Biophys. Acta 1798, 2296-2303.

Muchowski,P.J., Ning,K., D'Souza-Schorey,C., and Fields,S. (2002). Requirement of an intact microtubule cytoskeleton for aggregation and inclusion body formation by a mutant huntingtin fragment. Proc. Natl. Acad. Sci. U. S. A. 99, 727-732.

Mueller,T., Breuer,P., Schmitt,I., Walter,J., Evert,B.O., and Wullner,U. (2009). CK2-dependent phosphorylation determines cellular localization and stability of ataxin-3. Hum. Mol. Genet. 18, 3334-3343.

Mulders,S.A., van den Broek,W.J., Wheeler,T.M., Croes,H.J., van Kuik-Romeijn,P., de Kimpe,S.J., Furling,D., Platenburg,G.J., Gourdon,G., Thornton,C.A., Wieringa,B., and Wansink,D.G. (2009). Triplet-repeat oligonucleotide-mediated reversal of RNA toxicity in myotonic dystrophy. Proc. Natl. Acad. Sci. U. S. A. 106, 13915-13920.

Muller,Y.L., Reitstetter,R., and Yool,A.J. (2000). Antisense knockdown of calcium-dependent K+ channels in developing cerebellar Purkinje neurons. Brain Res. Dev. Brain Res. 120, 135-140.

Mykowska,A., Sobczak,K., Wojciechowska,M., Kozlowski,P., and Krzyzosiak,W.J. (2011). CAG repeats mimic CUG repeats in the misregulation of alternative splicing. Nucleic Acids Res. 39, 8938-8951.

Nagafuchi,S., Yanagisawa,H., Sato,K., Shirayama,T., Ohsaki,E., Bundo,M., Takeda,T., Tadokoro,K., Kondo,I., and Murayama,N. (1994). Dentatorubral and pallidoluysian atrophy expansion of an unstable CAG trinucleotide on chromosome 12p. Nat. Genet. 6, 14-18.

Naito,H. and Oyanagi,S. (1982). Familial myoclonus epilepsy and choreoathetosis: hereditary dentatorubral-pallidoluysian atrophy. Neurology 32, 798-807.

Nakamura,K., Jeong,S.Y., Uchihara,T., Anno,M., Nagashima,K., Nagashima,T., Ikeda,S., Tsuji,S., and Kanazawa,I. (2001). SCA17, a novel autosomal dominant cerebellar ataxia caused by an expanded polyglutamine in TATA-binding protein. Hum. Mol. Genet. 10, 1441-1448.

Nascimento-Ferreira,I., Santos-Ferreira,T., Sousa-Ferreira,L., Auregan,G., Onofre,I., Alves,S., Dufour,N., Colomer Gould,V.F., Koeppen,A., Deglon,N., and Pereira de,A.L. (2011). Overexpression of the autophagic beclin-1 protein clears mutant ataxin-3 and alleviates Machado-Joseph disease. Brain 134, 1400-1415.

Nasir,J., Floresco,S.B., O'Kusky,J.R., Diewert,V.M., Richman,J.M., Zeisler,J., Borowski,A., Marth,J.D., Phillips,A.G., and Hayden,M.R. (1995). Targeted disruption of the Huntington's disease gene results in embryonic lethality and behavioral and morphological changes in heterozygotes. Cell 81, 811-823.

Nguyen,H.P., Hubener,J., Weber,J.J., Grueninger,S., Riess,O., and Weiss,A. (2013). Cerebellar soluble mutant ataxin-3 level decreases during disease progression in Spinocerebellar Ataxia Type 3 mice. PLoS One 8, e62043.

Nicastro,G., Menon,R.P., Masino,L., Knowles,P.P., McDonald,N.Q., and Pastore,A. (2005). The solution structure of the Josephin domain of ataxin-3: structural determinants for molecular recognition. Proc. Natl. Acad. Sci. U. S. A. 102, 10493-10498.

Nobrega,C., Nascimento-Ferreira,I., Onofre,I., Albuquerque,D., Hirai,H., Deglon,N., and de Almeida,L.P. (2013). Silencing mutant ataxin-3 rescues motor deficits and neuropathology in Machado-Joseph disease transgenic mice. PLoS One 8, e52396.

Nucifora Jr,F.C., Sasaki,M., Peters,M.F., Huang,H., Cooper,J.K., Yamada,M., Takahashi,H., Tsuji,S., Troncoso,J., Dawson,V.L., Dawson,T.M., and Ross,C.A. (2001). Interference by huntingtin and atrophin-1 with cbp-mediated transcription leading to cellular toxicity. Science 291, 2423-2428.

Ogawa,M. (2004). Pharmacological treatments of cerebellar ataxia. Cerebellum. 3, 107-111.

Oliveira,J.M. (2010). Nature and cause of mitochondrial dysfunction in Huntington's disease: focusing on huntingtin and the striatum. J. Neurochem. 114, 1-12.

Ophoff,R.A., Terwindt,G.M., Vergouwe,M.N., van Eijk,E.R., Oefner,P.J., Hoffman,S.M., Lamerdin,J.E., Mohrenweiser,H.W., Bulman,D.E., Ferrari,M., Haan,J., Lindhout,D., van Ommen,G.J., Hofker,M.H., Ferrari,M.D., and Frants,R.R. (1996). Familial hemiplegic migraine and episodic ataxia type-2 are caused by mutations in the Ca2+ channel gene CACNL1A4. Cell 87, 543-552.

Orr,A.L., Li,S., Wang,C.E., Li,H., Wang,J., Rong,J., Xu,X., Mastroberardino,P.G., Greenamyre,J.T., and Li,X.J. (2008). N-terminal mutant huntingtin associates with mitochondria and impairs mitochondrial trafficking. J. Neurosci. 28, 2783-2792.

Orr,H.T., Chung,M.Y., Banfi,S., Kwiatkowski,T.J., Jr., Servadio,A., Beaudet,A.L., McCall,A.E., Duvick,L.A., Ranum,L.P., and Zoghbi,H.Y. (1993). Expansion of an unstable trinucleotide CAG repeat in spinocerebellar ataxia type 1. Nat. Genet. 4, 221-226.

Orr,H.T. and Zoghbi,H.Y. (2007). Trinucleotide repeat disorders. Annu. Rev. Neurosci. 30, 575-621.

Orr,H.T. (2012). Cell biology of spinocerebellar ataxia. J. Cell Biol. 197, 167-177.

Ostergaard,M.E., Southwell,A.L., Kordasiewicz,H., Watt,A.T., Skotte,N.H., Doty,C.N., Vaid,K., Villanueva,E.B., Swayze,E.E., Bennett,C.F., Hayden,M.R., and Seth,P.P. (2013). Rational design of antisense oligonucleotides targeting single nucleotide polymorphisms for potent and allele selective suppression of mutant Huntingtin in the CNS. Nucleic Acids Res. 41, 9634-9650.

Padiath,Q.S., Srivastava,A.K., Roy,S., Jain,S., and Brahmachari,S.K. (2005). Identification of a novel 45 repeat unstable allele associated with a disease phenotype at the MJD1/SCA3 locus. Am. J. Med. Genet. B Neuropsychiatr. Genet. 133B, 124-126.

Palmer,A.M. (2010). The blood-brain barrier. Neurobiol. Dis. 37, 1-2.

Panov,A.V., Gutekunst,C.A., Leavitt,B.R., Hayden,M.R., Burke,J.R., Strittmatter,W.J., and Greenamyre,J.T. (2002). Early mitochondrial calcium defects in Huntington's disease are a direct effect of polyglutamines. Nat. Neurosci. 5, 731-736.

Pardridge,W.M. (2007). Blood-brain barrier delivery. Drug Discov. Today 12, 54-61.

Park,J., Al-Ramahi,I., Tan,Q., Mollema,N., Diaz-Garcia,J.R., Gallego-Flores,T., Lu,H.C., Lagalwar,S., Duvick,L., Kang,H., Lee,Y., Jafar-Nejad,P., Sayegh,L.S., Richman,R., Liu,X., Gao,Y., Shaw,C.A., Arthur,J.S., Orr,H.T., Westbrook,T.F., Botas,J., and Zoghbi,H.Y. (2013a). RAS-MAPK-MSK1 pathway modulates ataxin 1 protein levels and toxicity in SCA1. Nature 498, 325-331.

Park,S.H., Kukushkin,Y., Gupta,R., Chen,T., Konagai,A., Hipp,M.S., Hayer-Hartl,M., and Hartl,F.U. (2013b). PolyQ proteins interfere with nuclear degradation of cytosolic proteins by sequestering the Sis1p chaperone. Cell 154, 134-145.

Parker,J.A., Connolly,J.B., Wellington,C., Hayden,M., Dausset,J., and Neri,C. (2001). Expanded polyglutamines in Caenorhabditis elegans cause axonal abnormalities and severe dysfunction of PLM mechanosensory neurons without cell death. Proc. Natl. Acad. Sci. U. S. A. 98, 13318-13323.

Passini,M.A., Bu,J., Richards,A.M., Kinnecom,C., Sardi,S.P., Stanek,L.M., Hua,Y., Rigo,F., Matson,J., Hung,G., Kaye,E.M., Shihabuddin,L.S., Krainer,A.R., Bennett,C.F., and Cheng,S.H. (2011). Antisense oligonucleotides delivered to the mouse CNS ameliorate symptoms of severe spinal muscular atrophy. Sci. Transl. Med. 3, 72ra18.

Paulsen,J.S., Ready,R.E., Hamilton,J.M., Mega,M.S., and Cummings,J.L. (2001). Neuropsychiatric aspects of Huntington's disease. J. Neurol. Neurosurg. Psychiatry 71, 310-314.

Paulsen,J.S. and Long,J.D. (2014). Onset of Huntington's disease: Can it be purely cognitive? Mov. Disord. 29, 1342-1350.

Paulson,H.L., Das,S.S., Crino,P.B., Perez,M.K., Patel,S.C., Gotsdiner,D., Fischbeck,K.H., and Pittman,R.N. (1997a). Machado-Joseph disease gene product is a cytoplasmic protein widely expressed in brain. Ann. Neurol. 41, 453-462.

Paulson,H.L., Perez,M.K., Trottier,Y., Trojanowski,J.Q., Subramony,S.H., Das,S.S., Vig,P., Mandel,J.L., Fischbeck,K.H., and Pittman,R.N. (1997b). Intranuclear inclusions of expanded polyglutamine protein in spinocerebellar ataxia type 3. Neuron 19, 333-344.

Perez,M.K., Paulson,H.L., Pendse,S.J., Saionz,S.J., Bonini,N.M., and Pittman,R.N. (1998). Recruitment and the role of nuclear localization in polyglutamine-mediated aggregation. J. Cell Biol. 143, 1457-1470.

Persichetti,F., Carlee,L., Faber,P.W., Mcneil,S.M., Ambrose,C.M., Srinidhi,J., Anderson,M., Barnes,G.T., Gusella,J.F., and MacDonald,M.E. (1996). Differential expression of normal and mutant Huntington's disease gene alleles. Neurobiol. Dis. 3, 183-190.

Perutz,M.F., Johnson,T., Suzuki,M., and Finch,J.T. (1994). Glutamine repeats as polar zippers: their possible role in inherited neurodegenerative diseases. Proc. Natl. Acad Sci U. S. A. 91, 5355-5358.

Pfaffl,M.W. (2001). A new mathematical model for relative quantification in real-time RT-PCR. Nucleic Acids Res. 29, e45.

Pfister,E.L., Kennington,L., Straubhaar,J., Wagh,S., Liu,W., Difiglia,M., Landwehrmeyer,B., Vonsattel,J.P., Zamore,P.D., and Aronin,N. (2009). Five siRNAs targeting three SNPs may provide therapy for three-quarters of Huntington's disease patients. Curr. Biol. 19, 774-778.

Pieretti,M., Zhang,F.P., Fu,Y.H., Warren,S.T., Oostra,B.A., Caskey,C.T., and Nelson,D.L. (1991). Absence of expression of the FMR-1 gene in fragile X syndrome. Cell 66, 817-822.

Pitts,M.W., Todorovic,C., Blank,T., and Takahashi,L.K. (2009). The central nucleus of the amygdala and corticotropin-releasing factor: insights into contextual fear memory. J. Neurosci. 29, 7379-7388.

Pouladi,M.A., Graham,R.K., Karasinska,J.M., Xie,Y., Santos,R.D., Petersen,A., and Hayden,M.R. (2009). Prevention of depressive behaviour in the YAC128 mouse model of Huntington disease by mutation at residue 586 of huntingtin. Brain 132, 919-932.

Pozzi,C., Valtorta,M., Tedeschi,G., Galbusera,E., Pastori,V., Bigi,A., Nonnis,S., Grassi,E., and Fusi,P. (2008). Study of subcellular localization and proteolysis of ataxin-3. Neurobiol. Dis. 30, 190-200.

Pringsheim,T., Wiltshire,K., Day,L., Dykeman,J., Steeves,T., and Jette,N. (2012). The incidence and prevalence of Huntington's disease: a systematic review and meta-analysis. Mov. Disord. 27, 1083-1091.

Qi,L., Zhang,X.D., Wu,J.C., Lin,F., Wang,J., Difiglia,M., and Qin,Z.H. (2012). The role of chaperone-mediated autophagy in huntingtin degradation. PLoS One 7, e46834.

Ranen,N.G., Stine,O.C., Abbott,M.H., Sherr,M., Codori,A.M., Franz,M.L., Chao,N.I., Chung,A.S., Pleasant,N., Callahan,C., Kasch,L.M., Ghaffari,M., Chase,G.A., Kazazian,H.H., Brandt,J., Folstein,S.E., and Ross,C.A. (1995). Anticipation and instability of IT-15 (CAG)n repeats in parent-offspring pairs with Huntington disease. Am. J. Hum. Gen. 57, 593-602.

Ranum,L.P., Lundgren,J.K., Schut,L.J., Ahrens,M.J., Perlman,S., Aita,J., Bird,T.D., Gomez,C., and Orr,H.T. (1995). Spinocerebellar ataxia type 1 and Machado-Joseph disease: incidence of CAG expansions among adult-onset ataxia patients from 311 families with dominant, recessive, or sporadic ataxia. Am. J. Hum. Genet. 57, 603-608.

Rao,D.D., Senzer,N., Cleary,M.A., and Nemunaitis,J. (2009). Comparative assessment of siRNA and shRNA off target effects: what is slowing clinical development. Cancer Gene Ther. 16, 807-809.

Raspe,M., Gillis,J., Krol,H., Krom,S., Bosch,K., van,V.H., and Reits,E. (2009). Mimicking proteasomal release of polyglutamine peptides initiates aggregation and toxicity. J. Cell Sci. 122, 3262-3271.

Ravikumar,B., Vacher,C., Berger,Z., Davies,J.E., Luo,S., Oroz,L.G., Scaravilli,F., Easton,D.F., Duden,R., O'Kane,C.J., and Rubinsztein,D.C. (2004). Inhibition of mTOR induces autophagy and reduces toxicity of polyglutamine expansions in fly and mouse models of Huntington disease. Nat. Genet. 36, 585-595.

Rawlins,M. (2010). Huntington's disease out of the closet? Lancet 376, 1372-1373.

Reedeker,W., van der Mast,R.C., Giltay,E.J., Kooistra,T.A., Roos,R.A., and van Duin,E. (2012). Psychiatric disorders in Huntington's disease: a 2-year follow-up study. Psychosomatics 53, 220-229.

Reina,C.P., Nabet,B.Y., Young,P.D., and Pittman,R.N. (2012). Basal and stress-induced Hsp70 are modulated by ataxin-3. Cell Stress. Chaperones. 17, 729-742.

Richards,R.I. and Sutherland,G.R. (1992). Dynamic mutations: a new class of mutations causing human disease. Cell 70, 709-712.

Riess,O., Schols,L., Bottger,H., Nolte,D., Vieira-Saecker,A.M., Schimming,C., Kreuz,F., Macek,M., Jr., Krebsova,A., Macek,M.S., Klockgether,T., Zuhlke,C., and Laccone,F.A. (1997). SCA6 is caused by moderate CAG expansion in the alpha1A-voltage-dependent calcium channel gene. Hum. Mol. Genet. 6, 1289-1293.

Riess,O., Rub,U., Pastore,A., Bauer,P., and Schols,L. (2008). SCA3: neurological features, pathogenesis and animal models. Cerebellum. 7, 125-137.

Rigamonti,D., Bauer,J.H., De-Fraja,C., Conti,L., Sipione,S., Sciorati,C., Clementi,E., Hackam,A., Hayden,M.R., Li,Y., Cooper,J.K., Ross,C.A., Govoni,S., Vincenz,C., and Cattaneo,E. (2000). Wild-type huntingtin protects from apoptosis upstream of caspase-3. J. Neurosci. 20, 3705-3713.

Rigo,F., Hua,Y., Krainer,A.R., and Bennett,C.F. (2012). Antisense-based therapy for the treatment of spinal muscular atrophy. J. Cell Biol. 199, 21-25.

Riley,B.E. and Orr,H.T. (2006). Polyglutamine neurodegenerative diseases and regulation of transcription: assembling the puzzle. Genes Dev. 20, 2183-2192.

Robberecht,W. (2000). Genetics of amyotrophic lateral sclerosis. J. Neurol. 247 Suppl 6, VI/2-VI/6.

Robbins,M., Judge,A., Liang,L., McClintock,K., Yaworski,E., and MacLachlan,I. (2007). 2′-O-methyl-modified RNAs act as TLR7 antagonists. Mol. Ther. 15, 1663-1669.

Rockabrand,E., Slepko,N., Pantalone,A., Nukala,V.N., Kazantsev,A., Marsh,J.L., Sullivan,P.G., Steffan,J.S., Sensi,S.L., and Thompson,L.M. (2007). The first 17 amino acids of Huntingtin modulate its sub-cellular localization, aggregation and effects on calcium homeostasis. Hum. Mol. Genet. 16, 61-77.

Rodrigues,A.J., Coppola,G., Santos,C., Costa,M.C., Ailion,M., Sequeiros,J., Geschwind,D.H., and Maciel,P. (2007). Functional genomics and biochemical characterization of the C. elegans orthologue of the Machado-Joseph disease protein ataxin-3. FASEB J. 21, 1126-1136.

Rodrigues,A.J., do Carmo,C.M., Silva,T.L., Ferreira,D., Bajanca,F., Logarinho,E., and Maciel,P. (2010). Absence of ataxin-3 leads to cytoskeletal disorganization and increased cell death. Biochim. Biophys. Acta 1803, 1154-1163.

Rodrigues,A.J., Neves-Carvalho,A., Teixeira-Castro,A., Rokka,A., Corthals,G., Logarinho,E., and Maciel,P. (2011). Absence of ataxin-3 leads to enhanced stress response in C. elegans. PLoS One 6, e18512.

Rodriguez-Lebron,E. and Paulson,H.L. (2006). Allele-specific RNA interference for neurological disease. Gene Ther. 13, 576-581.

Rolfs,A., Koeppen,A.H., Bauer,I., Bauer,P., Buhlmann,S., Topka,H., Schols,L., and Riess,O. (2003). Clinical features and neuropathology of autosomal dominant spinocerebellar ataxia (SCA17). Ann. Neurol. 54, 367-375.

Rooms,L., Reyniers,E., Scheers,S., van,L.R., Wauters,J., Van,A.L., Callaerts-Vegh,Z., D'Hooge,R., Mengus,G., Davidson,I., Courtens,W., and Kooy,R.F. (2006). TBP as a candidate gene for mental retardation in patients with subtelomeric 6q deletions. Eur. J. Hum. Genet. 14, 1090-1096.

Roos,R.A., Hermans,J., Vegter-van der Vlis,M., van Ommen,G.J., and Bruyn,G.W. (1993). Duration of illness in Huntington's disease is not related to age at onset. J. Neurol. Neurosurg. Psychiatry 56, 98-100.

Roos,R.A. (2010). Huntington's disease: a clinical review. Orphanet. J. Rare. Dis 5, 40.

Rosas,H.D., Koroshetz,W.J., Chen,Y.I., Skeuse,C., Vangel,M., Cudkowicz,M.E., Caplan,K., Marek,K., Seidman,L.J., Makris,N., Jenkins,B.G., and Goldstein,J.M. (2003). Evidence for more widespread cerebral pathology in early HD: an MRI-based morphometric analysis. Neurology 60, 1615-1620.

Rosas,H.D., Salat,D.H., Lee,S.Y., Zaleta,A.K., Pappu,V., Fischl,B., Greve,D., Hevelone,N., and Hersch,S.M. (2008). Cerebral cortex and the clinical expression of Huntington's disease: complexity and heterogeneity. Brain 131, 1057-1068.

Rose,D.M., Alon,R., and Ginsberg,M.H. (2007). Integrin modulation and signaling in leukocyte adhesion and migration. Immunol. Rev. 218, 126-134.

Rosenberg,R.N. (1992). Machado-Joseph disease: an autosomal dominant motor system degeneration. Mov. Disord. 7, 193-203.

Rosenblatt,A., Kumar,B.V., Mo,A., Welsh,C.S., Margolis,R.L., and Ross,C.A. (2012). Age, CAG repeat length, and clinical progression in Huntington's disease. Mov. Disord. 27, 272-276.

Ross,C.A. and Tabrizi,S.J. (2011). Huntington's disease: from molecular pathogenesis to clinical treatment. Lancet Neurol. 10, 83-98.

Rousseau,E., Kojima,R., Hoffner,G., Djian,P., and Bertolotti,A. (2009). Misfolding of proteins with a polyglutamine expansion is facilitated by proteasomal chaperones. J. Biol. Chem. 284, 1917-1929.

Rozen,S. and Skaletsky,H. (2000). Primer3 on the WWW for general users and for biologist programmers. Methods Mol. Biol. 132, 365-386.

Rub,U., de Vos,R.A., Brunt,E.R., Sebesteny,T., Schols,L., Auburger,G., Bohl,J., Ghebremedhin,E., Gierga,K., Seidel,K., den,D.W., Heinsen,H., Paulson,H., and Deller,T. (2006). Spinocerebellar ataxia type 3 (SCA3): thalamic neurodegeneration occurs independently from thalamic ataxin-3 immunopositive neuronal intranuclear inclusions. Brain Pathol. 16, 218-227.

Rub,U., Schols,L., Paulson,H., Auburger,G., Kermer,P., Jen,J.C., Seidel,K., Korf,H.W., and Deller,T. (2013). Clinical features, neurogenetics and neuropathology of the polyglutamine spinocerebellar ataxias type 1, 2, 3, 6 and 7. Prog. Neurobiol. 104, 38-66.

Rubinsztein,D.C. (2006). The roles of intracellular protein-degradation pathways in neurodegeneration. Nature 443, 780-786.

Ruijter,J.M., Ramakers,C., Hoogaars,W.M.H., Karlen,Y., Bakker,O., van den Hoff,M.J.B., and Moorman,A.F.M. (2009). Amplification efficiency: linking baseline and bias in the analysis of quantitative PCR data. Nucleic Acids Res. 37, e45.

Sah,D.W. and Aronin,N. (2011). Oligonucleotide therapeutic approaches for Huntington disease. J. Clin. Invest. 121, 500-507.

Saito,H., Okada,M., Miki,T., Wakamori,M., Futatsugi,A., Mori,Y., Mikoshiba,K., and Suzuki,N. (2009). Knockdown of Cav2.1 calcium channels is sufficient to induce neurological disorders observed in natural occurring Cacna1a mutants in mice. Biochem. Biophys. Res. Commun. 390, 1029-1033.

Sanchez,C.E., Tierney,T.S., Gale,J.T., Alavian,K.N., Sahin,A., Lee,J.S., Mulligan,R.C., and Carter,B.S. (2011). Recombinant adeno-associated virus type 2 pseudotypes: comparing safety, specificity, and transduction efficiency in the primate striatum. Laboratory investigation. J. Neurosurg. 114, 672-680.

Sarkar,S., Davies,J.E., Huang,Z.B., Tunnacliffe,A., and Rubinsztein,D.C. (2007). Trehalose, a novel mTOR-independent autophagy enhancer, accelerates the clearance of mutant huntingtin and alpha-synuclein. J. Biol. Chem. 282, 5641-5652.

Sasaki,H., Fukazawa,T., Yanagihara,T., Hamada,T., Shima,K., Matsumoto,A., Hashimoto,K., Ito,N., Wakisaka,A., and Tashiro,K. (1996). Clinical features and natural history of spinocerebellar ataxia type 1. Acta Neurol. Scand. 93, 64-71.

Sathasivam,K., Woodman,B., Mahal,A., Bertaux,F., Wanker,E.E., Shima,D.T., and Bates,G.P. (2001). Centrosome disorganization in fibroblast cultures derived from R6/2 Huntington's disease (HD) transgenic mice and HD patients. Hum. Mol. Genet. 10, 2425-2435.

Sathasivam,K., Neueder,A., Gipson,T.A., Landles,C., Benjamin,A.C., Bondulich,M.K., Smith,D.L., Faull,R.L., Roos,R.A., Howland,D., Detloff,P.J., Housman,D.E., and Bates,G.P. (2013). Aberrant splicing of HTT generates the pathogenic exon 1 protein in Huntington disease. Proc. Natl. Acad. Sci. U. S. A. 110, 2366-2370.

Saudou,F., Finkbeiner,S., Devys,D., and Greenberg,M.E. (1998). Huntingtin acts in the nucleus to induce apoptosis but death does not correlate with the formation of intranuclear inclusions. Cell 95, 55-66.

Saute,J.A., Castilhos,R., Monte,T., Schuh,A., Donis,K., D'Ávila,R., Souza,G.N., Russo,A.D., Furtado,G.V., Gheno,T.C., de Souza,D.O., Portela,L.V., Saraiva-Pereira,M.L., Camey,S.A., Torman,V.B., de Mello Rieder,C.R., and Jardim,L.B. (2013). Safety and effectiveness of lithium carbonate for the treatment of Machado-Joseph disease: A phase 2/3 randomised, double-blind, placebo-controlled trial [abstract]. Mov. Disord. 2013;28, Suppl 1 :713.

Scheel,H., Tomiuk,S., and Hofmann,K. (2003). Elucidation of ataxin-3 and ataxin-7 function by integrative bioinformatics. Hum. Mol. Genet. 12, 2845-2852.

Schmidt,T., Landwehrmeyer,G.B., Schmitt,I., Trottier,Y., Auburger,G., Laccone,F., Klockgether,T., Volpel,M., Epplen,J.T., Schols,L., and Riess,O. (1998). An isoform of ataxin-3 accumulates in the nucleus of neuronal cells in affected brain regions of SCA3 patients. Brain Pathol. 8, 669-679.

Schmidt,T., Lindenberg,K.S., Krebs,A., Schols,L., Laccone,F., Herms,J., Rechsteiner,M., Riess,O., and Landwehrmeyer,G.B. (2002). Protein surveillance machinery in brains with spinocerebellar ataxia type 3: redistribution and differential recruitment of 26S proteasome subunits and chaperones to neuronal intranuclear inclusions. Ann. Neurol. 51, 302-310.

Schmitt,I., Brattig,T., Gossen,M., and Riess,O. (1997). Characterization of the rat spinocerebellar ataxia type 3 gene. Neurogenetics. 1, 103-112.

Schmitt,I., Linden,M., Khazneh,H., Evert,B.O., Breuer,P., Klockgether,T., and Wuellner,U. (2007). Inactivation of the mouse Atxn3 (ataxin-3) gene increases protein ubiquitination. Biochem. Biophys. Res. Commun. 362, 734-739.

Schmitz-Hubsch,T., du Montcel,S.T., Baliko,L., Berciano,J., Boesch,S., Depondt,C., Giunti,P., Globas,C., Infante,J., Kang,J.S., Kremer,B., Mariotti,C., Melegh,B., Pandolfo,M., Rakowicz,M., Ribai,P., Rola,R., Schols,L., Szymanski,S., van de Warrenburg,B.P., Durr,A., Klockgether,T., and Fancellu,R. (2006). Scale for the assessment and rating of ataxia: development of a new clinical scale. Neurology 66, 1717-1720.

Scholefield,J., Greenberg,L.J., Weinberg,M.S., Arbuthnot,P.B., Abdelgany,A., and Wood,M.J. (2009). Design of RNAi hairpins for mutation-specific silencing of ataxin-7 and correction of a SCA7 phenotype. PLoS One 4, e7232.

Scholefield,J. and Wood,M.J.A. (2010). Therapeutic gene silencing strategies for polyglutamine disorders. Trends Genet. 26, 29-38.

Scholefield,J., Watson,L., Smith,D., Greenberg,J., and Wood,M.J. (2014). Allele-specific silencing of mutant Ataxin-7 in SCA7 patient-derived fibroblasts. Eur. J. Hum. Genet.

Schols,L., Kruger,R., Amoiridis,G., Przuntek,H., Epplen,J.T., and Riess,O. (1998). Spinocerebellar ataxia type 6: genotype and phenotype in German kindreds. J. Neurol. Neurosurg. Psychiatry 64, 67-73.

Schols,L., Bauer,P., Schmidt,T., Schulte,T., and Riess,O. (2004). Autosomal dominant cerebellar ataxias: clinical features, genetics, and pathogenesis. Lancet Neurol. 3, 291-304.

Schwarz,D.S., Ding,H., Kennington,L., Moore,J.T., Schelter,J., Burchard,J., Linsley,P.S., Aronin,N., Xu,Z., and Zamore,P.D. (2006). Designing siRNA that distinguish between genes that differ by a single nucleotide. PLoS Genet 2, e140.

Scott,L.J. (2011). Tetrabenazine: for chorea associated with Huntington's disease. CNS. Drugs 25, 1073-1085.

Seo,H., Sonntag,K.C., Kim,W., Cattaneo,E., and Isacson,O. (2007). Proteasome activator enhances survival of Huntington's disease neuronal model cells. PLoS One 2, e238.

Shao,J. and Diamond,M.I. (2007). Polyglutamine diseases: emerging concepts in pathogenesis and therapy. Hum. Mol. Genet. 16 Spec. No. 2, R115-R123.

Shen,Y., Lee,G., Choe,Y., Zoltewicz,J.S., and Peterson,A.S. (2007). Functional architecture of atrophins. J. Biol. Chem. 282, 5037-5044.

Shen,Y. and Peterson,A.S. (2009). Atrophins' emerging roles in development and neurodegenerative disease. Cell Mol. Life Sci. 66, 437-446.

Shimohata,T., Nakajima,T., Yamada,M., Uchida,C., Onodera,O., Naruse,S., Kimura,T., Koide,R., Nozaki,K., Sano,Y., Ishiguro,H., Sakoe,K., Ooshima,T., Sato,A., Ikeuchi,T., Oyake,M., Sato,T., Aoyagi,Y., Hozumi,I., Nagatsu,T., Takiyama,Y., Nishizawa,M., Goto,J., Kanazawa,I., Davidson,I., Tanese,N., Takahashi,H., and Tsuji,S. (2000). Expanded polyglutamine stretches interact with TAFII130, interfering with CREB-dependent transcription. Nat. Genet. 26, 29-36.

Shimojo,Y., Osawa,Y., Fukumizu,M., Hanaoka,S., Tanaka,H., Ogata,F., Sasaki,M., and Sugai,K. (2001). Severe infantile dentatorubral pallidoluysian atrophy with extreme expansion of CAG repeats. Neurology 56, 277-278.

Shoulson,I. and Young,A.B. (2011). Milestones in huntington disease. Mov. Disord. 26, 1127-1133.

Silveira,I., Lopes-Cendes,I., Kish,S., Maciel,P., Gaspar,C., Coutinho,P., Botez,M.I., Teive,H., Arruda,W., Steiner,C.E., Pinto-Junior,W., Maciel,J.A., Jerin,S., Sack,G., Andermann,E., Sudarsky,L., Rosenberg,R., MacLeod,P., Chitayat,D., Babul,R., Sequeiros,J., and Rouleau,G.A. (1996). Frequency of spinocerebellar ataxia type 1, dentatorubropallidoluysian atrophy, and Machado-Joseph disease mutations in a large group of spinocerebellar ataxia patients. Neurology 46, 214-218.

Simpson,S.A. (2007). Late stage care in Huntington's disease. Brain Res. Bull. 72, 179-181.

Sinadinos,C., Burbidge-King,T., Soh,D., Thompson,L.M., Marsh,J.L., Wyttenbach,A., and Mudher,A.K. (2009). Live axonal transport disruption by mutant huntingtin fragments in Drosophila motor neuron axons. Neurobiol. Dis. 34, 389-395.

Smith,R., Klein,P., Koc-Schmitz,Y., Waldvogel,H.J., Faull,R.L., Brundin,P., Plomann,M., and Li,J.Y. (2007). Loss of SNAP-25 and rabphilin 3a in sensory-motor cortex in Huntington's disease. J. Neurochem. 103, 115-123.

Smith,R.A., Miller,T.M., Yamanaka,K., Monia,B.P., Condon,T.P., Hung,G., Lobsiger,C.S., Ward,C.M., McAlonis-Downes,M., Wei,H., Wancewicz,E.V., Bennett,C.F., and Cleveland,D.W. (2006). Antisense oligonucleotide therapy for neurodegenerative disease. J. Clin. Invest. 116, 2290-2296.

Soong,B., Cheng,C., Liu,R., and Shan,D. (1997). Machado-Joseph disease: clinical, molecular, and metabolic characterization in Chinese kindreds. Ann. Neurol. 41, 446-452.

Sopher,B.L., Ladd,P.D., Pineda,V.V., Libby,R.T., Sunkin,S.M., Hurley,J.B., Thienes,C.P., Gaasterland,T., Filippova,G.N., and La Spada,A.R. (2011). CTCF regulates ataxin-7 expression through promotion of a convergently transcribed, antisense noncoding RNA. Neuron 70, 1071-1084.

Spiess,A.N. and Ivell,R. (2002). A highly efficient method for long-chain cDNA synthesis using trehalose and betaine. Anal. Biochem. 301, 168-174.

Spitali,P. and Aartsma-Rus,A. (2012). Splice modulating therapies for human disease. Cell 148, 1085-1088.

Steffan,J.S., Kazantsev,A., Spasic-Boskovic,O., Greenwald,M., Zhu,Y.Z., Gohler,H., Wanker,E.E., Bates,G.P., Housman,D.E., and Thompson,L.M. (2000). The Huntington's disease protein interacts with p53 and CREB-binding protein and represses transcription. Proc. Natl. Acad Sci U. S. A. 97, 6763-6768.

Steffan,J.S., Agrawal,N., Pallos,J., Rockabrand,E., Trotman,L.C., Slepko,N., Illes,K., Lukacsovich,T., Zhu,Y.Z., Cattaneo,E., Pandolfi,P.P., Thompson,L.M., and Marsh,J.L. (2004). SUMO modification of Huntingtin and Huntington's disease pathology. Science 304, 100-104.

Stevanin,G., Giunti,P., Belal,G.D., Durr,A., Ruberg,M., Wood,N., and Brice,A. (1998). De novo expansion of intermediate alleles in spinocerebellar ataxia 7. Hum. Mol. Genet. 7, 1809-1813.

Stine,O.C., Li,S.H., Pleasant,N., Wagster,M.V., Hedreen,J.C., and Ross,C.A. (1995). Expression of the mutant allele of IT-15 (the HD gene) in striatum and cortex of Huntington's disease patients. Hum. Mol. Genet. 4, 15-18.

Stochmanski,S.J., Therrien,M., Laganiere,J., Rochefort,D., Laurent,S., Karemera,L., Gaudet,R., Vyboh,K., Van Meyel,D.J., Di,C.G., Dion,P.A., Gaspar,C., and Rouleau,G.A. (2012). Expanded ATXN3 frameshifting events are toxic in Drosophila and mammalian neuron models. Hum. Mol. Genet. 21, 2211-2218.

Strehlow,A.N., Li,J.Z., and Myers,R.M. (2007). Wild-type huntingtin participates in protein trafficking between the Golgi and the extracellular space. Hum. Mol. Genet. 16, 391-409.

Strom,A.L., Forsgren,L., and Holmberg,M. (2005). A role for both wild-type and expanded ataxin-7 in transcriptional regulation. Neurobiol. Dis. 20, 646-655.

Strong,T.V., Tagle,D.A., Valdes,J.M., Elmer,L.W., Boehm,K., Swaroop,M., Kaatz,K.W., Collins,F.S., and Albin,R.L. (1993). Widespread expression of the human and rat Huntington's disease gene in brain and nonneural tissues. Nat. Genet. 5, 259-265.

Switonski,P.M., Fiszer,A., Kazmierska,K., Kurpisz,M., Krzyzosiak,W.J., and Figiel,M. (2011). Mouse ataxin-3 functional knock-out model. Neuromolecular. Med. 13, 54-65.

Tabrizi,S.J., Langbehn,D.R., Leavitt,B.R., Roos,R.A., Durr,A., Craufurd,D., Kennard,C., Hicks,S.L., Fox,N.C., Scahill,R.I., Borowsky,B., Tobin,A.J., Rosas,H.D., Johnson,H., Reilmann,R., Landwehrmeyer,B., and Stout,J.C. (2009). Biological and clinical manifestations of Huntington's disease in the longitudinal TRACK-HD study: cross-sectional analysis of baseline data. Lancet Neurol. 8, 791-801.

Tabrizi,S.J., Scahill,R.I., Owen,G., Durr,A., Leavitt,B.R., Roos,R.A., Borowsky,B., Landwehrmeyer,B., Frost,C., Johnson,H., Craufurd,D., Reilmann,R., Stout,J.C., and Langbehn,D.R. (2013). Predictors of phenotypic progression and disease onset in premanifest and early-stage Huntington's disease in the TRACK-HD study: analysis of 36-month observational data. Lancet Neurol. 12, 637-649.

Tait,D., Riccio,M., Sittler,A., Scherzinger,E., Santi,S., Ognibene,A., Maraldi,N.M., Lehrach,H., and Wanker,E.E. (1998). Ataxin-3 is transported into the nucleus and associates with the nuclear matrix. Hum. Mol. Genet. 7, 991-997.

Takahashi,T., Kikuchi,S., Katada,S., Nagai,Y., Nishizawa,M., and Onodera,O. (2008). Soluble polyglutamine oligomers formed prior to inclusion body formation are cytotoxic. Hum. Mol. Genet. 17, 345-356.

Takahashi,T., Katada,S., and Onodera,O. (2010). Polyglutamine diseases: where does toxicity come from? what is toxicity? where are we going? J. Mol. Cell Biol. 2, 180-191.

Takano,H. and Gusella,J.F. (2002). The predominantly HEAT-like motif structure of huntingtin and its association and coincident nuclear entry with dorsal, an NF-kB/Rel/dorsal family transcription factor. BMC. Neurosci. 3, 15.

Tanganyika-de Winter,C.L., Heemskerk,H., Karnaoukh,T.G., van Putten M., de Kimpe,S.J., van Deutekom J., and Aartsma-Rus,A. (2012). Long-term exon skipping studies with 2'-O-methyl phosphorothioate antisense oligonucleotides in dystrophic mouse models. Mol. Ther. Nucleic Acids 1, e44.

Tassone,F., Iwahashi,C., and Hagerman,P.J. (2004). FMR1 RNA within the intranuclear inclusions of fragile X-associated tremor/ataxia syndrome (FXTAS). RNA Biol. 1, 103-105.

Tebbenkamp,A.T., Green,C., Xu,G., Denovan-Wright,E.M., Rising,A.C., Fromholt,S.E., Brown,H.H., Swing,D., Mandel,R.J., Tessarollo,L., and Borchelt,D.R. (2011). Transgenic mice expressing caspase-6-derived N-terminal fragments of mutant huntingtin develop neurologic abnormalities with predominant cytoplasmic inclusion pathology composed largely of a smaller proteolytic derivative. Hum. Mol. Genet. 20, 2770-2782.

Teive,H.A., Munhoz,R.P., Arruda,W.O., Lopes-Cendes,I., Raskin,S., Werneck,L.C., and Ashizawa,T. (2012). Spinocerebellar ataxias: genotype-phenotype correlations in 104 Brazilian families. Clinics (Sao Paulo) 67, 443-449.

Teixeira-Castro,A., Ailion,M., Jalles,A., Brignull,H.R., Vilaca,J.L., Dias,N., Rodrigues,P., Oliveira,J.F., Neves-Carvalho,A., Morimoto,R.I., and Maciel,P. (2011). Neuron-specific proteotoxicity of mutant ataxin-3 in C. elegans: rescue by the DAF-16 and HSF-1 pathways. Hum. Mol. Genet. 20, 2996-3009.

The Huntington's Disease Collaborative Research Group (1993). A novel gene containing a trinucleotide repeat that is expanded and unstable on Huntington's disease chromosomes. Cell 72, 971-983.

Thompson,L.M., Aiken,C.T., Kaltenbach,L.S., Agrawal,N., Illes,K., Khoshnan,A., Martinez-Vincente,M., Arrasate,M., O'Rourke,J.G., Khashwji,H., Lukacsovich,T., Zhu,Y.Z., Lau,A.L., Massey,A., Hayden,M.R., Zeitlin,S.O., Finkbeiner,S., Green,K.N., LaFerla,F.M., Bates,G., Huang,L., Patterson,P.H., Lo,D.C., Cuervo,A.M., Marsh,J.L., and Steffan,J.S. (2009). IKK phosphorylates Huntingtin and targets it for degradation by the proteasome and lysosome. J. Cell Biol. 187, 1083-1099.

Todi,S.V., Laco,M.N., Winborn,B.J., Travis,S.M., Wen,H.M., and Paulson,H.L. (2007). Cellular turnover of the polyglutamine disease protein ataxin-3 is regulated by its catalytic activity. J. Biol. Chem. 282, 29348-29358.

Tomkins,O., Friedman,O., Ivens,S., Reiffurth,C., Major,S., Dreier,J.P., Heinemann,U., and Friedman,A. (2007). Blood-brain barrier disruption results in delayed functional and structural alterations in the rat neocortex. Neurobiol. Dis. 25, 367-377.

Toyoshima,Y., Yamada,M., Onodera,O., Shimohata,M., Inenaga,C., Fujita,N., Morita,M., Tsuji,S., and Takahashi,H. (2004). SCA17 homozygote showing Huntington's disease-like phenotype. Ann. Neurol. 55, 281-286.

Trottier,Y., Lutz,Y., Stevanin,G., Imbert,G., Devys,D., Cancel,G., Saudou,F., Weber,C., David,G., Tora,L., Agid,Y., Brice,A., and Mandel,J.L. (1995). Polyglutamine expansion as a pathological epitope in Huntington's disease and 4 dominant cerebellar ataxias. Nature 378, 403-406.

Trottier,Y., Cancel,G., An-Gourfinkel,I., Lutz,Y., Weber,C., Brice,A., Hirsch,E., and Mandel,J.L. (1998). Heterogeneous intracellular localization and expression of ataxin-3. Neurobiol. Dis. 5, 335-347.

Tsou,W.L., Soong,B.W., Paulson,H.L., and Rodriguez-Lebron,E. (2011). Splice isoform-specific suppression of the Cav2.1 variant underlying spinocerebellar ataxia type 6. Neurobiol. Dis. 43, 533-542.

Tsunemi,T., Ishikawa,K., Jin,H., and Mizusawa,H. (2008). Cell-type-specific alternative splicing in spinocerebellar ataxia type 6. Neurosci. Lett. 447, 78-81.

Ulusoy,A., Decressac,M., Kirik,D., and Bjorklund,A. (2010). Viral vector-mediated overexpression of alpha-synuclein as a progressive model of Parkinson's disease. Prog. Brain Res. 184, 89-111.

van Bilsen,P.H., Jaspers,L., Lombardi,M.S., Odekerken,J.C., Burright,E.N., and Kaemmerer,W.F. (2008). Identification and allele-specific silencing of the mutant huntingtin allele in Huntington's disease patient-derived fibroblasts. Hum. Gene Ther. 19, 710-719.

van Broeck,B., van Broeckhoven,C., and Kumar-Singh,S. (2007). Current Insights into Molecular Mechanisms of Alzheimer Disease and Their Implications for Therapeutic Approaches. Neurodegener. Dis. 4, 349-365.

van de Warrenburg,B.P., Frenken,C.W., Ausems,M.G., Kleefstra,T., Sinke,R.J., Knoers,N.V., and Kremer,H.P. (2001). Striking anticipation in spinocerebellar ataxia type 7: the infantile phenotype. J. Neurol. 248, 911-914.

van de Warrenburg,B.P., Hendriks,H., Durr,A., van Zuijlen,M.C., Stevanin,G., Camuzat,A., Sinke,R.J., Brice,A., and Kremer,B.P. (2005). Age at onset variance analysis in spinocerebellar ataxias: a study in a Dutch-French cohort. Ann. Neurol. 57, 505-512.

van Deutekom,J.C., Janson,A.A., Ginjaar,I.B., Frankhuizen,W.S., Aartsma-Rus,A., Bremmer-Bout,M., den Dunnen,J.T., Koop,K., van der Kooi,A.J., Goemans,N.M., de Kimpe,S.J., Ekhart,P.F., Venneker,E.H., Platenburg,G.J., Verschuuren,J.J., and van Ommen,G.J. (2007). Local dystrophin restoration with antisense oligonucleotide PRO051. N. Engl. J. Med. 357, 2677-2686.

van Putten,M. and Aartsma-Rus,A. (2011). Opportunities and challenges for the development of antisense treatment in neuromuscular disorders. Expert Opin. Biol. Ther. 11, 1025-1037.

van Roon-Mom,W.M., Reid,S.J., Jones,A.L., MacDonald,M.E., Faull,R.L., and Snell,R.G. (2002). Insoluble TATA-binding protein accumulation in Huntington's disease cortex. Brain Res. Mol Brain Res. 109, 1-10.

van Roon-Mom,W.M., Reid,S.J., Faull,R.L., and Snell,R.G. (2005). TATA-binding protein in neurodegenerative disease. Neuroscience 133, 863-872.

van Roon-Mom,W.M., Hogg,V.M., Tippett,L.J., and Faull,R.L. (2006). Aggregate distribution in frontal and motor cortex in Huntington's disease brain. Neuroreport 17, 667-670.

Venkatraman,P., Wetzel,R., Tanaka,M., Nukina,N., and Goldberg,A.L. (2004). Eukaryotic proteasomes cannot digest polyglutamine sequences and release them during degradation of polyglutamine-containing proteins. Mol. Cell 14, 95-104.

Verkerk,A.J., Pieretti,M., Sutcliffe,J.S., Fu,Y.H., Kuhl,D.P., Pizzuti,A., Reiner,O., Richards,S., Victoria,M.F., Zhang,F.P., Eussen,B.E., van Ommen,G.J., Blonden,L.A., Riggins,G.J., Chastain,J.L., Kunst,G.B., Galjaard,H., Caskey,C.T., Nelson,D.L., Oostraa,B.A., and Warren,S.T. (1991). Identification of a gene (FMR-1) containing a CGG repeat coincident with a breakpoint cluster region exhibiting length variation in fragile X syndrome. Cell 65, 905-914.

Vonsattel,J.P., Myers,R.H., Stevens,T.J., Ferrante,R.J., Bird,E.D., and Richardson,E.P. (1985). Neuropathological classification of Huntington's disease. J. Neuropathol. Exp. Neurol. 44, 559-577.

Vonsattel,J.P. and Difiglia,M. (1998). Huntington disease. J. Neuropathol. Exp. Neurol. 57, 369-384.

Waldron-Roby,E., Ratovitski,T., Wang,X., Jiang,M., Watkin,E., Arbez,N., Graham,R.K., Hayden,M.R., Hou,Z., Mori,S., Swing,D., Pletnikov,M., Duan,W., Tessarollo,L., and Ross,C.A. (2012). Transgenic mouse model expressing the caspase 6 fragment of mutant huntingtin. J. Neurosci. 32, 183-193.

Walker,F.O. (2007). Huntington's disease. Lancet 369, 218-228.

Wang,G., Sawai,N., Kotliarova,S., Kanazawa,I., and Nukina,N. (2000). Ataxin-3, the MJD1 gene product, interacts with the two human homologs of yeast DNA repair protein RAD23, HHR23A and HHR23B. Hum. Mol. Genet. 9, 1795-1803.

Wang,L.C., Chen,K.Y., Pan,H., Wu,C.C., Chen,P.H., Liao,Y.T., Li,C., Huang,M.L., and Hsiao,K.M. (2011). Muscleblind participates in RNA toxicity of expanded CAG and CUG repeats in Caenorhabditis elegans. Cell Mol. Life Sci. 68, 1255-1267.

Wang,Q., Li,L., and Ye,Y. (2006). Regulation of retrotranslocation by p97-associated deubiquitinating enzyme ataxin-3. J. Cell Biol. 174, 963-971.

Wang,Y.L., Liu,W., Wada,E., Murata,M., Wada,K., and Kanazawa,I. (2005). Clinico-pathological rescue of a model mouse of Huntington's disease by siRNA. Neurosci. Res. 53, 241-249.

Wanker,E.E. (2000). Protein aggregation and pathogenesis of Huntington's disease: mechanisms and correlations. Biol. Chem. 381, 937-942.

Warby,S.C., Doty,C.N., Graham,R.K., Carroll,J.B., Yang,Y.Z., Singaraja,R.R., Overall,C.M., and Hayden,M.R. (2008). Activated caspase-6 and caspase-6-cleaved fragments of huntingtin specifically colocalize in the nucleus. Hum. Mol. Genet. 17, 2390-2404.

Warby,S.C., Montpetit,A., Hayden,A.R., Carroll,J.B., Butland,S.L., Visscher,H., Collins,J.A., Semaka,A., Hudson,T.J., and Hayden,M.R. (2009). CAG expansion in the Huntington disease gene is associated with a specific and targetable predisposing haplogroup. Am. J. Hum. Genet. 84, 351-366.

Warner,J.P., Barron,L.H., and Brock,D.J. (1993). A new polymerase chain reaction (PCR) assay for the trinucleotide repeat that is unstable and expanded on Huntington's disease chromosomes. Mol. Cell Probes 7, 235-239.

Warrick,J.M., Morabito,L.M., Bilen,J., Gordesky-Gold,B., Faust,L.Z., Paulson,H.L., and Bonini,N.M. (2005). Ataxin-3 suppresses polyglutamine neurodegeneration in Drosophila by a ubiquitin-associated mechanism. Mol. Cell 18, 37-48.

Watase,K., Barrett,C.F., Miyazaki,T., Ishiguro,T., Ishikawa,K., Hu,Y., Unno,T., Sun,Y., Kasai,S., Watanabe,M., Gomez,C.M., Mizusawa,H., Tsien,R.W., and Zoghbi,H.Y. (2008). Spinocerebellar ataxia type 6 knockin mice develop a progressive neuronal dysfunction with age-dependent accumulation of mutant CaV2.1 channels. Proc. Natl. Acad. Sci. U. S. A. 105, 11987-11992.

Weiss,A., Klein,C., Woodman,B., Sathasivam,K., Bibel,M., Regulier,E., Bates,G.P., and Paganetti,P. (2008). Sensitive biochemical aggregate detection reveals aggregation onset before symptom development in cellular and murine models of Huntington's disease. J. Neurochem. 104, 846-858.

Wellington,C.L., Ellerby,L.M., Hackam,A.S., Margolis,R.L., Trifiro,M.A., Singaraja,R., McCutcheon,K., Salvesen,G.S., Propp,S.S., Bromm,M., Rowland,K.J., Zhang,T., Rasper,D., Roy,S., Thornberry,N., Pinsky,L., Kakizuka,A., Ross,C.A., Nicholson,D.W., Bredesen,D.E., and Hayden,M.R. (1998). Caspase cleavage of gene products associated with triplet expansion disorders generates truncated fragments containing the polyglutamine tract. J. Biol. Chem. 273, 9158-9167.

Wellington,C.L., Singaraja,R., Ellerby,L., Savill,J., Roy,S., Leavitt,B., Cattaneo,E., Hackam,A., Sharp,A., Thornberry,N., Nicholson,D.W., Bredesen,D.E., and Hayden,M.R. (2000). Inhibiting caspase cleavage of huntingtin reduces toxicity and aggregate formation in neuronal and nonneuronal cells. J. Biol. Chem. 275, 19831-19838.

Wellington,C.L., Ellerby,L.M., Gutekunst,C.A., Rogers,D., Warby,S., Graham,R.K., Loubser,O., van,R.J., Singaraja,R., Yang,Y.Z., Gafni,J., Bredesen,D., Hersch,S.M., Leavitt,B.R., Roy,S., Nicholson,D.W., and Hayden,M.R. (2002). Caspase cleavage of mutant huntingtin precedes neurodegeneration in Huntington's disease. J. Neurosci. 22, 7862-7872.

Wheeler,T.M. and Thornton,C.A. (2007). Myotonic dystrophy: RNA-mediated muscle disease. Curr. Opin. Neurol. 20, 572-576.

Wilburn,B., Rudnicki,D.D., Zhao,J., Weitz,T.M., Cheng,Y., Gu,X., Greiner,E., Park,C.S., Wang,N., Sopher,B.L., La Spada,A.R., Osmand,A., Margolis,R.L., Sun,Y.E., and Yang,X.W. (2011). An antisense CAG repeat transcript at JPH3 locus mediates expanded polyglutamine protein toxicity in Huntington's disease-like 2 mice. Neuron 70, 427-440.

Wilton,S.D., Fall,A.M., Harding,P.L., McClorey,G., Coleman,C., and Fletcher,S. (2007). Antisense oligonucleotide-induced exon skipping across the human dystrophin gene transcript. Mol. Ther. 15, 1288-1296.

Winborn,B.J., Travis,S.M., Todi,S.V., Scaglione,K.M., Xu,P., Williams,A.J., Cohen,R.E., Peng,J., and Paulson,H.L. (2008). The deubiquitinating enzyme ataxin-3, a polyglutamine disease protein, edits Lys63 linkages in mixed linkage ubiquitin chains. J. Biol. Chem. 283, 26436-26443.

Wojciechowska,M. and Krzyzosiak,W.J. (2011). CAG repeat RNA as an auxiliary toxic agent in polyglutamine disorders. RNA Biol. 8, 565-571.

Woldbye,D.P., Angehagen,M., Gotzsche,C.R., Elbrond-Bek,H., Sorensen,A.T., Christiansen,S.H., Olesen,M.V., Nikitidou,L., Hansen,T.V., Kanter-Schlifke,I., and Kokaia,M. (2010). Adeno-associated viral vector-induced overexpression of neuropeptide Y Y2 receptors in the hippocampus suppresses seizures. Brain 133, 2778-2788.

Wong,E. and Cuervo,A.M. (2010). Autophagy gone awry in neurodegenerative diseases. Nat. Neurosci. 13, 805-811.

Wu,H., Lima,W.F., Zhang,H., Fan,A., Sun,H., and Crooke,S.T. (2004). Determination of the role of the human RNase H1 in the pharmacology of DNA-like antisense drugs. J. Biol. Chem. 279, 17181-17189.

Xia,H., Mao,Q., Eliason,S.L., Harper,S.Q., Martins,I.H., Orr,H.T., Paulson,H.L., Yang,L., Kotin,R.M., and Davidson,B.L. (2004). RNAi suppresses polyglutamine-induced neurodegeneration in a model of spinocerebellar ataxia. Nat. Med. 10, 816-820.

Yabe,I., Sasaki,H., Takeichi,N., Takei,A., Hamada,T., Fukushima,K., and Tashiro,K. (2003). Positional vertigo and macroscopic downbeat positioning nystagmus in spinocerebellar ataxia type 6 (SCA6). J. Neurol. 250, 440-443.

Yamada,M., Shimohata,M., Sato,T., Tsuji,S., and Takahashi,H. (2006). Polyglutamine disease: recent advances in the neuropathology of dentatorubral-pallidoluysian atrophy. Neuropathology 26, 346-351.

Yamamoto,A., Lucas,J.J., and Hen,R. (2000). Reversal of neuropathology and motor dysfunction in a conditional model of Huntington's disease. Cell 101, 57-66.

Yu,D., Pendergraff,H., Liu,J., Kordasiewicz,H.B., Cleveland,D.W., Swayze,E.E., Lima,W.F., Crooke,S.T., Prakash,T.P., and Corey,D.R. (2012). Single-Stranded RNAs Use RNAi to Potently and Allele-Selectively Inhibit Mutant Huntingtin Expression. Cell 150, 895-908.

Yu,Y.C., Kuo,C.L., Cheng,W.L., Liu,C.S., and Hsieh,M. (2009). Decreased antioxidant enzyme activity and increased mitochondrial DNA damage in cellular models of Machado-Joseph disease. J. Neurosci. Res. 87, 1884-1891.

Zalachoras,I., Grootaers,G., van Weert,L.T., Aubert,Y., de Kreij,S.R., Datson,N.A., van Roon-Mom,W.M., Aartsma-Rus,A., and Meijer,O.C. (2013). Antisense-mediated isoform switching of steroid receptor coactivator-1 in the central nucleus of the amygdala of the mouse brain. BMC Neurosci. 14, 5.

Zeitlin,S., Liu,J.P., Chapman,D.L., Papaioannou,V.E., and Efstratiadis,A. (1995). Increased apoptosis and early embryonic lethality in mice nullizygous for the Huntington's disease gene homologue. Nat. Genet. 11, 155-163.

Zhang,M.Q. (1998). Statistical features of human exons and their flanking regions. Hum. Mol. Genet. 7, 919-932.

Zhang,S., Xu,L., Lee,J., and Xu,T. (2002). Drosophila atrophin homolog functions as a transcriptional corepressor in multiple developmental processes. Cell 108, 45-56.

Zhang,Y., Li,M., Drozda,M., Chen,M., Ren,S., Mejia Sanchez,R.O., Leavitt,B.R., Cattaneo,E., Ferrante,R.J., Hayden,M.R., and Friedlander,R.M. (2003). Depletion of wild-type huntingtin in mouse models of neurologic diseases. J. Neurochem. 87, 101-106.

Zhang,Y., Engelman,J., and Friedlander,R.M. (2009). Allele-specific silencing of mutant Huntington's disease gene. J. Neurochem. 108, 82-90.

Zhong,N., Ju,W., Pietrofesa,J., Wang,D., Dobkin,C., and Brown,W.T. (1996). Fragile X "gray zone" alleles: AGG patterns, expansion risks, and associated haplotypes. Am. J. Med. Genet. 64, 261-265.

Zhong,X. and Pittman,R.N. (2006). Ataxin-3 binds VCP/p97 and regulates retrotranslocation of ERAD substrates. Hum. Mol. Genet. 15, 2409-2420.

Zhou,H., Cao,F., Wang,Z., Yu,Z.X., Nguyen,H.P., Evans,J., Li,S.H., and Li,X.J. (2003). Huntingtin forms toxic NH2-terminal fragment complexes that are promoted by the age-dependent decrease in proteasome activity. J. Cell Biol. 163, 109-118.

Zhuchenko,O., Bailey,J., Bonnen,P., Ashizawa,T., Stockton,D.W., Amos,C., Dobyns,W.B., Subramony,S.H., Zoghbi,H.Y., and Lee,C.C. (1997). Autosomal dominant cerebellar ataxia (SCA6) associated with small polyglutamine expansions in the alpha 1A-voltage-dependent calcium channel. Nat. Genet. 15, 62-69.

Zoghbi,H.Y. and Orr,H.T. (2000). Glutamine repeats and neurodegeneration. Annu. Rev. Neurosci. 23, 217-247.

Zu,T., Duvick,L.A., Kaytor,M.D., Berlinger,M.S., Zoghbi,H.Y., Clark,H.B., and Orr,H.T. (2004). Recovery from polyglutamine-induced neurodegeneration in conditional SCA1 transgenic mice. J. Neurosci. 24, 8853-8861.

Zu,T., Gibbens,B., Doty,N.S., Gomes-Pereira,M., Huguet,A., Stone,M.D., Margolis,J., Peterson,M., Markowski,T.W., Ingram,M.A., Nan,Z., Forster,C., Low,W.C., Schoser,B., Somia,N.V., Clark,H.B., Schmechel,S., Bitterman,P.B., Gourdon,G., Swanson,M.S., Moseley,M., and Ranum,L.P. (2011). Non-ATG-initiated translation directed by microsatellite expansions. Proc. Natl. Acad. Sci. U. S. A. 108, 260-265.

Zuccato,C., Ciammola,A., Rigamonti,D., Leavitt,B.R., Goffredo,D., Conti,L., MacDonald,M.E., Friedlander,R.M., Silani,V., Hayden,M.R., Timmusk,T., Sipione,S., and Cattaneo,E. (2001). Loss of huntingtin-mediated BDNF gene transcription in Huntington's disease. Science 293, 493-498.

Zuccato,C., Belyaev,N., Conforti,P., Ooi,L., Tartari,M., Papadimou,E., MacDonald,M., Fossale,E., Zeitlin,S., Buckley,N., and Cattaneo,E. (2007). Widespread disruption of repressor element-1 silencing transcription factor/neuron-restrictive silencer factor occupancy at its target genes in Huntington's disease. J. Neurosci. 27, 6972-6983.

Zuhlke,C.H., Spranger,M., Spranger,S., Voigt,R., Lanz,M., Gehlken,U., Hinrichs,F., and Schwinger,E. (2003). SCA17 caused by homozygous repeat expansion in TBP due to partial isodisomy 6. Eur. J. Hum. Genet. 11, 629-632.

Zuker,M. (2003). Mfold web server for nucleic acid folding and hybridization prediction. Nucleic Acids Res. 31, 3406-3415.

Appendix

Summary
Samenvatting
List of abbreviations
List of publications
Curriculum Vitae
Dankwoord

Summary

Polyglutamine (polyQ) diseases are a group of nine neurodegenerative disorders, which are all caused by a CAG triplet repeat expansion, resulting in a gain of toxic polyQ protein function. The longer the CAG repeat, the earlier the disease manifestation and in most cases the disease onset is around midlife. Although the disorders have a monogenic cause and much research has been done the last decades, no therapies are available to cure or slow down the disease.

In **chapter 1** a short overview of the polyQ disorders and insight in the disease-causing polyQ proteins is given and their role in known disease mechanisms is described. The most prevalent and best studied polyQ disorders, being Huntington disease (HD) and spinocerebellar ataxia type 3 (SCA3), and the molecular biology of the disease causing proteins, huntingtin and ataxin-3, are extensively reviewed.

Furthermore, the opportunities for genetic therapies for polyQ disorders are discussed, focussing on what can be learned from other neurodegenerative disorders of which genetic therapies are in development or already used as therapy. Small molecules, called antisense oligonucleotides, are broadly used as potential treatment for neurodegenerative diseases. According to the specific chemical modifications and target binding site of the antisense oligonucleotide, they can either reduce expression or modify polyQ disease-causing proteins. Furthermore, the limitations and possibilities of the delivery of antisense oligonucleotides to the brain and into the affected neuronal cells are discussed.

While much research has been done on the underlying polyQ disease mechanisms, knowledge on regulation and expression of mRNA and protein expression are limited. **Chapter 2** describes subtle differences in huntingtin mRNA and protein expression in HD. In adult-onset HD less mutant huntingtin mRNA, but equal wild-type and mutant huntingtin protein levels are found. In juvenile HD subjects less mutant huntingtin protein compared to wild-type huntingtin protein is present. This indicates differences in huntingtin protein expression between adult-onset and juvenile HD.

In **chapter 3** CUG triplet-repeat antisense oligonucleotides are used to effectively reduce mutant polyQ transcript and protein levels in polyQ patient-derived fibroblasts. Although a reduction in wild-type CAG transcript levels was observed as well. This reduction was less pronounced than for the mutant transcript. Expression levels of other non-expanded CAG triplet repeat-containing transcripts investigated were not affected, verifying the specificity of the CUG triplet repeat antisense oligonucleotide for the mutant transcript. **Chapter 2** describes that the basal levels of mutant huntingtin mRNA and mutant huntingtin protein are equal or lower when compared to wild-type. This provides feasibility for genetic therapies like the CUG triplet-repeat antisense oligonucleotide that are not completely specific for the mutant huntingtin allele.

Next to specifically targeting the expanded CAG repeat transcripts to reduce the translation of mutant polyQ protein, **chapter 4** reports on removing the motifs that are implicated in the formation of toxic polyQ fragments. Soluble polyQ fragments, generated by proteolytic cleavage during the aggregation process, are considered to be the main toxic entities, resulting in neurodegeneration. In HD, removing a proteolytic cleavage site, implicated in the formation of huntingtin fragments containing the polyQ repeat has been shown to result in reduced toxicity. **Chapter 4** describes a potential therapeutic approach of preventing the formation of toxic huntingtin polyQ fragments by antisense oligonucleotides that induce skipping of exon 12 in huntingtin pre-mRNA. This antisense oligonucleotide-mediated protein modification resulted in a huntingtin protein lacking disease-implied cleavage motifs and subsequently reduced formation of toxic huntingtin polyQ fragments. This proof of concept shows a completely novel approach to reduce mutant huntingtin toxicity not by reducing expressing levels, but by modifying polyQ protein.

A more direct genetic approach to reduce polyQ-induced toxicity is shown in **chapter 5**. Here antisense oligonucleotide-mediated exon skipping is used to remove the toxic polyQ repeat from the ataxin-3 protein. Two different approaches are proposed with the same aim: removal of the CAG repeat-containing exon. Both approaches result in the formation of modified ataxin-3 protein that lacks the toxic polyQ repeat. The modified ataxin-3 protein lacks only a small part and maintains important wild-type functions of the protein.

The feasibility of the in **chapter 4 and 5** described antisense oligonucleotides was tested *in vivo* by injections of antisense oligonucleotides directly into the brain of mice. The *in vivo* and *in vitro* data described in this thesis suggest that both targeting the CAG repeat directly and antisense oligonucleotide-mediated exon skipping are promising potential therapeutic approaches to reduce polyQ-induced toxicity in HD, SCA3 and other polyQ disorders.

In **chapter 6** the main findings from this thesis are summarized. Recent developments are described and reflected how they relate to the results reported in this thesis. In addition, a reflection is given on how to get to clinical trials of genetic therapies like antisense oligonucleotide-mediated treatments for polyQ disease patients.

This thesis proposes various novel genetic therapies for polyQ disorders, aiming at reducing and/or modifying polyQ disease-causing proteins. Although extensive *in vitro* and *in vivo* research is important to rule out toxic off-target effects of the various antisense oligonucleotides and resulting modified proteins, these preclinical antisense oligonucleotide-mediated treatments look promising as therapeutic candidates for polyQ disorders.

Samenvatting

Polyglutamine (polyQ) ziekten is een groep van negen neurodegeneratieve aandoeningen die allen worden veroorzaakt door een verlengde CAG herhaling resulterend in een extra schadelijke polyQ eiwitfunctie. Hoe langer deze CAG herhaling, des te eerder de ziekte zich manifesteert. In de meeste gevallen begint de ziekte rond middelbare leeftijd. Hoewel alle polyQ ziekten veroorzaakt worden door een mutatie in één gen, en er de laatste decennia veel onderzoek gedaan is, zijn er tot dusverre geen therapieën beschikbaar die de ziekte genezen of vertragen.

In **hoofdstuk 1** wordt een kort overzicht gegeven van de polyQ aandoeningen en worden de ziekte-veroorzakende polyQ eiwitten en hun rol in de ziektemechanismen beschreven. De meest voorkomende en best bestudeerde polyQ aandoeningen, de ziekte van Huntington (ZvH) en spinocerebellaire ataxie type 3 (SCA3) en de moleculaire biologie van hun ziekteverwekkende huntingtine en ataxine-3 worden beschreven.

Vervolgens zijn in **hoofdstuk 1** de mogelijkheden voor genetische therapieën voor polyQ aandoeningen besproken, met de nadruk op wat kan worden geleerd van andere neurodegeneratieve aandoeningen waarvoor genetische therapieën in ontwikkeling zijn of al worden gebruikt als therapie. Kleine moleculen, zogenaamde antisense oligonucleotiden, worden algemeen gebruikt als potentiële behandeling voor neurodegeneratieve ziekten. Afhankelijk van de specifieke chemische modificaties en plaats waarop het bindt kunnen antisense oligonucleotiden de expressie verlagen of polyQ eiwitten modificeren. De beperkingen en mogelijkheden van de toediening van antisense oligonucleotiden in de hersenen en het bereiken van de getroffen zenuwcellen wordt besproken.

Ondanks het vele onderzoek naar de onderliggende polyQ ziektemechanismen, blijft de kennis over regulering en expressie van mRNA en eiwit beperkt. **Hoofdstuk 2** beschrijft subtiele verschillen in huntingtine mRNA en eiwit expressie in ZvH. In volwassen ZvH is iets minder mutant huntingtine mRNA, maar gelijke hoeveelheden wild-type en mutant huntingtin eiwit hoeveelheden gevonden. Juveniele ZvH proefpersonen vertoonden minder mutant huntingtin eiwit vergeleken met wild-type huntingtine eiwit. Dit duidt op verschillen in huntingtine eiwitexpressie tussen volwassen ZvH en juveniel ZvH.

In **hoofdstuk 3** worden CUG triplet antisense oligonucleotiden gebruikt om, in van polyQ patiënten verkregen fibroblasten, specifiek mutant polyQ transcripten en eiwit te verminderen. Een vermindering van wild-type CAG transcript niveaus werd ook waargenomen, maar deze afname was minder opvallend dan voor het mutant mRNA. Andere niet verlengde CAG triplet bevattende transcripten waren niet verminderd, wat de specificiteit van de CUG triplet antisense oligonucleotide voor het mutant mRNA bevestigt. **Hoofdstuk 2** beschrijft dat de basale niveaus van mutant huntingtin mRNA en mutant huntingtine eiwit gelijk of lager zijn in vergelijking met wild-type. Dit bevestigt de potentie van gentherapieën die niet geheel specifiek voor het mutante huntingtine allel, zoals de CUG triplet antisense oligonucleotide.

Naast het doelgericht aanpakken van verlengde CAG triplet transcripten om de translatie van mutant polyQ eiwit te verminderen, beschrijft **hoofdstuk 4** het verwijderen van motieven die betrokken zijn bij de vorming van toxische polyQ fragmenten. Tijdens het aggregatieproces worden oplosbare polyQ fragmenten gegenereerd door het proteolytisch knippen van volledige polyQ eiwitten. Deze polyQ fragmenten worden beschouwd als de belangrijkste schadelijke entiteiten voor het ontstaan van neurodegeneratie. In de ZvH is reeds aangetoond dat het verwijderen van een proteolytische knipplaats, wat betrokken is bij de vorming van huntingtine polyQ fragmenten, leidt tot verminderde toxiciteit. **Hoofdstuk 4** beschrijft een mogelijke therapeutische benadering door middel van antisense oligonucleotiden die ervoor zorgen dat exon 12 uit het huntingtine mRNA verwijderd wordt. Deze antisense oligonucleotide geïnduceerde eiwitmodificatie resulteert in een huntingtine eiwit wat de knipplaats mist en wat vervolgens leidt tot verminderde vorming van toxische huntingtine polyQ fragmenten. Deze eerste studie beschrijft een compleet nieuwe aanpak voor het verminderen van de toxiciteit van mutant huntingtine door niet de expressieniveaus te verminderen, maar door het polyQ eiwit te modificeren.

Een meer directe genetische benadering om de polyQ geïnduceerde toxiciteit te verminderen is in **hoofdstuk 5** beschreven. Hier wordt het verwijderen van de toxische polyQ herhaling uit het ataxine-3 eiwit door middel van het verwijderen van exonen met behulp van antisense oligonucleotiden beschreven. Twee verschillende benaderingen werden aangedragen met hetzelfde doel, het verwijderen van het verlengde CAG triplet bevattende exon. Beide benaderingen resulteren in gemodificeerd ataxine-3 eiwit wat de toxische polyQ verlenging mist. Het gemodificeerde ataxine-3 eiwit mist slechts een klein deel en behoudt belangrijke wild-type functies van het eiwit.

De haalbaarheid van de in **hoofdstuk 4 en 5** beschreven antisense oligonucleotiden is *in vivo* aangetoond door antisense oligonucleotiden direct in de hersenen van muizen te injecteren. De in dit proefschrift beschreven *in vivo* en *in vitro* resultaten suggereren dat antisense oligonucleotiden gericht tegen de verlengde CAG triplet rechtstreeks en het verwijderen van exonen veelbelovende therapeutische benaderingen zijn om de polyQ geïnduceerde toxiciteit te verminderen in de ZvH, SCA3 en andere polyQ aandoeningen.

In **hoofdstuk 6** zijn de belangrijkste bevindingen van dit proefschrift samengevat. Recente ontwikkelingen worden beschreven en gerelateerd aan de verkregen resultaten beschreven in dit proefschrift. Daarnaast wordt er een blik in de toekomst geworpen hoe voor polyQ patiënten klinische studies met genetische therapieën zoals antisense oligonucleotiden behandelingen op te zetten.

Dit proefschrift beschrijft enkele nieuwe genetische therapieën voor polyQ aandoeningen welke gericht zijn op het verminderen en/of modificeren van polyQ ziekte-veroorzakende eiwitten. Hoewel uitgebreid *in vitro* en *in vivo* onderzoek nodig is om toxische bijwerkingen van de verschillende antisense oligonucleotiden en de resulterende gemodificeerde eiwitten uit te sluiten, zijn deze preklinische antisense oligonucleotide behandelingen veelbelovend als mogelijke therapeutische behandelingen voor polyQ aandoeningen.

List of abbreviations

AAV	adeno-associated virus
AD	Alzheimer disease
ALS	amyotrophic lateral sclerosis
AON	antisense oligonucleotide
APP	amyloid β precursor protein
AR	androgen receptor
ATN1	atrophin-1
ATP	Adenosine triphosphate
ATXN	ataxin
Aβ	β-amyloid peptide
BBB	blood brain barrier
BDNF	brain-derived neurotrophic factor
CA1	Cornu ammonis area 1
CACNA1A	alpha 1A subunit of the voltage-dependent P/Q type calcium channel ($Ca_V2.1$)
CBP	cAMP response element-binding protein binding protein
CELF2	CUGBP, Elav-like family member 2
cET	ethyl nucleic acid
CNS	central nervous system
CSF	cerebrospinal fluid
DM1	myotonic dystrophy-1
DMD	Duchenne muscular dystrophy
DMPK	dystrophia myotonica protein kinase
DRPLA	dentatorubro-pallidoluysian atrophy
EA-2	episodic ataxia type-2
ER	endoplasmic-reticulum
ERAD	endoplasmic-reticulum-associated protein degradation
ESE	exonic splicing silencer
FHM	familial hemiplegic migraine
FMRP	fragile X mental retardation protein
FOXO	forkhead box O (FOXO) transcription factor
FXTAS	fragile X-associated tremor/ataxia syndrome
gDNA	genomic DNA
GFAP	glial fibrillary acidic protein
GLS	glutaminase
GLUT	glucose transporter
HD	Huntington disease
HDAC	histone deacetylase
HDL2	Huntington disease-like-2
HEAT	htt, elongation factor 3, protein phosphatase 2A, and the yeast PI3-kinase TOR1

hHR23	human homologues of yeast protein RAD23
Hip	htt interacting protein
HTT	huntingtin
HTTAS	huntingtin antisense
ICV	intracerebroventricular
ISS	intronic splicing silencer
LNA	locked nucleic acid
MBNL1	muscleblind-like protein 1
Me	methyl
miRNA	microRNA
MJD	Machado-Joseph disease
MMP-2	matrix metalloproteinase-2
MOE	methoxyethyl
MS	multiple sclerosis
NCoR1	nuclear receptor co-repressor
NES	nuclear export signal
NLS	nuclear localisation signal
PCAF	p300/CBP-associated factor
PMO	phosphorodiamidate morpholino oligomer
PNA	peptide nucleic acid
polyA	polyalanine
polyQ	polyglutamine
polyS	polyserine
PPMO	peptide-linked phosphorodiamidate morpholino oligomer
PS	phosphorothioate
qRT-PCR	quantitative real-time polymerase chain reaction
REST	RE1 silencing transcription factor
RNase H	ribonuclease H
RT-PCR	reverse transcription polymerase chain reaction
SARA	scale for the assessment and rating of ataxia
SBMA	bulbar muscular atrophy
SCA	spinocerebellar ataxia
SCAANT1	SCA7 antisense noncoding transcript 1
shRNA	short hairpin RNA
siRNA	small interfering RNA
SLiC	SNP linkage by circularization
SMA	spinal muscular atrophy
SMN	survival motor neuron
SNP	single nucleotide polymorphism
SOD1	superoxide dismutase 1
ss-siRNA	single-stranded silencing RNA

TAF4	TBP-associated factor 4
TARDBP	TAR DNA-binding protein
TBP	TATA box-binding protein
UHDRS	unified Huntington disease rating scale
UIM	ubiquitin interacting motif
UPS	ubiquitin-proteasome system
UTR	untranslated region
VCP/p97	valosin-containing protein
YAC	yeast artificial chromosome
ZNF384	zinc finger protein 384

List of publications

van Vlijmen T, Vleugel M, **Evers MM**, Mohammed S, Wulf PS, Heck AJ, Hoogenraad CC, van der Sluijs P. (2008). A unique residue in rab3c determines the interaction with novel binding protein Zwint-1. FEBS Lett. 582(19):2838-42.

Evers MM, Pepers BA, van Deutekom JC, Mulders SA, den Dunnen JT, Aartsma-Rus A, van Ommen GJ, van Roon-Mom WM. (2011). Targeting several CAG expansion diseases by a single antisense oligonucleotide. PLoS One. 6(9):e24308.

Zalachoras I, **Evers MM**, van Roon-Mom WM, Aartsma-Rus AM, Meijer OC. (2011). Antisense-mediated RNA targeting: versatile and expedient genetic manipulation in the brain. Front Mol Neurosci. 4:10.

Evers MM, Vlamings R, Temel Y, van Roon-Mom WM. (2012). Ameliorating Huntington's Disease by Targeting Huntingtin mRNA. Huntington's Disease - Core Concepts and Current Advances, Dr Nagehan Ersoy Tunali (Ed.), ISBN: 978-953-307-953-0, InTech

Rook MB, **Evers MM**, Vos MA, Bierhuizen MF. (2012). Biology of cardiac sodium channel Nav1.5 expression. Cardiovasc Res. 93(1):12-23.

Evers MM, Tran HD, Zalachoras I, Pepers BA, Meijer OC, den Dunnen JT, van Ommen GJ, Aartsma-Rus A, van Roon-Mom WM. (2013) Ataxin-3 protein modification as a treatment strategy for Spinocerebellar Ataxia type 3: Removal of the CAG containing exon. Neurobiol Dis. 58:49-56.

Evers MM, Toonen LJA, van Roon-Mom WM. (2014) Ataxin-3 protein and RNA toxicity in spinocerebellar ataxia type 3: current insights and emerging therapeutic strategies. Mol Neurobiol. 49(3):1513-31.

Evers MM, Tran HD, Zalachoras I, Meijer OC, den Dunnen JT, van Ommen GJ, Aartsma-Rus A, van Roon-Mom WM. (2014) Preventing formation of toxic N-terminal huntingtin fragments through antisense oligonucleotide-mediated protein modification. Nucleic Acid Ther. 24(1):4-12.

Evers MM, Schut MH, Pepers BA, Atalar M, van Belzen MJ, Faull RLM, Roos RAC, and van Roon-Mom WM. (2014) Making (anti-) sense out of huntingtin levels in Huntington disease. Neurobiol Dis. Under review.

Evers MM, Toonen LJA, van Roon-Mom WM. (2014) Antisense oligonucleotides in therapy of central nervous system diseases. Adv Drug Deliv Rev. Under review.

Curriculum Vitae

Melvin Evers is geboren op 12 december 1982 te Rhenen. In 2001 heeft hij zijn VWO diploma behaald op het Christelijk Lyceum te Veenendaal. Na een jaar Informatiekunde aan de Universiteit van Utrecht, begon hij in 2003 aan de studie Biomedische Wetenschappen aan de Universiteit van Utrecht. Na het verkrijgen van zijn Bachelors diploma in 2006 heeft hij de Biomedical Sciences Master Biology of Disease gevolgd aan de Universiteit van Utrecht. Voor deze Master heeft hij twee maal een onderzoeksstage gelopen. De eerste stage vond plaats in het Universitair Medisch Centrum Utrecht bij de afdeling celbiologie onder leiding van Dr. Thijs van Vlijmen en Dr. Peter van der Sluijs. Hier deed hij onderzoek naar de interactie van Zwint-1 met Rab3c en hun betrokkenheid bij de secretie van synaptische vesikels. Zijn tweede stage vond plaats in het Leids Universitair Medisch Centrum bij de afdeling Humane Genetica in de Huntington disease onderzoeksgroep onder leiding van Dr. Willeke van Roon-Mom. Tijdens deze stageperiode werkte hij nauw samen met het biotechnologiebedrijf Prosensa Therapeutics B.V. waar hij zich bezig hield met het uitvoeren van pilot studies met antisense oligonucleotiden gericht tegen de CAG verlenging in de ziekte van Huntington. Zijn Masterscriptie over de biologie van een specifiek natriumkanaal in het hart heeft hij vervolgens geschreven bij de afdeling Medische Fysiologie van het Universitair Medisch Centrum Utrecht onder supervisie van Dr. Martin Rook en Dr. Marti Bierhuizen.

Na het verkrijgen van zijn Master diploma was hij van september 2008 tot augustus 2013 werkzaam als promovendus aan de afdeling Humane Genetica van het Leids Universitair Medisch Centrum onder leiding van Dr. Willeke van Roon-Mom en Prof. Dr. Gert-Jan van Ommen. De resultaten van dit onderzoek staan beschreven in dit proefschrift. Vanaf september 2013 is hij werkzaam als postdoctoraal onderzoeker in de Polyglutamine Disease Research Group binnen de afdeling Humane Genetica van het Leids Universitair Medisch Centrum.

Dankwoord

Tijdens het promotietraject heb ik veel goede samenwerkingen gehad en vriendschappen opgebouwd. Het is dan ook onmogelijk iedereen persoonlijk te bedanken en mijn oprechte excuses als je je naam niet in het dankwoord ziet staan.

Als eerste zou ik graag mijn promotor **Gert-Jan** willen bedanken. Bedankt voor je betrokkenheid en kritische kijk op mijn manuscripten. Je complimenten na afloop van mijn eerste praatje op een groot congres in Cold Spring Harbor hebben mij erg goed gedaan.

Beste **Willeke**, jou ben ik heel veel dank verschuldigd. Bedankt dat je me de kans hebt gegeven om na mijn stage als promovendus aan de slag te gaan. Je stond altijd klaar voor me om over wetenschappelijke én niet-wetenschappelijke zaken te praten. Wetenschappelijk en sociaal een topper, het is echt geweldig om in jouw groep te mogen werken.

De motor van de groep, **Barry**, bedankt voor al je hulp en suggesties gedurende de afgelopen 6 jaar. We hebben er een paar mooie papers en vriendschap aan overgehouden! Fijn dat je mijn paranimf wilt zijn.

Er zijn nog enkele groepsgenoten die ik zou willen bedanken. **Lodewijk**, we hebben de afgelopen 2 jaar fijn samengewerkt en mooie reviews samen geschreven, ik wens je heel veel succes met je promotietraject. Blijf positief, dan komt er iets moois uit, daar ben ik van overtuigd! **Menno**, buurman, bedankt voor al je feitjes en weetjes. We hebben samen een artikel gepipetteerd wat hopelijk snel geaccepteerd zal worden. Αγαπητέ **Tassos**, καλή τύχη με την της διατριβής. εύχομαι ό, τι καλύτερο και ευτυχία στη μελλοντική σας σταδιοδρομία. Omdat ik toch in het steenkolen Grieks bezig ben, αγαπητή **Eleni**, είστε ένα δροσερό κορίτσι και είχαμε ωραία συνομιλίες κατά τη διάρκεια ποτά. Καλή τύχη με την οριστικοποίηση PhD σας! Ook **Maurice** en **Iris**, bedankt voor jullie hulp in het lab.

In de loop der jaren heb ik veel studenten mogen begeleiden waarvan enkele zelf nu ook als promovendus aan de slag zijn (#trots): **Alex**, thank you for your great help with two manuscripts and good luck with your PhD. Ook **José** en **Juliette** bedankt voor jullie inzet en heel veel succes met jullie promotietraject. **Astrid**, **Eline**, **Gido**, **Maria** en **Marlous**, bedankt voor jullie harde werken en succes met jullie opleidingen. Also **Neil** and **Tim** thanks for your work and good luck with your careers.

I would like to thank the following (ex)colleagues for your help, input, getting to know you better and providing a nice working environment: **Annemieke**, **Christa**, **Cindy**, **Cor**, **Cynthia**, **Dwi**, **Eleonora**, **Emile**, **Emmelien**, **Hans**, **Henk**, **Ingrid**, **Isabella**, **Ivo**, **Jeroen**, **Johan**, **Joke**, **Jos**, **Julie**, **Laura**, **Laure**, **Linda**, **Louise**, **Maaike**, **Maarten**, **Majella**, **Marcel**, **Margriet**, **Monika**, **Nisha**, **Peter²**, **Peter-Bram**, **Petra**, **Piet**, **Pietro**, **Polina**, **Richard**, **Rolf**, **Sandra**, **Saskia**, **Silvana**, **Silvère**, **Steven**, **Svetlana**, **Willem**, **Wouter**, **Yahya** en **Yavuz**. Ook **Babs** heel erg bedankt met je hulp om door alle promotieregelgeving heen te komen.

Verder zou ik graag de andere collega's van **LabJ**, de afdeling **Humane Genetica** en de **exonskip werkgroep** willen bedanken voor alle hulp en gezelligheid. Het werkt erg stimulerend om in zo'n wetenschappelijk hoogstaande afdeling te mogen werken.

This thesis could not be completed without good collaborations. I would therefore like to thank **Onno** and **Ioannis** for their valuable help with the *in vivo* experiments, which resulted in three papers. From Prosensa Therapeutics I would like to thank **Anchel**, **Jeroen**, **Judith**, **Nicole** and **Susan** for the close collaborations on the (CUG)7 work. From the Maastricht University Medical Center, I would like to thank **Ali**, **João**, **Rinske** and **Yasin** for their collaborations that are still ongoing. Ich möchte auch **Bernd**, **Peter**, **Philipp**, **Thomas** und **Ullrich** vom Universitätsklinikum Bonn danken und ich hoffe, dass unsere Zusammenarbeit uns einen Schritt näher bringt, eine mögliche Therapie für SCA3 Patienten zu finden.

Mijn studievrienden **Mark**, **Pascal**, **Stefan** en **Timo** bedankt voor de fijne studiejaren. Je weet wel waarvoor. Ik ben mij ervan bewust dat ik te vaak afhaak als er een biertje gedronken wordt, maar áls ik erbij ben is het erg gezellig mannen. De volgende dag minder.

Mijn schoolvrienden en collegapapas **Bart**, **Gerben Jan** en **Michiel**, tof dat we na al die jaren, verschillende woonadressen, gezinsuitbreidingen en totaal verschillende carrières nog steeds veel contact hebben. Michiel bedankt voor de mooie cover.

Verder zou ik graag de volgende vrienden **Boy**, **Elisah**, **Eva**, **Jaap**, **Jennifer**, **Jojanneke**, **Josje**, **Judith**, **Karlijn**, **Kim**, **Marije**, **Michael**, **René**, **Sandra** willen bedanken voor de gezellige avonden de afgelopen jaren.

Johannes erg bedankt dat ik je maat mag zijn. Je bent een geweldig persoon waar ik altijd mijn ei bij kwijt kan.

Mies, **Ingrid**, **Mieske**, bedankt voor jullie Brabantse gezelligheid en jullie support de afgelopen jaren.

Lieve **Priscalla**, we verschillen 10 jaar in leeftijd, waardoor we vroeger nog al eens onze broer-zus conflicten hadden. Maar nu we allebei wat ouder en ouders zijn, zijn we steeds meer naar elkaar toegegroeid. Ik had me geen betere grote zus kunnen wensen! Mijn (bijna) zwager en paranimf **Martijn**, jij bent al bijna 25 jaar in mijn leven en je bent als een broer voor me. Ik wens jullie samen met mijn lieve neefje **Justin** en nichtje **Esmée** een hele fijne bruiloft, hè hè eindelijk, en al het geluk van de wereld toe.

Lieve **ma**, lieve **pa**. Het is aan jullie te danken dat ik ben waar ik nu ben. Jullie hebben me de opvoeding en kans gegeven om mij te ontwikkelen tot wie ik nu ben. Jullie "doe gewoon je best, niet zeuren en ga ervoor" mentaliteit heeft me de afgelopen jaren erg geholpen. Ik ben jullie dankbaar voor de concessies die jullie hebben moeten doen zodat ik onbezorgd kon studeren. Ik hou van jullie en ik hoop dat jullie trots zijn op de bijzondere mijlpaal die ik nu bereikt heb.

Lieve **Linde**, wat heb jij ons leven in positieve zin veranderd! Door jou heb ik beter leren relativeren en ik weet nu wat écht belangrijk is in het leven. Je bent een mooi, lief, stralend, slim meisje en papa houdt zielsveel van je!

Lieve **Inkie**, ik ben zo blij dat ik jou aan de haak geslagen heb. Je bent een mooie vrouw, mijn beste maatje en de liefste mama ter wereld in één. Je gelooft in me, begrijpt me en staat altijd onvoorwaardelijk voor me klaar. Wat kan ik me nog meer wensen?

Ik vind jou lief!